YGS Miscellaneous Report MR-11

Case studies of high resolution resistivity/IP surveying over known mineral deposits: Yukon, Canada

M. Best, Bemex Consulting International
I.Fage and R. Daigle, Groundtruth Exploration

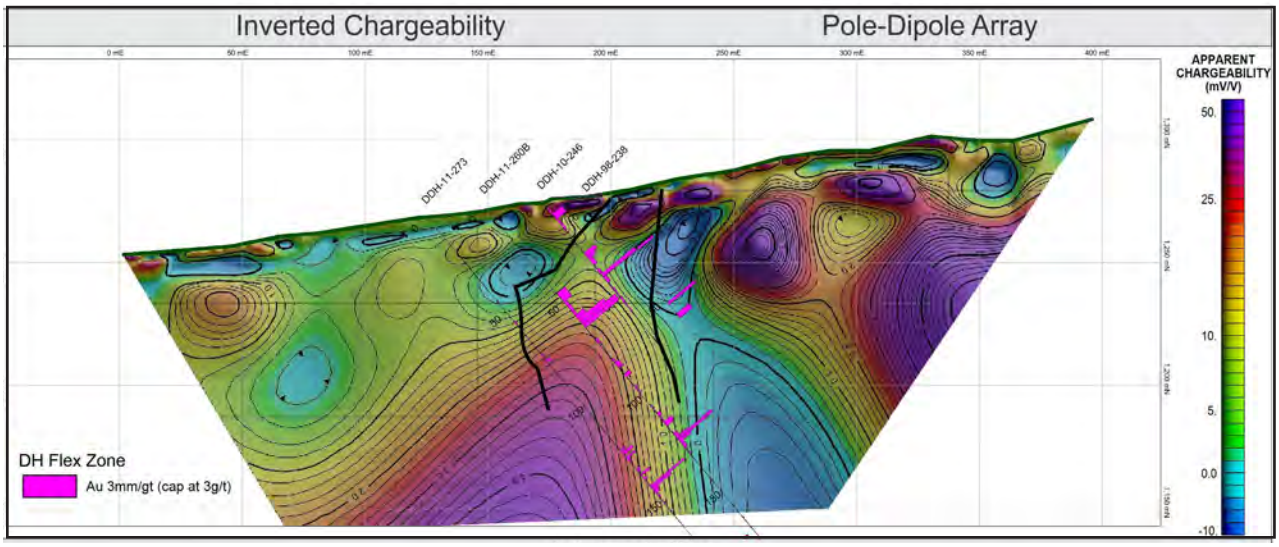

Yukon Geological Survey
Yukon Energy, Mines and Resources

Published under the authority of the Department of Energy, Mines and Resources, Government of Yukon
http://www.emr.gov.yk.ca.

Printed in Whitehorse, Yukon, 2014.

Publié avec l'autorisation du Ministères de l'Énergie, des Mines et des Ressources du gouvernement du Yukon, ***http://www.emr.gov.yk.ca.***

Imprimé à Whitehorse (Yukon) en 2014.

A copy of this report can be obtained by download from: www.geology.gov.yk.ca or by emailing: ***geology@gov.yk.ca***

In referring to this publication, please use the following citation:
Best, M., Fage, I., and Daigle, R., 2014. Case studies of high resolution resistivity/IP surveying over known mineral deposits: Yukon, Canada. Yukon Geological Survey, Miscellaneous Report 11, 146 p.

Cover image: Interpretation of inverted chargeability, pole-dipole array on line CS5-S050N (Flex Zone).

ABSTRACT

Multi-electrode, high resolution DC resistivity/IP systems have been used within the environmental and engineering geophysical community for several decades. The objective of these systems is to map the resistivity and IP structure of the Earth's subsurface to approximately 100 m depth. Typical applications include locating aggregate, groundwater mapping, salt water intrusion into fresh water aquifers, contaminant and leachate mapping, shallow landslide hazard mapping of slip planes, porosity, and potential debris volumes. Additionally the technique can be used to locate buried tunnels and sink holes. These high resolution resistivity/IP systems are therefore ideal for follow-up in non-glaciated environments since they are effective for mapping the shallow resistivity and IP structures potentially associated with mineralization and/or alteration products.

High resolution resistivity/IP (HRRIP) surveys were carried out over nine mineral deposits within Yukon. The objectives of this study were 1) to investigate whether HRRIP surveys could map mineralization and structure associated with known deposits, and 2) to determine which arrays, if any, were the most diagnostic for a given deposit type. The study included a copper porphyry deposit, a lead-zinc-silver vein deposit, and several different styles of gold mineralization/deposits. The location of the HRRIP line(s) were chosen based on the known mineralization and geology of the deposit. On average 3 different arrays were carried out along each line. Variations of dipole-dipole, inverse Schlumberger and pole-dipole arrays, as well as an array developed by Advanced Geosciences Inc. of Austin, Texas were used. Two-dimensional inversions of each array for each line were carried out to produce 2D resistivity and IP cross sections. These sections provided the fundamental information for the study.

The inversion results show that HRRIP surveys are able to produce resistivity and IP sections that generally correlate with the known mineralization and structure of the deposits. However, there are often differences between the inversion results (both resistivity and IP) of the different arrays along a given profile, and the location of resistivity and IP features is sometimes offset or missing relative to known structure and/or mineralization. The depth of penetration of the HRRIP method employed is estimated to be approximately 60 to 70 m for all arrays used except the pole-dipole array which has a depth of penetration estimated to be closer to 90 m. The study shows the HRRIP method can be effective for mapping a range of mineral deposits. However, care must be exercised when interpreting the inversion results because 1) there can be subtleties within the data and 2) not all resistivity and chargeability values from the inversions can be assumed to be associated with mineralization and/or structure. These comments apply to any resistivity/IP survey, not just HRRIP surveys. The arrays that were most effective for the HRRIP surveys were the dipole-dipole and inverse Schlumberger arrays with their variations.

CONTENTS

INTRODUCTION

Multi-electrode, high resolution DC resistivity/IP systems have been used within the environmental and engineering geophysical community for several decades. The objective of these systems is to map the resistivity and IP structure of the Earth's subsurface to approximately 100 m depth. Typical applications include locating aggregate, groundwater mapping, salt water intrusion into fresh water aquifers, contaminant and leachate mapping, shallow landslide hazard mapping of slip planes, porosity, and potential debris volumes. Additionally the technique can be used to locate buried tunnels and sink holes. These high resolution resistivity/IP (HRRIP) systems are therefore ideal for follow-up in non-glaciated environments since they are effective for mapping the shallow resistivity and IP structures potentially associated with mineralization and/or alteration products.

To our knowledge the application of these HHRIP surveys to mineral exploration has not been documented in literature. Several review articles on state of the art mining geophysics have been published during the last two decades (Lowe *et al.*, 1999; Nabighian and Asten, 2002; Vallee *et al.*, 2011) that provide examples of case histories using resistivity/IP systems but none provide examples of using the HHRIP method. There have been a large number of case studies specifically related to resistivity/IP surveying, for example Gasprikova *et al.*, 2005 and Pare and Legault, 2010, but again none using the HHRIP method.

There are mineral deposits within Yukon that are located in non-glaciated terrain. Such deposits provide an opportunity to test the HRRIP method since they are relatively shallow, their geology is known, and a number of holes have been drilled to outline them. The mineral deposits in this study were selected to provide different deposit types, different structural styles, and different metal content (Au, Ag, Cu, Pb, Zn). The IP response depends on the type of mineralization associated with the deposit. For example a porphyry copper deposit provides an opportunity to map stockwork structures containing disseminated sulphide mineralization. There are several different types of gold mineralization such as 1) oxides with no sulphide mineralization and hence no IP response, and 2) vein and breccia gold structures with sulphide mineralization and hence an IP response.

The primary goal was to investigate if high resolution multi-electrode resistivity/IP surveys could potentially be used to map known mineralization and structure. In particular, for which deposit types and/or geological situations does the method work and are there deposits where the inversions are inconclusive or incomplete. By understanding the geophysical response over deposits with known geology and mineralization we expect to learn how the HRRIP method can be more effectively utilized in prospective areas where the geology and mineralization are not so well known. A second goal was to investigate which array type(s), if any, were most effective for mapping the different deposit types. The nine deposits selected to test the HRRIP method provided a cross section of the target types outlined above.

The report starts with a description of the HRRIP method and then provides information on the location and regional setting of the case study targets. Sections on resistivity/IP arrays and procedures and data processing and inversion are provided. The results of case studies CS1 through CS9 are then presented. Each case study contains the geological description of the deposit, the geophysical parameters and arrays used, and the geophysical results. This is

followed with a section on the rock property measurements carried out on several of the cases studies. The report ends with two sections; one on results and discussion and one with a few concluding remarks.

MULTI-ELECTRODE HIGH RESOLUTION DC RESISTIVITY/IP SURVEYS

General description

Multi-electrode, high resolution, shallow resistivity/IP systems are a more portable version of the standard resistivity/IP systems used for mineral exploration. Their main advantage is they are portable, light-weight, and do not require large generators for generating the current. For example, an 84-electrode 2D array with an electrode spacing of 5 m covers a distance of 415 m and, depending on the array used, images the upper 50 to 150 m of the subsurface. In addition, the smaller electrode spacing provides good lateral resolution. Longer lines are obtained using roll-along techniques similar to those utilized within the seismic industry. These systems can collect data using common arrays (Fig. 1) such as dipole-dipole, pole-dipole, pole-pole, and Wenner-Schlumberger (inverse Wenner-Schlumberger), as well as specialized arrays such as the strong gradient array developed by AGI (see Appendix A for further details of these arrays). Each array has its strengths and weaknesses when imaging the subsurface. Small, light-weight generators or batteries can be used to supply the current for these systems (Fig. 2), although batteries are the preferred choice since they provide a more stable current to the current electrodes as discussed in case study one.

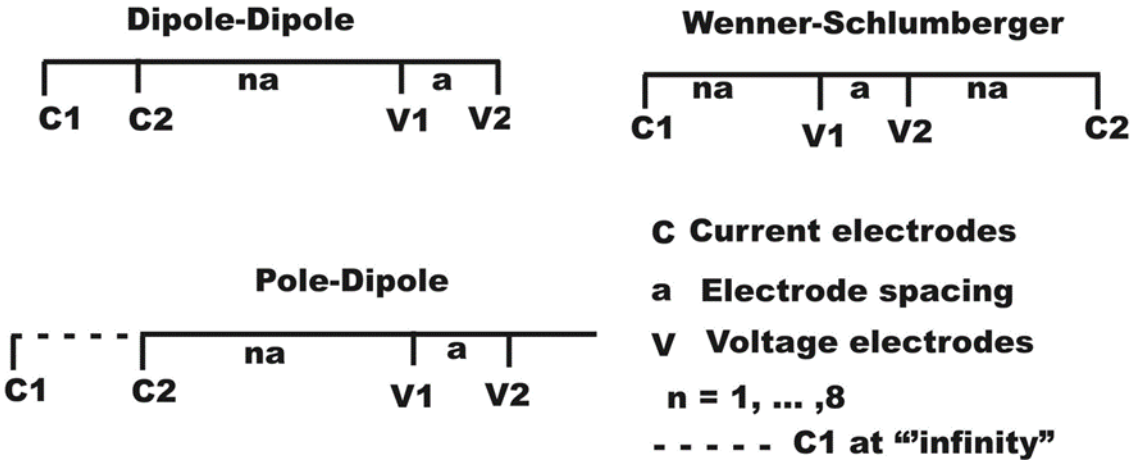

Figure 1. *Common electrode arrays.*

Figure 2. *AGI Supersting R8 system console (right), switchbox (upper left), and battery power source (lower left).*

Field operation

Each electrode must be planted in the ground to make good electrical contact. The contact resistance for an electrode is the resistance between the electrode and the ground and is independent of the bulk resistivity of the earth. Figure 3 is an example showing the contact resistance for each electrode of an 84 electrode system. Contact resistances of 2000 ohm-m or less provide the best coupling between the ground and the electrode; however 5000 ohm-m or less is acceptable. In this example electrode numbers 50 to 60 have contact resistances greater than 6000 ohm-m, even reaching 15 000 ohm-m in some cases. These high contact resistances limit the amount of current that can be injected into the ground. A couple of methods used to reduce the contact resistance are: 1) soaking the grounded electrodes with water with or without a conductive electrolyte, and 2) planting multiple electrodes at the same place and connecting them together to increase the area of contact between the electrodes and the ground. If time permits leaving the electrodes in the ground overnight or longer also reduces the contact resistance.

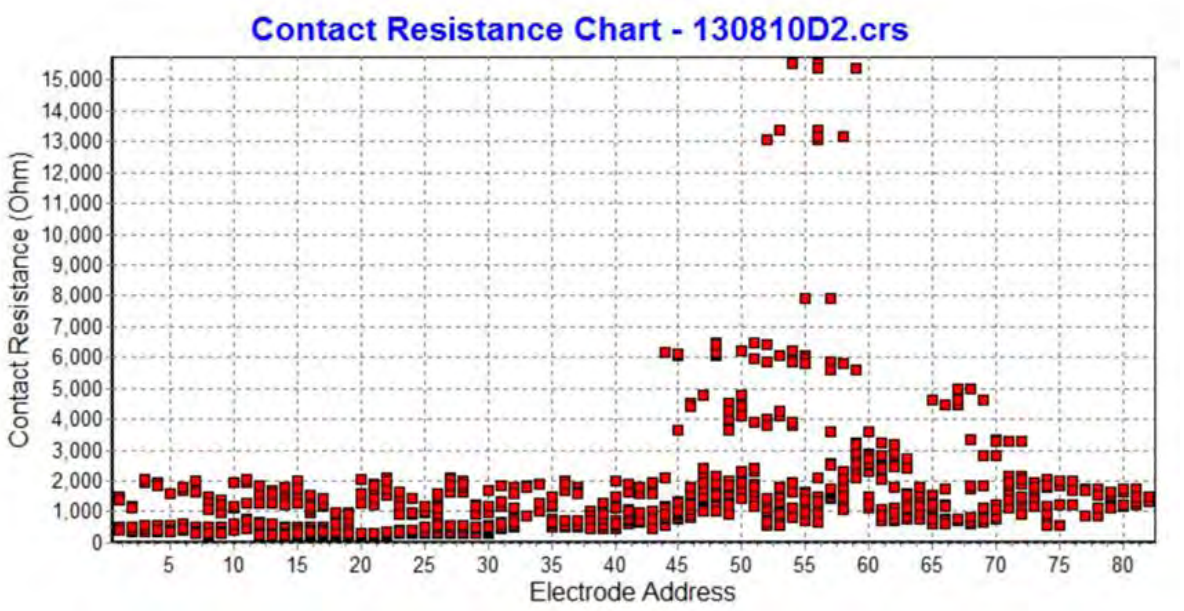

Figure 3. *Example of contact resistance for an 84 electrode system.*

Each electrode is connected to a takeout on the multi-electrode cable (Fig. 4). The connection must be sufficiently tight to ensure good electrical contact between the electrode and the cable. The cables are connected to a switching box (Fig. 2) which controls which two electrodes provide the current and which two electrodes measure the voltage. The console (Fig. 2) controls

Figure 4. *Multi-electrode laid along profile (left) and electrode connected to cable (right).*

the order of switching the electrodes so that all combinations of electrodes are used for a given array.

Figure 5 is a schematic showing the different combinations of current and voltage electrodes for a dipole-dipole array with n values from 1 to 8. The "a" spacing between the current and voltage electrodes takes on all possible values of a, 2a, 3a, etc., where “a” is the electrode spacing until the maximum separation is reached for the number of electrodes in the array. For example for 84 electrodes with an electrode spacing of 5 m, a = 5, 10, 15, 20, 25, 30, 35, 40, etc., although not all of the n = 1, etc., 8 values can be obtained for the larger values of “a” since the total length of the array is 415 m. Figure 6 is an example of a dipole-dipole apparent resistivity pseudosection. Note that for large “a” values (*i.e.*, effective depth since larger values of a spacing penetrate deeper into the sub-surface - see Kearey and Brooks, 1984) there are fewer measurement points as expected.

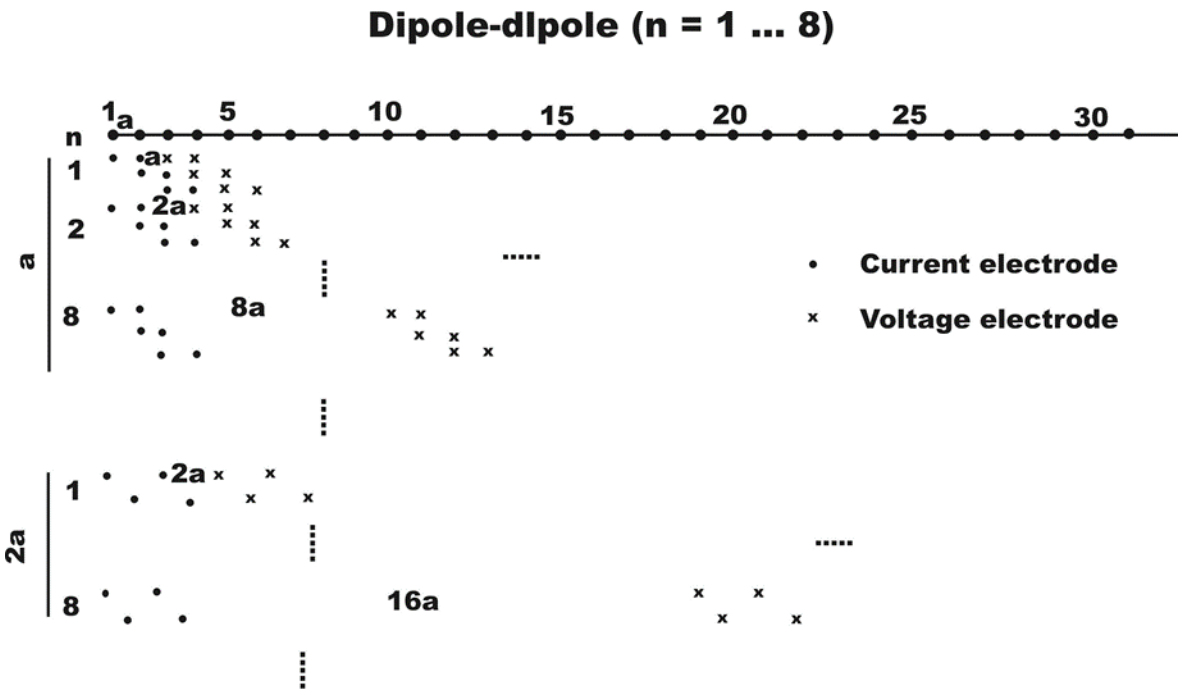

Figure5. *Example of current and voltage electrode locations for dipole array.*

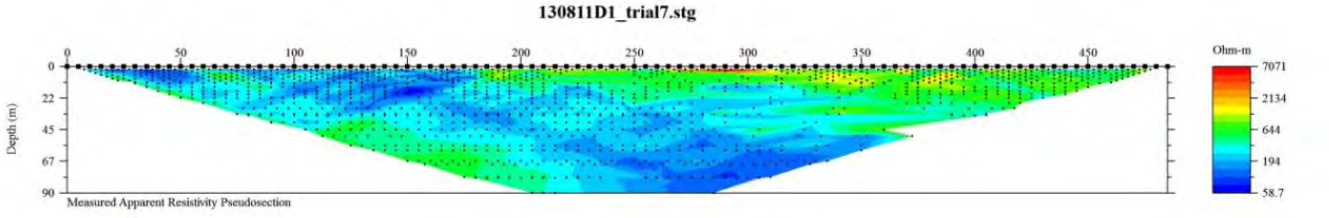

Figure 6. *Example of a resistivity pseudosection for a dipole-dipole array.*

LOCATION AND REGIONAL SETTING

The locations of the 9 case studies are shown in Figures 7 and 8 (overlain on terrane and geology maps respectively). Table 1 lists the case study targets and identifies the deposit type, NTS sheet, and main metals.

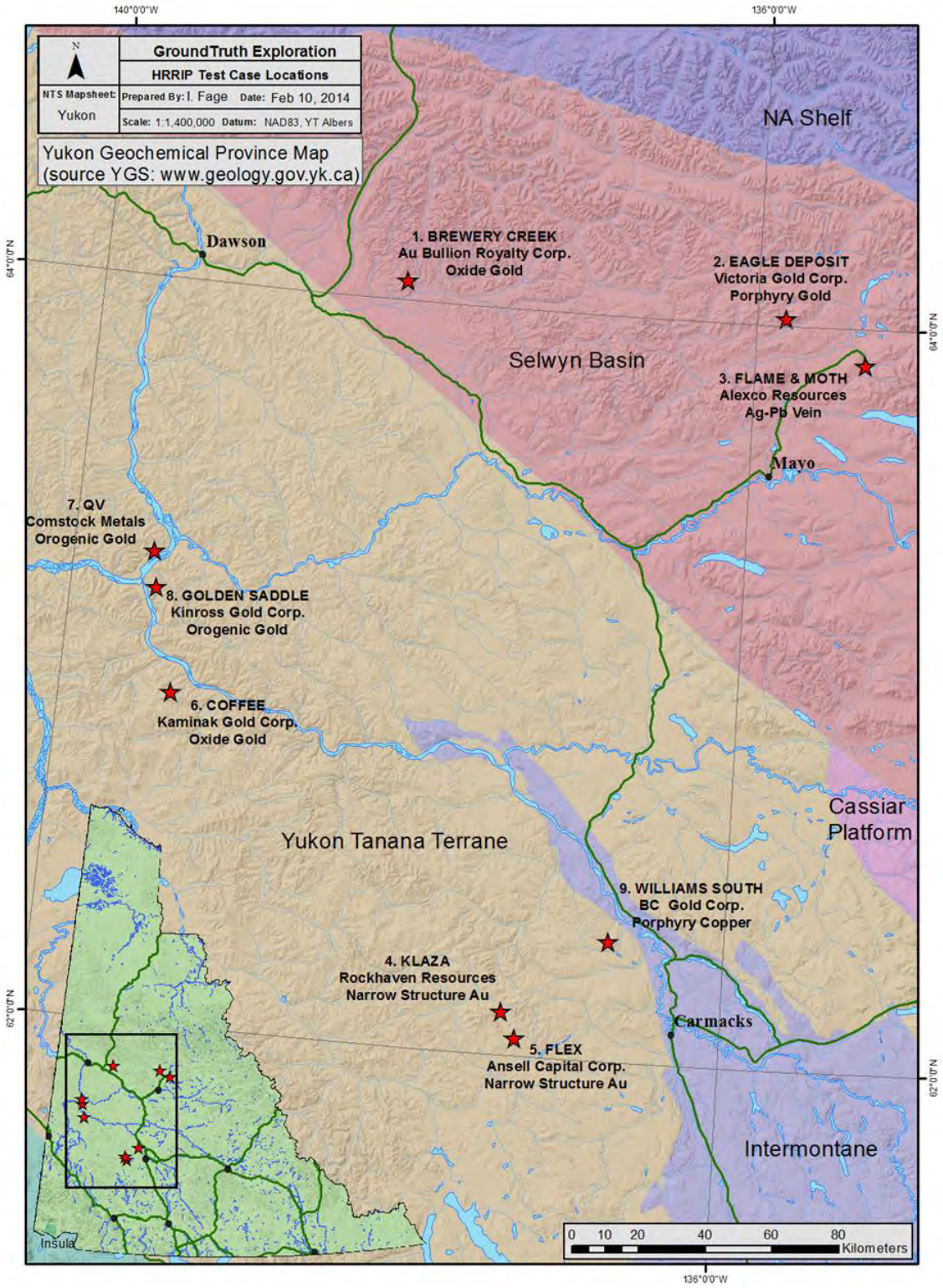

Figure 7. *Locations of the 9 case studies overlain on the Yukon terrane map.*

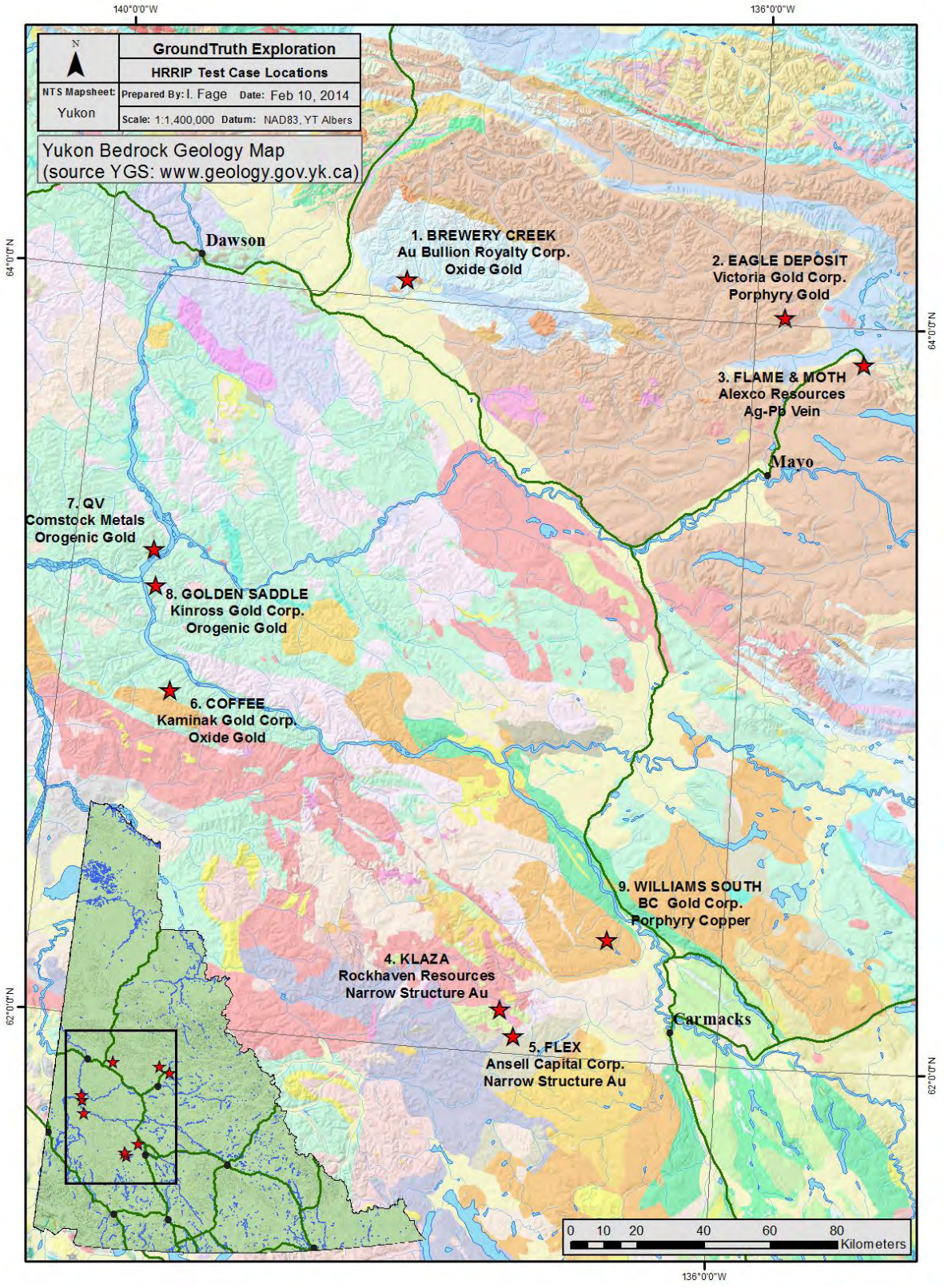

Figure 8. *Locations of the 9 case studies overlain on the Yukon regional geology map.*

Table 1. *Case study deposits.*

CASE STUDY	NAME	DEPOSIT TYPE	MAIN METALS	NTS SHEET
CS-1	BREWERY CREEK	OXIDE GOLD /PORPHYRY, SHEETED VEIN	Au	116B/01
CS-2	DUBLIN GULCH	PORPHYRY GOLD	Au	106D/04
CS-3	FLAME/MOTH	SEDIMENTARY Pb, Zn, Ag	Pb, Zn, Ag	105M/14
CS-4	KLAZA	NARROW GOLD STRUCTURE / VEIN BRECCIA	Au, Ag	115I/03
CS-5	CHARLOTTE	NARROW GOLD STRUCTURE / VOCANIC ASSOCIATED	Au	115I/03
CS-6	COFFEE	OXIDE GOLD / VEIN BRECCIA	Au	115J/14
CS-7	VG ZONE	WHITE STYLE	Au	115O/05
CS-8	GOLDEN SADDLE	WHITE STYLE	Au	115O/03
CS-9	WILLIAMS CREEK	PORPHYRY	Cu, Au	115I/07

Brewery Creek (CS-1), Dublin Gulch (CS-2), and Flame/Moth (CS-3) are east of the Tintina fault and lie within the Selwyn basin. The other case study targets are located west of the Tintina fault and lie within the Yukon Tanana terrane, a pericratonic sequence that extends from northern British Columbia, through Yukon, and into southern Alaska (Colpron *et al.*, 2006; Wainwright *et al.*, 2011). The Yukon Tanana terrane consists of Paleozoic schist and gneiss that were deformed and metamorphosed in the late Paleozoic, and intruded by several suites of Mesozoic intrusions that range in age from Jurassic to Eocene (Mortensen, 1992; Colpron *et al.*, 2006). From Late Permian to Early Jurassic, the rocks were tectonically stacked along foliation-parallel thrust faults (Mortensen, 1992; Berman *et al.*, 2007).

OVERVIEW OF RESISTIVITY/IP ARRAYS AND PROCEDURES

An Advanced Geosciences lnc. (AGI) Supersting multi-electrode resistivity/IP system with 84 electrodes was used to collect the resistivity and induced polarization (IP) data (Appendix A). The electrode spacing was fixed at 5 m for this case study, providing a spread length of 83 x 5 = 415 m. Most lines were short enough so that only a single spread length was necessary. Those lines longer than a spread length were obtained using the roll-along option of the Supersting System (Appendix A).

The current (I) and voltage (V) are measured for each electrode pair and are converted to an apparent resistivity (ρ_a) using the following formulas (Sumner, 1976).

Dipole-dipole

$\rho_a = \pi$ (V/I) n(n+1)(n+2)a

Pole-dipole

$\rho_a = \pi$ (V/I) n(n+1)a

Schlumberger (inverse Schlumberger)

$\rho_a = \pi$ (V/I) n(n+1)a

Wenner

$\rho_a = 2\pi$ (V/I) a

where V is the measured voltage (volts), I is the injected current (amperes), and a is the spacing between the electrodes and is a multiple of the 5 m electrode spacing (5, 10, 15 m, etc.). The apparent resistivity computed from the above equations equals the actual resistivity of the subsurface only for the case of a homogenous earth.

The Schlumberger array used with multi-electrode systems like the AGI system is the Wenner-Schlumberger array shown in Figure 1. The inverse Schlumberger array has the same configuration but the voltage and current electrodes are interchanged (Fig. 1 and Appendix B). The strong gradient array is a special array designed by AGI and combines the standard gradient array with the Wenner-Schlumberger array. The gradient array uses a short, fixed electrode spacing to measure the voltage within the central portion between the two current electrodes which are placed a significant distance apart (*i.e.*, "infinity" similar to the traditional pole-dipole array). The strong gradient array places the current electrodes much closer to the voltage electrodes, hence the name strong gradient. The dipole-dipole enhanced array, enhanced pole-dipole array, and the modified inverse Schlumberger array are discussed in Appendix B.

The resistivity data are presented as an apparent resistivity pseudosection (Fig. 6). If the subsurface is not a simple homogenous layer then the apparent resistivity must be determined from inversion of a forward model. The forward model can be a 1D, 2D or 3D forward model. If the subsurface geology consists of slowly varying layering then a one dimensional model may be appropriate. However subsurface geology is usually more complex so two or three-dimensional inversion programs are normally used. Generally two-dimensional inversion programs are used because 1) 3D data collection is time-consuming and expensive, and 2) most surveys collect a number of 2D profiles with lines placed as close to perpendicular to the known strike as possible in order to keep the interpretation as close to 2D as possible.

The Supersting system can measure the induced polarization and apparent resistivity at the same time. The unit of induced polarization measured by the Supersting is chargeability (M) with units of mV/V or ms. Chargeability is a measure of the integrated decay voltage as shown in Figure 9 (Sumner, 1976) and is computed from integrating the voltage decay curve after the current is turned off.

$$M = 1/V_p \qquad \int V(t)\, dt \text{ (integrated from } t_1 \text{ to } t_2)$$

The voltage V_p is the voltage used in the equations given earlier for the apparent resistivity and is the voltage just before the current is turned off.

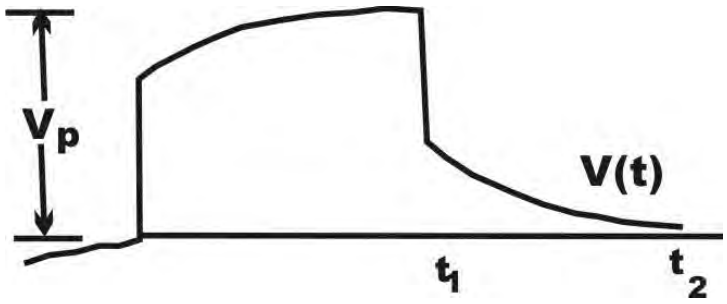

Figure 9. *Schematic of IP decay parameters (from Sumner, 1976).*

The Supersting collects the IP data in 6 time windows starting from time zero and spaced logarithmically. The six voltages (or subset of them) are averaged and divided by the initial (time zero) voltage V to provide the chargeability. The voltages in the 6 time windows are stored so the user can determine which ones to use during further processing. At least 4 of the voltages must be used in order to produce statistically meaningful chargeability values. The IP data are plotted as an IP pseudosection, similar to resistivity pseudosections. Inversion using a forward model (Sumner, 1976) must be carried out in order to obtain the sub-surface chargeability distribution, similar to the process carried out for resistivity inversion.

Table 2 lists which electrode arrays were used for each of the case study targets. At the first target, Brewery Creek, signal-to-noise levels were checked using a dipole-dipole array on line EW for a generator source and a battery source. The conclusion was that a battery source produced less noise than a generator source. Consequently a battery source was subsequently used for the entire study. Standard arrays (dipole-dipole, pole-dipole, and inverse Schlumberger, Wenner), along with the enhanced dipole-dipole array, the strong gradient array developed by AGI, the enhanced pole-pole array, and the enhanced pole-dipole and inverse Schlumberger arrays (appendix B) were used depending on the particular case study.

Minimal line cutting was needed for the AGI Supersting system since the multi-element cable is lightweight and requires little effort to move it in the field (Figure 4). The cable is segregated into 6 sections, each with 14 electrodes to make up the 84 electrode system. Three sections are placed behind the console and 3 are placed in front of the console, making the console the center point of the spread. When a line requires roll-along either one or three of the back sections are moved to the front and the console is moved to the new center position. In most instances it only takes a few hours to get a single spread ready for data acquisition. Soaking the electrodes to reduce the contact resistance and ensuring they are properly connected to the cable takeouts requires the most time. Once all of the electrodes are connected and soaked it takes several hours per array type to collect all combinations of current and voltage electrodes for a single spread. A significant amount of the time is for averaging the voltage signal to improve signal-to-noise. The same spread however can be used for multiple array types without making any physical changes to the cable layout.

Table 2. *Array type used over each case study target.*

TARGET	PROJECT	LINE	DD	DDx	ISCH	ISCHx	PD	SG	WENNER
CS-1	BREWERY CREEK	0-Gen	x						
		0-Bat	x		X				
		100	x		X			x	
CS-2	DUBLIN GULCH	35		x	X			x	
		50		x	X			x	
CS-3	FLAME/MOTH	102	x		X			x	
CS-4	KLAZA	10-50		x	X			x	
		10-600		x	X			x	
CS-5	CHARLOTTE	50		x	X		x	x	x
		200		x	X			x	
CS-6	COFFEE	Latte		x		x	x(2)		
		Supremo				x	x(2)		
CS-7	VG ZONE	03		x		x	x	x	
CS-8	GOLDEN SADDLE	01		x		x	x(3)		
CS-9	WILLIAMS CREEK	01	x	x	X			x	

0-Gen = line 0 with generator source, 0-Bat = line 0 with battery source, All other lines used battery source. The x after the array type means the enhanced version (DD dipole-dipole, ISCH inverse Schlumberger, PD pole-dipole, SG strong gradient, WEN = Wenner).

DATA PROCESSION AND INVERSION

Once the data are collected they can be transferred to the AGI EarthImager software (or any other standard 2D resistivity/IP inversion program such as res2dInv, Loke and Barker 1996a,b). These programs provide editing options to remove noisy or unwanted data points before inverting the 2D apparent resistivity data. The Earthimager two-dimensional (2D) inversion software computes the best fit 2D electrical model of the subsurface to the apparent resistivity data using an iterative process for a given trial. Each trial allows the user to remove a certain amount of noisy data from the resistivity and/or chargeability data. The root mean square (RMS) error is computed after each iteration and the iterations continues until the maximum number of iterations selected is reached or the RMS error is less than the value set by the user. Once the best fit resistivity model has been computed a one iteration inversion of the apparent IP data is carried out to produce a best fit two-dimensional IP model of the subsurface. If no IP data were collected the Earthimager software only carries out resistivity inversion.

There are more details in the Earthimager operating manual on how the software works for those who are interested. In addition the following references provide additional information on the algorithms used to carry out 2D resistivity/IP forward and inverse modelling: Constable *et al.*, 1987; Dey and Morrison, 1979; Loke and Barker, 1996a,b; Oldenburg and Li, 1994; Stummer *et al.*, 2004; Wannamaker, 1992; and Ward, 1990a,b,c.

The final resistivity and chargeability inversions were output as xyz files so they could be manipulated using Geosoft, thus allowing more control over the use of colour bars and other parameters. The final Geosoft plots were output as jpeg bit map files so that drillhole and geological information could easily be placed as an overlay using Coral Draw.

Once the final best fit resistivity and IP models are obtained the 2D resistivity and IP cross sections can be interpreted in terms of geological models of the earth. This requires knowledge of the relationship between resistivity, chargeability, and geology (rocks and minerals). Although the model assumes the geology is two-dimensional there may be 3D effects as well. This process of interpreting the data in terms of realistic geological models is when the input from a knowledgeable interpreter is required.

The final plots produced for each case study are 1) plots of resistivity and chargeability (paired plots) labelled with case study name, array type, and any other additional information required but without any interpretation and 2) plots of resistivity (chargeability) with borehole information (geology and mineralization) plus a section beneath the image for comments on interpretation.

PRESENTATION OF CASE STUDY SURVEYS

The final data for each case study is presented in the following sections. Each case study section explains the geological setting, geophysical data acquisition, and the geophysical results. In addition a plan map showing the surface geology and the location of the geophysical line(s) is included. Paired plots of inverted resistivity and IP are provided for every array used (line by line - see Table 2) for each case study as well as a selection of individual plots of inverted resistivity (or IP) with drillhole and geology information. Only a subset of these sections are included because the paired plots contain all the inverted geophysical sections. The reader can therefore use the paired plots, along with these sections, to extrapolate to other paired plot arrays not presented with drillhole information.

CS-1 BREWERY CREEK

Final Inversions and Interpretation

Geological setting

The Brewery Creek project is located off the Dempster Highway approximately 60 km east of Dawson City. It is situated on the western edge of the epicratonic Selwyn basin, just north of the Tintina fault. Selwyn basin stratigraphy, described by Gordey and Makepeace (2003) and Gustavson Associates (2013), consists of late Proterozoic to Paleozoic marginal basinal and platformal clastic and pelitic sediments derived from the North American Craton. On the Brewery Creek property, calcareous phyllite of the Rabbitkettle Formation (Cambrian-Ordovician) are overlain by Road River Group volcanic rocks (Ordovician-Silurian), which in turn are overlain by siliciclastic rocks of the Earn Group (Lower Devonian). These rocks are imbricated by a series of NNE-directed thrust faults, and intruded by Cretaceous monzonite to quartz monzonite thrust-parallel sills and younger discordant stocks of the Tombstone plutonic suite.

The majority of the gold mineralization at the Brewery Creek project is hosted within sills of the Tombstone plutonic suite, with lower-grade mineralization in the younger stocks. The high resolution resistivity and IP survey was carried out over the Bohemian-Schooner zone at the eastern end of the property where a monzonite sill complex intrudes a section of siltstone and carbonaceous argillite (Figure CS1-1). Gold mineralization at Bohemian/Schooner occurs primarily in clay-altered quartz monzonite sills and subordinately in adjacent siltstone in the footwall of the sill. It occurs most commonly in association with strong argillic altered and locally silicified quartz monzonite plutons (Gustavson Associates, 2013).

Geophysical survey

Line CS1-LS-0 has lengths of 485 m for the dipole-dipole array and 415 m for the inverse Schlumberger array. Line CS1-100N is 415 m in length for all arrays. Data were collected twice for the dipole-dipole array along line CS1-LS-0 since this was the first line of the entire case study: once using the AGI generator and once using battery power. The battery proved to be more stable and provided data with a higher signal-to-noise ratio than the generator. Consequently data for all case studies were collected using battery power for the transmitter. The surface geology of the Brewery Creek survey, locations of the two lines, and a photo of the area are shown in the figures below. The next set of figures are plots of the final inverted resistivity and IP for both lines, dipole-dipole and inverse Schlumberger arrays for line CS1-LS-0 and dipole-dipole, inverse Schlumberger and strong gradient for line CS1-100N. In general the data for Brewery Creek has a reasonable signal-to-noise ratio. The average RMS error of fit is approximately 6% which is quite good.

Geophysical interpretation

The figures below provide borehole geology and mineralization overlain on selected inverted resistivity and IP sections for the two lines. Not all arrays are provided; however the reader can use the paired plots if they wish to investigate other arrays.

Dipole-dipole inversion of resistivity and chargeability with borehole geology and mineralization overlain are shown below for line CS1-100N. The black curve is an example showing one location of the contact between the monzonite sill and sediments using the inverted resistivity. Note the contact does not appear to be as well defined in the IP section. The mineralization is located at the monzonite-sediment contact. The low resistivity zones are associated with the sediments and the higher values (not at the surface where there is permafrost) are associated with the monzonite sills. Similar results, although more diffuse, can be seen on the inverse Schlumberger and strong gradient inverted resistivity and IP sections.

Inversion results for dipole-dipole resistivity and inverse Schlumberger resistivity and IP with borehole geology and mineralization overlain for line CS1-100N are given below. The top of the monzonite sill shows up clearly on both the dipole-dipole and inverse Schlumberger resistivity sections, although there is an area at hole BC12-423 where the inverse Schlumberger matches the borehole geology and mineralization better. The dipole-dipole resistivity section has a large low resistivity zone where one might expect monzonite based on the drilling results (near the west end). The inverse Schlumberger and dipole-dipole IP sections are significantly different from each other and neither one match borehole chargeability data. There is more detail in the dipole-dipole section near the west end but that may be artifacts.

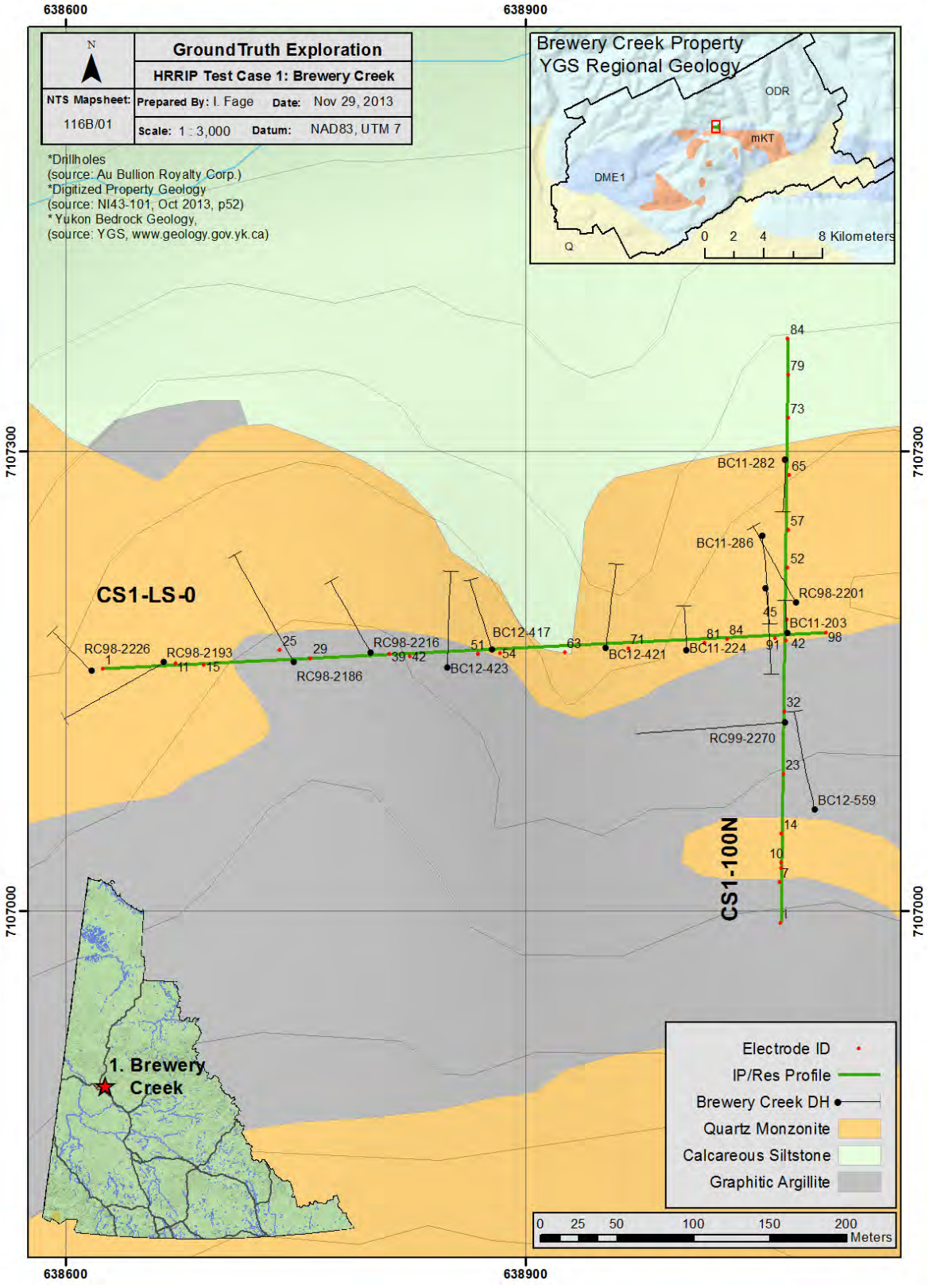

Figure CS1-1. *Location of geophysical survey lines and surface geology for Brewery Creek.*

Figure CS1-2. *Survey Location at CS-1, Brewery Creek Property.*

Figure CS1-3. *Crew examining Graphitic Argillite at Brewery Creek Property.*

PAIRED PLOTS

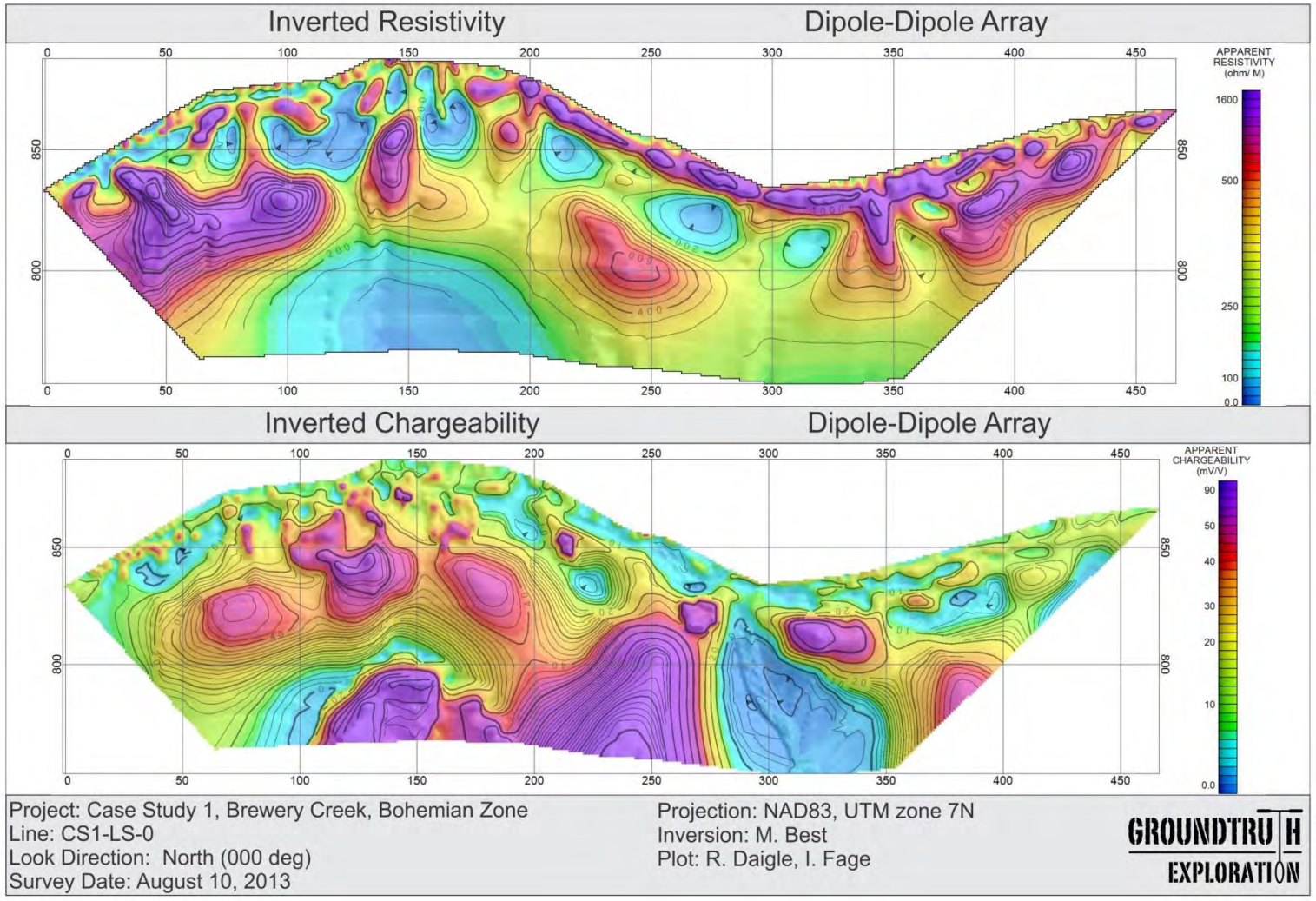

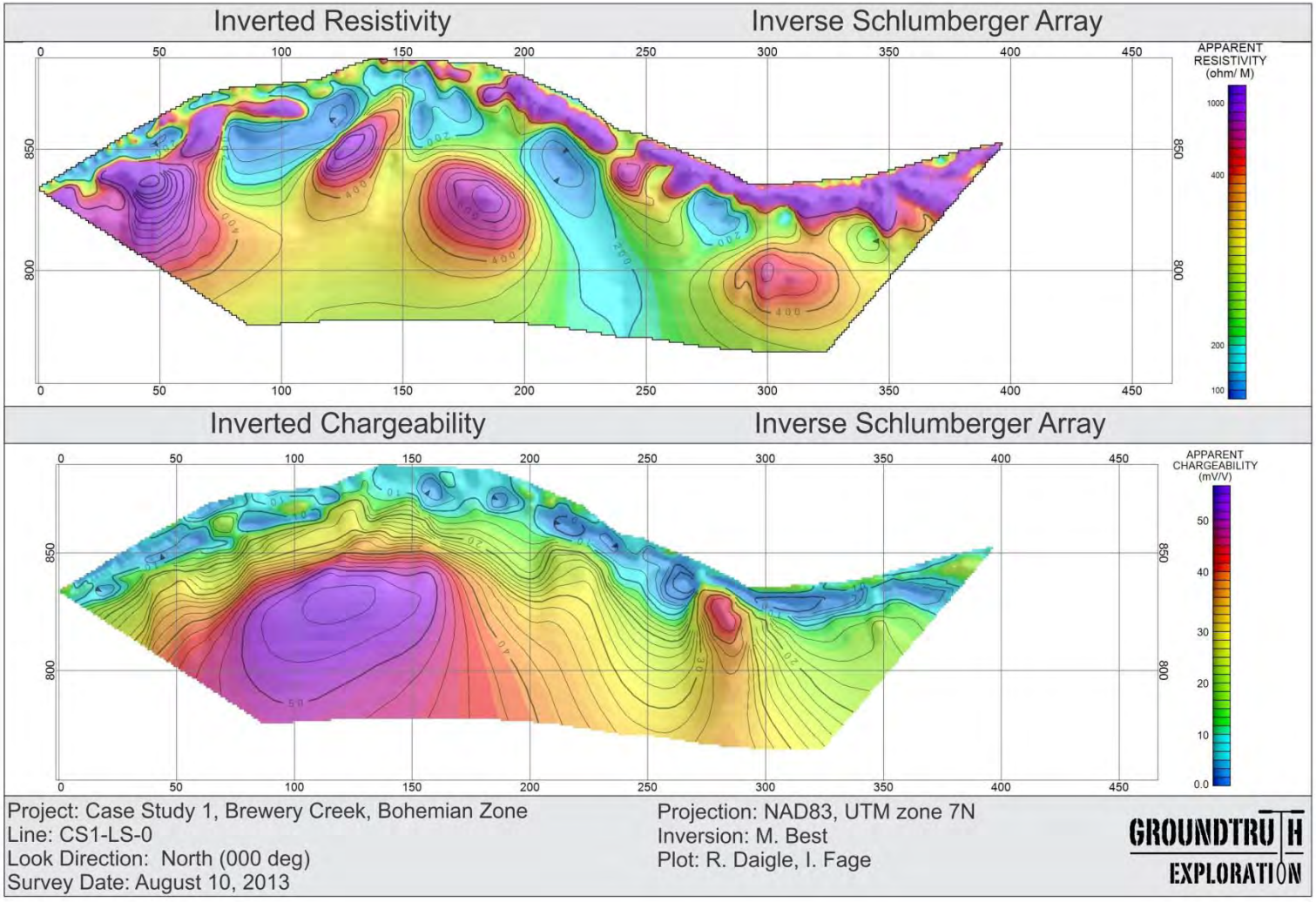
Inverted Resistivity
Inverse Schlumberger Array
APPARENT RESISTIVITY (ohm/ M)
1000
400
200
100
Inverted Chargeability
Inverse Schlumberger Array
APPARENT CHARGEABILITY (mV/V)
50
40
30
20
10
0.0
Project: Case Study 1, Brewery Creek, Bohemian Zone
Line: CS1-LS-0
Look Direction: North (000 deg)
Survey Date: August 10, 2013
Projection: NAD83, UTM zone 7N
Inversion: M. Best
Plot: R. Daigle, I. Fage
GROUNDTRUTH EXPLORATION

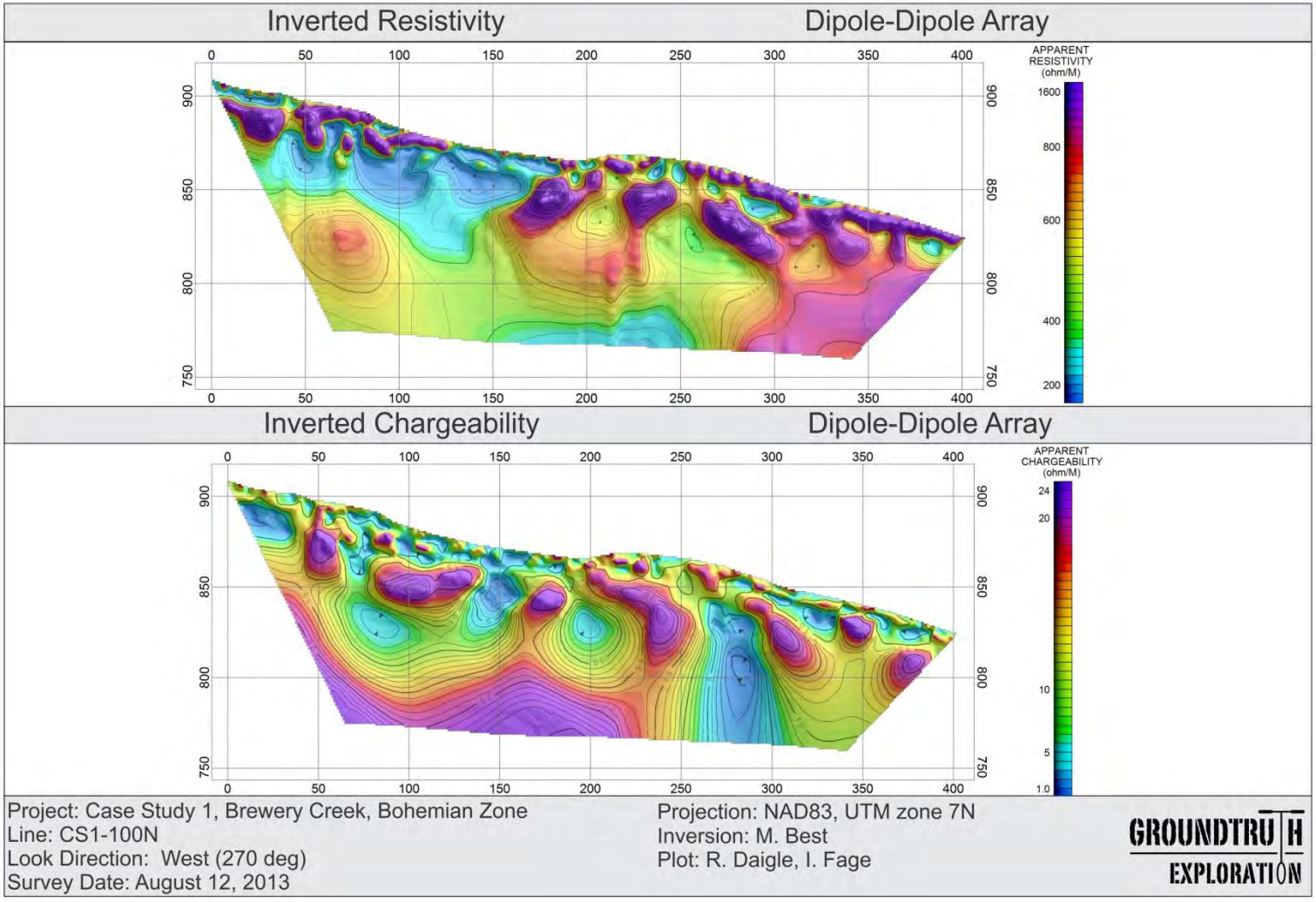
Inverted Resistivity
Dipole-Dipole Array
APPARENT RESISTIVITY (ohm/M)
1600
800
600
400
200
Inverted Chargeability
Dipole-Dipole Array
APPARENT CHARGEABILITY (ohm/M)
24
20
10
5
1.0
0
50
100
150
200
250
300
350
400
900
850
800
750
Project: Case Study 1, Brewery Creek, Bohemian Zone
Line: CS1-100N
Look Direction: West (270 deg)
Survey Date: August 12, 2013
Projection: NAD83, UTM zone 7N
Inversion: M. Best
Plot: R. Daigle, I. Fage
GROUNDTRUTH EXPLORATION

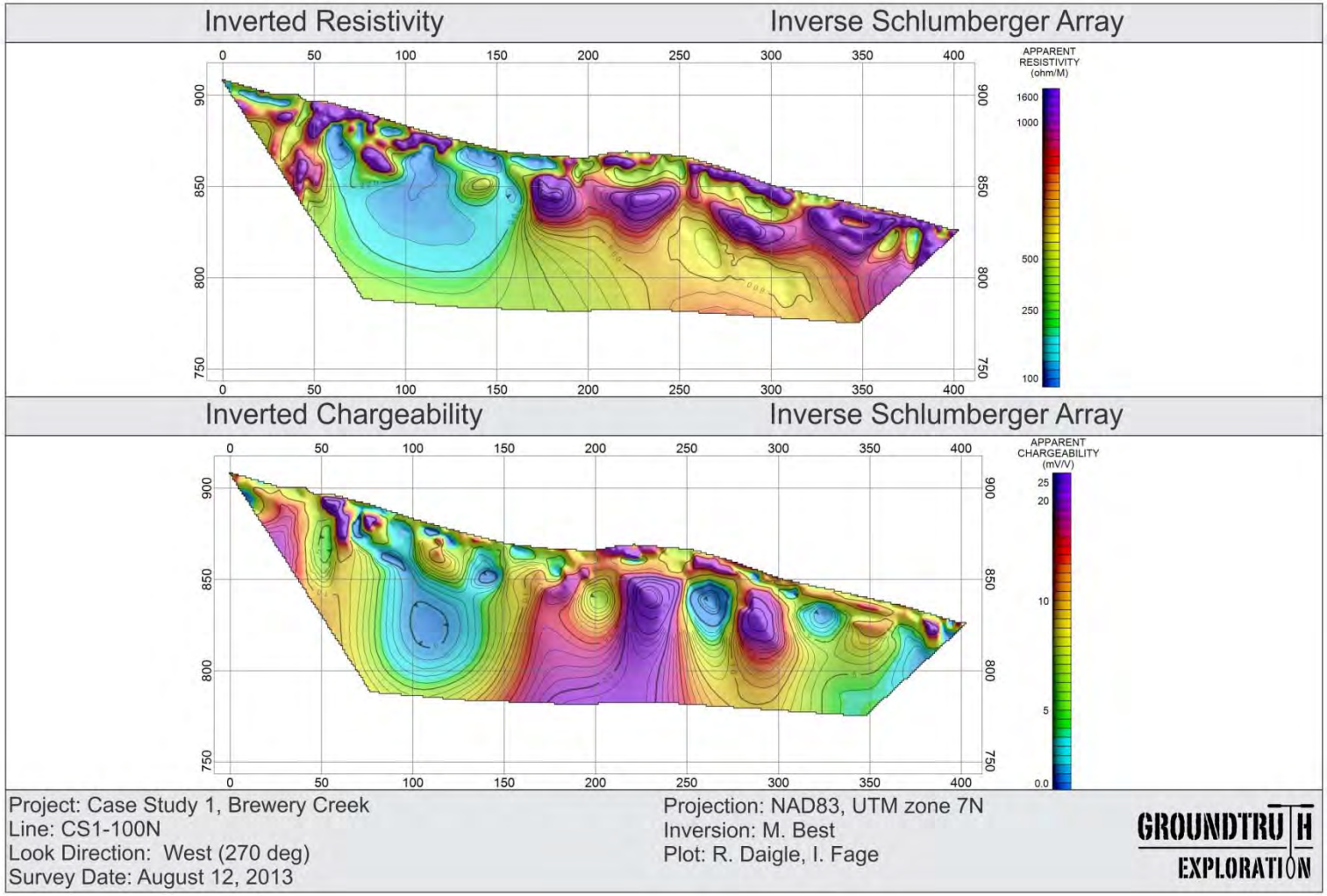
Inverted Resistivity
Inverse Schlumberger Array
APPARENT RESISTIVITY (ohm/M)
1600
1000
500
250
100
Inverted Chargeability
Inverse Schlumberger Array
APPARENT CHARGEABILITY (mV/V)
25
20
10
5
0.0
0
50
100
150
200
250
300
350
400
900
850
800
750
Project: Case Study 1, Brewery Creek
Line: CS1-100N
Look Direction: West (270 deg)
Survey Date: August 12, 2013
Projection: NAD83, UTM zone 7N
Inversion: M. Best
Plot: R. Daigle, I. Fage
GROUNDTRUTH EXPLORATION

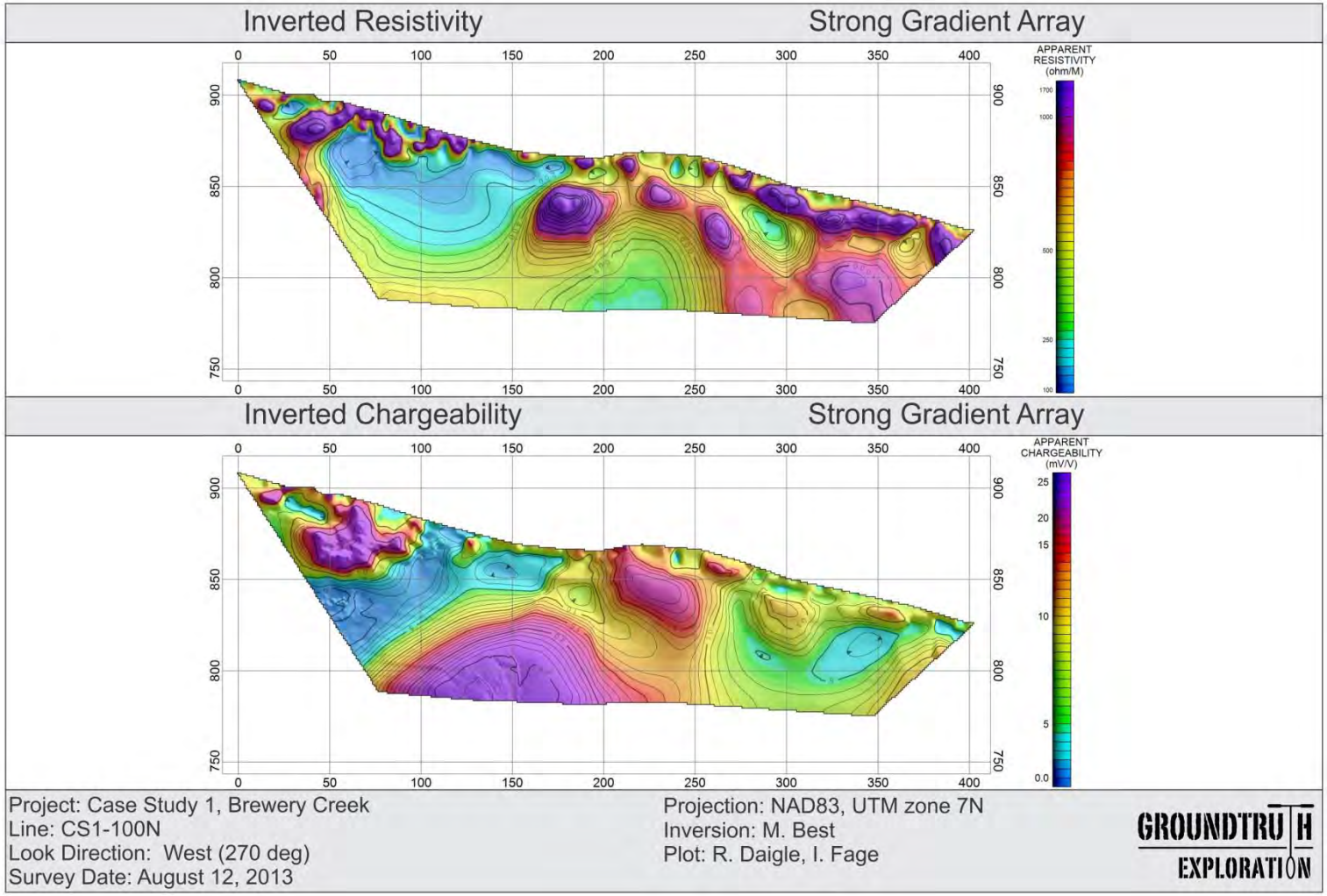
Inverted Resistivity
Strong Gradient Array
APPARENT RESISTIVITY (ohm/M)
1700
1000
500
250
100
Inverted Chargeability
Strong Gradient Array
APPARENT CHARGEABILITY (mV/V)
25
20
15
10
5
0.0
0
50
100
150
200
250
300
350
400
750
800
850
900
Project: Case Study 1, Brewery Creek
Line: CS1-100N
Look Direction: West (270 deg)
Survey Date: August 12, 2013
Projection: NAD83, UTM zone 7N
Inversion: M. Best
Plot: R. Daigle, I. Fage
GROUNDTRUTH EXPLORATION

INTERPRETATION

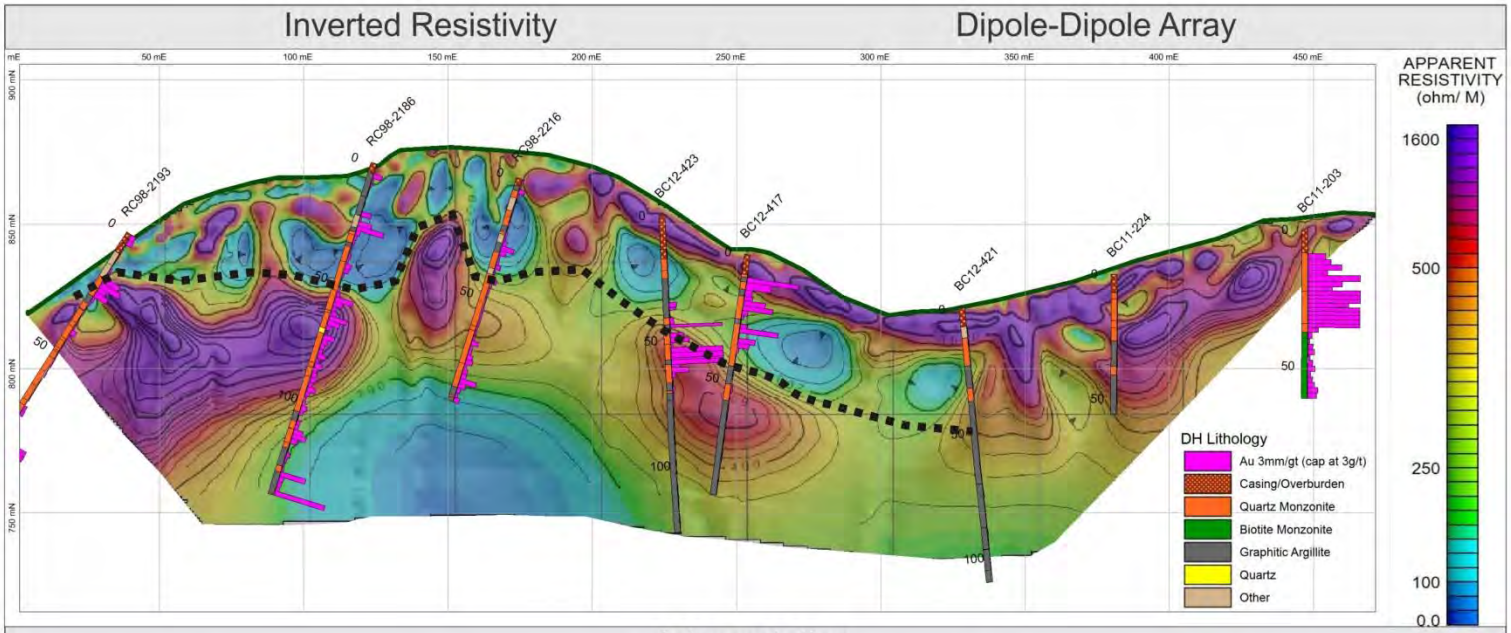

Interpretation

- o mineralization associated with monzonite or near contact with graphitic sediments
- o graphitic argillite has low resistivity values as expected
- o monzonite sills show up as resistivity highs
- o hole 2186 upper section shows monzonite from borehole but has low resistivity, however mineralization at contact
- o dashed black line shows potential location of top of sill
- o inverse Schlumberger resistivity section near hole 423 better represents borehole geology

Project: Case Study 1, Brewery Creek, Bohemian Zone	Projection: NAD83, UTM zone 7N
Line: CS1-LS-0	Scale: 1 : 2,000
Look Direction: North (000 deg)	Inversion: M. Best
Survey Date: August 10, 2013	Plot: R. Daigle, I. Fage

GROUNDTRUTH EXPLORATION

Inverted Resistivity

Inverse Schlumberger Array

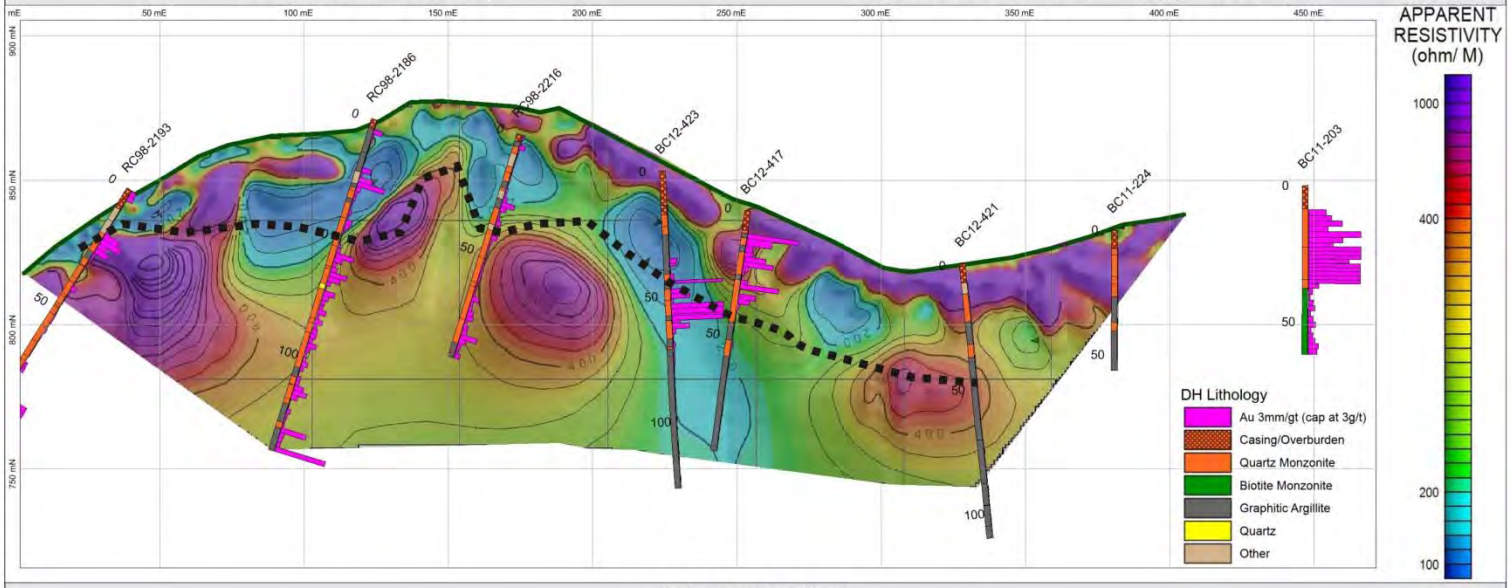

Interpretation

o top of sill location similar to dipole-dipoloe except near hole 423

o at hole 423 monzonite zone missed by inversion - probably too small

Project: Case Study 1, Brewery Creek, Bohemian Zone
Line: CS1-LS-0
Look Direction: North (000 deg)
Survey Date: August 10, 2013

Projection: NAD83, UTM zone 7N
Scale: 1 : 2,000
Inversion: M. Best
Plot: R. Daigle, I. Fage

GROUNDTRUTH EXPLORATION

Inverted Chargeability

Inverse Schlumberger Array

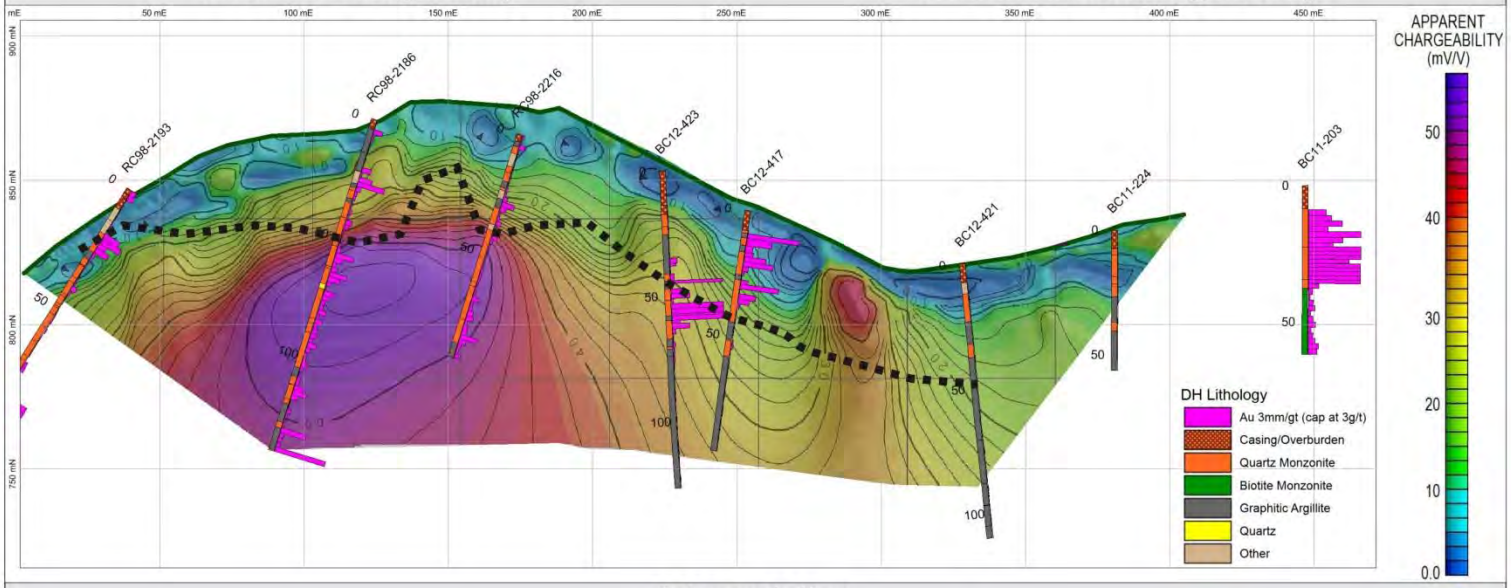

Interpretation

- o west end of line shows high chargeability below contact from resistivity section
- o chargeability does not corelate with mineralization on this and dipole dipole IP sections
- o more detail on dipole dipole IP section but could be artifacts

Project: Case Study 1, Brewery Creek, Bohemian Zone
Line: CS1-LS-0
Look Direction: North (000 deg)
Survey Date: August 10, 2013

Projection: NAD83, UTM zone 7N
Scale: 1 : 2,000
Inversion: M. Best
Plot: R. Daigle, I. Fage

GROUNDTRUTH EXPLORATION

Inverted Resistivity — Dipole-Dipole Array

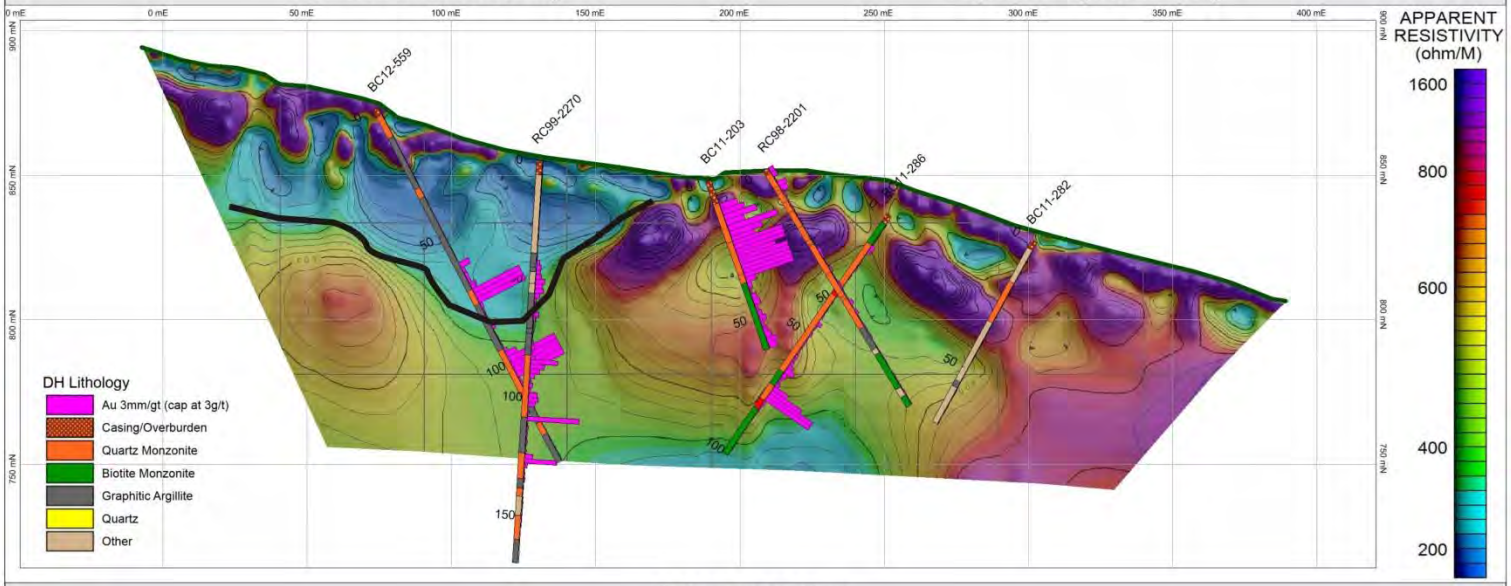

Interpretation

- o argillites and siltstones are associated with more conductive (lower resistivity) values.
- o intermittent near-surface (shallow) high resistivity values are patches of permafrost
- o mineralization is near contact between sediments and monzonite sills (example shown as black curve in figure)
- o the dip-dip array (resistivity) better defines the contact between sills and sediments (see paired plot figures for inverse Schlumberger and strong gradient)

Project: Case Study 1, Brewery Creek, Bohemian Zone
Line: CS1-100N
Look Direction: West (270 deg)
Survey Date: August 12, 2013

Projection: NAD83, UTM zone 7N
Scale: 1 : 2,000
Inversion: M. Best
Plot: R. Daigle, I. Fage

GROUNDTRUTH EXPLORATION

Inverted Chargeability — Dipole-Dipole Array

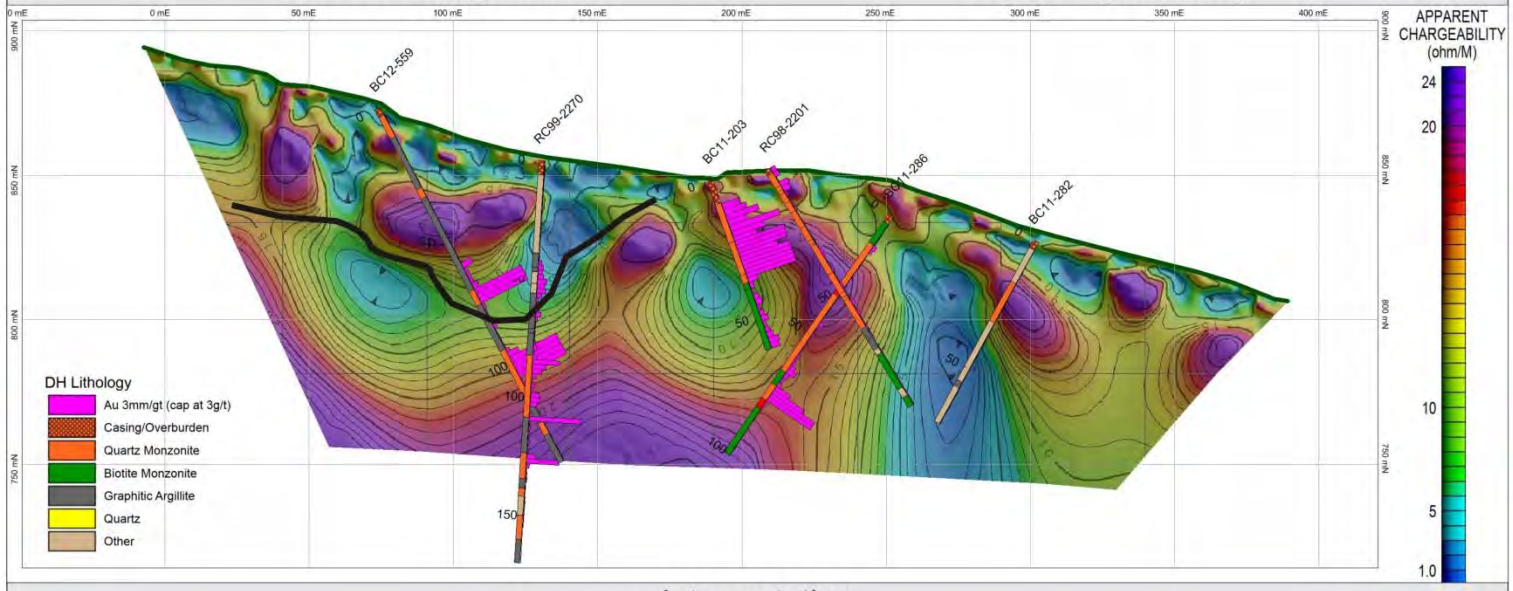

Interpretation

- o chargeability high associated with mineralization close to monzonite sediment contact
- o chargeability of deeper mineralization near south end of line shows up on strong gradient but not very well defined on inverse Schlumberger
- o mineralization near 200E shows up nicely on all three arrays
- o geology better mapped using resistivity on this line

Project: Case Study 1, Brewery Creek, Bohemian Zone
Line: CS1-100N
Look Direction: West (270 deg)
Survey Date: August 12, 2013

Projection: NAD83, UTM zone 7N
Scale: 1 : 2,000
Inversion: M. Best
Plot: R. Daigle, I. Fage

GROUNDTRUTH EXPLORATION

CS-2 DUBLIN GULCH

Final Inversions and Interpretation

Geological setting

The Dublin Gulch Eagle property is located in the northwestern Selwyn basin, approximately 50 km north of the village of Mayo. The region is underlain by deformed Upper Proterozoic to Lower Cambrian clastic rocks of the Hyland Group and intruded by a linear belt of middle Cretaceous intrusions comprising the Tombstone plutonic suite (Maloof *et al.*, 2001). The Dublin Gulch intrusion is part of this suite and consists of medium-grained granodiorite cut by minor late dikes. The Eagle zone is located in the southwestern part of the Dublin Gulch intrusion (see Fig. CS2-1). Gold occurs in a series of east-striking, steeply south-dipping sheeted veins that occur primarily within the intrusion but locally extend into the adjacent metasedimentary country rock. The veins consist of early quartz-scheelite-pyrrhotite-pyrite-arsenopyrite, and are associated with K-feldspar-albite alteration envelopes. These grade out to and are overprinted by sericite-carbonate-chlorite alteration. The same assemblage also occurs in veinlets that refracture sheeted quartz veins and contain the majority of the gold.

Geophysical survey

Two lines of HRRIP data were collected for the Dublin Gulch case study along Lines S35 and S50 (location map and photo below) with a length of 415 m, *i.e.*, a single spread length. The RMS error for the strong gradient arrays was 25.4% and 32.4% for lines S35 and S50 respectively. Line 50 was noisy on all three arrays (dipole-dipole extended, inverse Schlumberger and strong gradient) with the lowest RMS error of fit equal to 9.2 % for the dipole-dipole extended array. The inverse Schlumberger and dipole-dipole extended arrays for Line S35 however had RMS errors of fit less than 3.5%. The ground was very rough and contained rubble piles making it difficult to plant electrodes; consequently the contact resistance was high. The paired plots of resistivity and chargeability for most of the arrays on lines S35 and S50 are presented after the location map.

Geophysical interpretation

The figures below provide borehole geology and mineralization overlain on selected inverted resistivity and IP sections for the two lines. Not all arrays are provided; however the reader can use the paired plots if they wish to investigate other arrays.

The inverse Schlumberger interpreted resistivity and IP sections on line S35 are shown below. There is a resistivity low and a chargeability associated with the upper zone of mineralization near the centre of the section. The black lines outline the zones of mineralization within the section, although the majority of the mineralization occurs in the central part of the section. The drilling indicates that most of the mineralization is located deeper than the exploration depth of the HRRIP system. However the upper middle mineralized zone does correlate with the HHRIP inversions thus providing a drill target that would have intersect this zone. Individual fractures cannot be observed on the inversions but the low resistivity/high chargeability zone is likely the bulk effect of many fractures containing pyrite arsenopyrite and pyrrhotite. The dipole-dipole

extended array has high chargeability at both places outlined in black; however the resistivity section has lows in the same areas but not as well defined.

The interpreted inverse Schlumberger inverse resistivity array and the interpreted strong gradient chargeability array for line S50 are given below. The mineralization only occurs in the centre of the section on this lime and again only the upper zone has been mapped with the HRRIP system. The upper mineralized zone is at the contact between low and high resistivity values for the inverse Schlumberger and strong gradient arrays but the dipole-dipole extended array has a resistivity low at the same place. The strong gradient and inverse Schlumberger arrays have a chargeability high associated with the upper mineralized zone but the dipole-dipole extended array has a chargeability low.

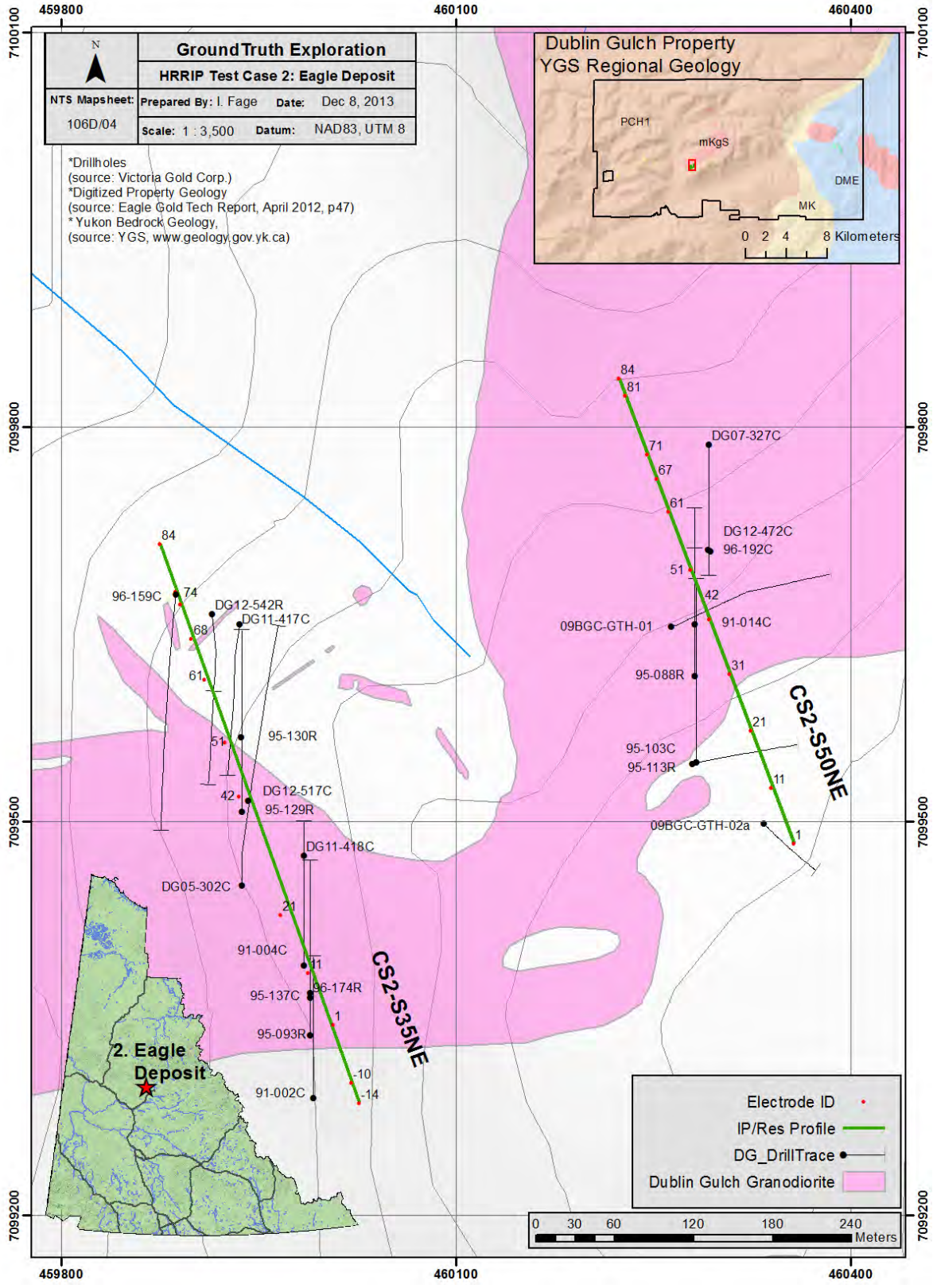

Figure CS2-1. *Location of geophysical survey lines and surface geology for Eagle Deposit.*

Figure CS2-2. *Survey Landscape at CS-2, Dublin Gulch Property.*

Figure CS2-3. *Sheeted Veins at CS-2, Dublin Gulch Property.*

PAIRED PLOTS

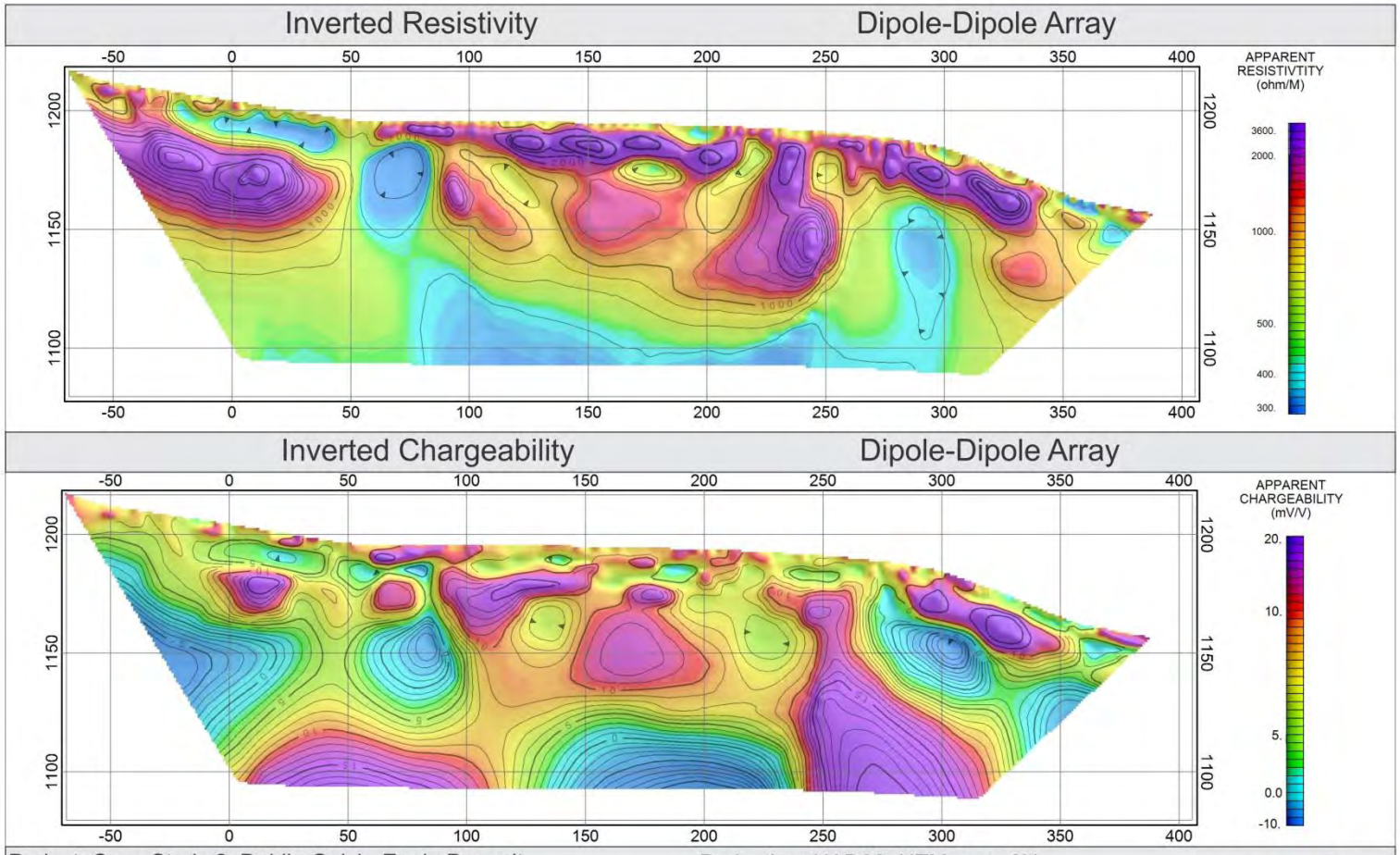

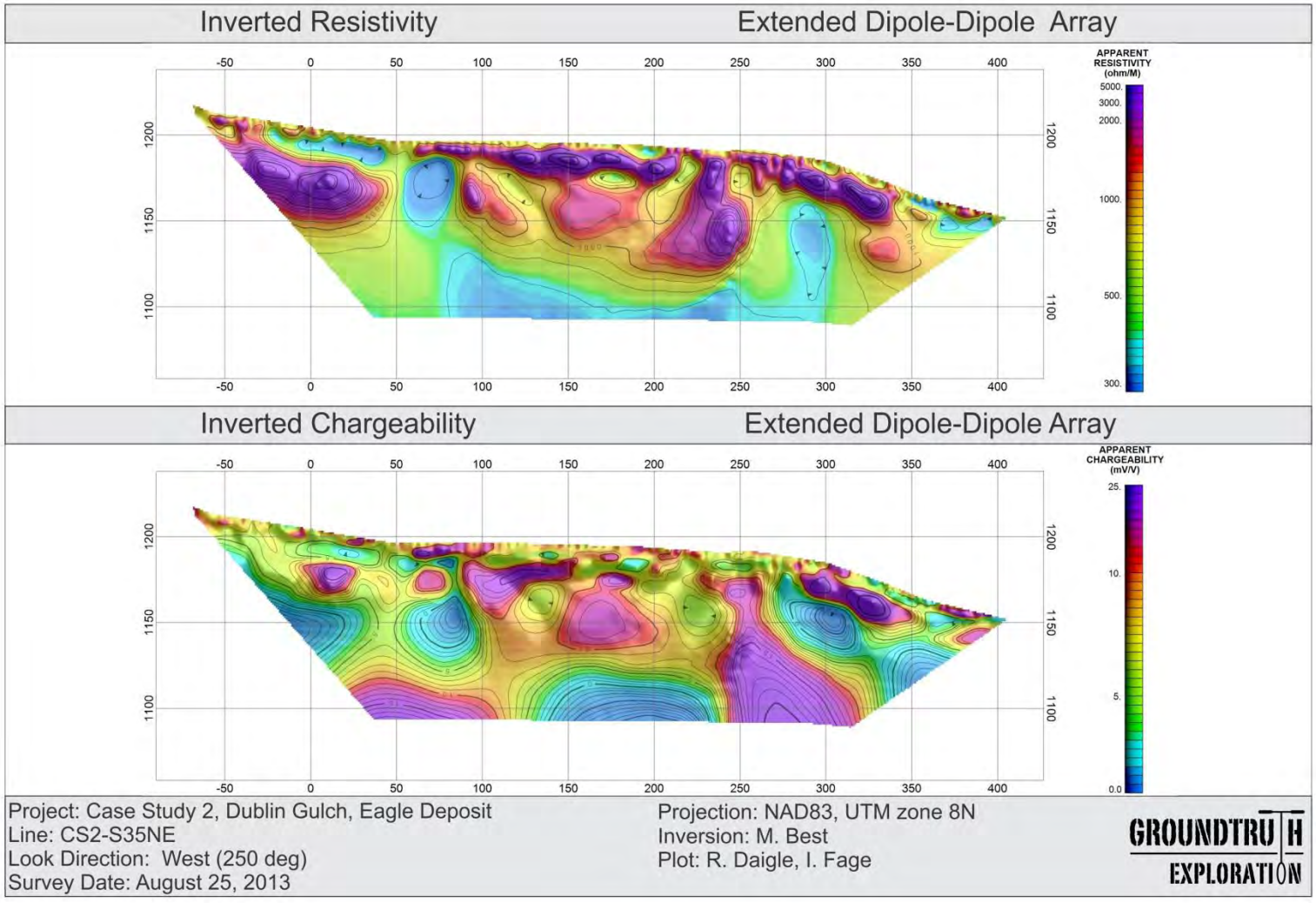
Inverted Resistivity
Extended Dipole-Dipole Array
APPARENT RESISTIVITY (ohm/M)
5000.
3000.
2000.
1000.
500.
300.
-50 0 50 100 150 200 250 300 350 400
1200
1150
1100
Inverted Chargeability
Extended Dipole-Dipole Array
APPARENT CHARGEABILITY (mV/V)
25.
10.
5.
0.0
Project: Case Study 2, Dublin Gulch, Eagle Deposit
Line: CS2-S35NE
Look Direction: West (250 deg)
Survey Date: August 25, 2013
Projection: NAD83, UTM zone 8N
Inversion: M. Best
Plot: R. Daigle, I. Fage
GROUNDTRUTH EXPLORATION

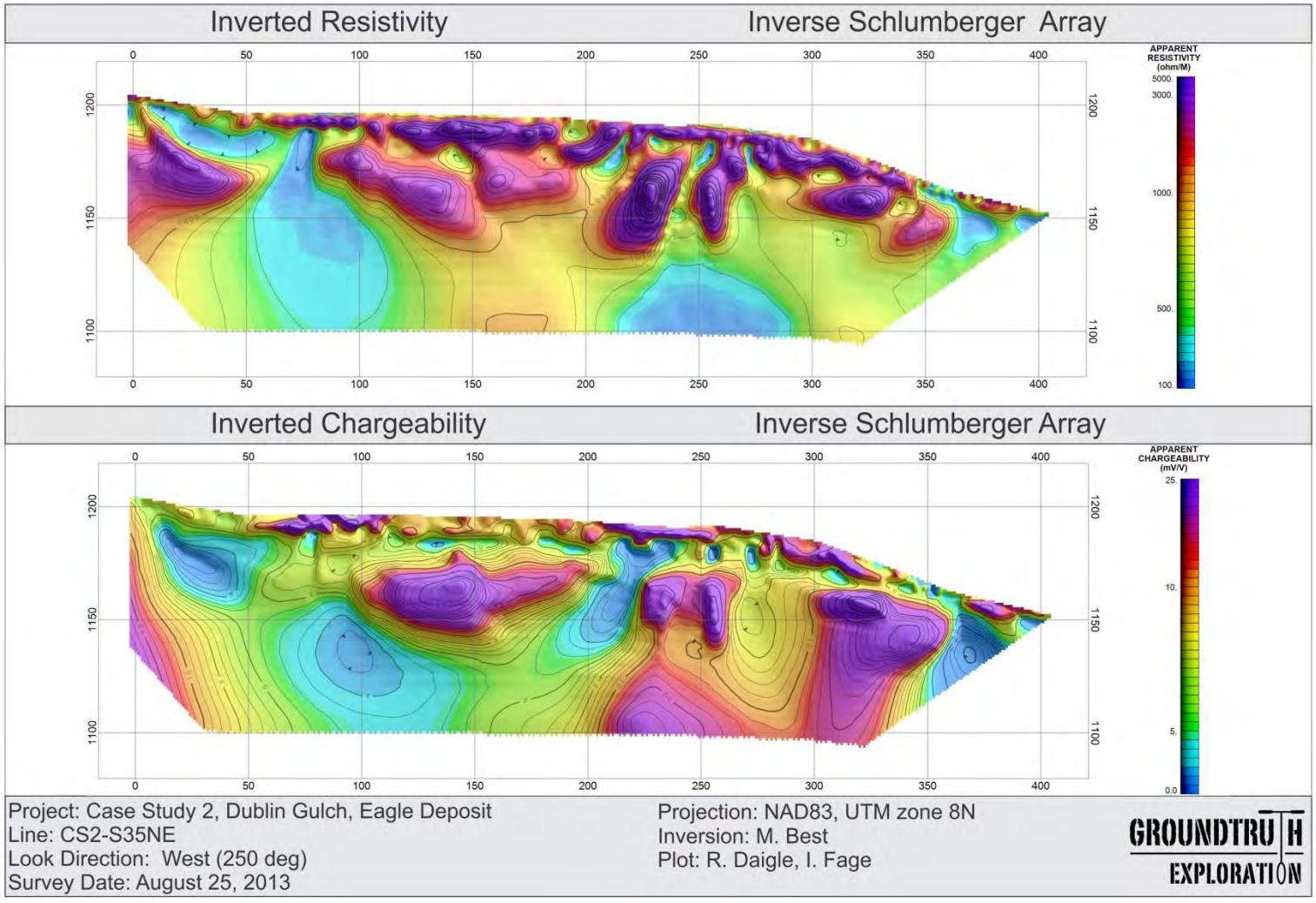
Inverted Resistivity
Inverse Schlumberger Array
APPARENT RESISTIVITY (ohm/M)
5000.
3000.
1000.
500.
100.
Inverted Chargeability
Inverse Schlumberger Array
APPARENT CHARGEABILITY (mV/V)
25.
10.
5.
0.0
0
50
100
150
200
250
300
350
400
1200
1150
1100
Project: Case Study 2, Dublin Gulch, Eagle Deposit
Line: CS2-S35NE
Look Direction: West (250 deg)
Survey Date: August 25, 2013
Projection: NAD83, UTM zone 8N
Inversion: M. Best
Plot: R. Daigle, I. Fage
GROUNDTRUTH EXPLORATION

Inverted Resistivity — Extended Dipole-Dipole Array

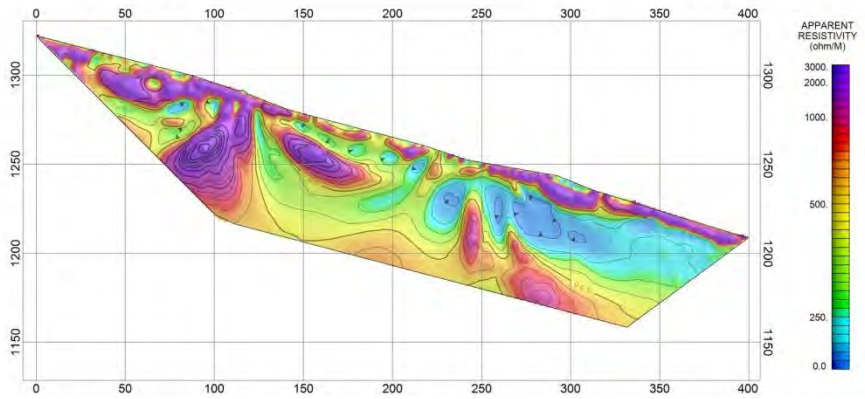

Inverted Chargeability — Extended Dipole-Dipole Array

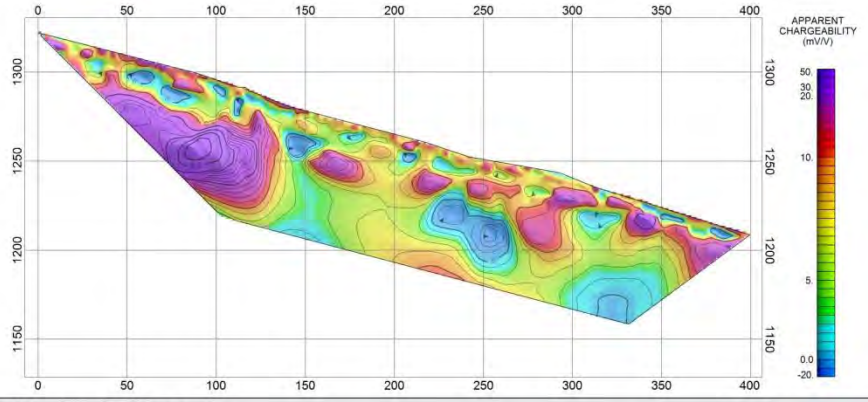

Project: Case Study 2, Dublin Gulch, Eagle Deposit
Line: CS2-S50NE
Look Direction: West (250 deg)
Survey Date: August 26, 2013

GROUNDTRUTH EXPLORATION

Inverted Resistivity — Inverse Schlumberger Array

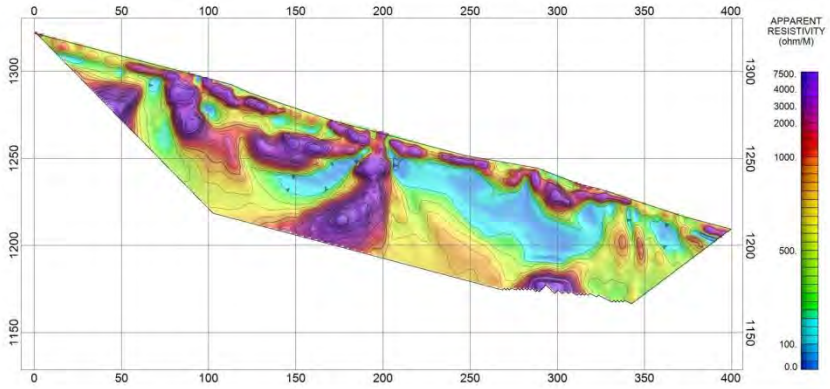

Inverted Chargeability — Inverse Schlumberger Array

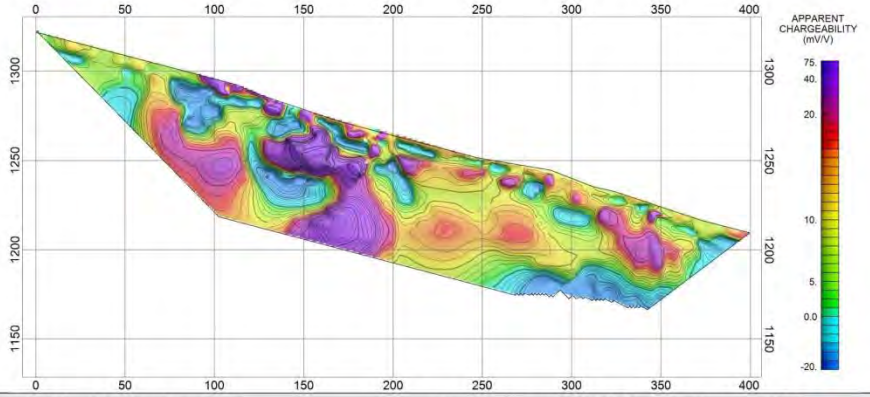

Project: Case Study 2, Dublin Gulch, Eagle Deposit
Line: CS2-S50NE
Look Direction: West (250 deg)
Survey Date: August 26, 2013

Projection: NAD83, UTM zone 8N
Inversion: M. Best
Plot: R. Daigle, I. Fage

GROUNDTRUTH EXPLORATION

Inverted Resistivity — Strong Gradient Array

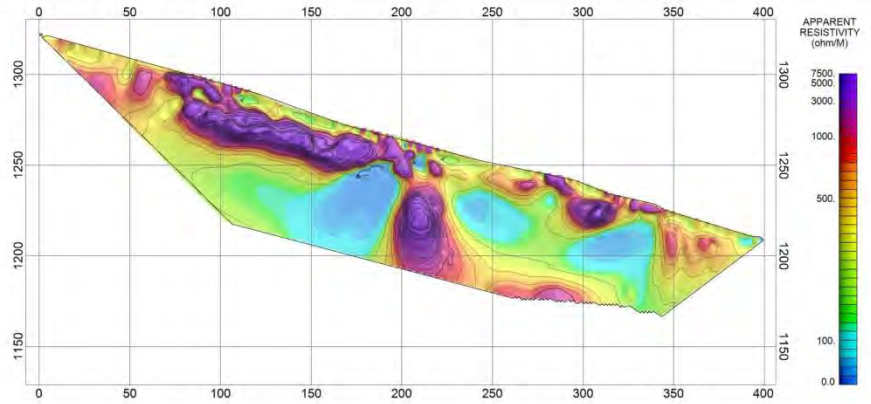

Inverted Chargeability — Strong Gradient Array

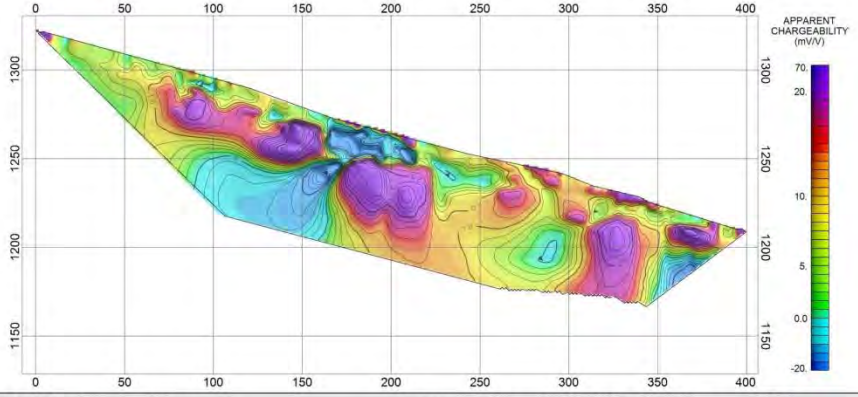

Project: Case Study 2, Dublin Gulch, Eagle Deposit
Line: CS2-S50NE
Look Direction: West (250 deg)
Survey Date: August 26, 2013

Projection: NAD83, UTM zone 8N
Inversion: M. Best
Plot: R. Daigle, I. Fage

GROUNDTRUTH EXPLORATION

INTERPRETATION

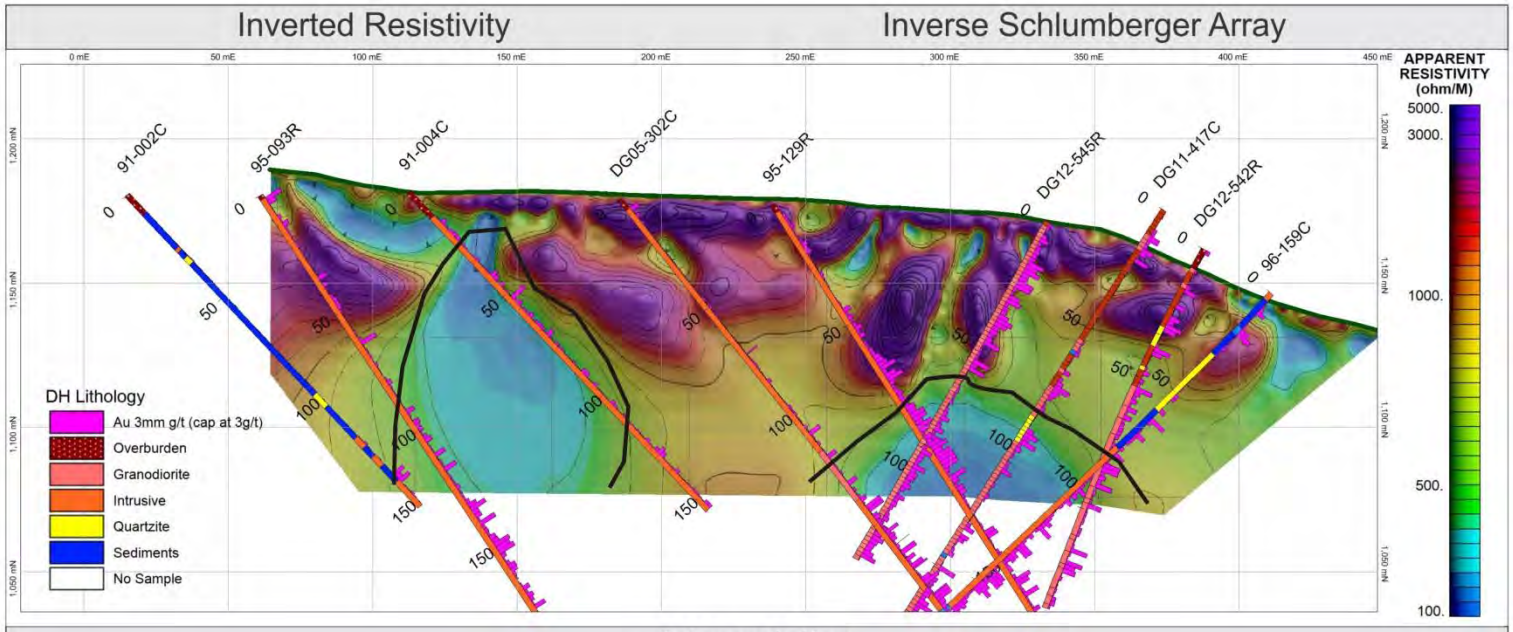

Interpretation

- o majority of mineralization below depth of HRRIP resolution (also for dipole-dipole extended)
- o shallow mineralization is within resistivity low (or at edge) that appears to extend to depth
- o resistivity low may be associated with pyrite and pyrrhotite arsenopyrite zones
- o black outlines encompass most of shallow mineralization
- o dipole-dipole extended resistiviy section has same low areas but not as well defined

Project: Case Study 2, Dublin Gulch, Eagle Deposit	Projection: NAD83, UTM zone 8N
Line: CS2-S35NE	Scale: 1 : 2,000
Look Direction: West (250 deg)	Inversion: M. Best
Survey Date: August 25, 2013	Plot: R. Daigle, I. Fage

GROUNDTRUTH EXPLORATION

Inverted Chargeability — Inverse Schlumberger Array

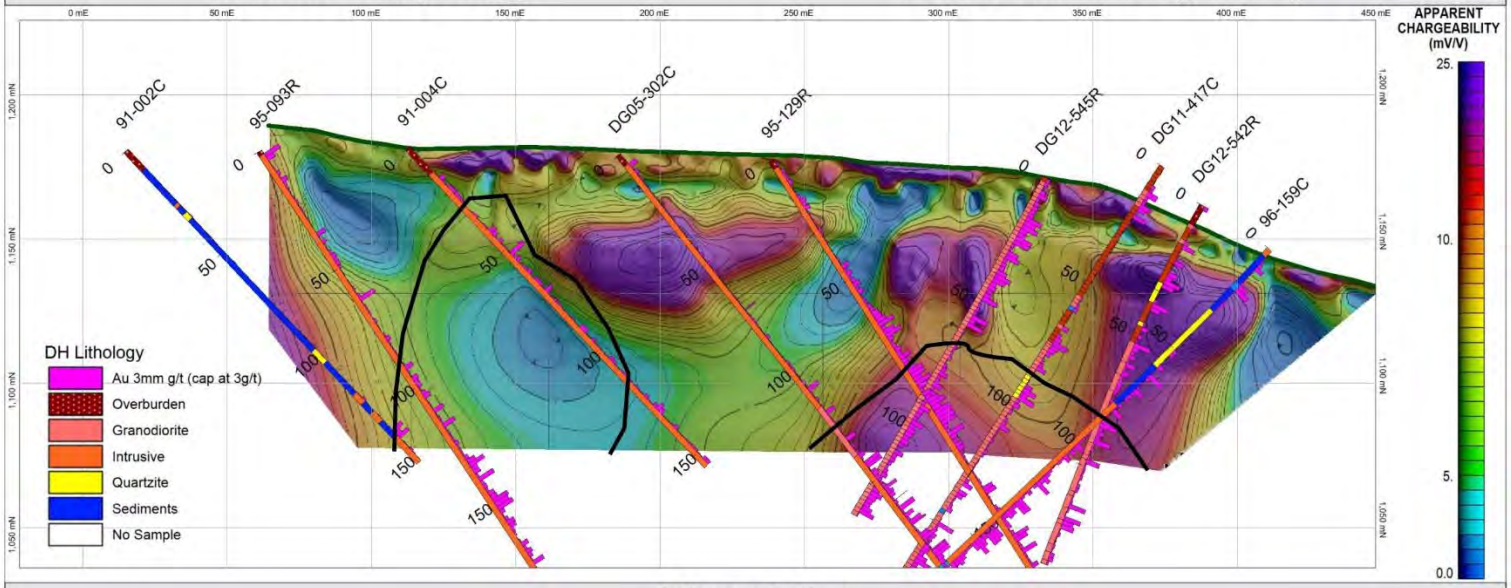

Interpretation

- o south end of line mineralization is in chargeability low
- o north end of line has chargeability high associated with resistivity low and mineralization
- o dipole-dipole IP has high chargeability at both ends of line (where mineralization occurs)
- o even though mineralization deeper than depth resolution of HRRIP system upper portion was mapped providing drill target

Project: Case Study 2, Dublin Gulch, Eagle Deposit
Line: CS2-S35NE
Look Direction: West (250 deg)
Survey Date: August 25, 2013

Projection: NAD83, UTM zone 8N
Scale: 1 : 2,000
Inversion: M. Best
Plot: R. Daigle, I. Fage

GROUNDTRUTH EXPLORATION

Inverted Resistivity

Inverse Schlumberger Array

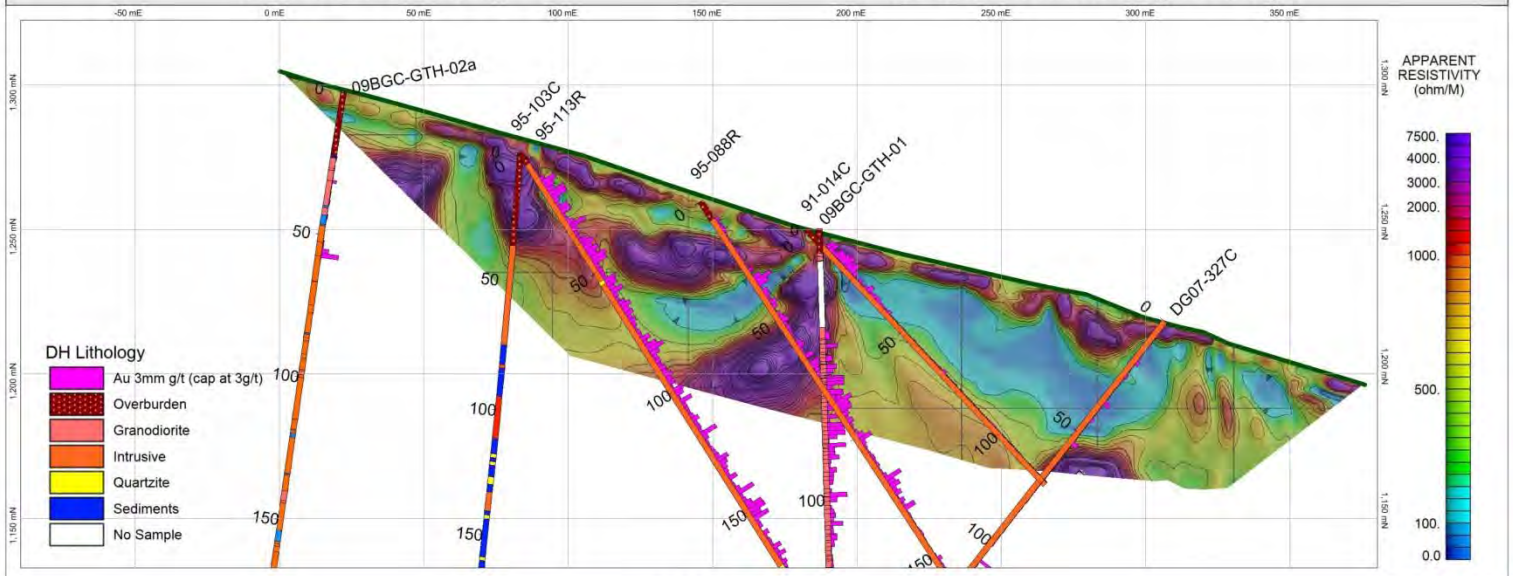

Interpretation

- o upper zone of mineralization (centre) is at contact between high and low resistivity zones.
- o strong gradient inverse resistivity similar to inverse Schlumbeger
- o dipole-dipole extended inverse resistivity array has resistivity low in same place (perhaps maps mineralized zone more effectively?)

Project: Case Study 2, Dublin Gulch, Eagle Deposit
Line: CS2-S50NE
Look Direction: West (250 deg)
Survey Date: August 26, 2013

Projection: NAD83, UTM zone 8N
Scale: 1 : 2,000
Inversion: M. Best
Plot: R. Daigle, I. Fage

GROUNDTRUTH EXPLORATION

Inverted Chargeability — Strong Gradient Array

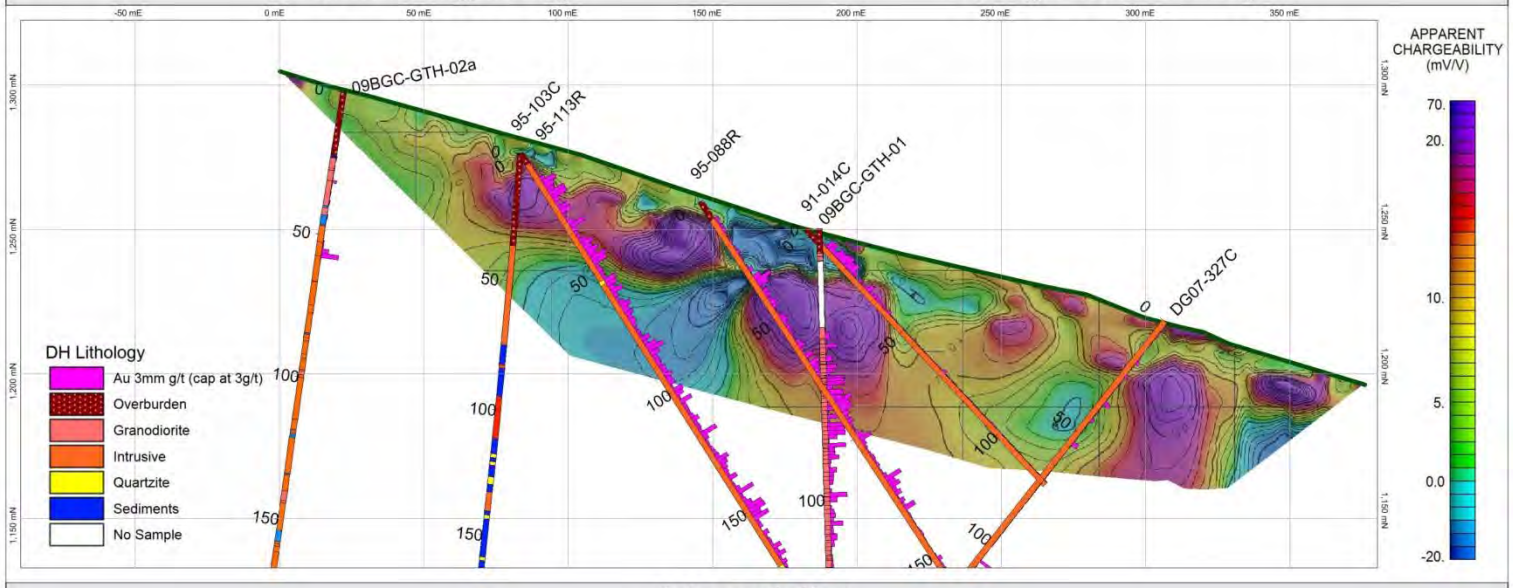

Interpretation

- o chargeability high in upper mineralized zone (centre of figure)
- o chargeability low in same place for dipole-dipole extended inverse IP array
- o inverse Schlumberger inverted IP array at same location is at contact between high and low chargeability values

Project: Case Study 2, Dublin Gulch, Eagle Deposit
Line: CS2-S50NE
Look Direction: West (250 deg)
Survey Date: August 26, 2013

Projection: NAD83, UTM zone 8N
Scale: 1 : 2,000
Inversion: M. Best
Plot: R. Daigle, I. Fage

GROUNDTRUTH EXPLORATION

CS-3 FLAME & MOTH DEPOSIT

Final Inversions and Interpretation

Geological setting

The Keno Hill mining camp is located in the northwestern part of the Selwyn basin. It is bounded to the south by the Robert Service thrust, and to the north by the Tombstone thrust. The Keno Hill Ag-Pb-Zn deposits, which sit in the hanging wall of the Tombstone thrust, are hosted by a thick Mississippian quartzite unit and underlain by Devonian phyllite, felsic meta-tuffs, and metaclastic rocks of Earn Group. To the south, the Robert Service thrust has emplaced Late Proterozoic to Early Cambrian siliciclastic rocks of the Hyland Group northward and structurally above the Keno Hill Quartzite. The quartzite is locally thickened due to folding and/or thrusting and hosts the silver-lead-zinc mineralization of the Keno Hill camp (Farrow and McOnie, 2013).

Much of the Flame & Moth area is blanketed by a thick cover of fluvioglacial overburden deposited on an irregular erosional surface that is in places up to 50 m thick. The mineralization occurs within the upper section of the Basal Quartzite Member of the Keno Hill Quartzite. The host rocks predominantly comprise medium to thick bedded quartzite with interbedded graphitic schist (Fig. CS3-1). The mineralized sequence is overlain by the Upper Quartzite, Sericite Schist, and Graphitic Schist marker units of the Sourdough Hill Member. The sequence generally strikes to the east to east-southeast and dips moderately to the southwest. The Flame and Moth zones consists of a north-northeast striking vein containing polymetallic silver-lead-zinc mineralization.

Geophysical survey

Data from three arrays were collected for line CS3-S102, length equal to 415 m (single spread length). The arrays were dipole-dipole, inverse Schlumberger, and strong gradient. The average RMS error of fit is 14.1 % with the highest being 19.1 % for the inverse Schlumberger. This was a difficult line because there was active drilling nearby during acquisition (see location map and photo below). At one point drilling fluid shorted out several electrodes during acquisition. The paired plots for all three arrays are presented below after the location map.

Geophysical interpretation

The Pb-Zn-Ag mineralization occurs in narrow, steeply dipping veins making this a difficult target for HRRIP methods. The black curve shown on the interpreted sections outlines an area with low to moderate resistivity which is mapped mostly as quartzite with several narrow zones of sericite and graphitic schist. A quartzite dominated zone is normally expected to have moderate to high resistivity values. The inverted inverse Schlumberger and dipole-dipole resistivity sections have low to moderate resistivity values within the black outline but the inverse Schlumberger section also has a zone of higher resistivity towards eth SE end of the outlined zone. The SE section of the 3 inverted resistivity arrays all have moderate resistivity values associated with the mapped quartzite, sericite schist, and graphitic schist mixed zone.

The black curve shown on the inverted dipole-dipole chargeability section has relatively high chargeability although there is no mineralization observed in boreholes. The inverted strong

gradient chargeability section also has moderate to high resistivity values but the inverse Schlumberger chargeability array has low chargeability values. The SE end of all three inverted arrays has low to moderate resistivity with moderate to high chargeability probably associated with the graphitic schist.

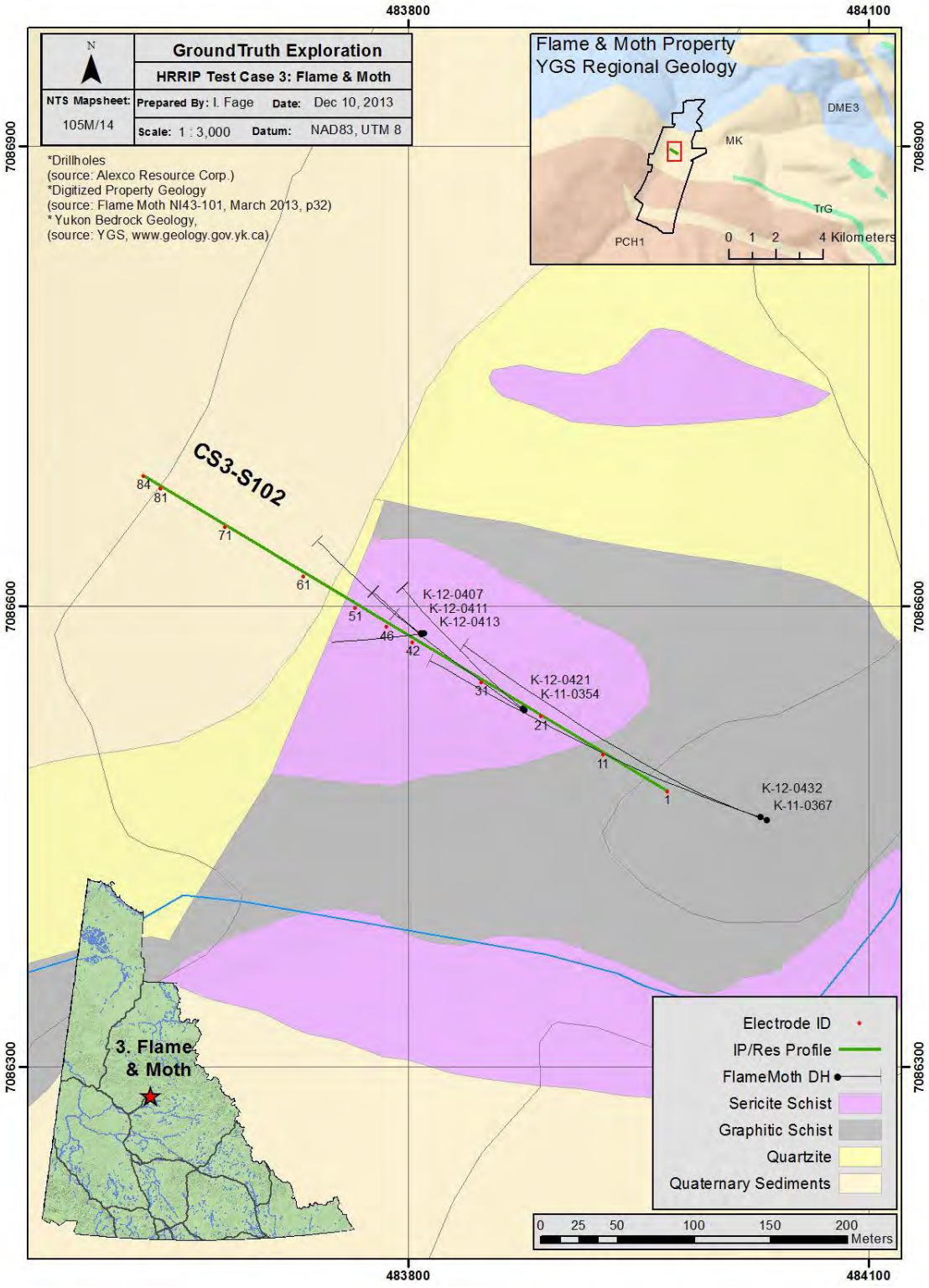

Figure CS3-1. *Location of the geophysical line and the surface geology at Flame and Moth.*

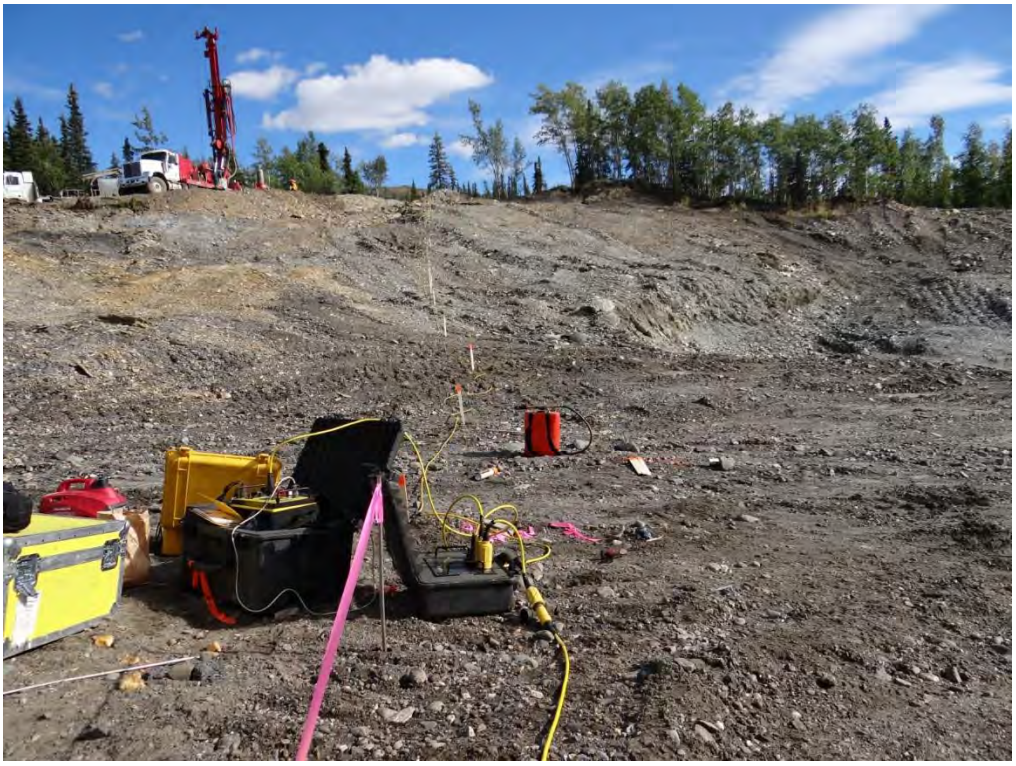

Figure CS3-2. *Survey profile at Flame & Moth.*

Figure CS3-3. *Survey line proximal to drill rig at Flame & Moth.*

PAIRED PLOTS

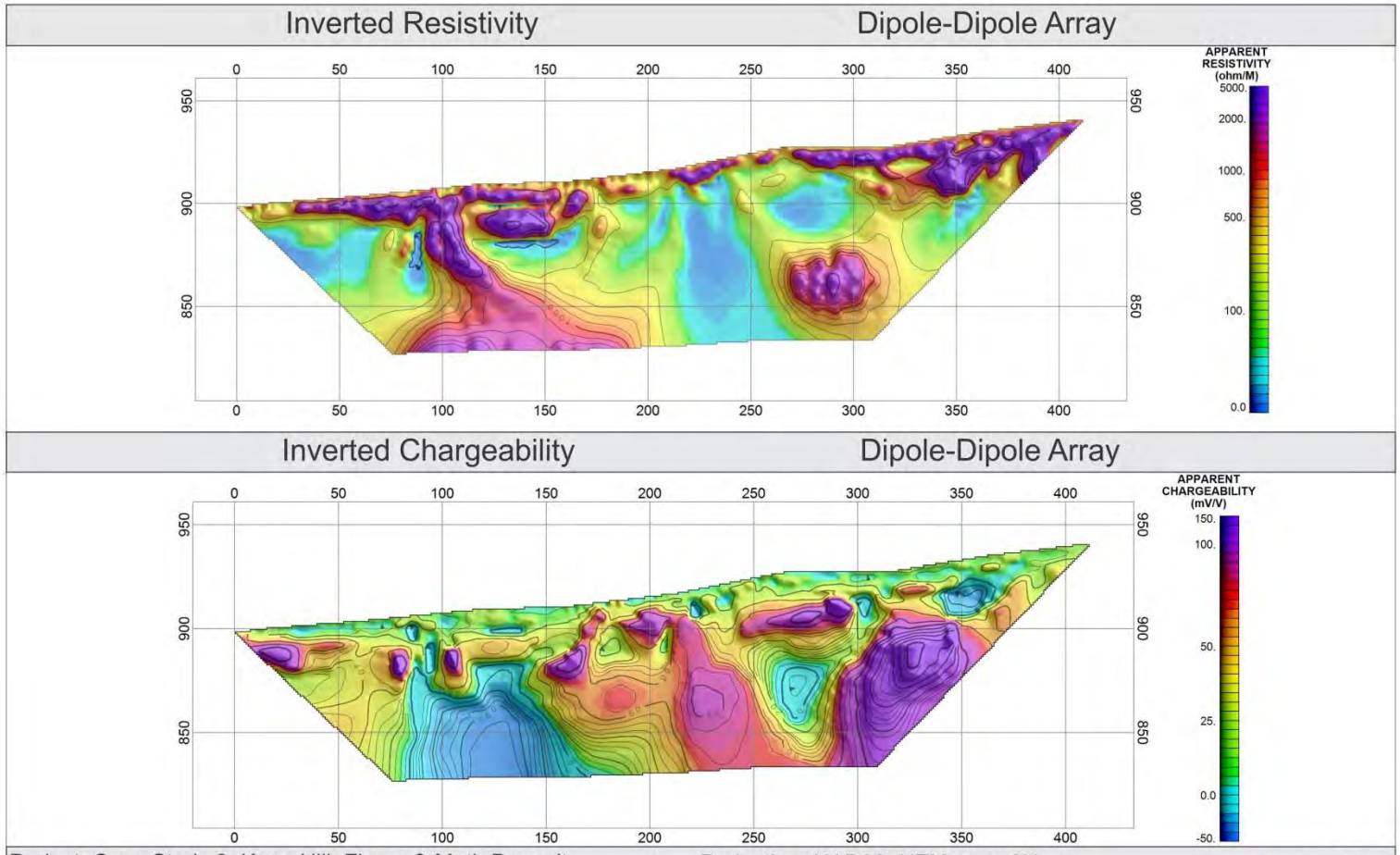

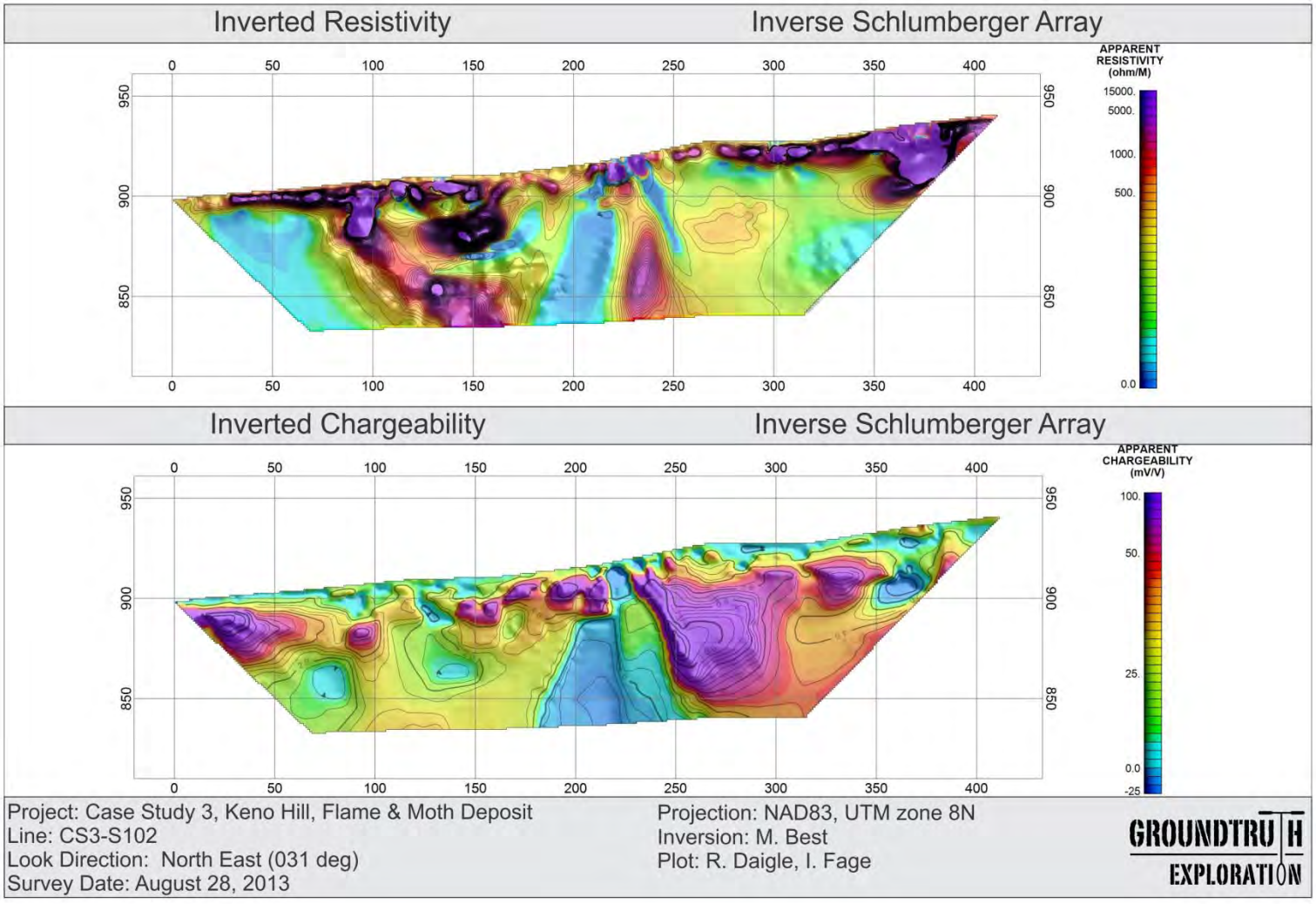
Inverted Resistivity
Inverse Schlumberger Array
APPARENT RESISTIVITY (ohm/M)
15000.
5000.
1000.
500.
0.0
Inverted Chargeability
Inverse Schlumberger Array
APPARENT CHARGEABILITY (mV/V)
100.
50.
25.
0.0
-25
0
50
100
150
200
250
300
350
400
850
900
950
Project: Case Study 3, Keno Hill, Flame & Moth Deposit
Line: CS3-S102
Look Direction: North East (031 deg)
Survey Date: August 28, 2013
Projection: NAD83, UTM zone 8N
Inversion: M. Best
Plot: R. Daigle, I. Fage
GROUNDTRUTH EXPLORATION

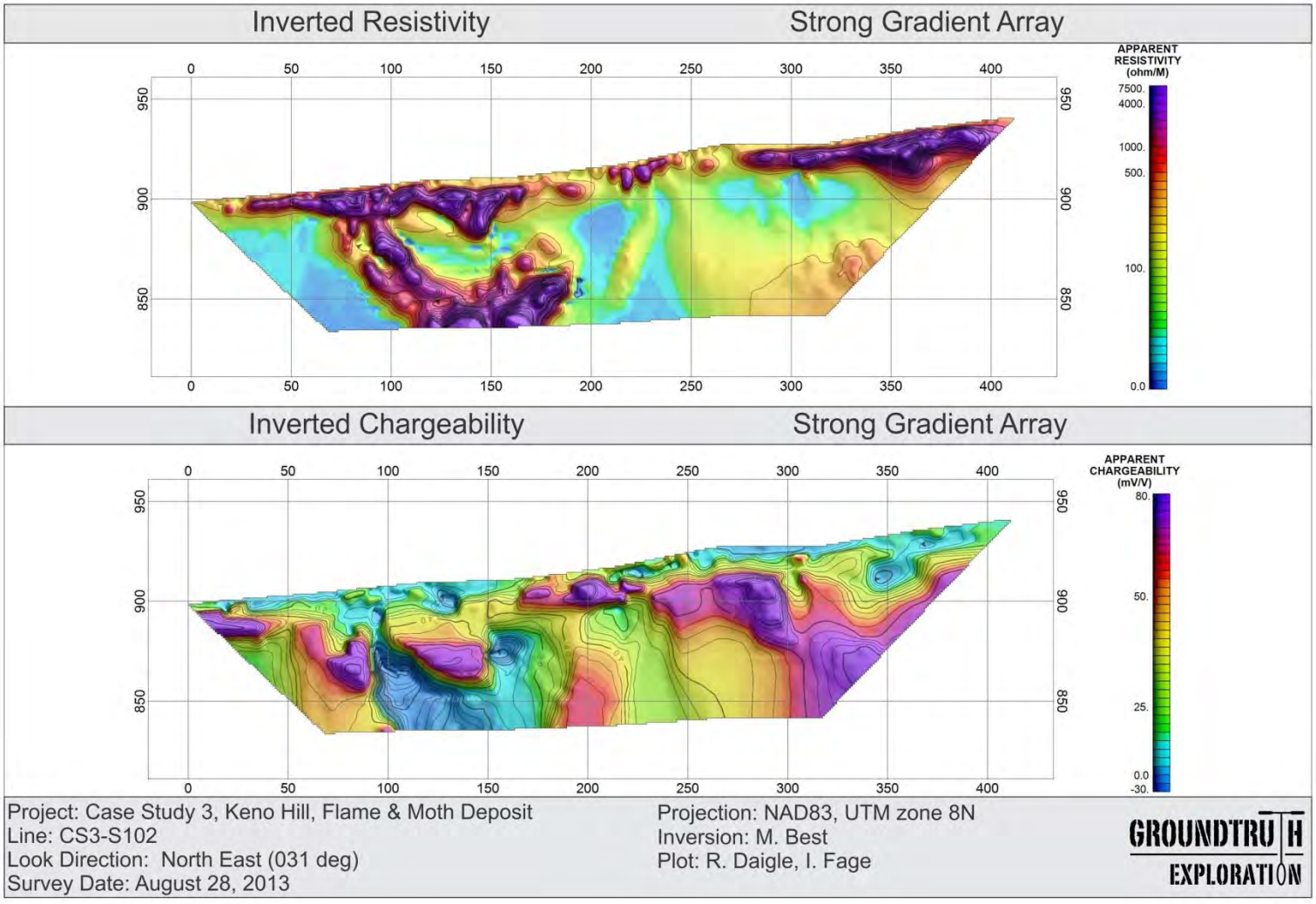
Inverted Resistivity
Strong Gradient Array
APPARENT RESISTIVITY (ohm/M)
7500.
4000.
1000.
500.
100.
0.0
Inverted Chargeability
Strong Gradient Array
APPARENT CHARGEABILITY (mV/V)
80.
50.
25.
0.0
-30.
0
50
100
150
200
250
300
350
400
950
900
850
Project: Case Study 3, Keno Hill, Flame & Moth Deposit
Line: CS3-S102
Look Direction: North East (031 deg)
Survey Date: August 28, 2013
Projection: NAD83, UTM zone 8N
Inversion: M. Best
Plot: R. Daigle, I. Fage
GROUNDTRUTH EXPLORATION

INTERPRETATION

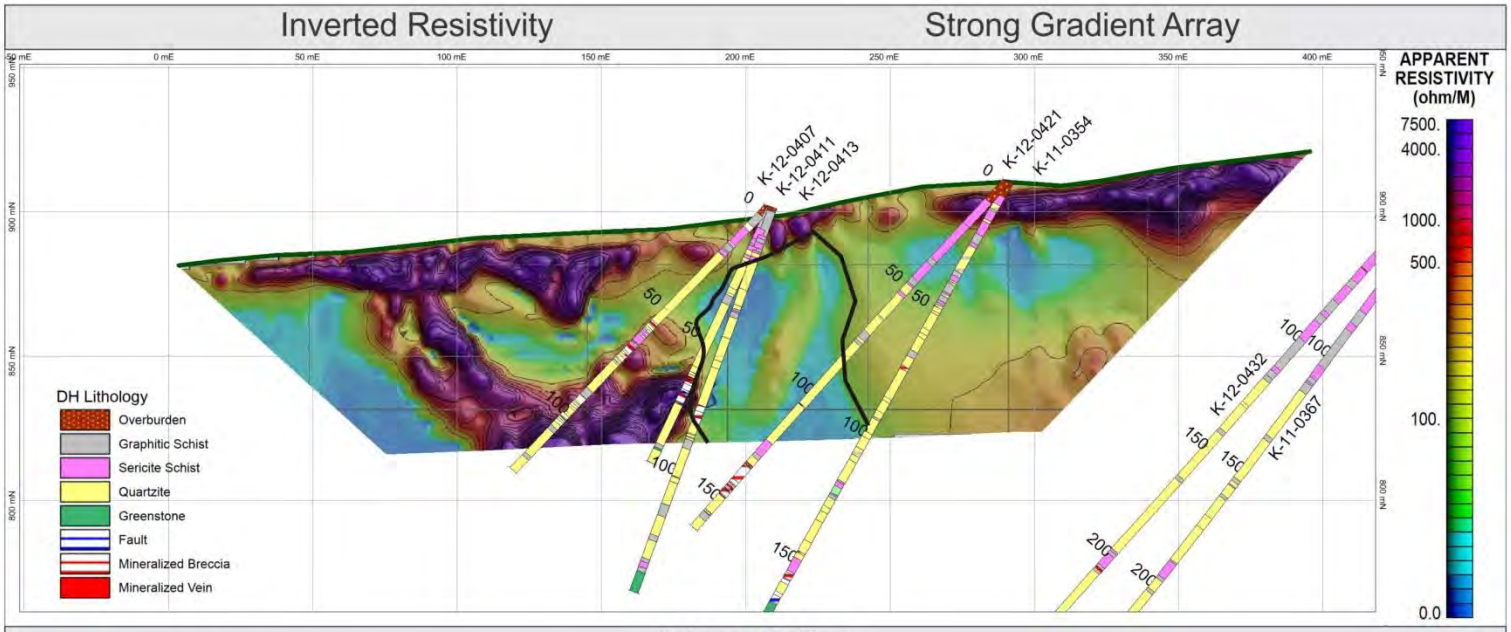

Interpretation

- o mineralization occurs in narrow veins - not easy target to map
- o black curve outlines area of low to moderate resistivity values
- o same area mapped as quartzite from boreholes - usually has higher resistivity values
- o area to SE of black outline mostly sericite schist and quartzite - has moderate resistivity values
- o dipole-dipole and inverse Schlumberger inverted resistivity sections similar but have zones of higher resistivity within black outlined area

Project: Case Study 3, Keno Hill, Flame & Moth Deposit
Line: CS3-S102
Look Direction: North East (031 deg)
Survey Date: August 28, 2013

Projection: NAD83, UTM zone 8N
Scale: 1 : 2,000
Inversion: M. Best
Plot: R. Daigle, I. Fage

GROUNDTRUTH EXPLORATION

Inverted Chargeability — Dipole-Dipole Array

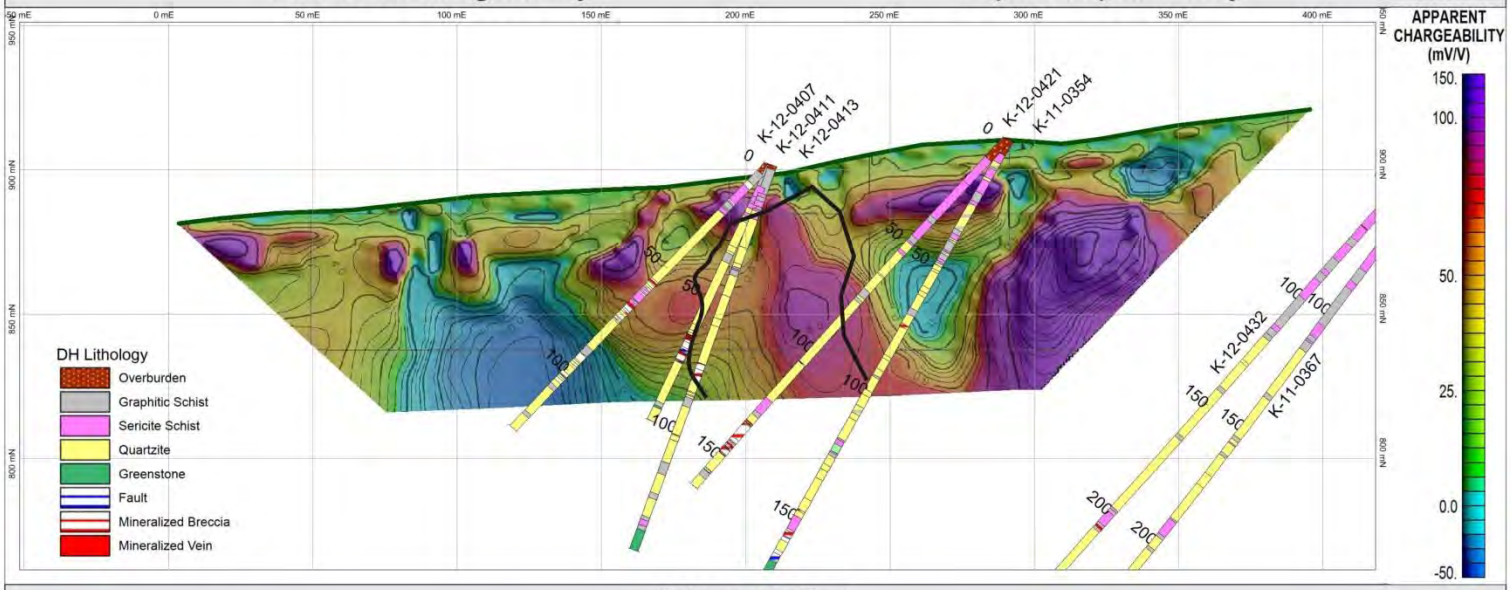

Interpretation

- o black zone outlines moderate to high chargeability region - no mineralization observed in boreholes
- o inverted strong gradient chargeability similar in character in black outline but inverse Schlumberger has chargeability low
- o SE end of line has low to moderate resistivity with moderate to high chargeablity for all three arrays - appears to be associated with graphitic schist

Project: Case Study 3, Keno Hill, Flame & Moth Deposit	Projection: NAD83, UTM zone 8N
Line: CS3-S102	Scale: 1 : 2,000
Look Direction: North East (031 deg)	Inversion: M. Best
Survey Date: August 28, 2013	Plot: R. Daigle, I. Fage

GROUNDTRUTH EXPLORATION

CS-4 KLAZA

Final Inversions and Interpretation

Geological setting

The Klaza property, a gold-silver vein/breccia occurrence in the south Dawson Range, is located in the Mt. Nansen area west of Carmacks, within the Paleozoic Yukon-Tanana terrane. Mineralization is hosted in Mid-Cretaceous granodiorite and is associated with four distinct southwest-dipping faulted zones: the Klaza, BYG, Herc, and BRX zones. Lewis and Burke (2011) described galena, arsenopyrite, pyrite and sphalerite-bearing veins and breccia, and noted phyllic and argillic alteration of breccia clasts and in the adjacent granodiorite wallrock. The high resolution resistivity/IP survey was carried out over the BRX and Klaza zones (Fig. CS4-1).

Geophysical survey

Dipole-dipole extended, inverse Schlumberger, and strong gradient array data were collected on lines KL-050E and BRX-600E at the Klaza BRX zone (see location map and photo below). The length of these lines was 415 m (a single spread length) for all the arrays. The average RMS error of fit for these 6 arrays was 2.91% with the highest value equal to 4.2% for the dipole-dipole extended array on line BRX-600E. These lines had a very high signal-to-noise ratio providing excellent high quality data. The paired plots for all 3 arrays along both lines are presented below after the location map.

Geophysical interpretation

The figures below provide borehole geology and mineralization overlain on selected inverted resistivity and IP sections for the two lines. Not all arrays are provided; however the reader can use the paired plots if they wish to investigate other arrays.

The inverted resistivity and chargeability from the dipole-dipole extended array on line KL-050E with interpretation is shown below. The black outline shows a resistivity low associated with a chargeability high over the mineralized vein and breccia zone. The HRRIP survey indicates these features extend in depth which is consistent with the borehole results showing the mineralization continues. All 3 arrays (dipole-dipole extended, inverse Schlumberger, and strong gradient) on this line show similar results. The granodiorite shows up as a resistivity high as expected but the chargeability values are variable over the granodiorite. The individual veins and fracture zones do not show up since they are too narrow. However the mineralized zone containing these individual fractures show up quite nicely.

The inverted resistivity and chargeability from the inverse Schlumberger array on line BRX-600E is presented below. In general the results are consistent with those for line KL-050E. There are two mineralized zones along this line (outlined by black lines) with resistive granodiorite surrounding them. As before the inverted resistivity tends to agree more closely with the mineralization than the chargeability, although they both outline the general mineralized zones. The mineralized zone at the NE end of the line has a large chargeability feature associated with it but the zone near the SW end only has a moderate chargeability. This is consistent with all three

of the arrays. The black lines indicate only partial overlap between resistivity lows and chargeability highs on this line.

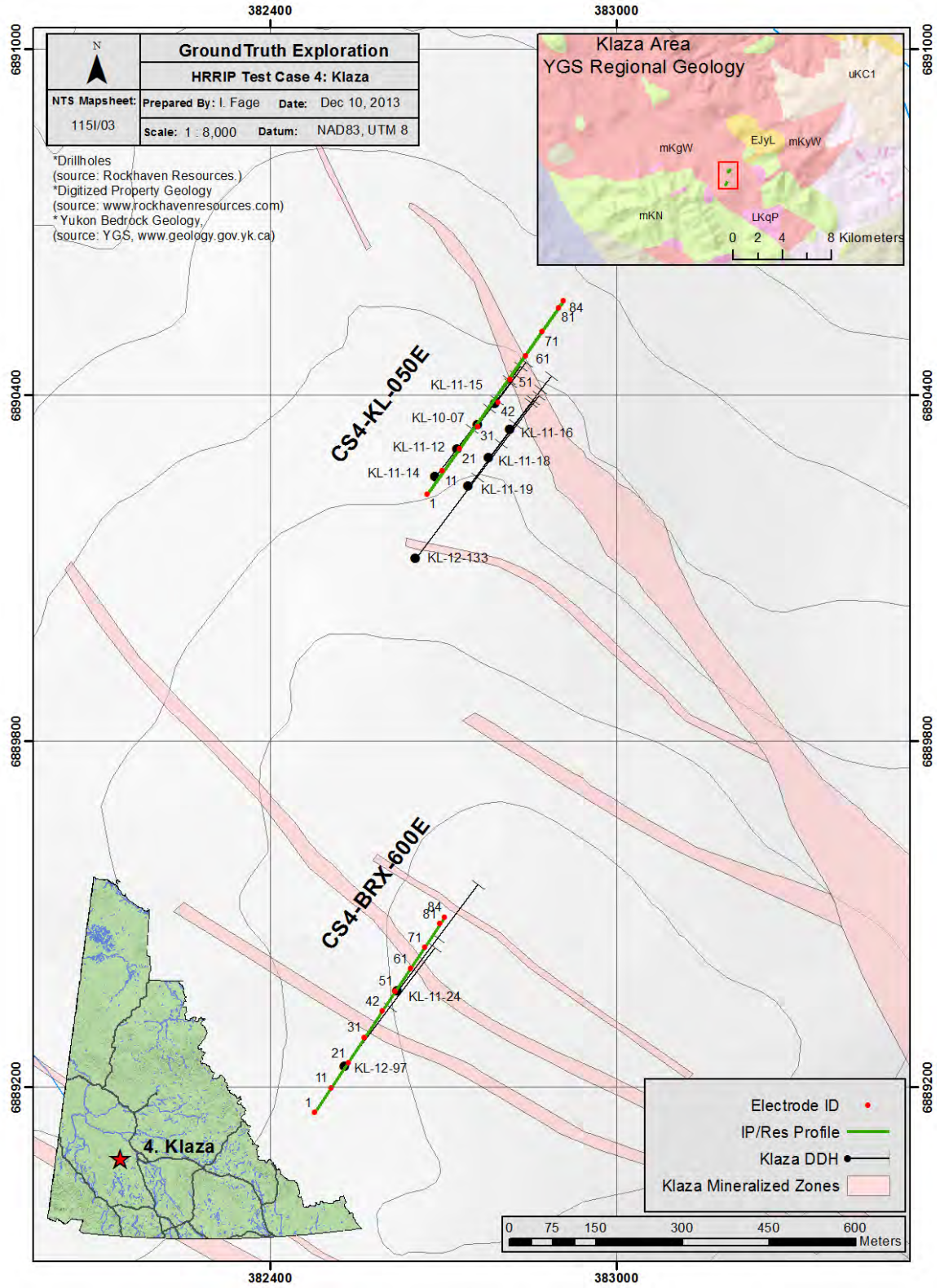

Figure CS4-1. *Map showing location of geophysical survey lines and surface geology at Klaza.*

Figure CS4-2. *Survey landscape for Klaza Project.*

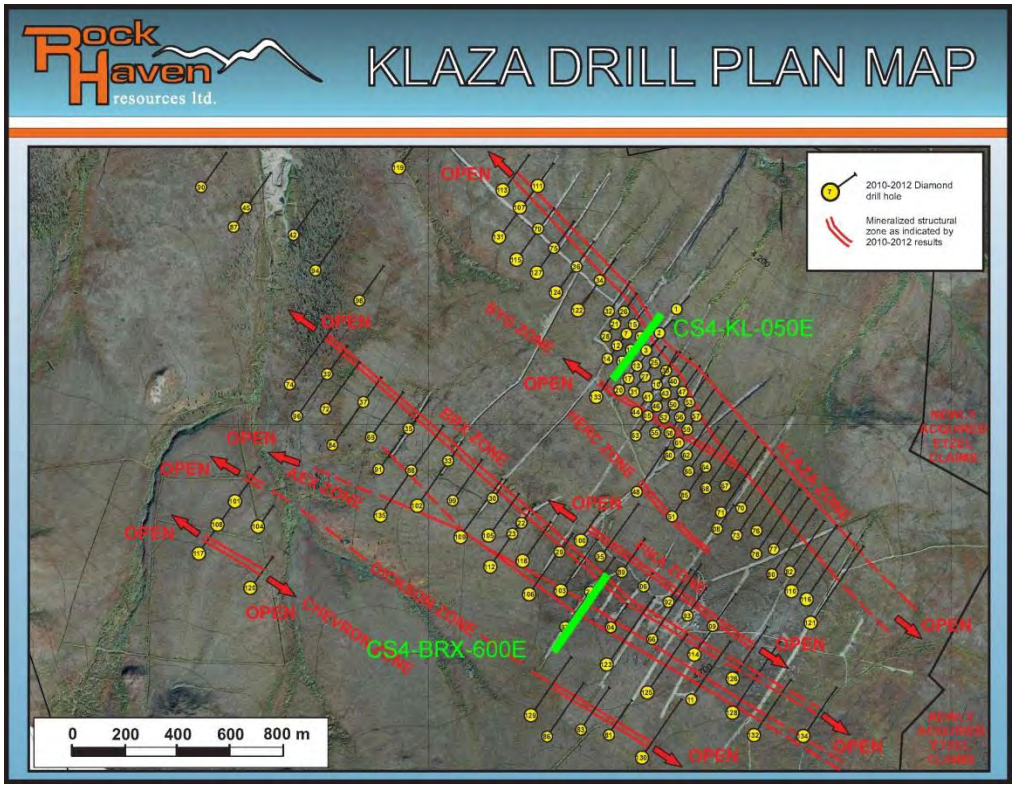

Figure CS4-3. *Plan Map with imagery and deposit overly, from Rockhaven Resources Ltd.*

PAIRED PLOTS

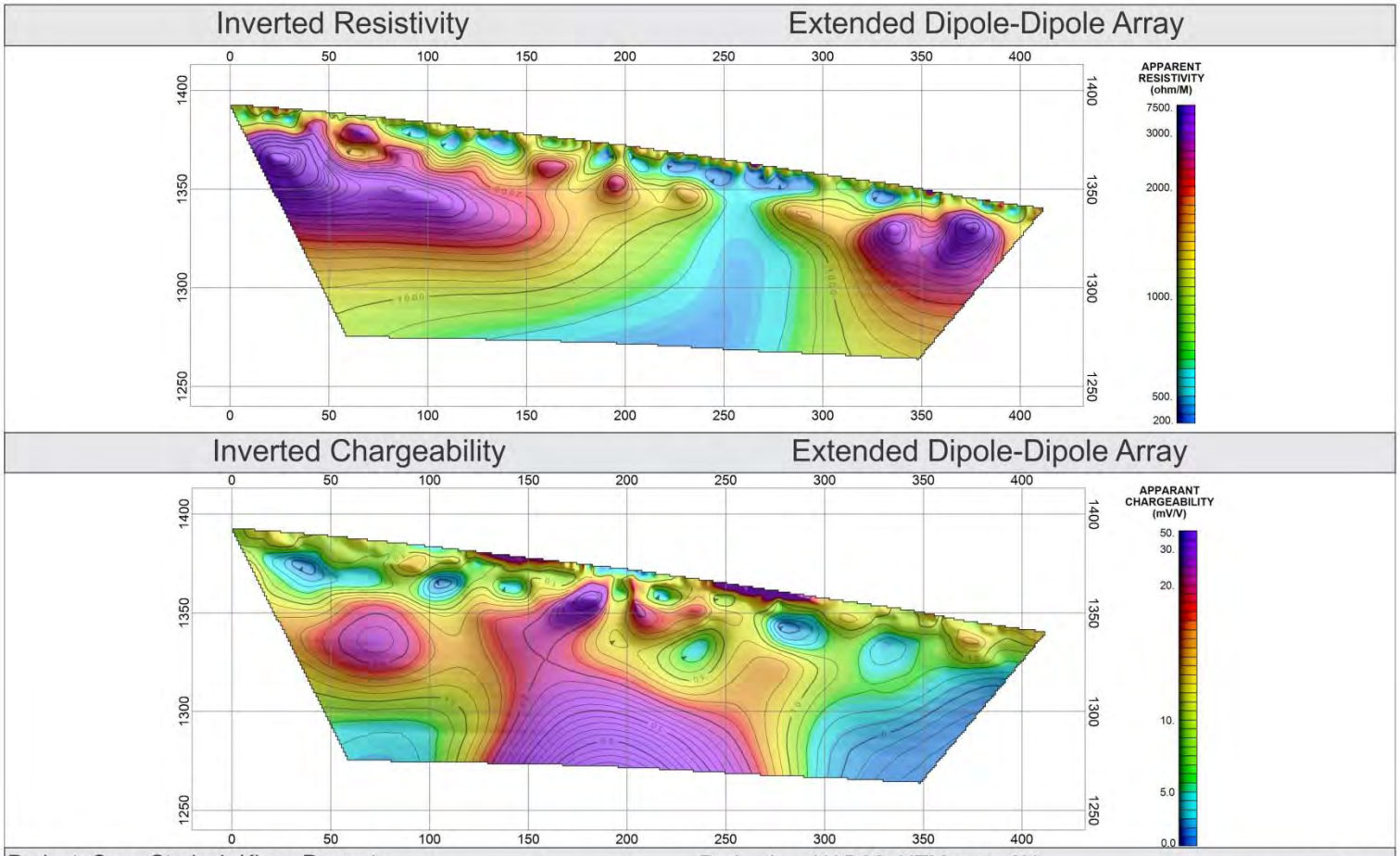

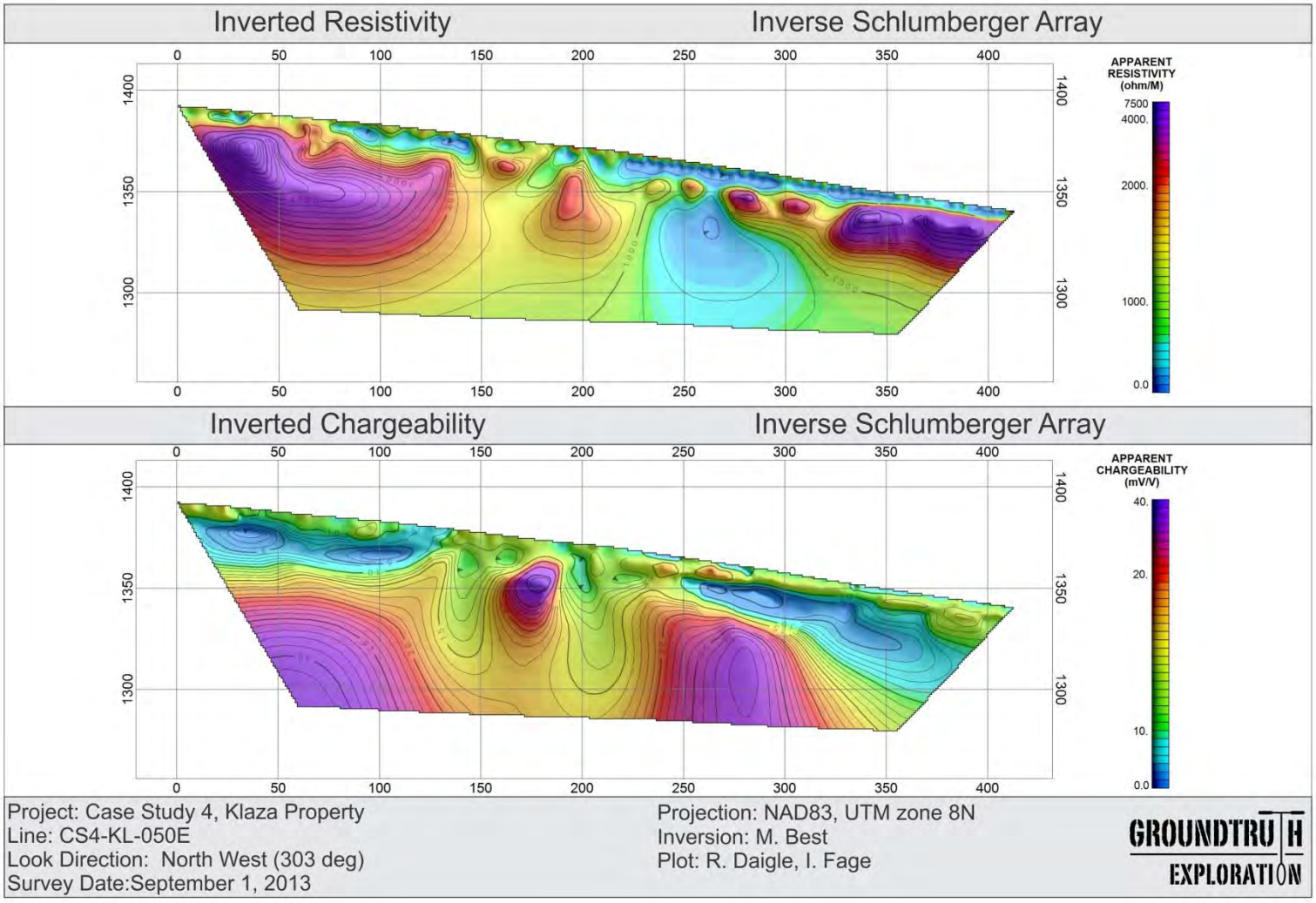
Inverted Resistivity
Inverse Schlumberger Array
APPARENT RESISTIVITY (ohm/M)
7500
4000.
2000.
1000.
0.0
Inverted Chargeability
Inverse Schlumberger Array
APPARENT CHARGEABILITY (mV/V)
40.
20.
10.
0.0
0
50
100
150
200
250
300
350
400
1400
1350
1300
Project: Case Study 4, Klaza Property
Line: CS4-KL-050E
Look Direction: North West (303 deg)
Survey Date:September 1, 2013
Projection: NAD83, UTM zone 8N
Inversion: M. Best
Plot: R. Daigle, I. Fage
GROUNDTRUTH EXPLORATION

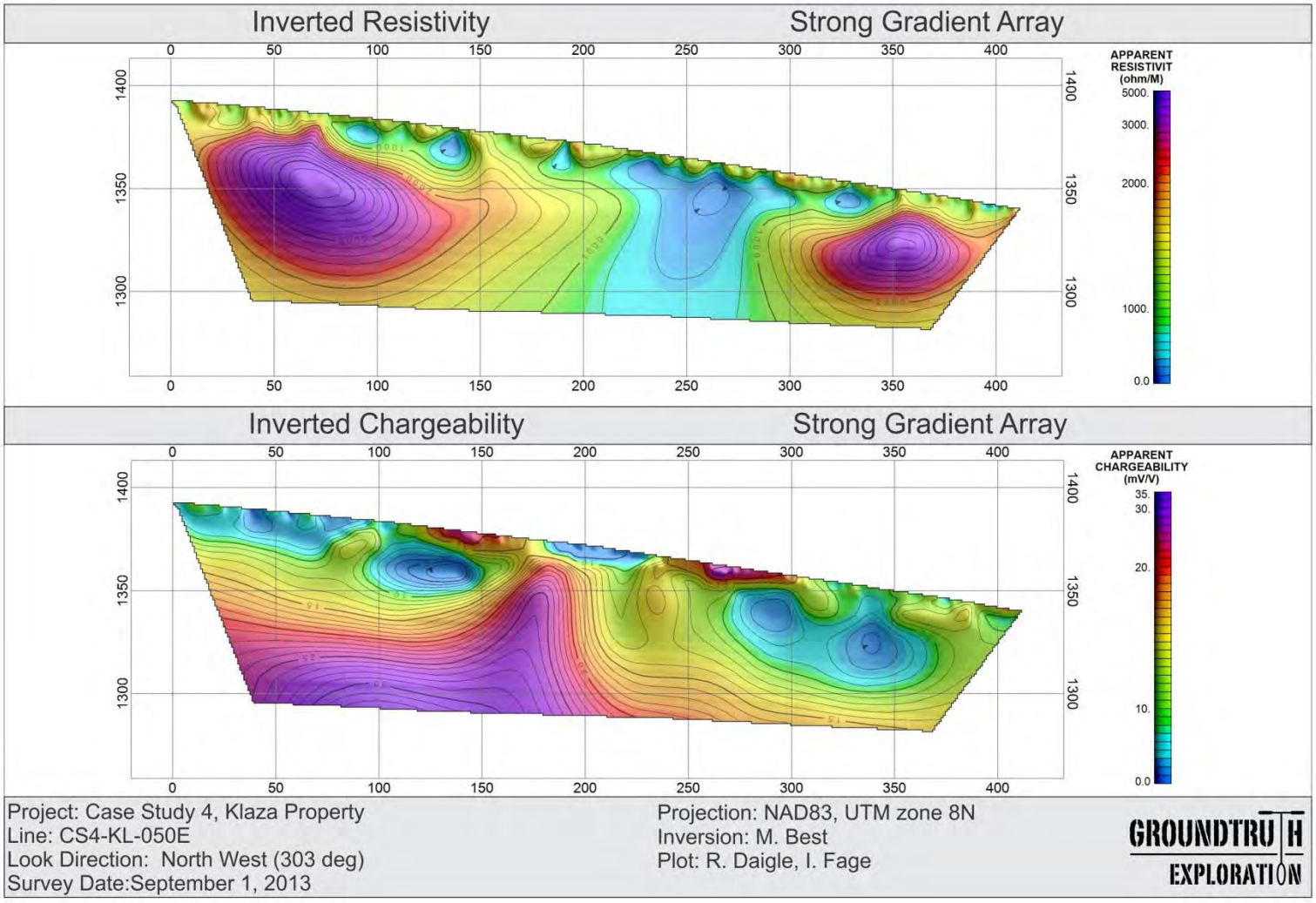
Inverted Resistivity
Strong Gradient Array
APPARENT RESISTIVIT (ohm/M)
5000.
3000.
2000.
1000.
0.0
Inverted Chargeability
Strong Gradient Array
APPARENT CHARGEABILITY (mV/V)
35.
30.
20.
10.
0.0
0
50
100
150
200
250
300
350
400
1400
1350
1300
Project: Case Study 4, Klaza Property
Line: CS4-KL-050E
Look Direction: North West (303 deg)
Survey Date:September 1, 2013
Projection: NAD83, UTM zone 8N
Inversion: M. Best
Plot: R. Daigle, I. Fage
GROUNDTRUTH EXPLORATION

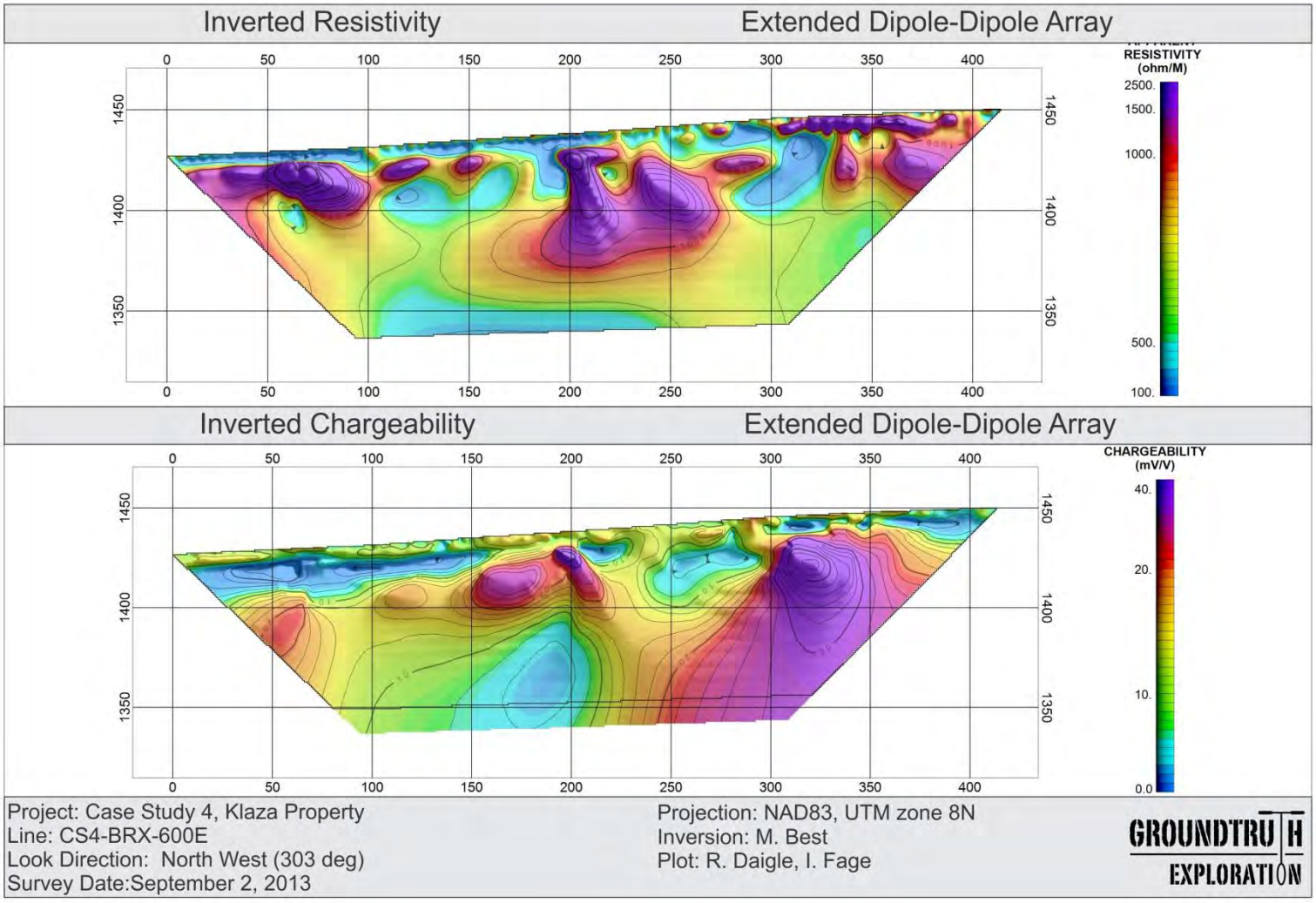
Inverted Resistivity
Extended Dipole-Dipole Array
0
50
100
150
200
250
300
350
400
1450
1400
1350
RESISTIVITY
(ohm/M)
2500.
1500.
1000.
500.
100.
Inverted Chargeability
Extended Dipole-Dipole Array
CHARGEABILITY
(mV/V)
40.
20.
10.
0.0
Project: Case Study 4, Klaza Property
Line: CS4-BRX-600E
Look Direction: North West (303 deg)
Survey Date:September 2, 2013
Projection: NAD83, UTM zone 8N
Inversion: M. Best
Plot: R. Daigle, I. Fage
GROUNDTRUTH
EXPLORATION

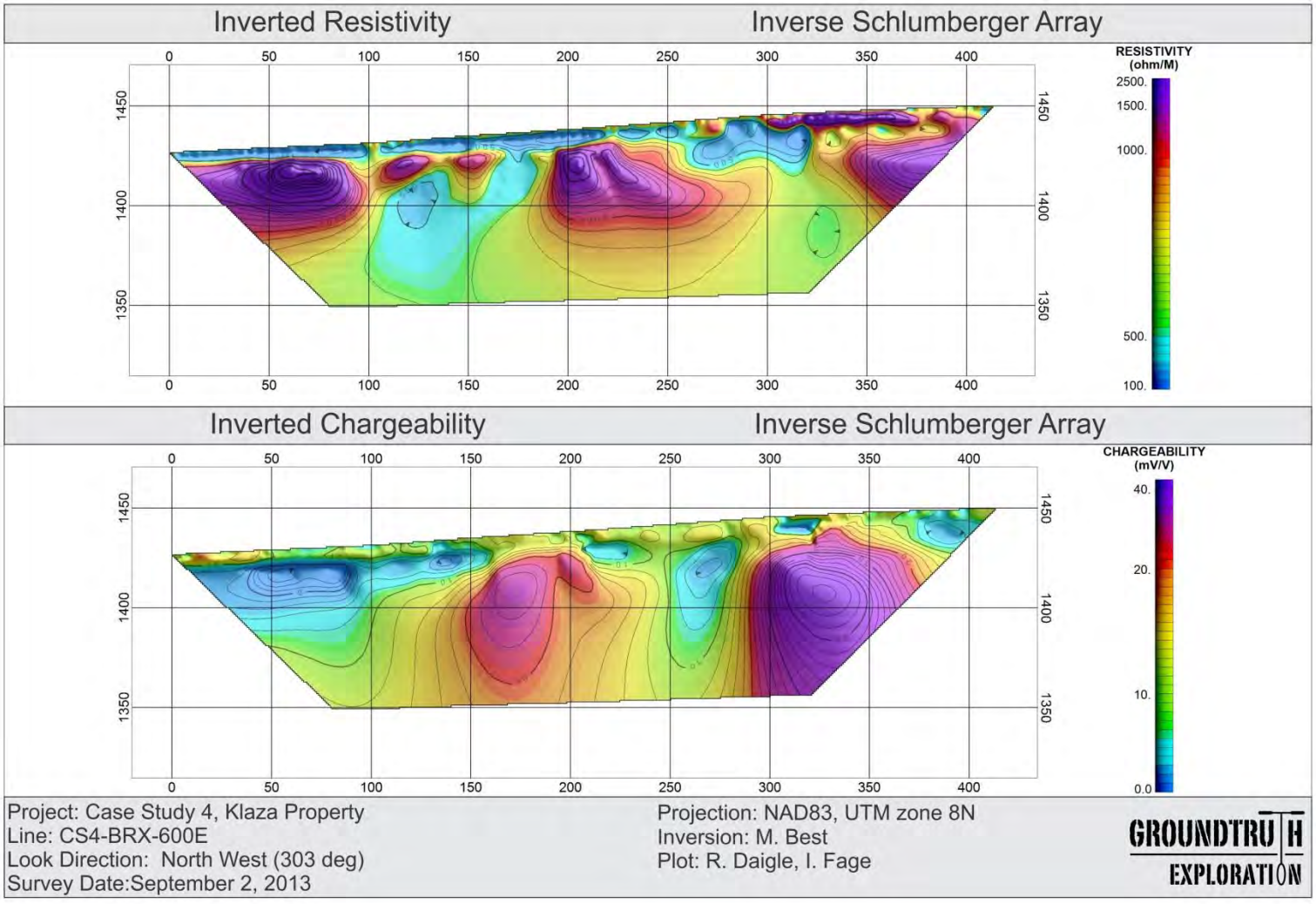
Inverted Resistivity
Inverse Schlumberger Array
RESISTIVITY
(ohm/M)
2500.
1500.
1000.
500.
100.
Inverted Chargeability
Inverse Schlumberger Array
CHARGEABILITY
(mV/V)
40.
20.
10.
0.0
0
50
100
150
200
250
300
350
400
1450
1400
1350
Project: Case Study 4, Klaza Property
Line: CS4-BRX-600E
Look Direction: North West (303 deg)
Survey Date:September 2, 2013
Projection: NAD83, UTM zone 8N
Inversion: M. Best
Plot: R. Daigle, I. Fage
GROUNDTRUTH
EXPLORATION

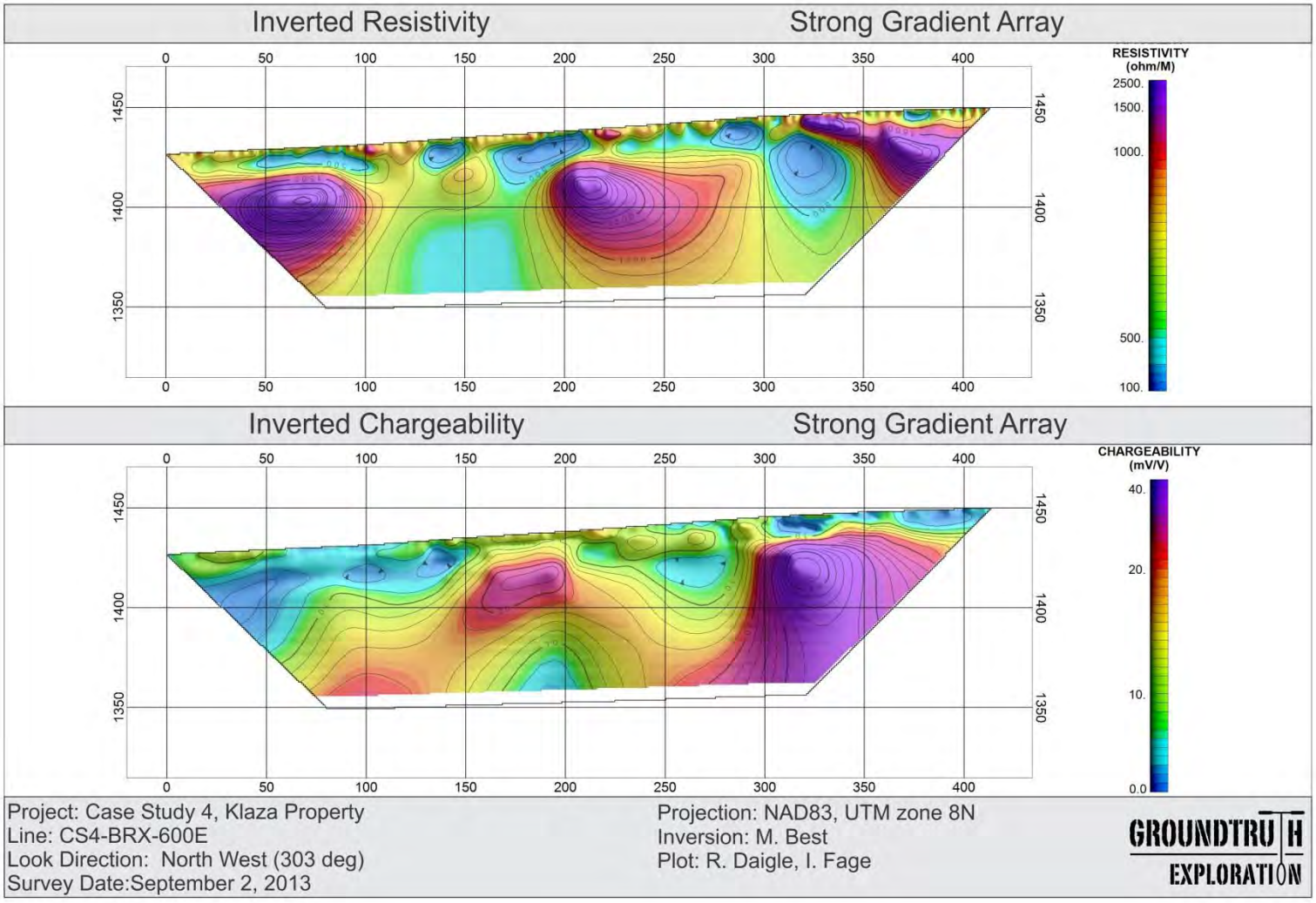
Inverted Resistivity
Strong Gradient Array
RESISTIVITY
(ohm/M)
2500.
1500.
1000.
500.
100.
Inverted Chargeability
Strong Gradient Array
CHARGEABILITY
(mV/V)
40.
20.
10.
0.0
0
50
100
150
200
250
300
350
400
1450
1400
1350
Project: Case Study 4, Klaza Property
Line: CS4-BRX-600E
Look Direction: North West (303 deg)
Survey Date:September 2, 2013
Projection: NAD83, UTM zone 8N
Inversion: M. Best
Plot: R. Daigle, I. Fage
GROUNDTRUTH
EXPLORATION

INTERPRETATION

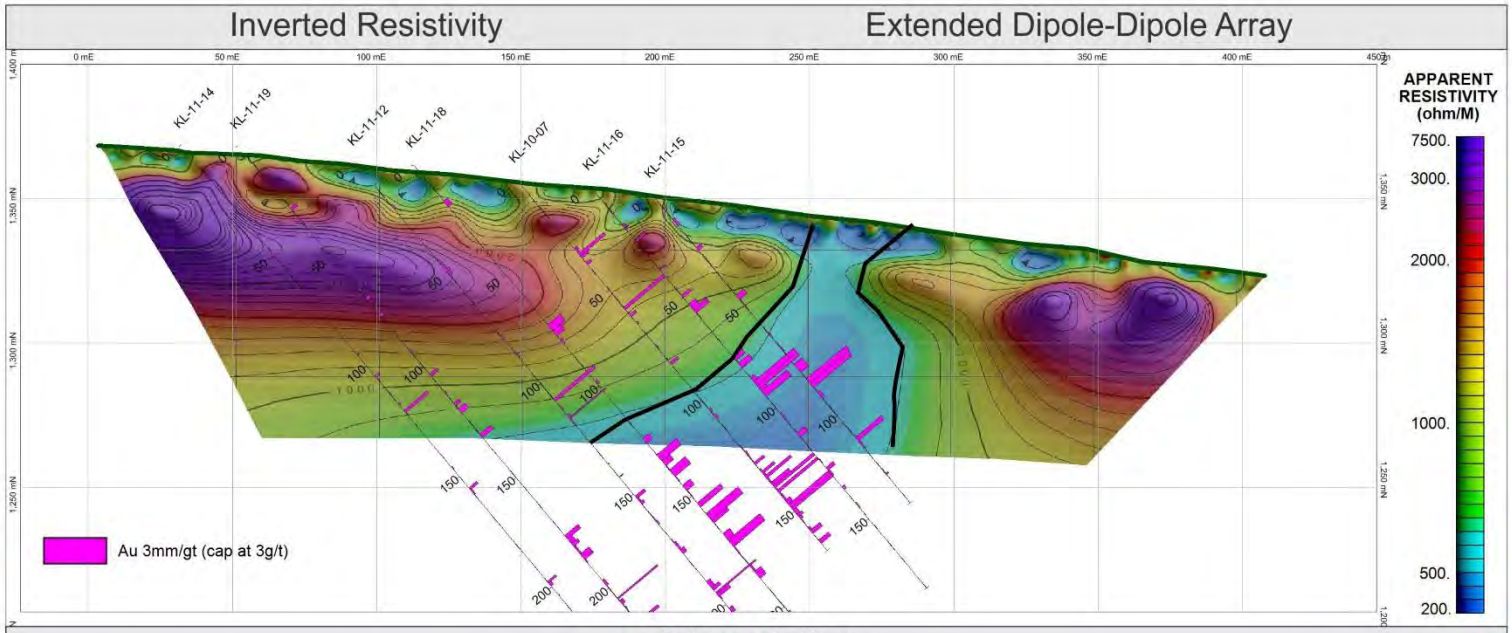

Interpretation

- o black lines outline mineralized veins and breccias associated with porphyry dikes
- o mineralized zone is a resistivity low and appears to continue at depth
- o all 3 inverted resistivity arrays outline mineralized zone very effectively
- o granodiorite shows up as resistivity highs on all 3 inverted resistivity arrays

Project: Case Study 4,Klaza Property	Projection: NAD83, UTM zone 8N
Line: CS4-KL-050E	Scale: 1 : 2,000
Look Direction: North West (303 deg)	Inversion: M. Best
Survey Date: September 2, 2013	Plot: R. Daigle, I. Fage

GROUNDTRUTH EXPLORATION

Inverted Chargeability — Extended Dipole-Dipole Array

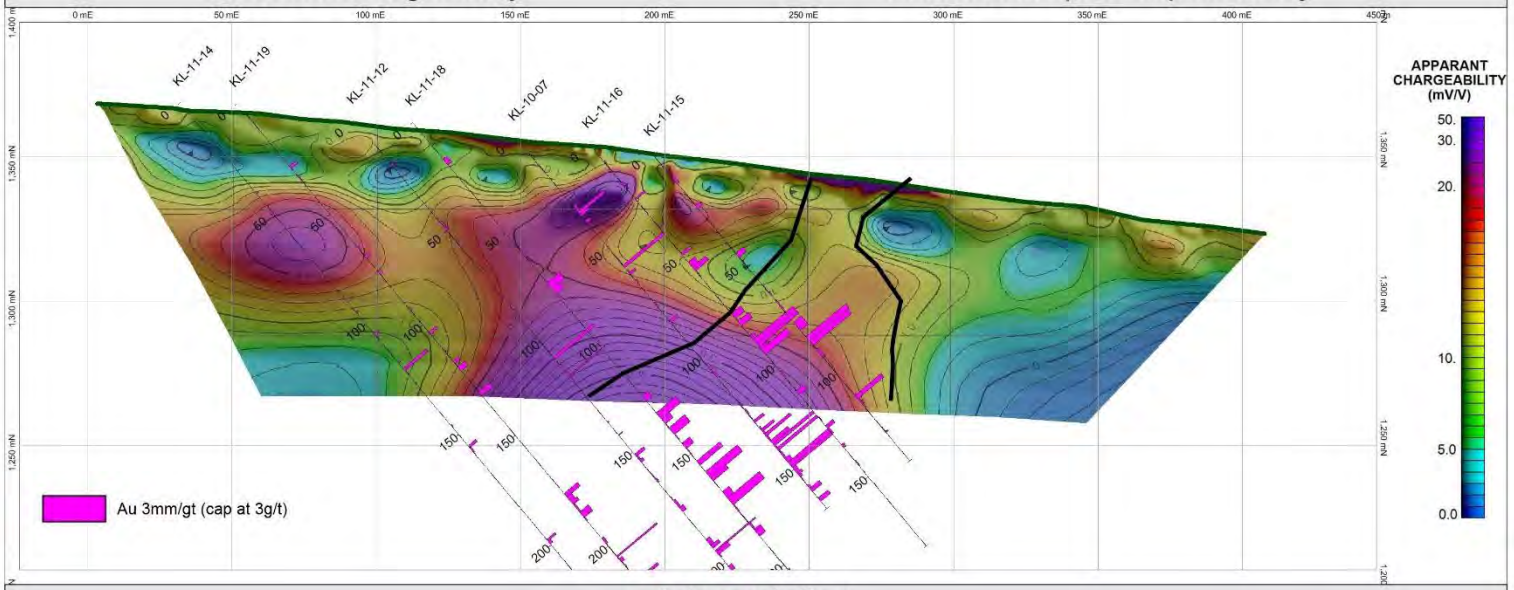

Interpretation

- o inverted chargeability outlines mineralized zone but extends to the SW farther than corresponding resistivity low
- o inverted strong gradient chargeablility similar to dipole-dipole extended array
- o inverted inverse Schlumberger chargeability extends farther to the east and has smaller chargeability value

Project: Case Study 4,Klaza Property
Line: CS4-KL-050E
Look Direction: North West (303 deg)
Survey Date: September 2, 2013

Projection: NAD83, UTM zone 8N
Scale: 1 : 2,000
Inversion: M. Best
Plot: R. Daigle, I. Fage

GROUNDTRUTH EXPLORATION

Inverted Resistivity — Inverse Schlumberger Array

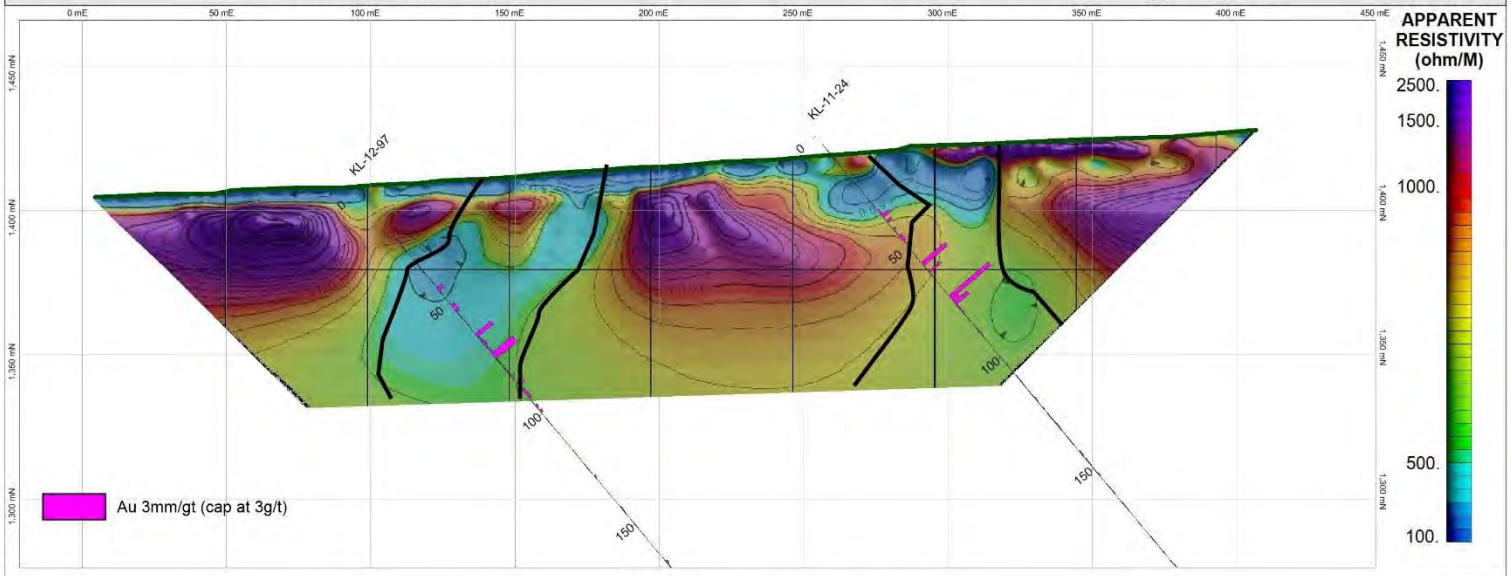

Interpretation

- o black lines outline low resistivity zones associated with mineralized veins and breccias
- o granodiorites are high resistivity zones similar to Line KL-050
- o all 3 arrays have low resistivity zones associated with mineralized zones
- o best correlation with mineralized zones is with the inverse Schlumberger and strong gradient on this line

Project: Case Study 4,Klaza Property
Line: CS4-BRX-600E
Look Direction: North West (303 deg)
Survey Date: September 2, 2013

Projection: NAD83, UTM zone 8N
Scale: 1 : 2,000
Inversion: M. Best
Plot: R. Daigle, I. Fage

GROUNDTRUTH EXPLORATION

Inverted Chargeability

Inverse Schlumberger Array

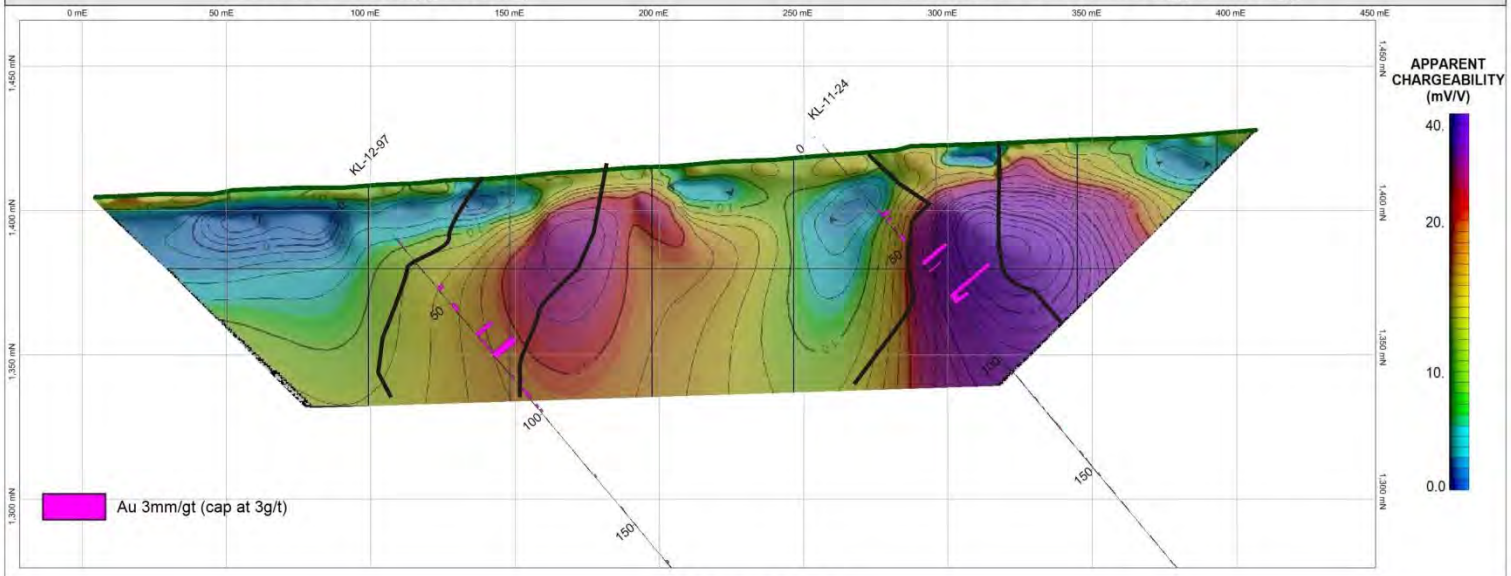

Interpretation

- o a chargeability high is clearly associated with the NE mineralized zone
- o mineralized zone near SW end is in moderate chargeability high for all 3 arrays
- o black lines indicate only partial overlap of resistivity lows and chargeablilty highs
- o all 3 arrays have chargeability highs at the NE end of lines

Project: Case Study 4,Klaza Property
Line: CS4-BRX-600E
Look Direction: North West (303 deg)
Survey Date: September 2, 2013

Projection: NAD83, UTM zone 8N
Scale: 1 : 2,000
Inversion: M. Best
Plot: R. Daigle, I. Fage

GROUNDTRUTH EXPLORATION

CS-5 CHARLOTTE

Final Inversions and Interpretation

Geological setting

The Charlotte epithermal gold-silver property, a few kilometres southeast of the Klaza case study (CS-4), is also in the Mt Nansen Mine area and lies within the Yukon-Tanana terrane. It is characterized by a number of mineralized vein systems associated with west to southwest-dipping shear zones. The Flex zone lies in the southeast corner of the property (Fig. CS5-1) and consists of several anastamosing quartz-sulphide veins crosscutting quartz-feldspar chlorite gneiss that is intercalated with amphibolite gneiss (Abbado *et al.*, 2005). Veins host gold and silver mineralization with abundant pyrite and lesser arsenopyrite, stibnite, galena, and sphalerite. Veins commonly exhibit propylitic, phyllic, argillic, and silicic alteration (Lewis and Burke, 2011).

Geophysical survey

The two HHRIP lines were surveyed over the flex zone and were offset from the borehole locations by approximately 20 to 50 m depending on the individual lines and boreholes (see location map and photo). The average RMS error of fit for the entire inverted data set is 3.2% with the largest error of fit equal to 5.21%. The data quality for this case study is therefore excellent. All arrays had a length of 415 m (single spread length). Data from five arrays were collected over line S050N (dipole-dipole extended, pole-dipole, inverse Schlumberger, strong gradient, and Wenner) and three arrays over line S200N (dipole-dipole extended, inverse Schlumberger, and strong gradient).

Geophysical interpretation

Examples of inverted sections with borehole information overlain for the inverted dipole-dipole extended resistivity array, the inverse Schlumberger IP array, and the pole-dipole resistivity and IP arrays are presented below for line S050N. The mineralized zone observed on the borehole information shows up as a resistivity low for both the dipole-dipole extended and pole-dipole arrays. There is a second low resistivity zone approximately 100 m to the northeast of the known mineralized zone that shows up on all 5 arrays but does not correlate very well with high chargeability on the arrays. The pole-dipole array provides better depth coverage than the other arrays. Generally the dipole-dipole and pole-dipole arrays provide the best lateral coverage with the inverse Schlumberger and Wenner arrays better at defining layering (depth information). The mineralized zone from the borehole data consists of multiple moderately conductive veins and fractures. Consequently the HRRIP surveys are averaging the effects of these multiple zones. They are too narrow to resolve individually; however the inversions provide a reasonable estimate of the entire zone.

Inverted strong gradient resistivity and dipole-dipole extended IP sections with borehole information overlain are presented below for line S200N. The results are similar to Line S050N. There is a low resistivity zone associated with the known mineralization on all three inverted resistivity arrays. The inverse chargeability for the strong gradient and dipole-dipole extended IP arrays have high chargeability at the same location as the resistivity low but the same zone is in a

chargeability low for the inverted inverse Schlumberger array. A similar low resistivity zone to the northeast, as mentioned above for line S050N, also exists on all three inverted resistivity arrays, indicating this zone extends between the two lines similar to the mineralized zone.

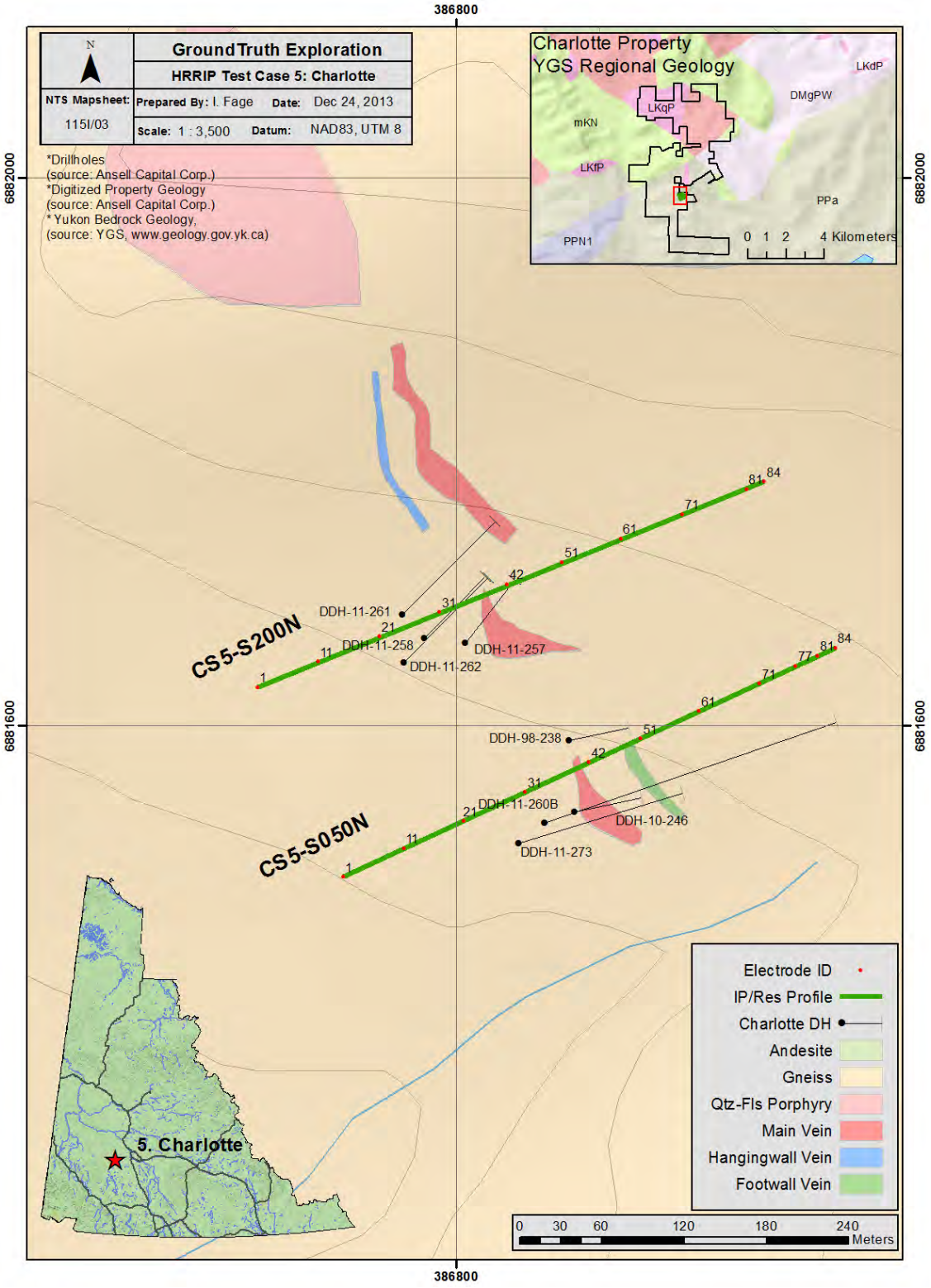

Figure CS5-1. *Location of geophysical lines and surface geology for Charlotte Property, Flex Zone.*

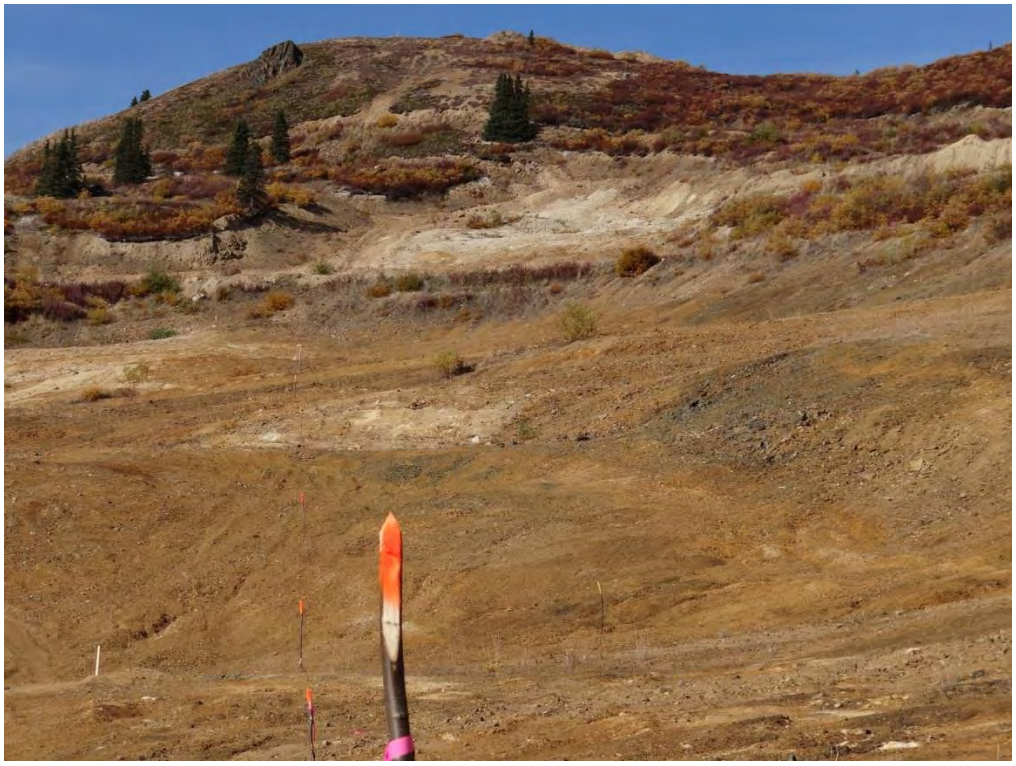

Figure CS5-2. *Survey over historic stripped area on Charlotte Property, Flex Zone.*

Figure CS5-3. *Landscape of Charlotte Property, Flex Zone*

PAIR PLOTS

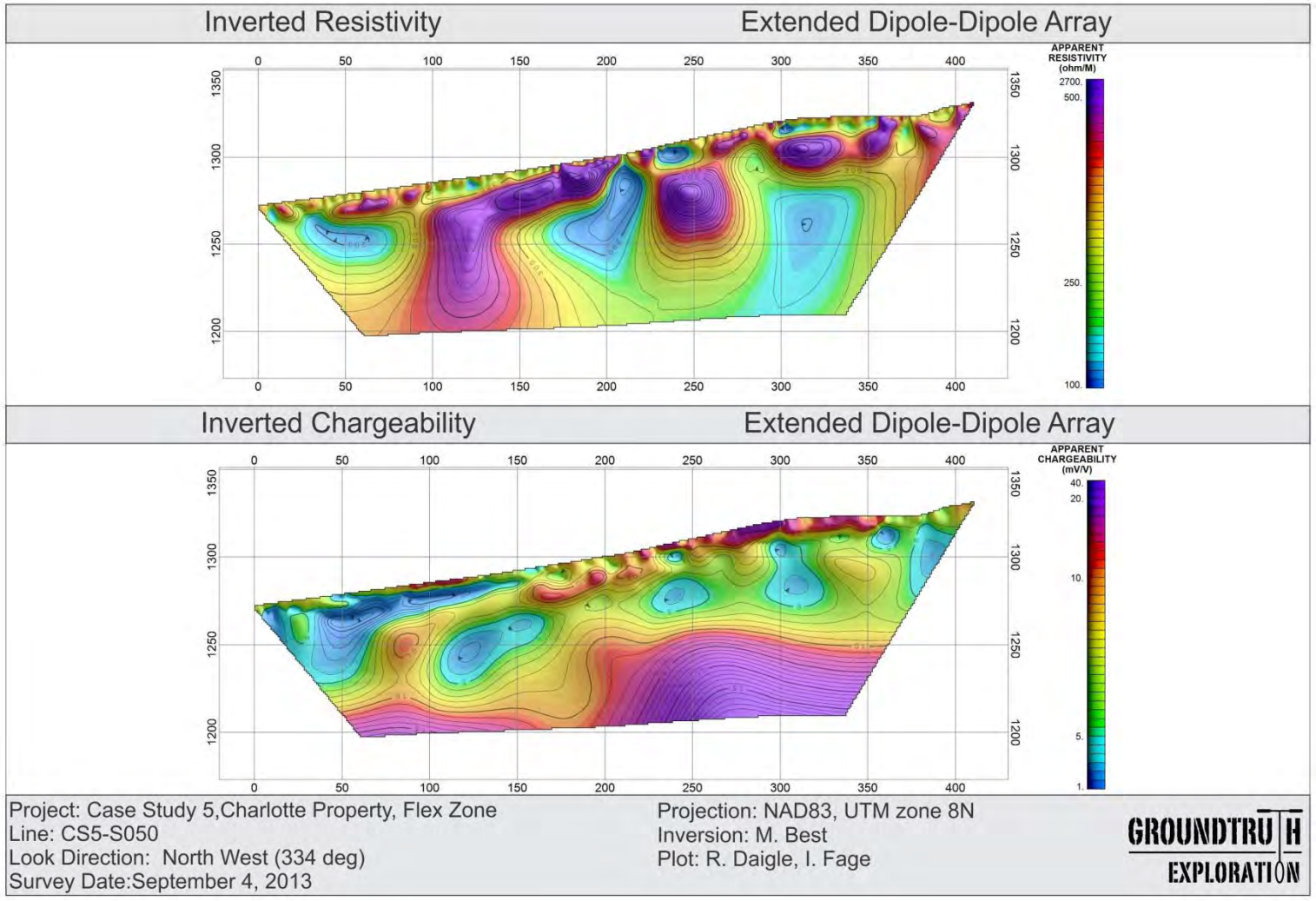
Inverted Resistivity
Extended Dipole-Dipole Array
APPARENT RESISTIVITY (ohm/M)
2700.
500.
250.
100.
Inverted Chargeability
Extended Dipole-Dipole Array
APPARENT CHARGEABILITY (mV/V)
40.
20.
10.
5.
1.
Project: Case Study 5,Charlotte Property, Flex Zone
Line: CS5-S050
Look Direction: North West (334 deg)
Survey Date:September 4, 2013
Projection: NAD83, UTM zone 8N
Inversion: M. Best
Plot: R. Daigle, I. Fage
GROUNDTRUTH EXPLORATION

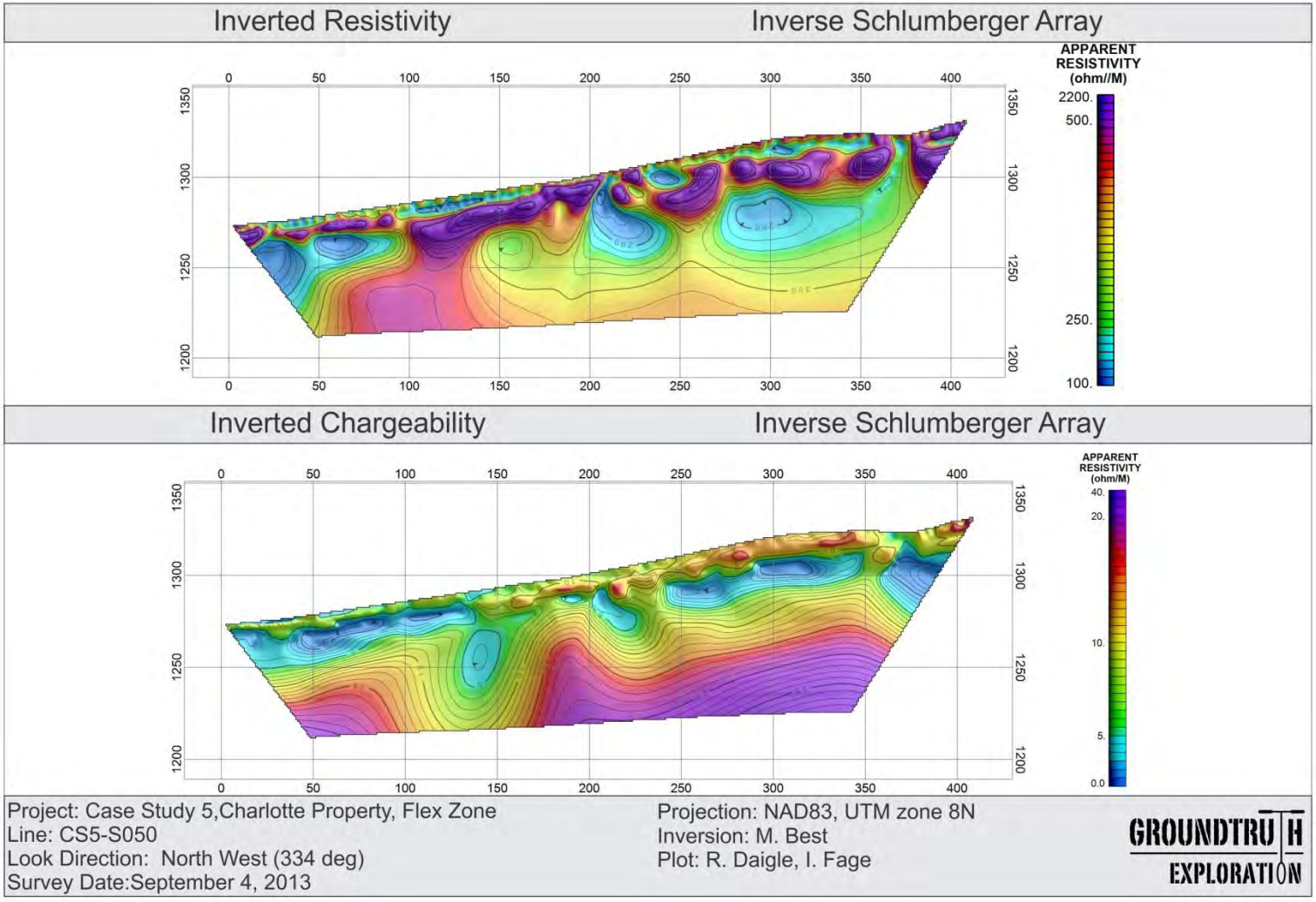
Inverted Resistivity
Inverse Schlumberger Array
APPARENT RESISTIVITY (ohm//M)
2200.
500.
250.
100.
0
50
100
150
200
250
300
350
400
1350
1300
1250
1200
Inverted Chargeability
Inverse Schlumberger Array
APPARENT RESISTIVITY (ohm/M)
40.
20.
10.
5.
0.0
Project: Case Study 5,Charlotte Property, Flex Zone
Line: CS5-S050
Look Direction: North West (334 deg)
Survey Date:September 4, 2013
Projection: NAD83, UTM zone 8N
Inversion: M. Best
Plot: R. Daigle, I. Fage
GROUNDTRUTH
EXPLORATION

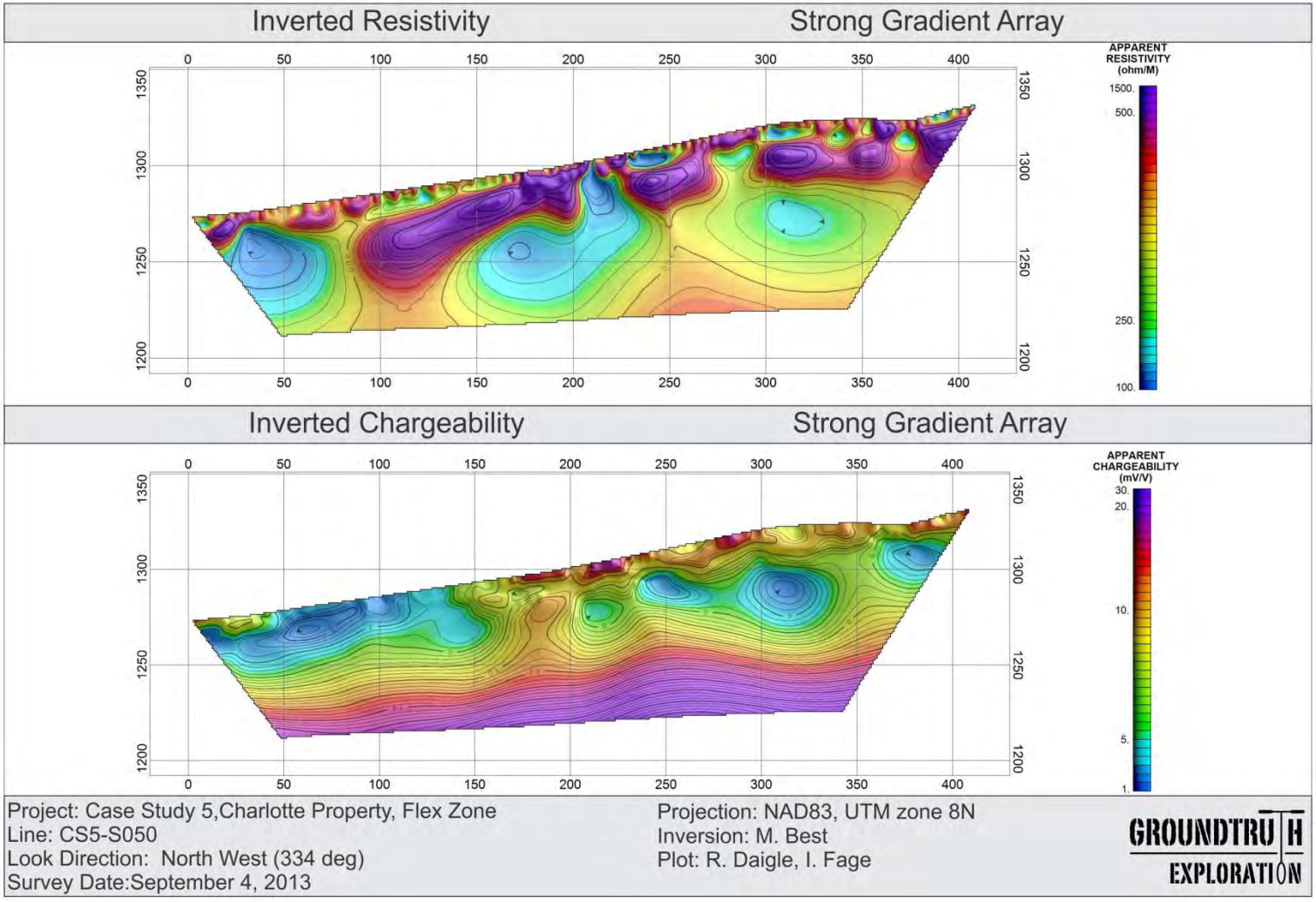
Inverted Resistivity
Strong Gradient Array
APPARENT RESISTIVITY (ohm/M)
1500.
500.
250.
100.
Inverted Chargeability
Strong Gradient Array
APPARENT CHARGEABILITY (mV/V)
30.
20.
10.
5.
1.
0
50
100
150
200
250
300
350
400
1350
1300
1250
1200
Project: Case Study 5,Charlotte Property, Flex Zone
Line: CS5-S050
Look Direction: North West (334 deg)
Survey Date:September 4, 2013
Projection: NAD83, UTM zone 8N
Inversion: M. Best
Plot: R. Daigle, I. Fage
GROUNDTRUTH EXPLORATION

Inverted Resistivity — Pole-Dipole Array

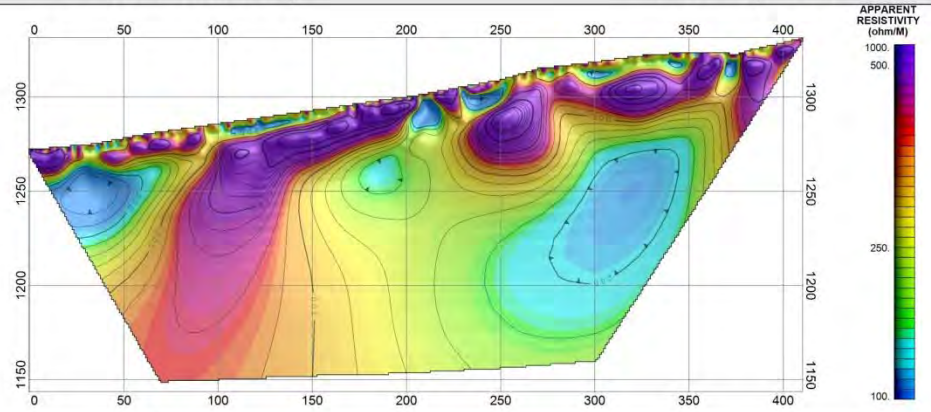

Inverted Chargeability — Pole-Dipole Array

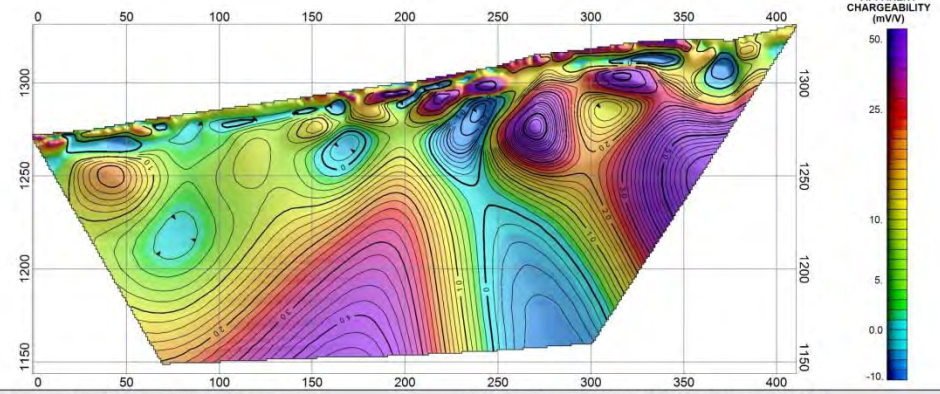

Project: Case Study 5,Charlotte Property, Flex Zone
Line: CS5-S050
Look Direction: North West (334 deg)
Survey Date:September 4, 2013

Projection: NAD83, UTM zone 8N
Inversion: M. Best
Plot: R. Daigle, I. Fage

GROUNDTRUTH EXPLORATION

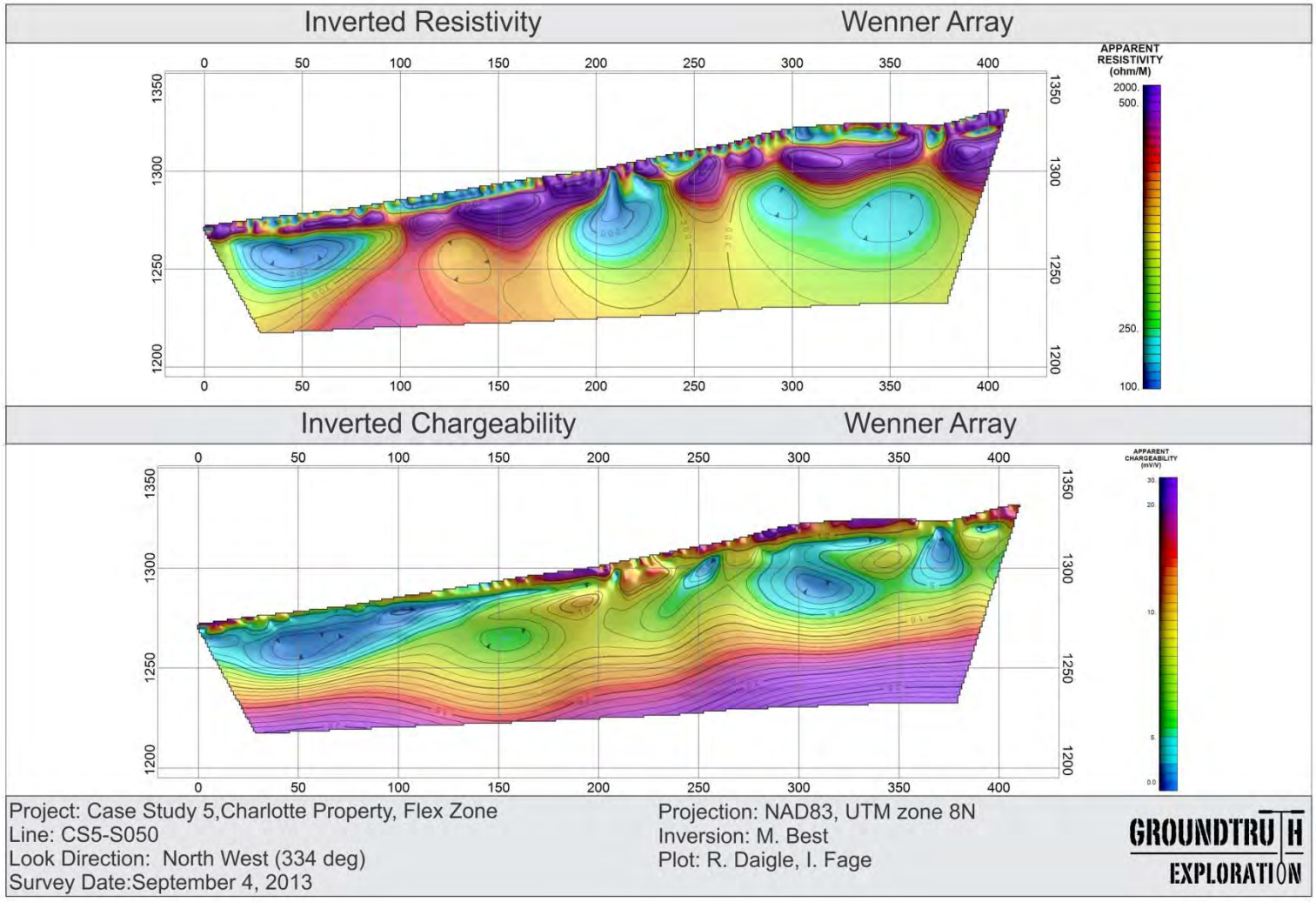
Inverted Resistivity
Wenner Array
APPARENT RESISTIVITY (ohm/M)
2000.
500.
250.
100.
Inverted Chargeability
Wenner Array
APPARENT CHARGEABILITY (mV/V)
Project: Case Study 5,Charlotte Property, Flex Zone
Line: CS5-S050
Look Direction: North West (334 deg)
Survey Date:September 4, 2013
Projection: NAD83, UTM zone 8N
Inversion: M. Best
Plot: R. Daigle, I. Fage
GROUNDTRUTH EXPLORATION

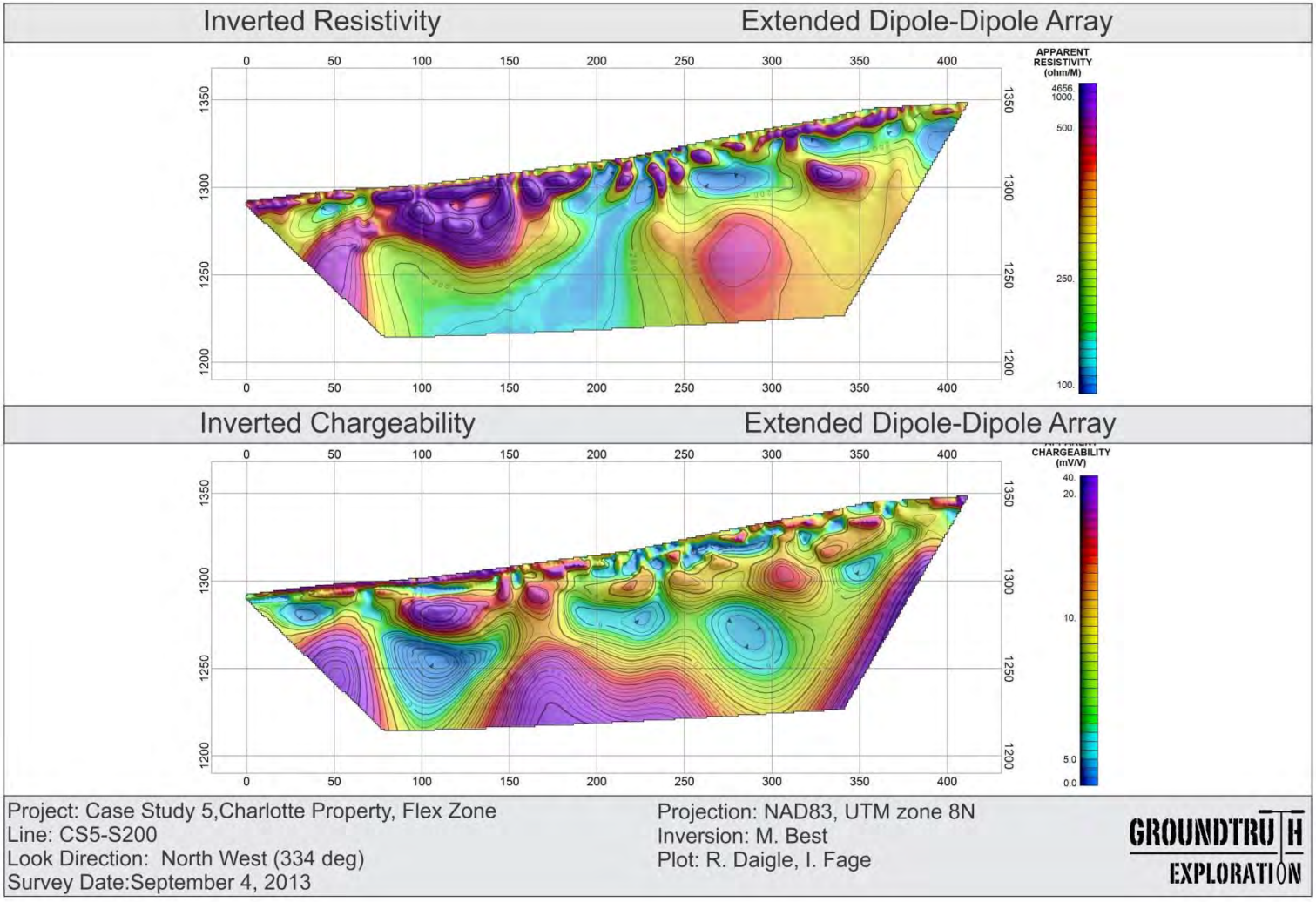
Inverted Resistivity
Extended Dipole-Dipole Array
APPARENT RESISTIVITY (ohm/M)
4656.
1000.
500.
250.
100.
Inverted Chargeability
Extended Dipole-Dipole Array
CHARGEABILITY (mV/V)
40.
20.
10.
5.0
0.0
0
50
100
150
200
250
300
350
400
1350
1300
1250
1200
Project: Case Study 5,Charlotte Property, Flex Zone
Line: CS5-S200
Look Direction: North West (334 deg)
Survey Date:September 4, 2013
Projection: NAD83, UTM zone 8N
Inversion: M. Best
Plot: R. Daigle, I. Fage
GROUNDTRUTH
EXPLORATION

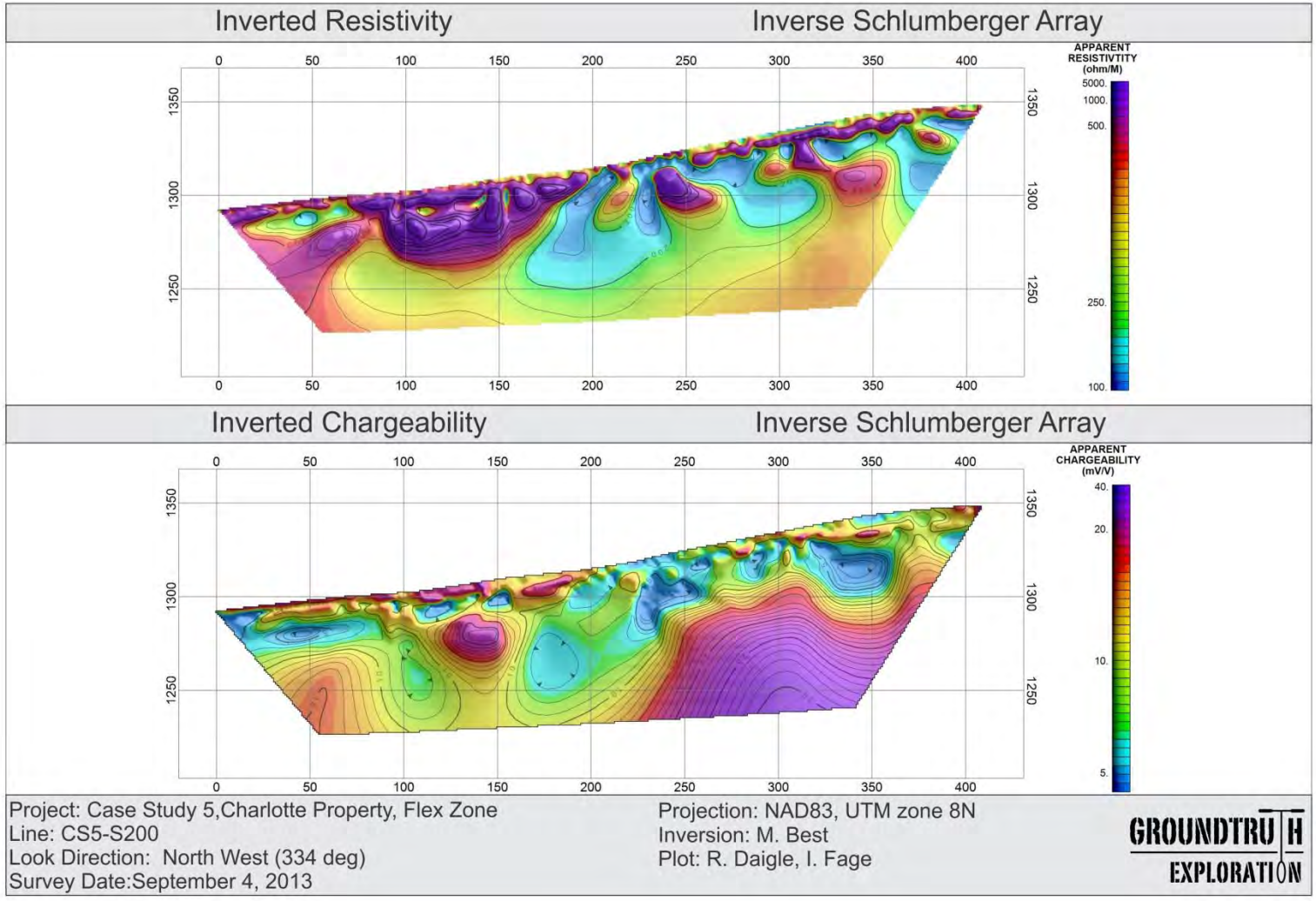
Inverted Resistivity
Inverse Schlumberger Array
APPARENT RESISTIVTITY (ohm/M)
5000.
1000.
500.
250.
100.
0
50
100
150
200
250
300
350
400
1350
1300
1250
Inverted Chargeability
Inverse Schlumberger Array
APPARENT CHARGEABILITY (mV/V)
40.
20.
10.
5.
Project: Case Study 5,Charlotte Property, Flex Zone
Line: CS5-S200
Look Direction: North West (334 deg)
Survey Date:September 4, 2013
Projection: NAD83, UTM zone 8N
Inversion: M. Best
Plot: R. Daigle, I. Fage
GROUNDTRUTH EXPLORATION

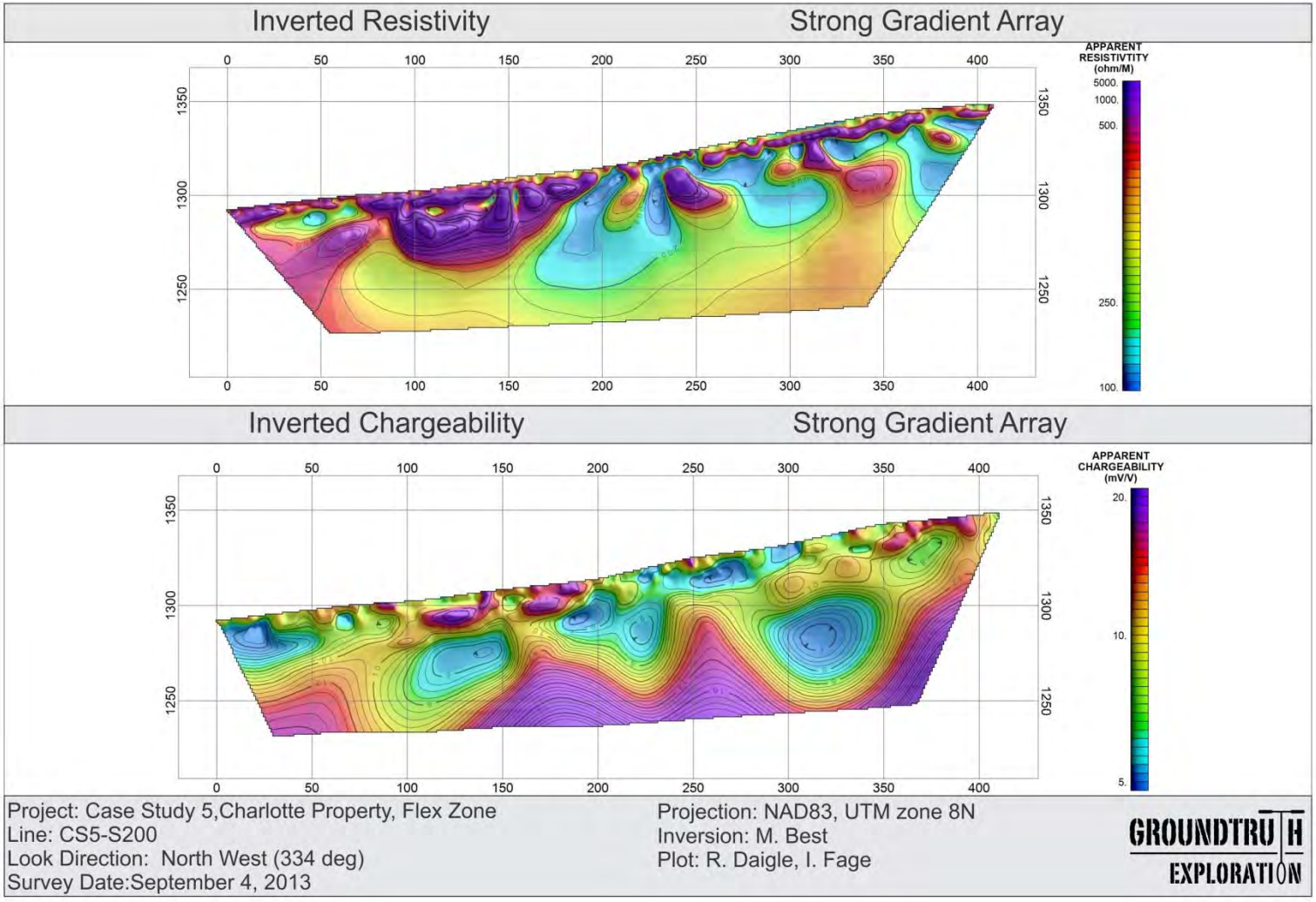
Inverted Resistivity
Strong Gradient Array
APPARENT RESISTIVTITY (ohm/M)
5000.
1000.
500.
250.
100.
Inverted Chargeability
Strong Gradient Array
APPARENT CHARGEABILITY (mV/V)
20.
10.
5.
0
50
100
150
200
250
300
350
400
1350
1300
1250
Project: Case Study 5,Charlotte Property, Flex Zone
Line: CS5-S200
Look Direction: North West (334 deg)
Survey Date:September 4, 2013
Projection: NAD83, UTM zone 8N
Inversion: M. Best
Plot: R. Daigle, I. Fage
GROUNDTRUTH EXPLORATION

INTERPRETATION

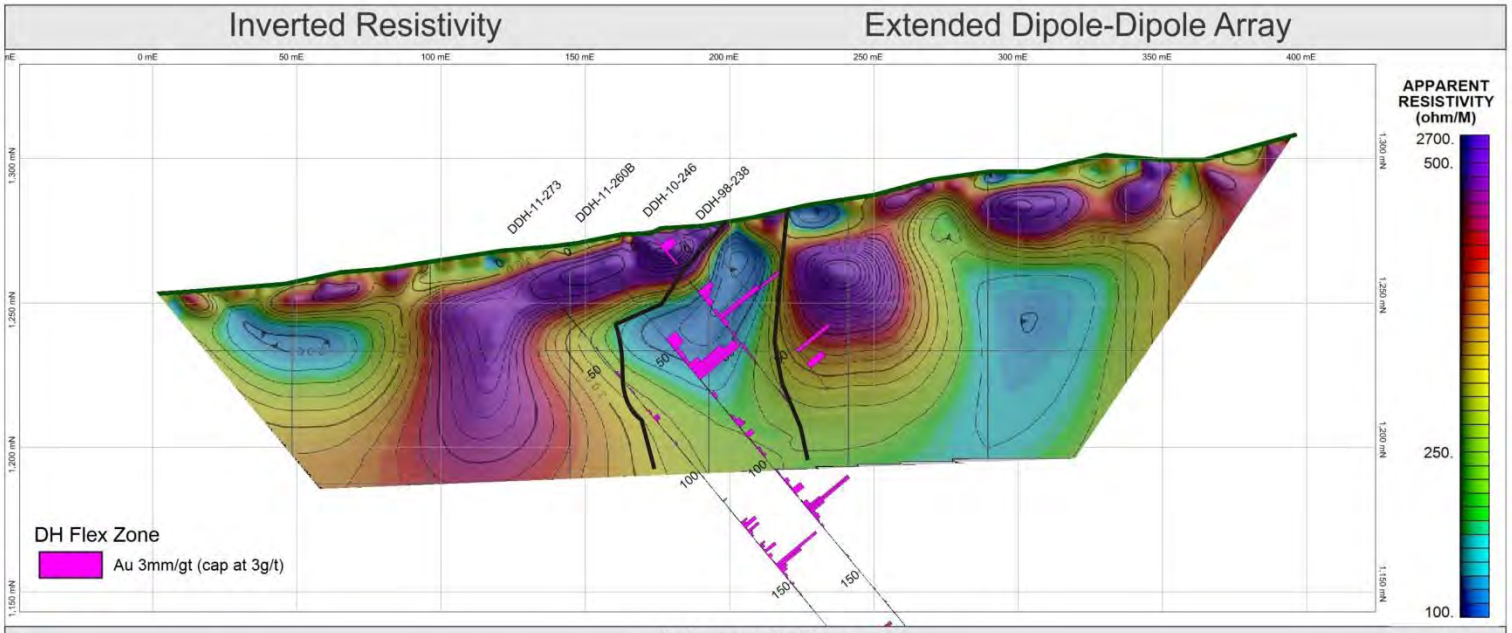

Interpretation

- o mineralization in veins with conductive sulphides
- o individual veins not seen - see low resistivity caused by sulphides associated with overall zone
- o mineralization extends beyond depth of HRRIP system but still mapped upper portion
- o black lines outline extent of mineralization
- o low resistivity zone also on inverse Schlumberger, Wenner and strong gradient

Project: Case Study 5,Charlotte Property, Flex Zone
Line: CS5-S050N
Look Direction: North West (334 deg)
Survey Date: September 5, 2013

Projection: NAD83, UTM zone 8N
Scale: 1 : 2,000
Inversion: M. Best
Plot: R. Daigle, I. Fage

GROUNDTRUTH EXPLORATION

Inverted Resistivity — Pole-Dipole Array

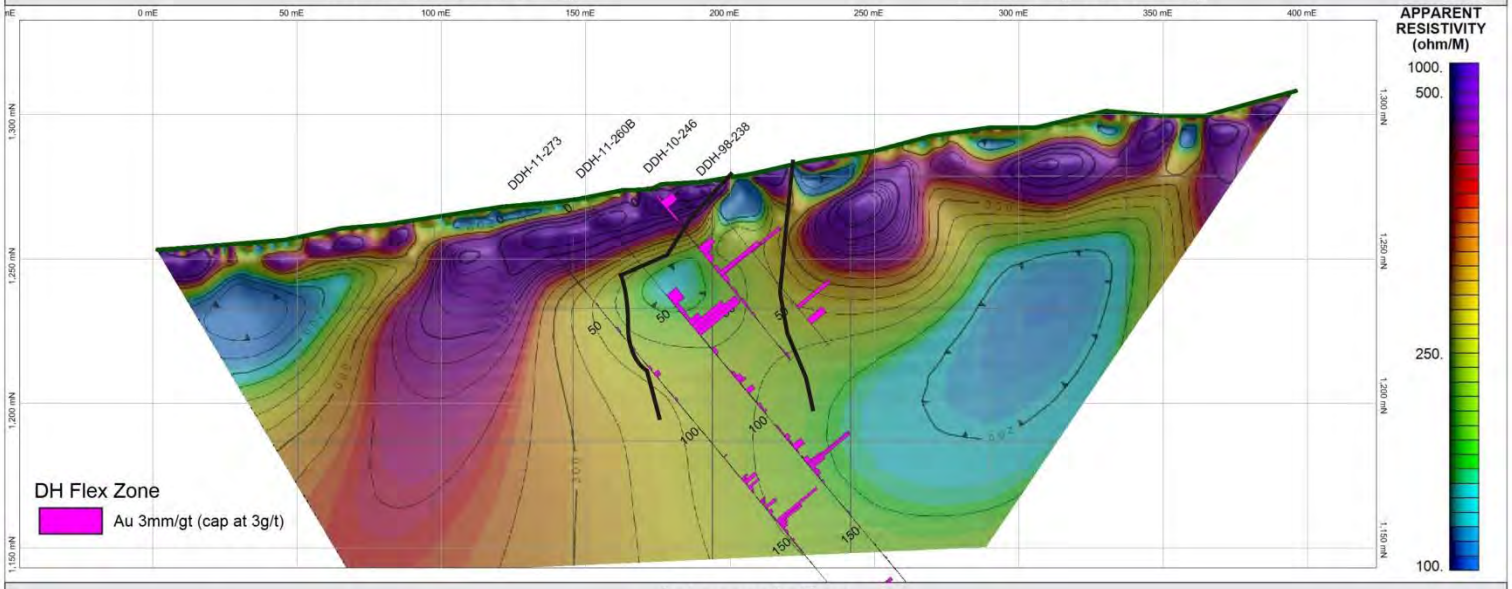

Interpretation

- o pole-dipole outlines deeper mineralized (low resistivity) zone
- o zone at depth has slightly higher values than upper portion but upper portion consistent with other arrays
- o black lines from dipole-dipole extended array consistent with upper portion of pole-dipole resistivity array
- o higher resistivity at southwest end of section associated with gneissic rocks

Project: Case Study 5,Charlotte Property, Flex Zone	Projection: NAD83, UTM zone 8N
Line: CS5-S050N	Scale: 1 : 2,000
Look Direction: North West (334 deg)	Inversion: M. Best
Survey Date: September 4, 2013	Plot: R. Daigle, I. Fage

GROUNDTRUTH EXPLORATION

Inverted Chargeability — Inverse Schlumberger Array

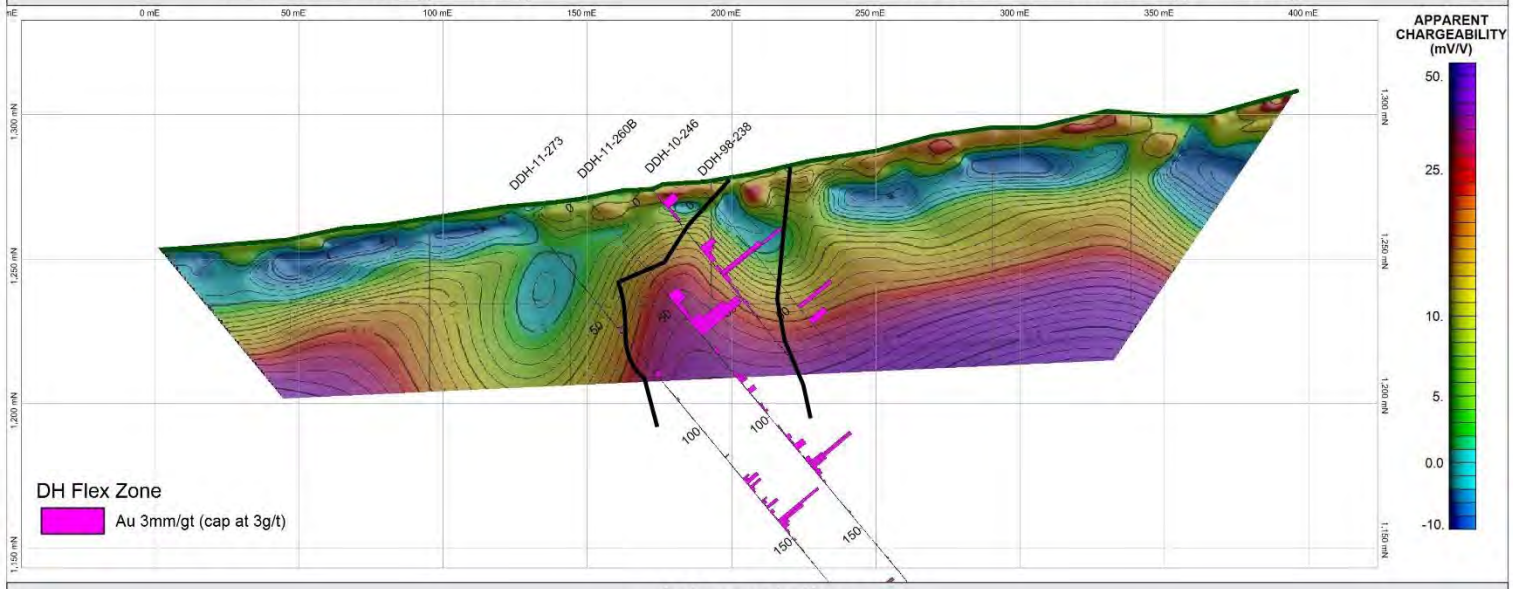

Interpretation

- o black lines from dipole-dipole extended resistivity outline high chargeability zone over mineralization
- o high chargeability appears to extend deeper consistent with mineralization
- o not clear what the deeper high chargeability values to northeast of zone represents
- o dipole-dipole extended chargeability does not agree as well as the inverse Schlumberger array
- o Wenner chargeability does not appear to correlate with mineralization

Project: Case Study 5,Charlotte Property, Flex Zone
Line: CS5-S050N
Look Direction: North West (334 deg)
Survey Date: September 5, 2013

Projection: NAD83, UTM zone 8N
Scale: 1 : 2,000
Inversion: M. Best
Plot: R. Daigle, I. Fage

GROUNDTRUTH EXPLORATION

Inverted Chargeability — Pole-Dipole Array

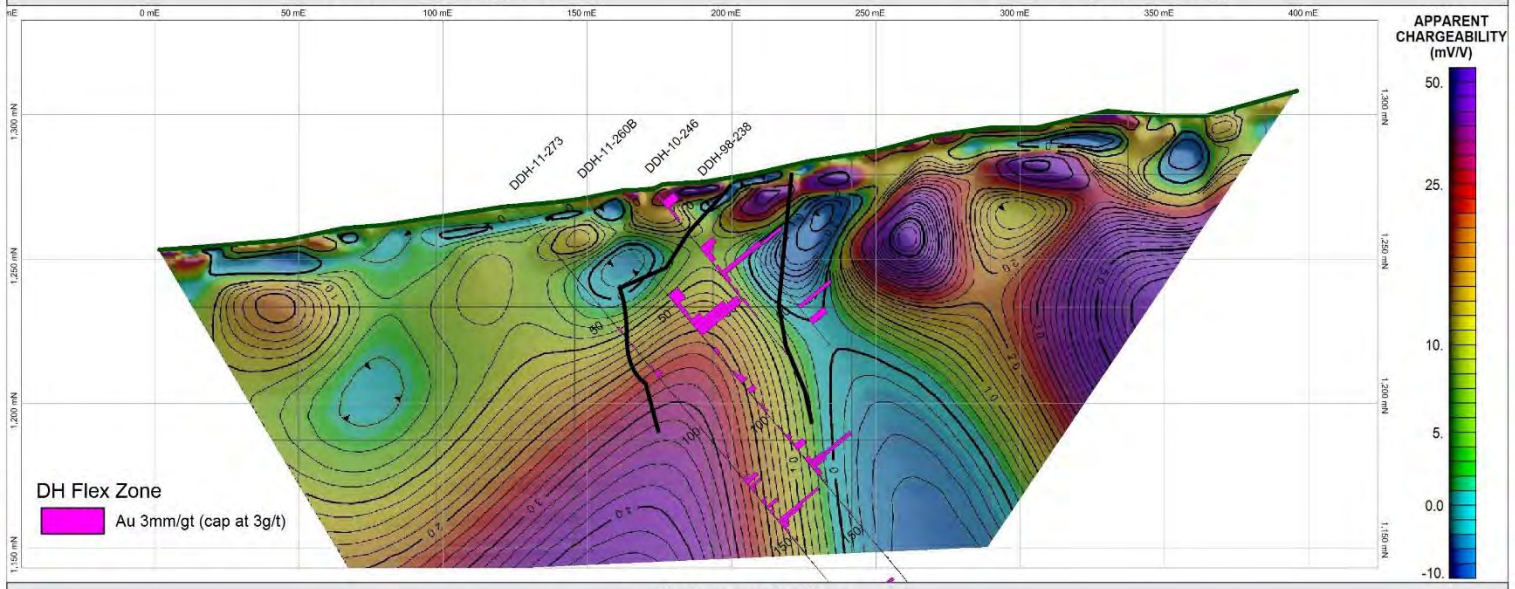

Interpretation

- o black lines outline high chargeability zone associated with mineralization and show the pole-dipole array extends zone at depth
- o upper chargeability zone agrees with the other arrays except the Wenner array
- o not clear what higher chargeability values to northeast represent

Project: Case Study 5,Charlotte Property, Flex Zone	Projection: NAD83, UTM zone 8N
Line: CS5-S050N	Scale: 1 : 2,000
Look Direction: North West (334 deg)	Inversion: M. Best
Survey Date: September 4, 2013	Plot: R. Daigle, I. Fage

GROUNDTRUTH EXPLORATION

Inverted Resistivity — Strong Gradient Array

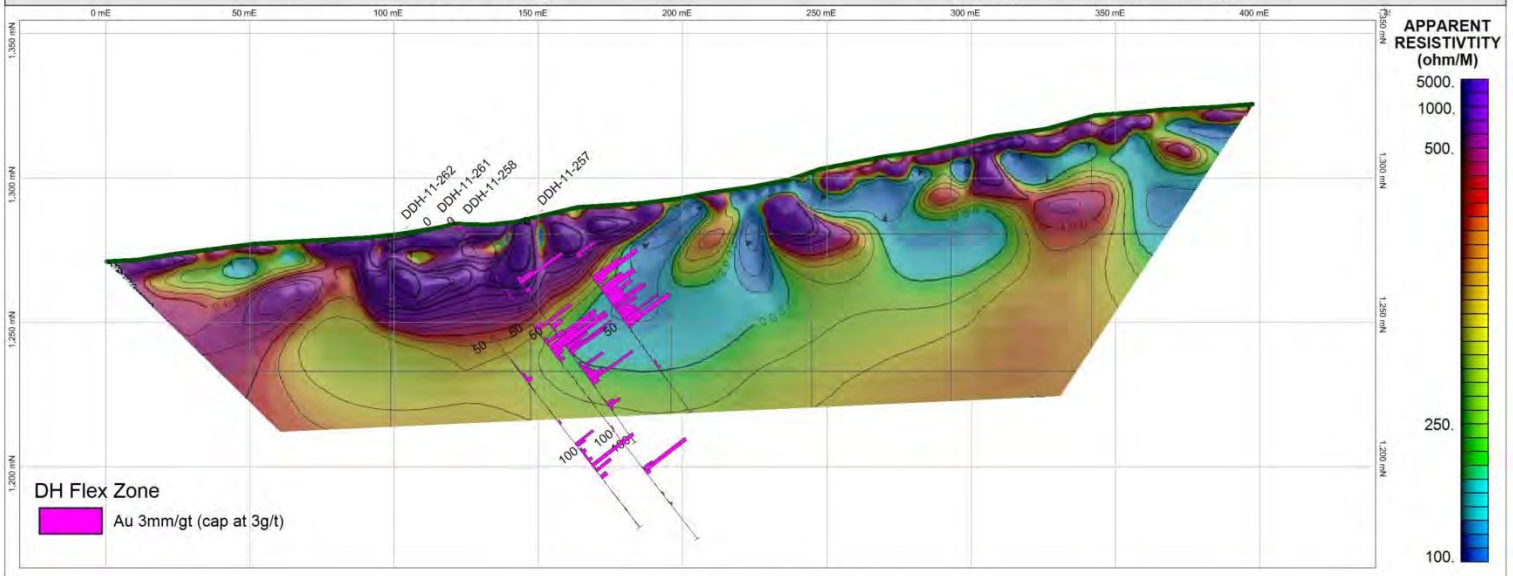

Interpretation

- o mineralization associated with low resistivity zone in upper part but becomes less clear with depth
- o dipole-dipole extended similar but inverse Schlumberger has less well defined low
- o not clear what the high resistivity zone to the SW of low resistivity represents
- o low resistivity zone 200 to 300 m to the northeast of mineralization could be a potential mineralized zone

Project: Case Study 5,Charlotte Property, Flex Zone	Projection: NAD83, UTM zone 8N
Line: CS5-S200N	Scale: 1 : 2,000
Look Direction: North West (334 deg)	Inversion: M. Best
Survey Date: September 6, 2013	Plot: R. Daigle, I. Fage

GROUNDTRUTH EXPLORATION

Inverted Chargeability — Extended Dipole-Dipole Array

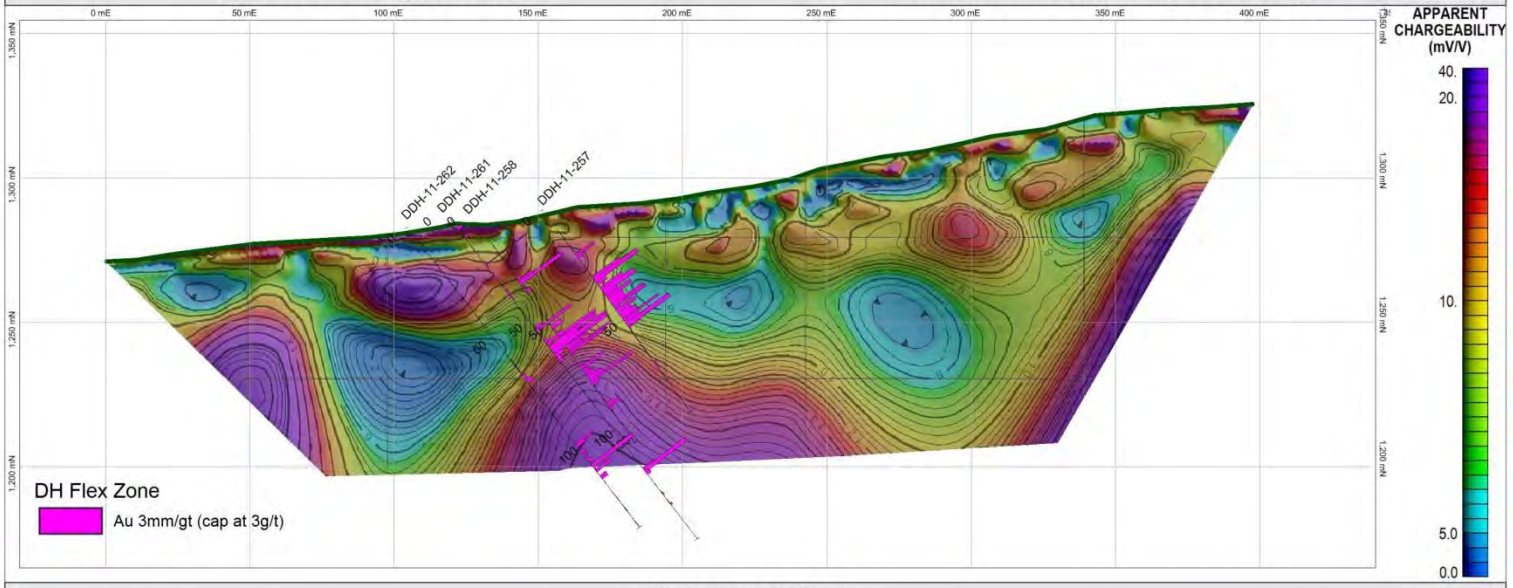

Interpretation

o high chargeability associated with mineralization as expected

o high chargeability extends to depth

o dipole-dipole extended and strong gradient arrays have greater depth extent compared with the inverse Schlumberger array

Project: Case Study 5,Charlotte Property, Flex Zone	Projection: NAD83, UTM zone 8N
Line: CS5-S200N	Scale: 1 : 2,000
Look Direction: North West (334 deg)	Inversion: M. Best
Survey Date: September 6, 2013	Plot: R. Daigle, I. Fage

GROUNDTRUTH EXPLORATION

CS-6 COFFEE

Final Inversions and Interpretation

Geological setting

The Coffee property is located in the Dawson Range about 130 km south of Dawson City. The geology consists of Paleozoic shallowly to moderately southwest-dipping metamorphic rocks of the Yukon-Tanana terrane intruded by Early to Mid-Cretaceous granite (the Coffee Creek granite). Gold is associated with silica, sericite and clay alteration, and occurs in quartz-rich hydrothermal and tectonic breccia, stockworks, and veins. Mineralization is hosted by both granitic and metasedimentary rocks, and appears to be controlled by faults in a number of orientations that cut all rock units. Gold is also associated with a suite of dacite dikes of unknown age (Lewis and Burke, 2011; Wainwright *et al.*, 2011).

In the Supremo and Latte zones, which were investigated in this study (see Fig. CS6-1), the primary structures associated with gold are sub-vertical north-trending faults (Supremo) and steeply south-dipping faults (Latte). Based on overprinting alteration assemblages, these structures are interpreted to have been active fluid conduits during both Jurassic orogenesis and subsequent brittle Cretaceous faulting events. The bulk of the gold appears to have been deposited during the late Cretaceous (MacKenzie *et al.*, 2014).

Geophysical survey

The two HRRIP lines (see location map and photo) have lengths of 415 m (single spread length). The average RMS error of fit is 4.2 % for the entire inverted data set with the largest error equal to 13 % for the pole-dipole (E-infinity) array. Consequently the data quality for this case study is excellent. Two pole-dipole arrays were obtained for each of the two lines, one with the infinity current electrode placed 500 m off one end of the line and the other with the infinity current electrode placed 500 m off the other end. On the Latte line data for the inverse Schlumberger and dipole-dipole extended arrays were also collected. On the Supremo line data for the inverse Schlumberger array were also collected.

Geophysical interpretation

Examples of inverted sections with borehole information overlain for the dipole-dipole extended, pole-dipole (S-infinity) and the inverse Schlumberger are presented below for the Latte line. Mineralization is associated with low to high resistivity values and moderate to high chargeability values. Low resistivity zones on the inverted sections may be related to metasedimentary rocks and/or alteration. Mineralization is within quartz veins, breccia, and veinlets with or without alteration/sulphide, so low to high resistivity values are expected. Disseminated sulphide and/or alteration products within the mineralized zones are the likely cause of the higher chargeability values. Indications are that the chargeability extends beyond the depth limit of the HRRIP surveys consistent with known mineralization. The pole-dipole arrays are sensitive to which end of the line the infinity current electrode is placed. The pole-dipole (N-infinity) and the pole-dipole (S-infinity) have significant differences that are caused by the asymmetry of the pole-dipole array. One way of eliminating this asymmetry is to merge the data from opposite directions into a single merged file for the inversion. For the same spread length

however the pole-dipole array provides greater depth of exploration than the other arrays discussed in this report.

Examples of inverted sections with borehole information overlain for the pole-dipole (E-infinity) and inverse Schlumberger arrays for the Supremo line are presented below. Moderate to high chargeability values are associated with the mineralized zones for the inverted inverse Schlumberger IP section except for the shallow one at the east end of the line. The mineralized zone near the middle of the section on the two pole-dipole arrays however shows up as a chargeability low. High chargeability is associated with the western mineralized zone for all three arrays. Low to high resistivity values are associated with all the mineralize zones for all three arrays. The inverted resistivity for all three arrays over the two main mineralized zones indicate these zones extend deeper than the limit of the HRRIP survey which is consistent with the known mineralization. Both the Latte and Supremo lines have similar behaviour over the mineralized zones, *i.e.* low to high resistivity and moderate to high chargeability.

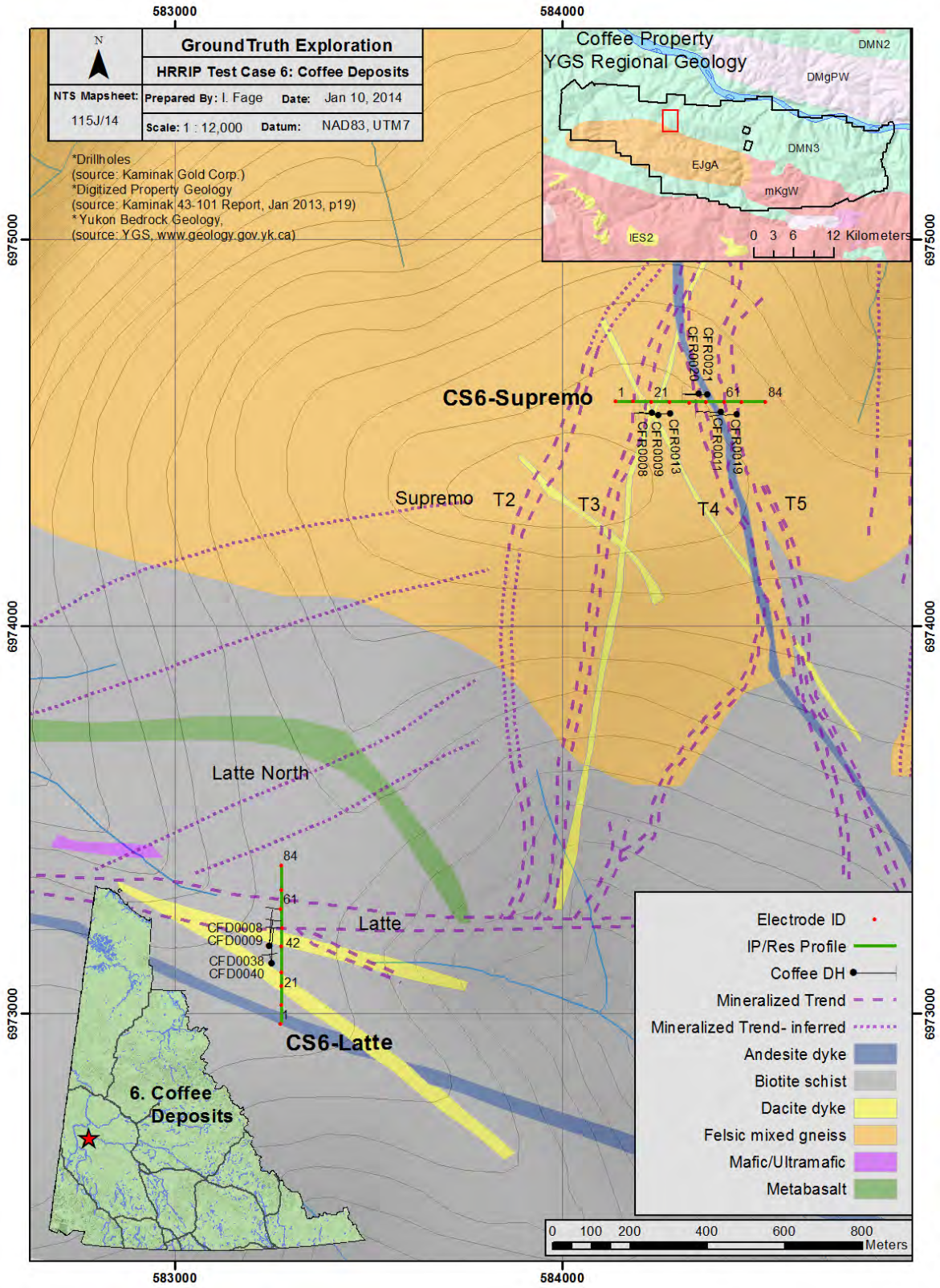

Figure CS6-1. *Location of geophysical lines and surface geology for CS-6, Coffee deposits.*

Figure CS6-2. *Survey over Latte Deposit.*

Figure CS6-3. *Survey over Latte Deposit, Coffee project.*

PAIRED PLOTS

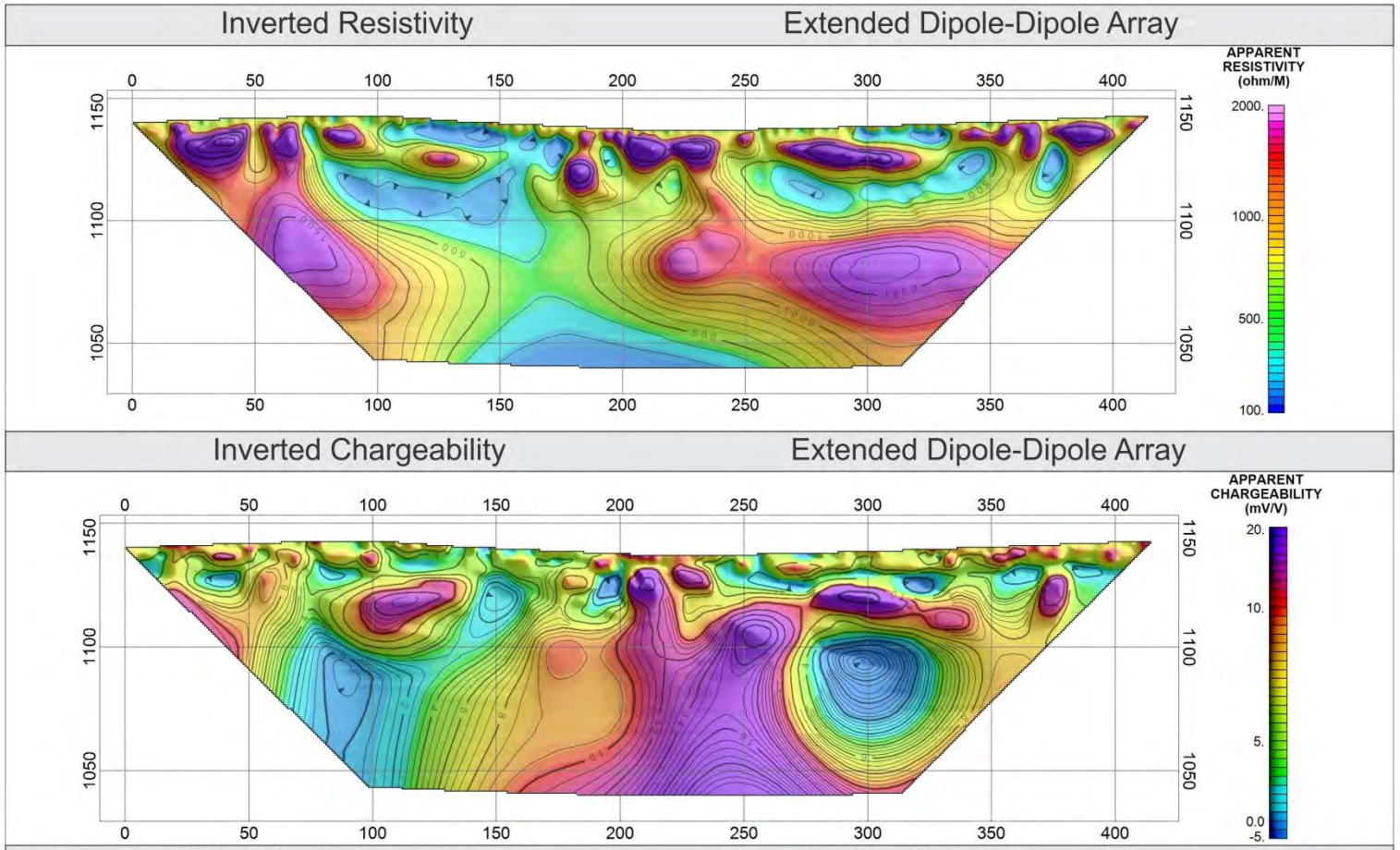

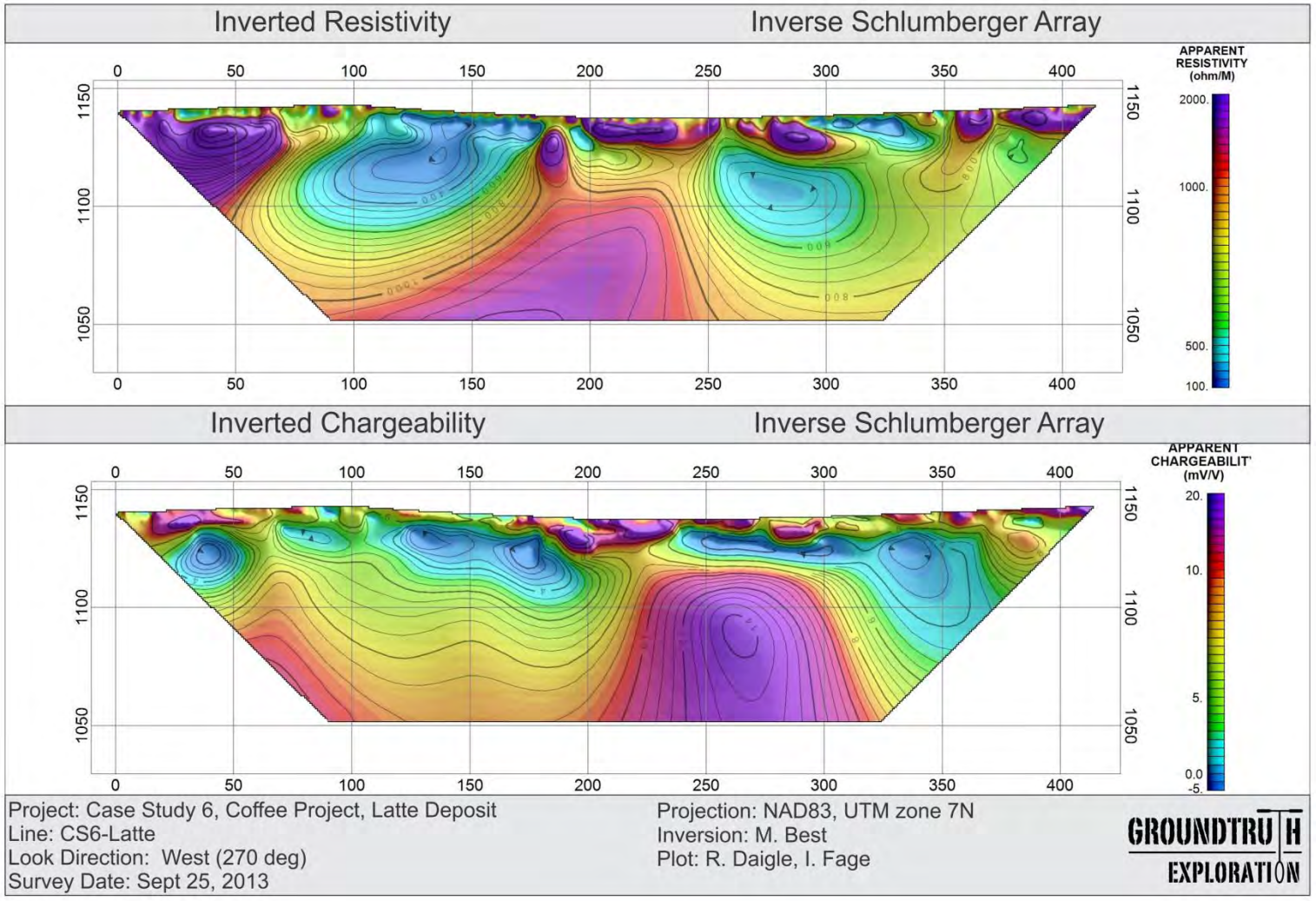
Inverted Resistivity
Inverse Schlumberger Array
APPARENT RESISTIVITY (ohm/M)
2000.
1000.
500.
100.
Inverted Chargeability
Inverse Schlumberger Array
APPARENT CHARGEABILIT' (mV/V)
20.
10.
5.
0.0
-5.
0
50
100
150
200
250
300
350
400
1150
1100
1050
Project: Case Study 6, Coffee Project, Latte Deposit
Line: CS6-Latte
Look Direction: West (270 deg)
Survey Date: Sept 25, 2013
Projection: NAD83, UTM zone 7N
Inversion: M. Best
Plot: R. Daigle, I. Fage
GROUNDTRUTH EXPLORATION

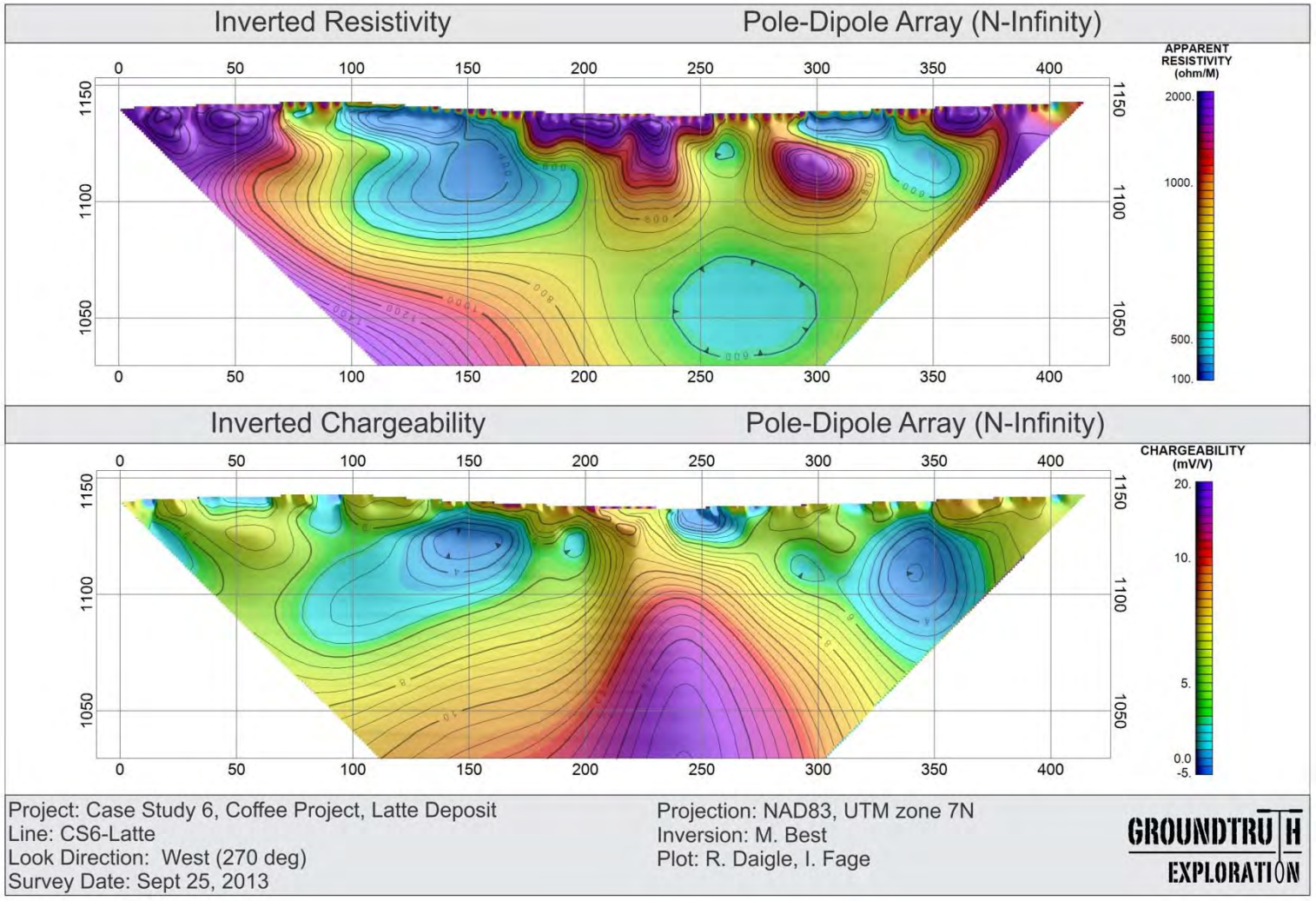
Inverted Resistivity
Pole-Dipole Array (N-Infinity)
APPARENT RESISTIVITY (ohm/M)
2000.
1000.
500.
100.
Inverted Chargeability
Pole-Dipole Array (N-Infinity)
CHARGEABILITY (mV/V)
20.
10.
5.
0.0
-5.
0
50
100
150
200
250
300
350
400
1150
1100
1050
Project: Case Study 6, Coffee Project, Latte Deposit
Line: CS6-Latte
Look Direction: West (270 deg)
Survey Date: Sept 25, 2013
Projection: NAD83, UTM zone 7N
Inversion: M. Best
Plot: R. Daigle, I. Fage
GROUNDTRUTH EXPLORATION

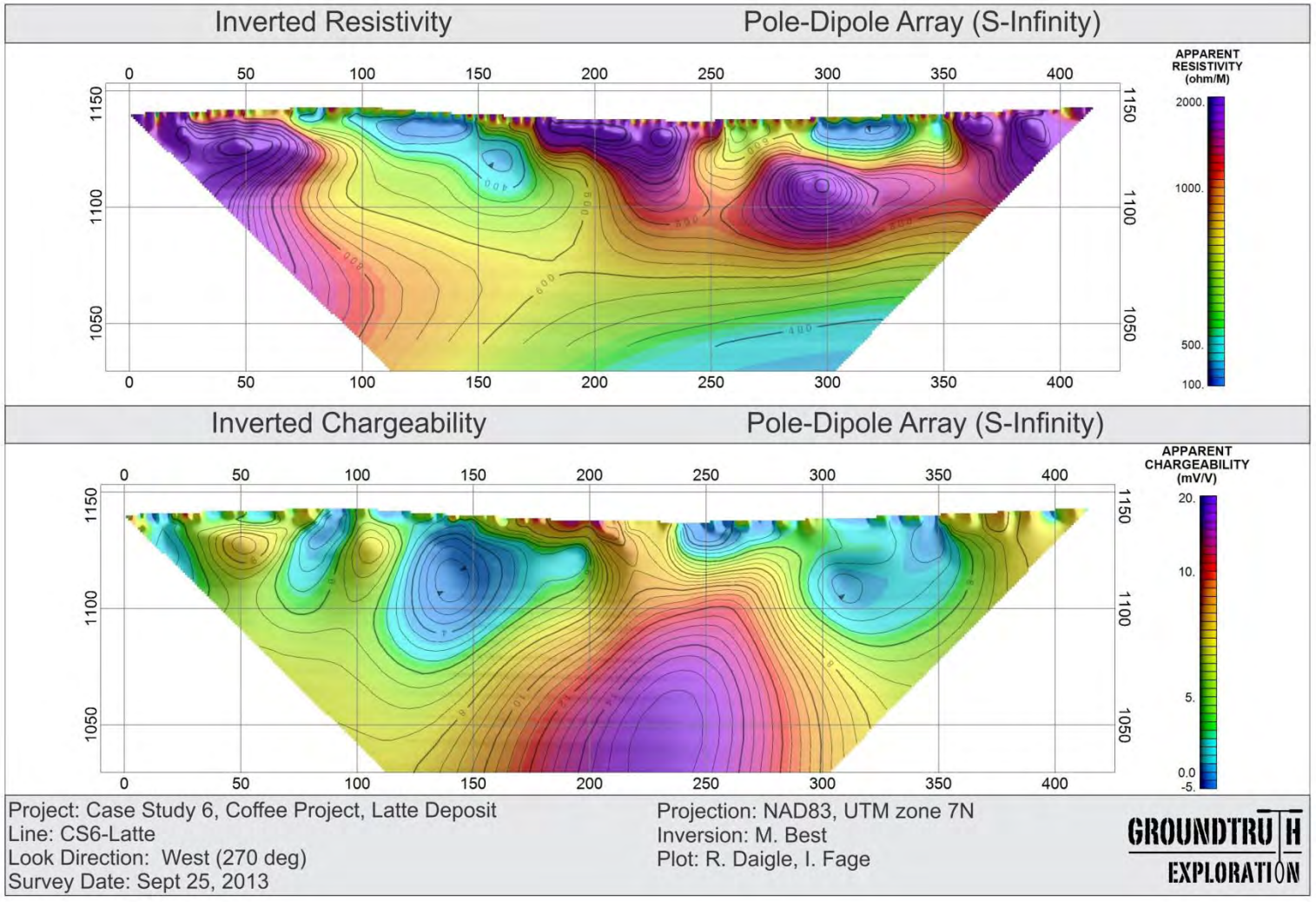
Inverted Resistivity
Pole-Dipole Array (S-Infinity)
APPARENT RESISTIVITY (ohm/M)
2000.
1000.
500.
100.
Inverted Chargeability
Pole-Dipole Array (S-Infinity)
APPARENT CHARGEABILITY (mV/V)
20.
10.
5.
0.0
-5.
0
50
100
150
200
250
300
350
400
1150
1100
1050
Project: Case Study 6, Coffee Project, Latte Deposit
Line: CS6-Latte
Look Direction: West (270 deg)
Survey Date: Sept 25, 2013
Projection: NAD83, UTM zone 7N
Inversion: M. Best
Plot: R. Daigle, I. Fage
GROUNDTRUTH EXPLORATION

Inverted Resistivity — Inverse Schlumberger Array

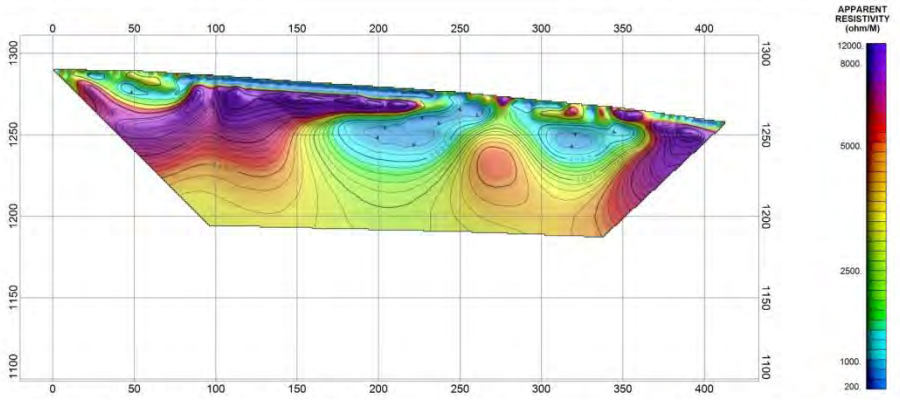

Inverted Chargeability — Inverse Schlumberger Array

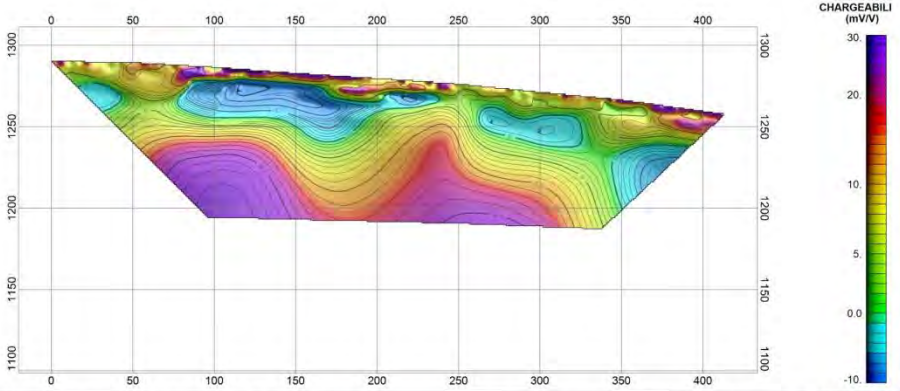

Project: Case Study 6, Coffee Project, Supremo Deposit
Line: CS6-Supremo
Look Direction: North (000 deg)
Survey Date: Sept 26, 2013

Projection: NAD83, UTM zone 7N
Inversion: M. Best
Plot: R. Daigle, I. Fage

GROUNDTRUTH EXPLORATION

Inverted Resistivity — Pole-Dipole Array (E-Infinity)

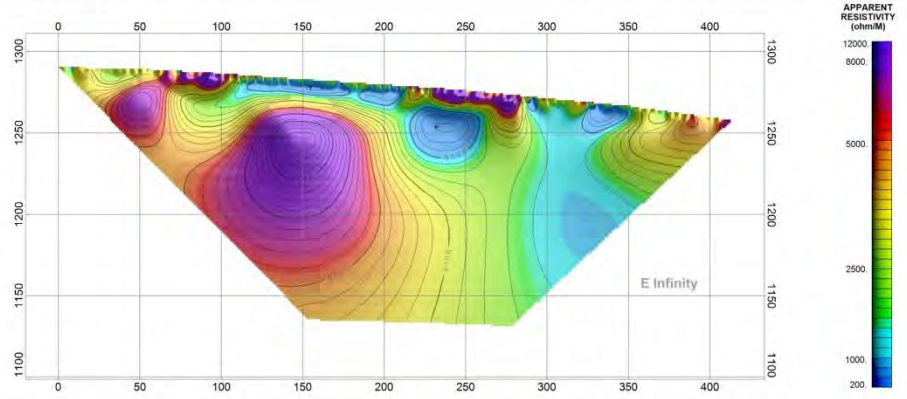

Inverted Chargeability — Pole-Dipole Array (E-Infinity)

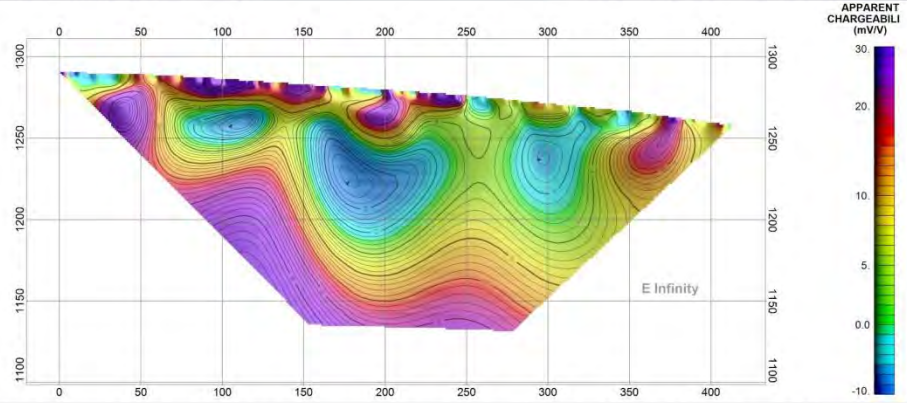

Project: Case Study 6, Coffee Project, Supremo Deposit
Line: CS6-Supremo
Look Direction: North (000 deg)
Survey Date: Sept 26, 2013

Projection: NAD83, UTM zone 7N
Inversion: M. Best
Plot: R. Daigle, I. Fage

GROUNDTRUTH EXPLORATION

Inverted Resistivity — Pole-Dipole Array (W-Infinity)

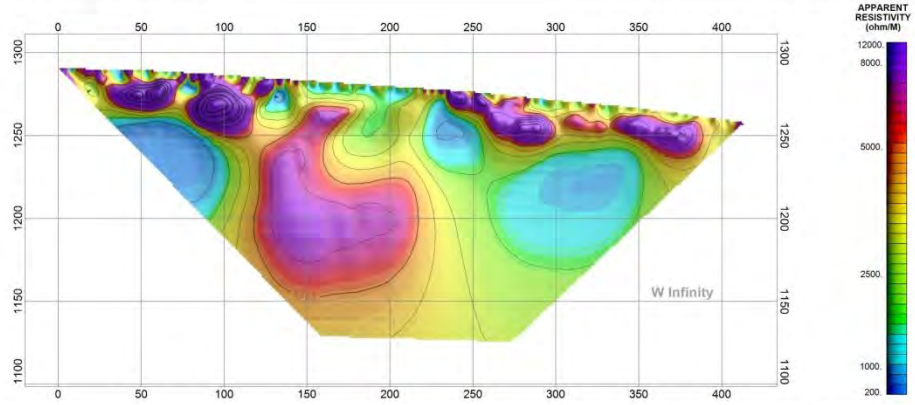

Inverted Chargeability — Pole-Dipole Array (W-Infinity)

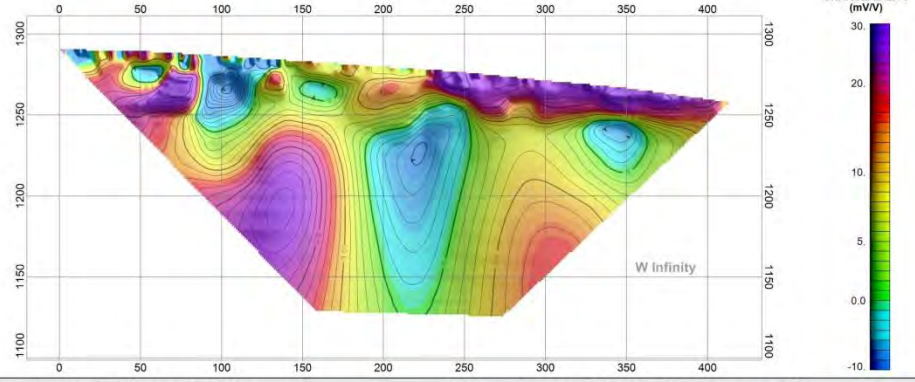

Project: Case Study 6, Coffee Project, Supremo Deposit
Line: CS6-Supremo
Look Direction: North (000 deg)
Survey Date: Sept 26, 2013

Projection: NAD83, UTM zone 7N
Inversion: M. Best
Plot: R. Daigle, I. Fage

GROUNDTRUTH EXPLORATION

INTERPRETATION

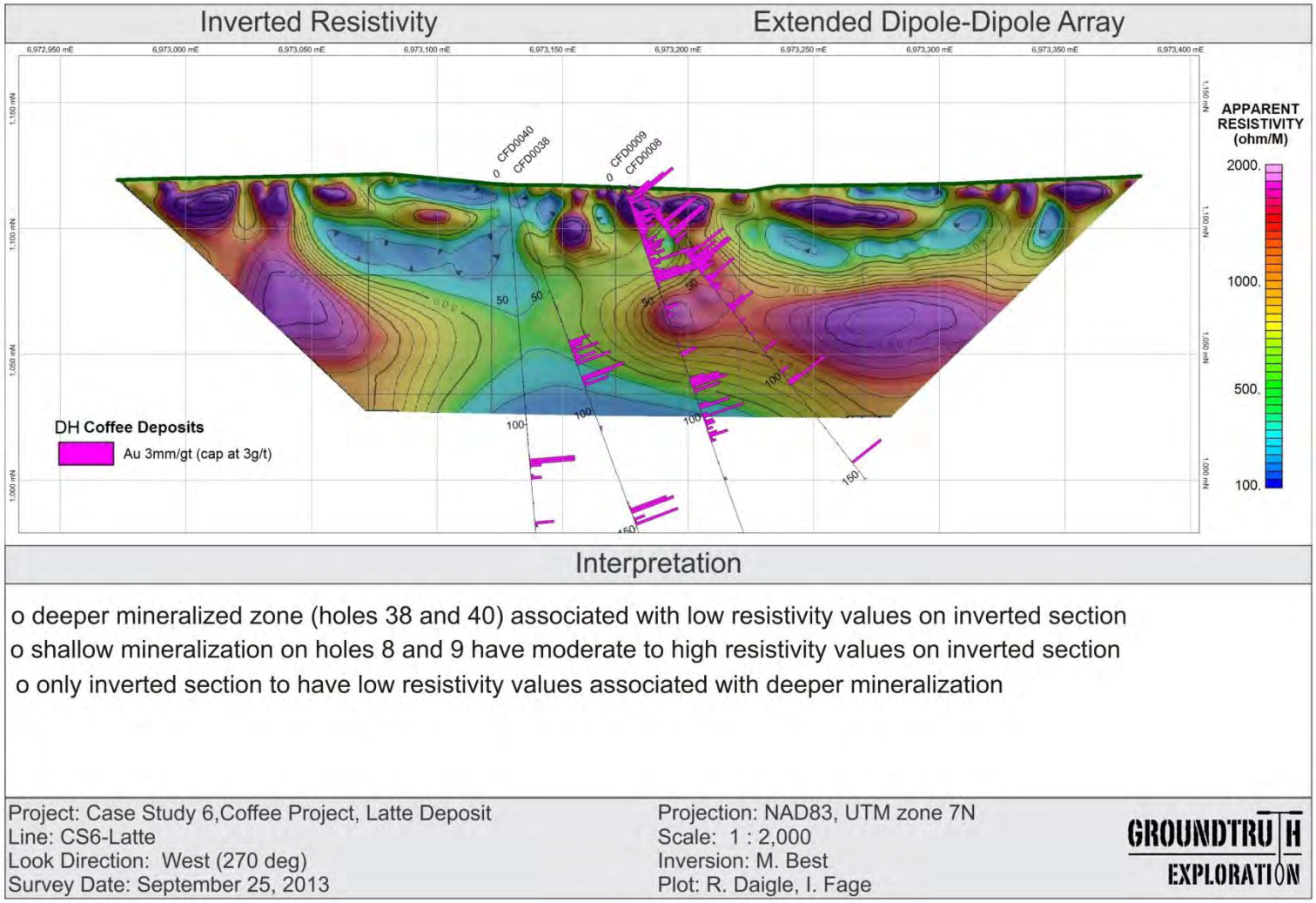

Inverted Resistivity — Pole-Dipole Array (S-Infinity)

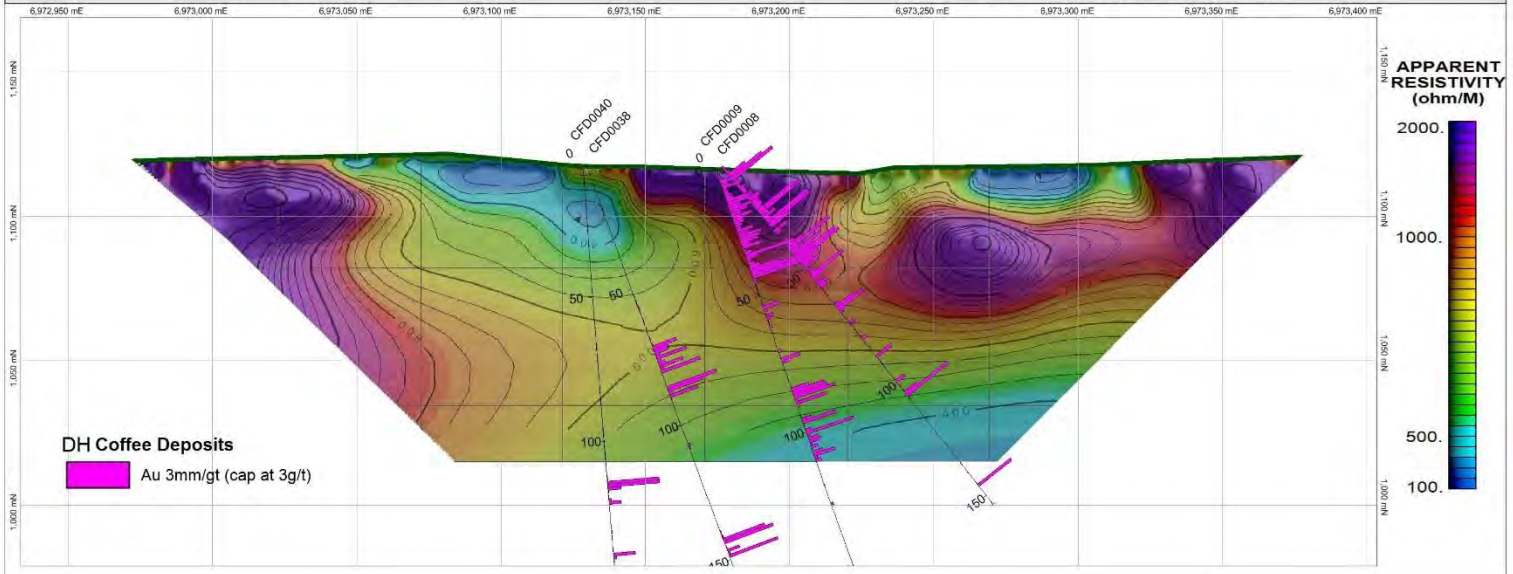

Interpretation

- o shallow mineralization near centre of line associated with high resistivity zone
- o deeper mineralization associated with moderate values of resistivity
- o resistivity lows near surface may be metasedimentary rocks
- o mineralization is within quartz veins, breccias and veinlets - expect moderate to high resistivity values
- o high resistivity is associated with shallow mineralization for all 4 arrays
- o all arrays have moderate resistivity near deeper mineralization except the dipole-dipole extended array

Project: Case Study 6,Coffee Project, Latte Deposit
Line: CS6-Latte
Look Direction: West (270 deg)
Survey Date: September 25, 2013

Projection: NAD83, UTM zone 7N
Scale: 1 : 2,000
Inversion: M. Best
Plot: R. Daigle, I. Fage

GROUNDTRUTH EXPLORATION

Inverted Chargeability — Extended Dipole-Dipole Array

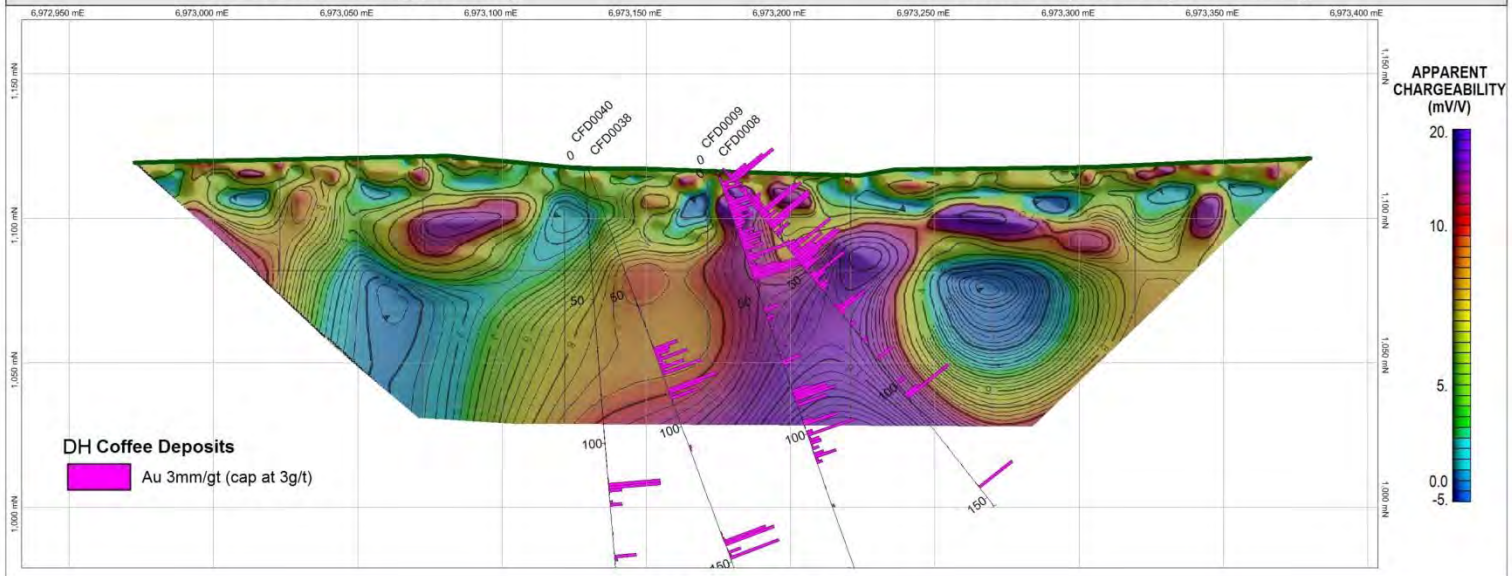

Interpretation

o moderate to high chargeability on inverted section associated with shallow and deep mineralization
o chargeability provides better definition of mineralization than resistivity for this case study

Project: Case Study 6,Coffee Project, Latte Deposit
Line: CS6-Latte
Look Direction: West (270 deg)
Survey Date: September 25, 2013

Projection: NAD83, UTM zone 7N
Scale: 1 : 2,000
Inversion: M. Best
Plot: R. Daigle, I. Fage

GROUNDTRUTH EXPLORATION

Inverted Chargeability — Inverse Schlumberger Array

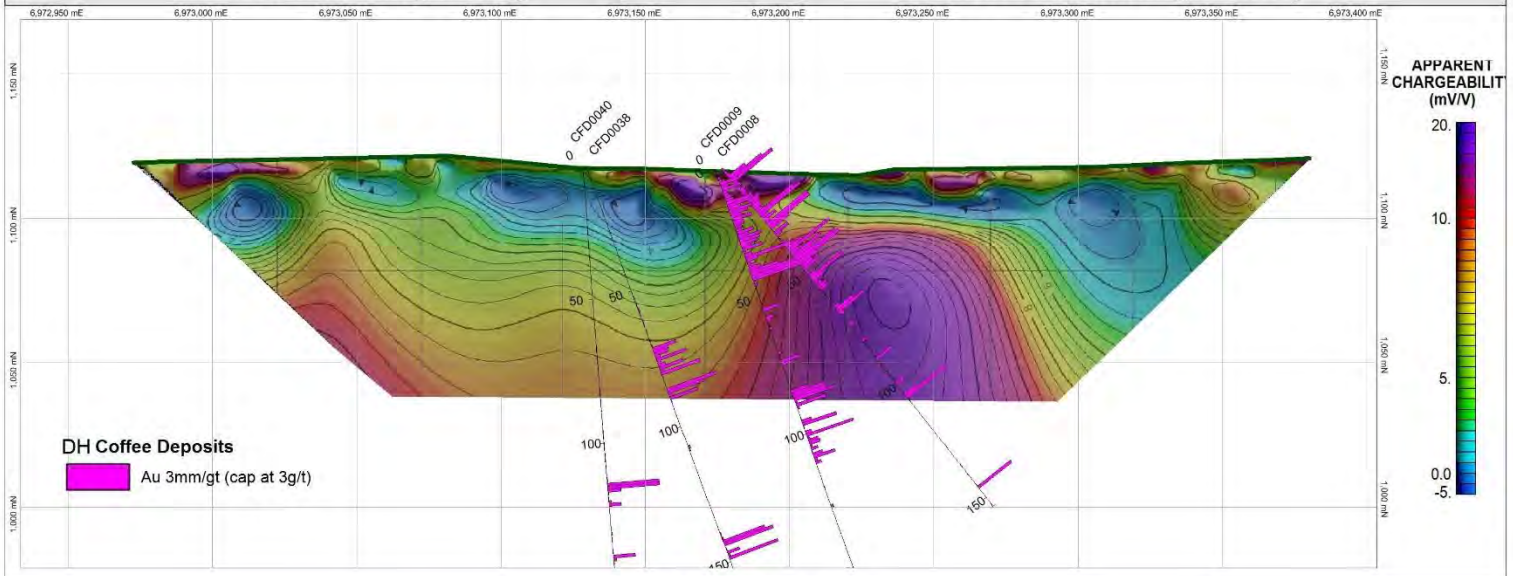

Interpretation

- o mineralized zone in centre of line associated with high chargeability values
- o chargeability values are moderate for deeper mineralization near south end of line
- o chargeability appears to continue at depth consistent with mineralization
- o disseminate pyrite produces the moderate and high chargeability values in mineralized zones
- o pole-dipole arrays provide deeper information than the other arrays
- o high chargeability values occur over the central mineralized zone for all arrays

Project: Case Study 6,Coffee Project, Latte Deposit	Projection: NAD83, UTM zone 7N
Line: CS6-Latte	Scale: 1 : 2,000
Look Direction: West (270 deg)	Inversion: M. Best
Survey Date: September 25, 2013	Plot: R. Daigle, I. Fage

GROUNDTRUTH EXPLORATION

Inverted Resistivity — Pole-Dipole Array (E-Infinity)

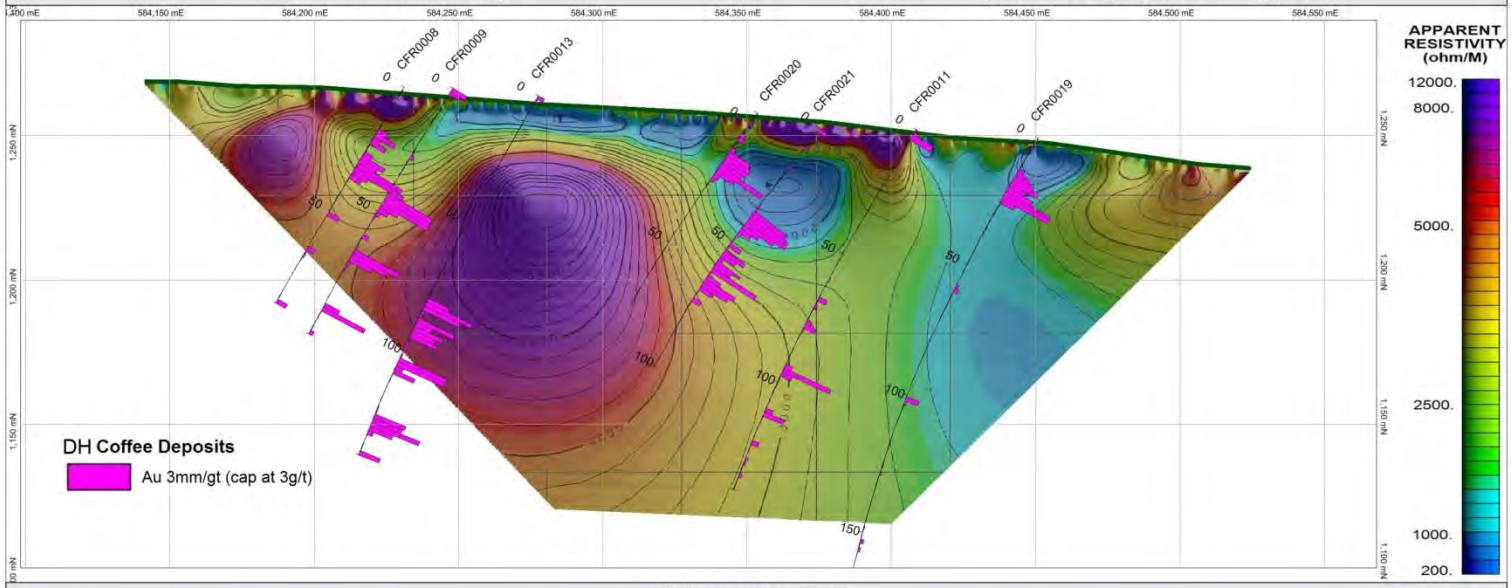

Interpretation

- o mineralization correlates with moderate to high resistivity except near east end of section
- o large resistivity high at west end continues at depth mimicking mineralization
- o shallow mineralization at east end of line appears to be associated with low resistivity metasediments
- o pole-dipole (W-infinity) has low resistivity at west end of line opposite of pole-dipole(E-infinity)
- o moderate resistivity for the inverse Schlumberger array is consistent with pole-diole(E-infinity) at west end of line
- o mineralization with moderate to high resistivity is consistent for the two lines at the coffee case study

Project: Case Study 6,Coffee Project, Supremo Deposit
Line: CS6-Supremo
Look Direction: North (000 deg)
Survey Date: September 26, 2013

Projection: NAD83, UTM zone 7N
Scale: 1 : 2,000
Inversion: M. Best
Plot: R. Daigle, I. Fage

GROUNDTRUTH EXPLORATION

Inverted Chargeability — Inverse Schlumberger Array

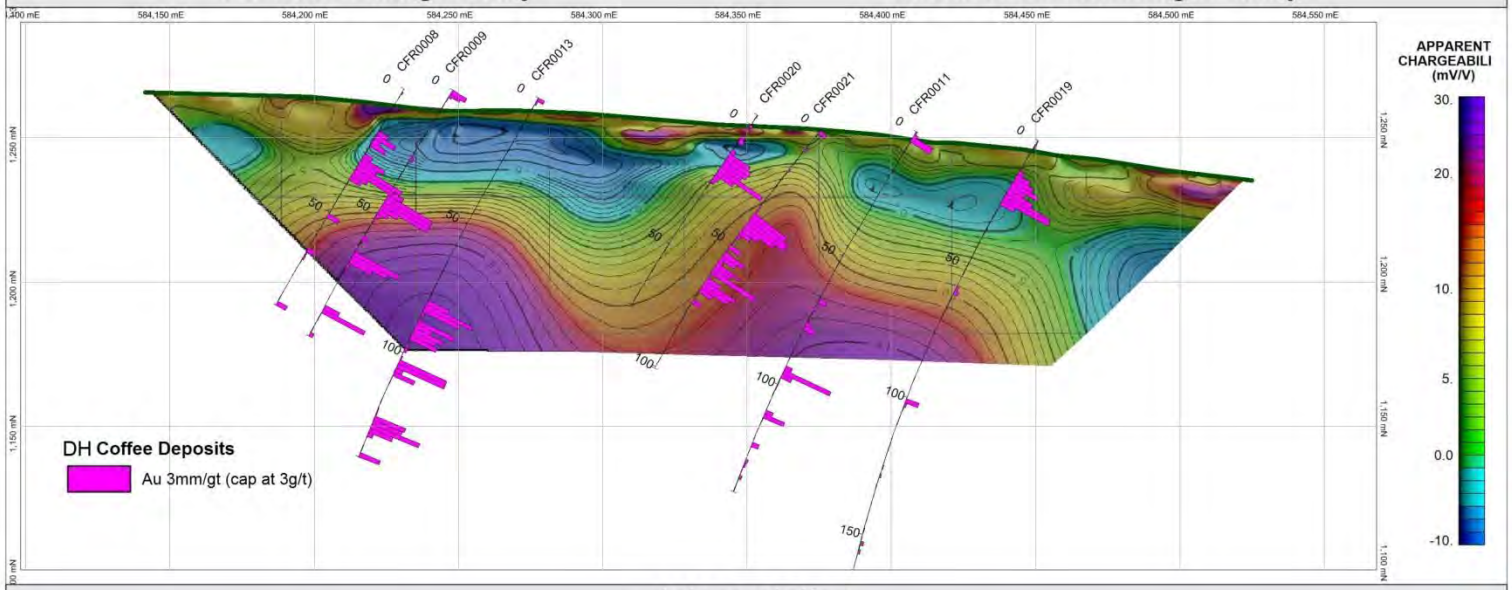

Interpretation

- o high chargeability values are associated with all mineralized zones except the shallow east one
- o high chargeability continues at depth following the main mineralized zones
- o the shallow east mineralization has low chargeability
- o the pole-dipole (E-infinity) array has mixed chargeability associated with the mineralization except at depth at the west end of the line
- o the pole-dipole (W-infinity) has mixed chargeability associated with mineralization along the entire line

Project: Case Study 6,Coffee Project, Supremo Deposit
Line: CS6-Supremo
Look Direction: North (000 deg)
Survey Date: September 26, 2013

Projection: NAD83, UTM zone 7N
Scale: 1 : 2,000
Inversion: M. Best
Plot: R. Daigle, I. Fage

GROUNDTRUTH EXPLORATION

CS-7 QV PROPERTY, VG ZONE

Final Inversions and Interpretation

Geological setting

The QV Property is on the west side of the Yukon River along the same geologic trend as the White Gold property (Golden Saddle deposit; this study). The QV property is underlain by mid to late Paleozoic, amphibolite grade metamorphic rocks of the Yukon-Tanana terrane that include amphibolite, a variety of felsic-intermediate gneiss and age equivalent feldspar porphyry dikes/sills, and metasediments (Gibson, 2013). The entire package strikes north-northwest and dips moderately to the east, and appears to be a continuation of the same rock package that occurs on the Golden Saddle case study.

Gold mineralization at the VG zone is hosted in a package of metavolcanic and meta-intrusive rocks broadly consisting of felsic-intermediate gneiss, amphibolite, and mafic-ultramafic gneiss (Fig. CS7-1). These rocks are in turn crosscut by at least two generations of feldspar porphyry dikes and mafic dikes/sills. The gold mineralization at VG is dominated by vein-fracture controlled and disseminated pyrite within lode and stockworked quartz veins, quartz vein breccia, zones of pervasive silicification, and locally as limonite within strongly oxidized zones. Minor molybdenite, galena, and chalcopyrite are also observed and are generally associated with stockworked quartz veins and breccia zones. Sulphide minerals typically comprise <10% of the mineralized zones and there appears to be a correlation between pyrite volume and gold grades within areas of strong quartz-kspar > sericite-carbonate alteration. Based on drilling, gold mineralization is preferentially located within felsic-intermediate gneiss and feldspar porphyry dikes, and gold grades rapidly decrease when the mineralized structure(s) intersect mafic-ultramafic units.

Geophysical survey

A single line of HRRIP data were collected for the QV case study (see plan map below) with a length of 415 m, *i.e.*, a single spread length. The average RMS error of fit is 3.09% with the highest error equal to 3.36%. The data quality was excellent for this case study. The boreholes are slightly offset from line L03 but no more than a few tens of metres. Data for the dipole-dipole extended, inverse Schlumberger (new array design), strong gradient, and pole-dipole arrays were collected. Paired plots of the inverted resistivity and chargeability for all 4 arrays are presented below.

Geophysical interpretation

Examples of inverted sections with borehole information overlain for the pole-dipole array (both resistivity and chargeability) and dipole-dipole extended (chargeability) are provided below. Mineralization is generally associated with high resistivity values and moderate to high chargeability values. The high resistivity values are related to the metavolcanic and meta-intrusive rocks hosting the gold mineralization. The quartz vein fracture system containing the mineralization also has high resistivity values. Chargeability is likely associated with the disseminated pyrite and other sulphide minerals associated with the gold mineralization. The pole-dipole array illustrates how different arrays provide different depths of exploration. In this

case the deeper mineralization has high resistivity and chargeability values that can only be inferred from the other three arrays. The absolute values of chargeability are relatively low for this case study so the use of moderate and high are misleading. The values for all 4 arrays are really moderate at most. The fault tectonic breccia zone appears to have mixed resistivity values depending on the depth and its location along the line. This is most obvious on the dipole-dipole extended inverted array.

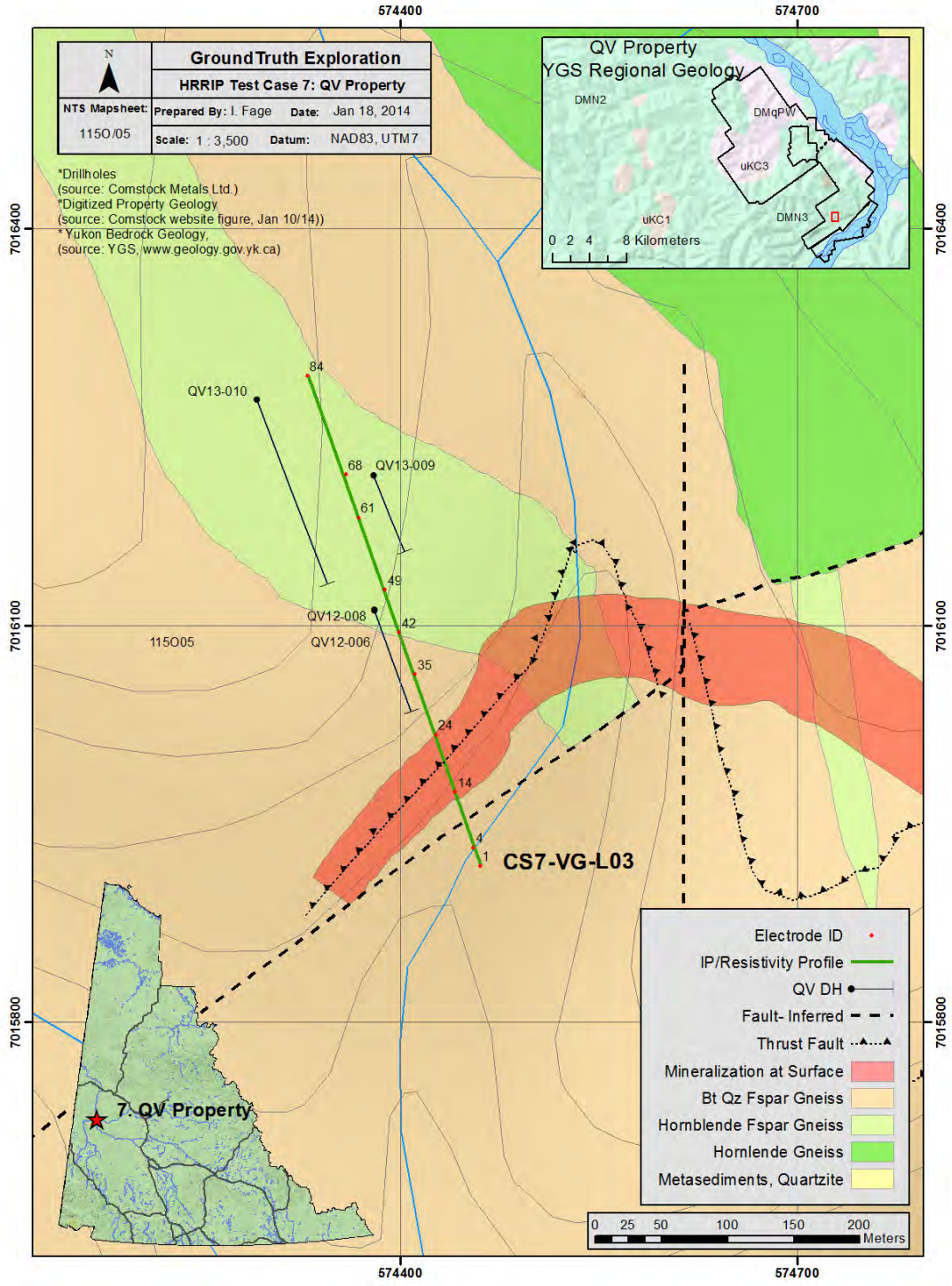

Figure CS7-1. *Location of geophysical survey line and surface geology for VG Zone on QV Project.*

Figure CS7-2. *Prepping line at VG Zone on QV Project.*

Figure CS7-3. *Survey line at VG Zone.*

PAIRED PLOTS

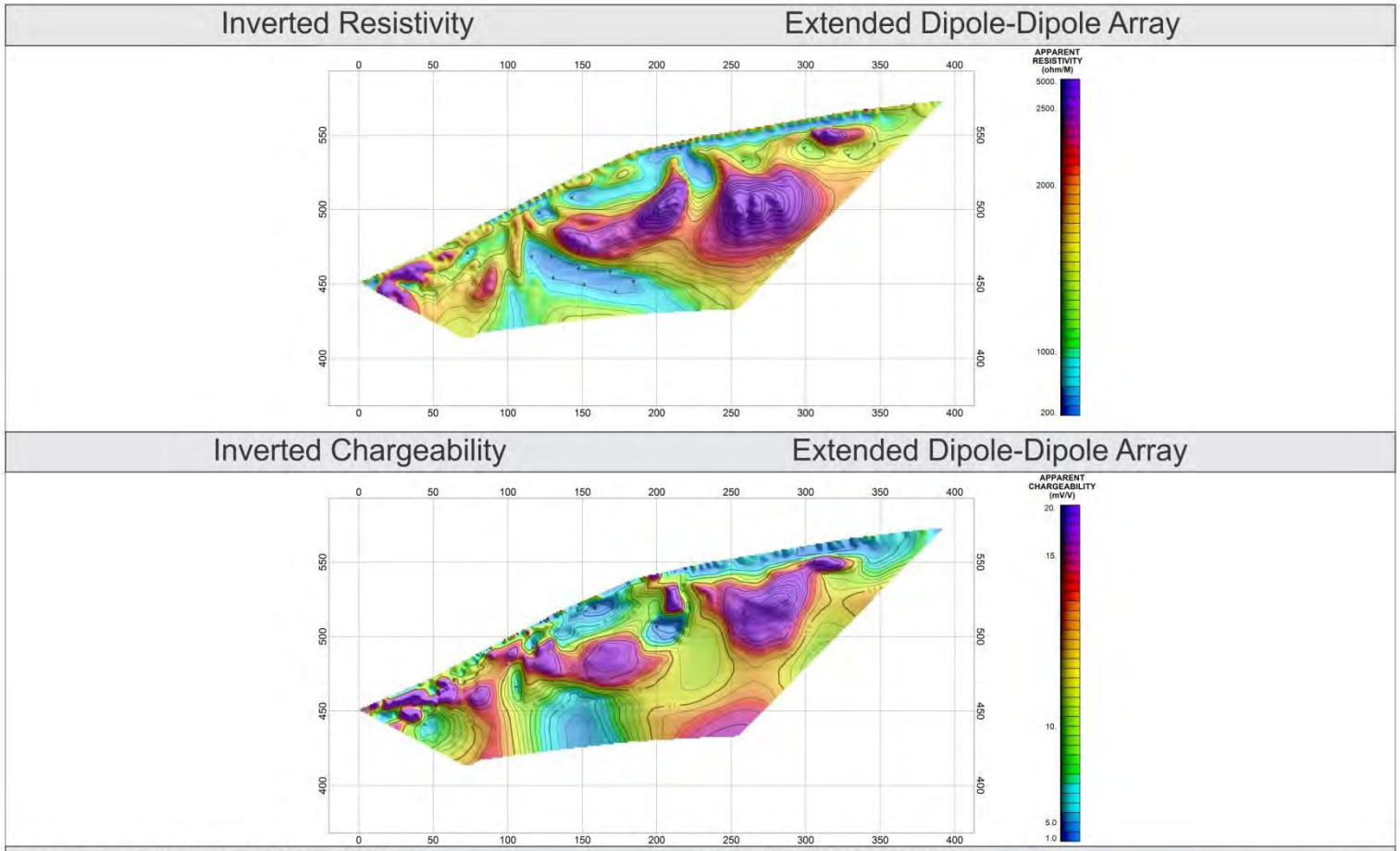

Inverted Resistivity — Inverse Schlumberger Array

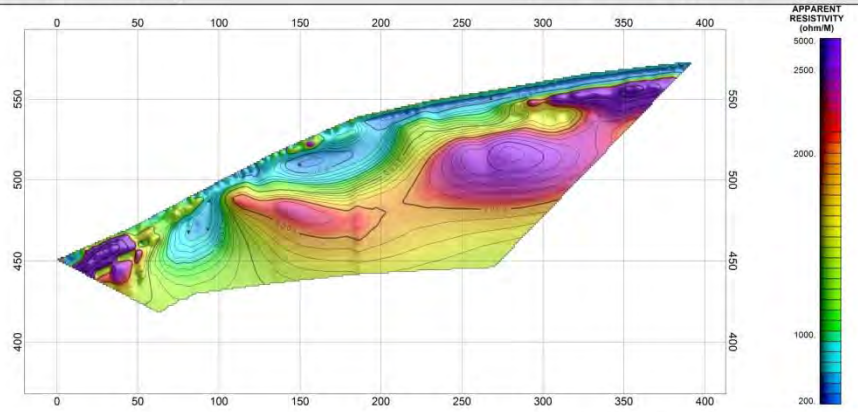

Inverted Chargeability — Inverse Schlumberger Array

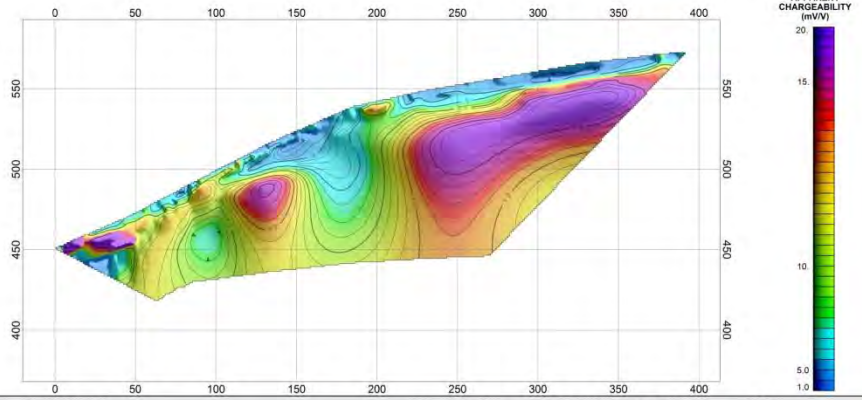

Project: Case Study 7, QV Project, VG Zone
Line: CS7-VG-L03
Look Direction: West (252 deg)
Survey Date: October 7, 2013

Projection: NAD83, UTM zone 7N
Inversion: M. Best
Plot: R. Daigle, I. Fage

GROUNDTRUTH EXPLORATION

Inverted Resistivity — Strong Gradient Array

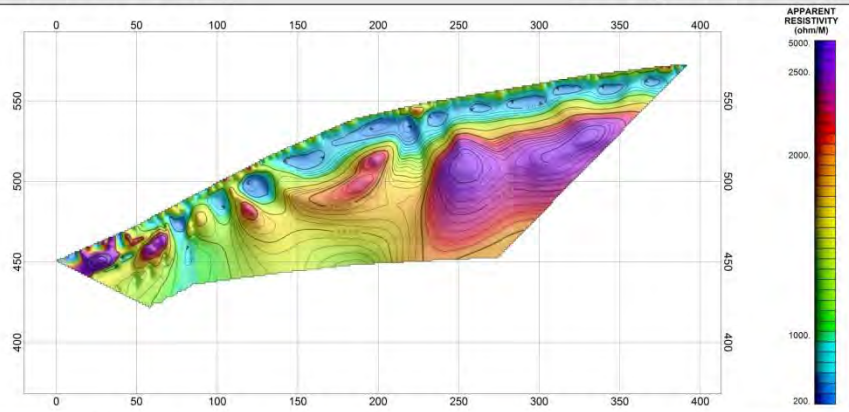

Inverted Chargeability — Strong Gradient Array

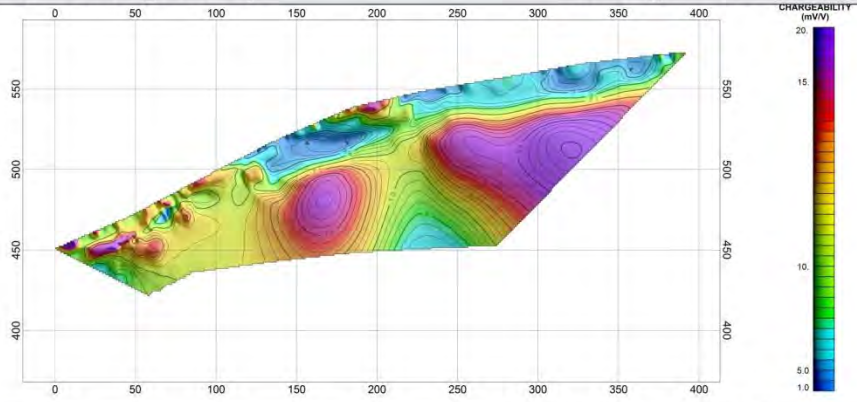

Project: Case Study 7, QV Project, VG Zone
Line: CS7-VG-L03
Look Direction: West (252 deg)
Survey Date: October 7, 2013

Projection: NAD83, UTM zone 7N
Inversion: M. Best
Plot: R. Daigle, I. Fage

GROUNDTRUTH EXPLORATION

Inverted Resistivity — Pole-Dipole Array

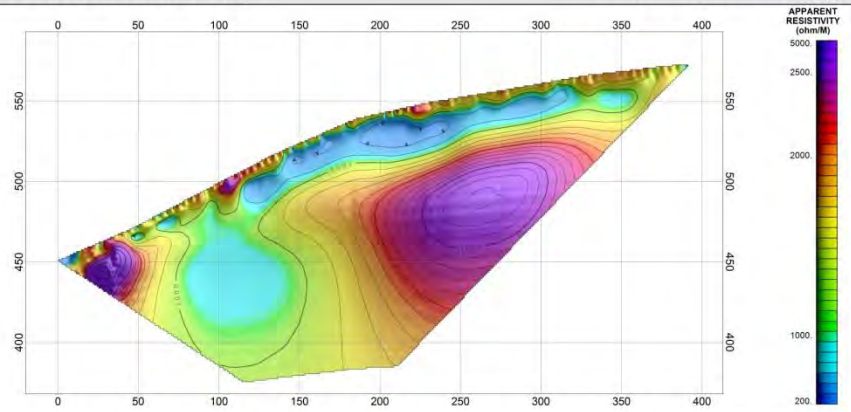

Inverted Chargeability — Pole-Dipole Array

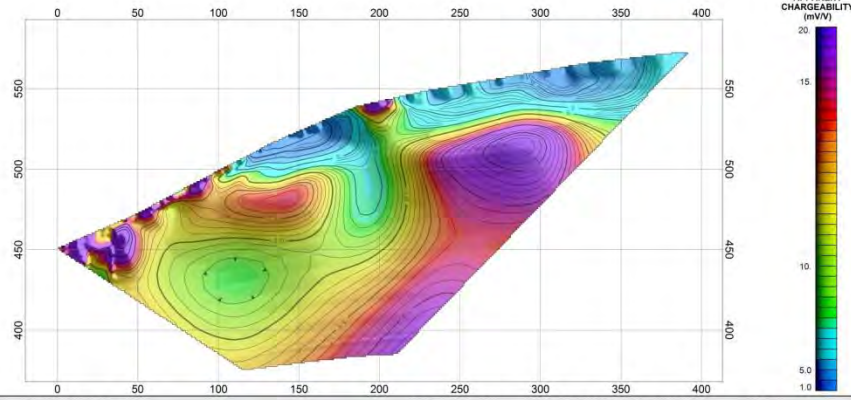

Project: Case Study 7, QV Project, VG Zone
Line: CS7-VG-L03
Look Direction: West (252 deg)
Survey Date: October 7, 2013

Projection: NAD83, UTM zone 7N
Inversion: M. Best
Plot: R. Daigle, I. Fage

GROUNDTRUTH EXPLORATION

INTERPRETATION

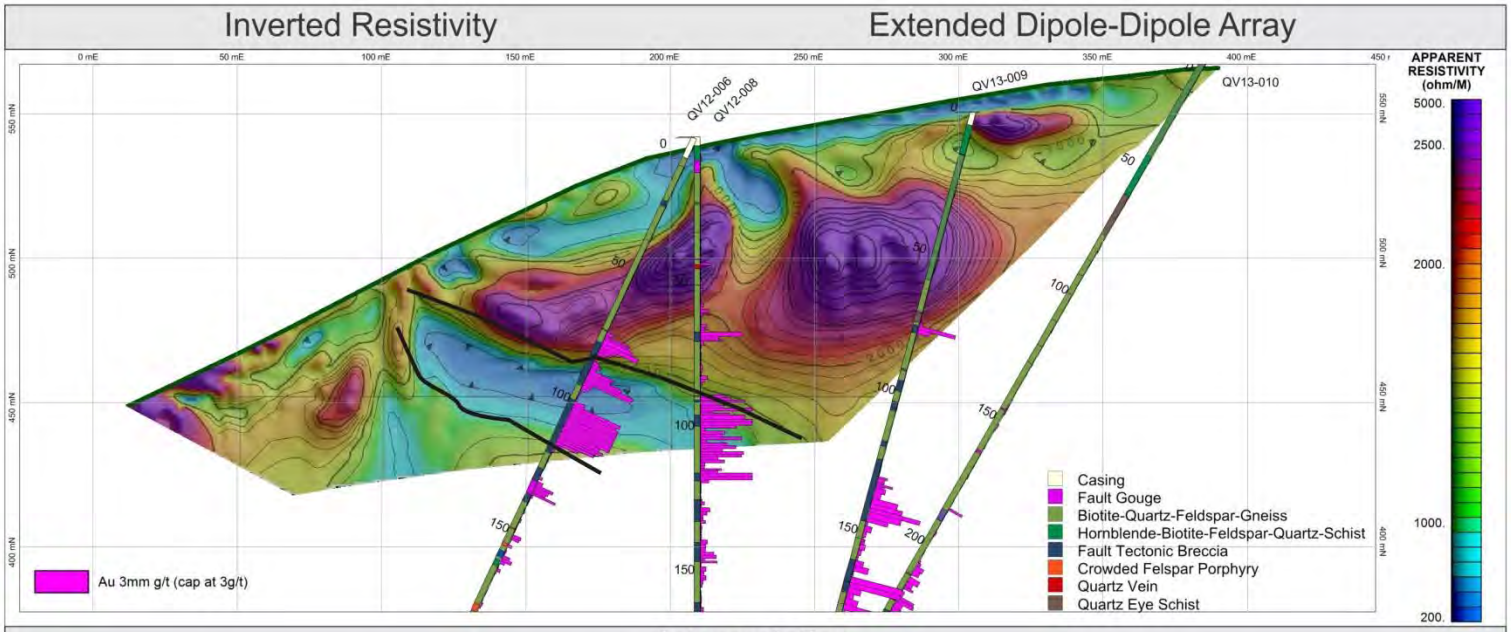

Interpretation

- o mineralization has low to moderate resistivity values
- o similar for all resistivity arrays - pole-dipole slightly higher than other 3 arrays
- o low to moderate resistivity expected because association of mineralized zone with breccia and sulphides
- o pole-dipole sees deeper mineralization as expected
- o black lines outline mineralized zone

Project: Case Study 7, QV Project, VG Zone
Line: CS7-VG-L03
Look Direction: West (252 deg)
Survey Date: October 7, 2013

Projection: NAD83, UTM zone 7N
Scale: 1 : 2,000
Inversion: M. Best
Plot: R. Daigle, I. Fage

GROUNDTRUTH EXPLORATION

Inverted Resistivity — Pole-Dipole Array

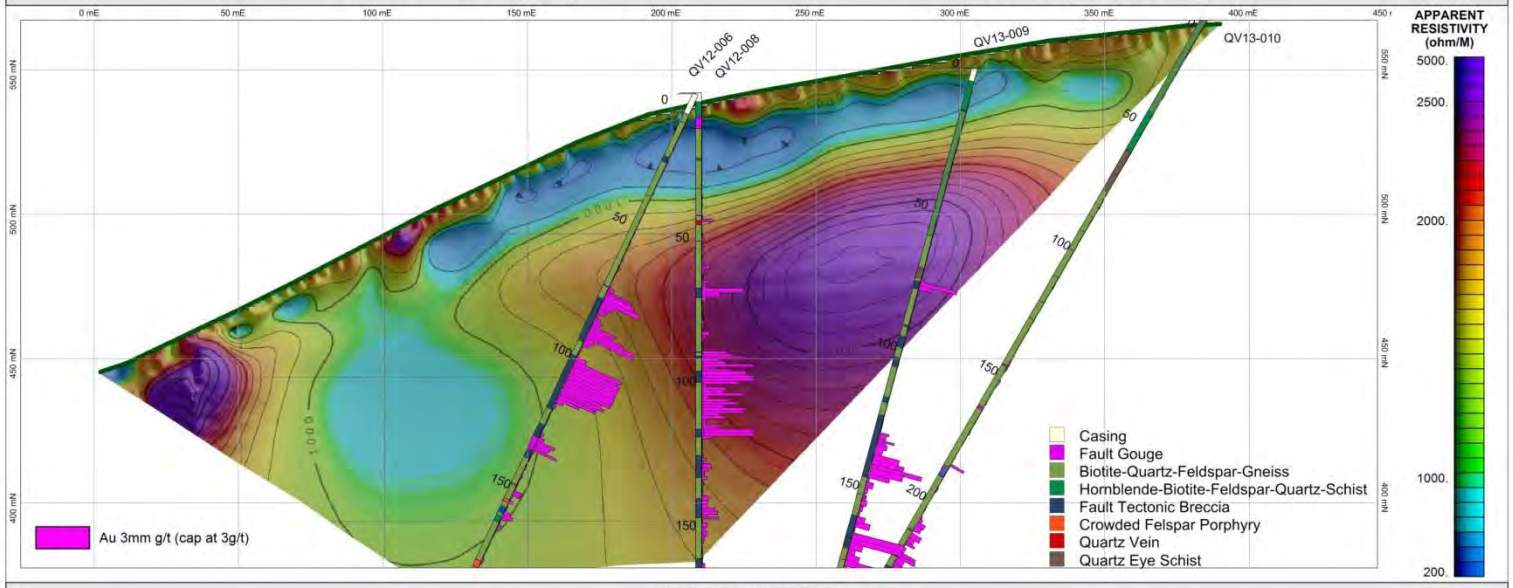

Interpretation

- o mineralization associated with moderate to high resistivity values
- o pole-dipole array extends depth sufficiently to encompass more of the deeper mineralization
- o low resistivity zones not clear - likely is breccia or schist
- o all 3 other arrays have similar behaviour at shallower depths except dipole-dipole extended has lower resistivity than other three associated with mineralization on hole QV12-006.
- o moderate resistivity expected since mineralization in breccia even though host rocks are meta-volcanic and intrusive rocks

Project: Case Study 7, QV Project, VG Zone
Line: CS7-VG-L03
Look Direction: West (252 deg)
Survey Date: October 7, 2013

Projection: NAD83, UTM zone 7N
Scale: 1 : 2,000
Inversion: M. Best
Plot: R. Daigle, I. Fage

GROUNDTRUTH EXPLORATION

Inverted Chargeability

Extended Dipole-Dipole Array

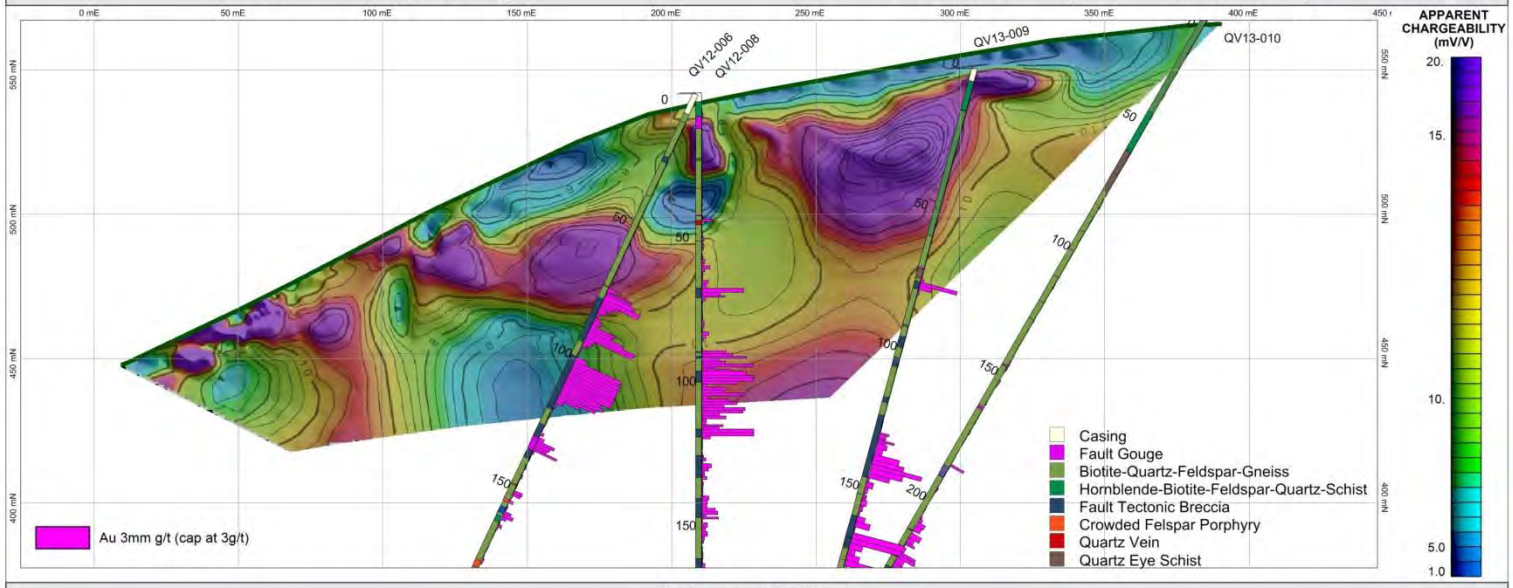

Interpretation

o only inverted array with low chargeability for hole QV12-006

o indications are the chargeability increases going to the north end of the line

Project: Case Study 7, QV Project, VG Zone
Line: CS7-VG-L03
Look Direction: West (252 deg)
Survey Date: October 7, 2013

Projection: NAD83, UTM zone 7N
Scale: 1 : 2,000
Inversion: M. Best
Plot: R. Daigle, I. Fage

GROUNDTRUTH EXPLORATION

Inverted Chargeability — Pole-Dipole Array

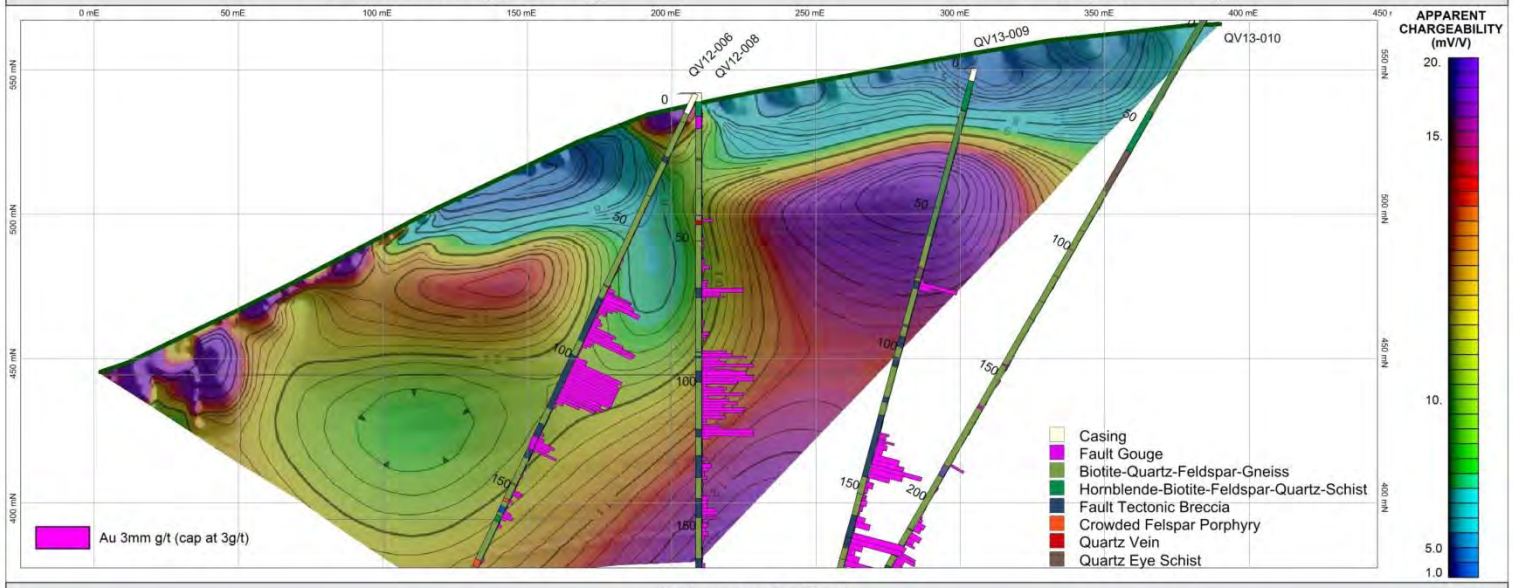

Interpretation

- o mineralization appears to be associated with moderate chargeability
- o moderate to high chargeability related to disseminated pyrite and other sulphides associated with the gold mineralization
- o strong gradient and inverse Schlumberger similar to pole-dipole at north end of line but have differences between chargeability values and mineralization in middle of line

Project: Case Study 7, QV Project, VG Zone
Line: CS7-VG-L03
Look Direction: West (252 deg)
Survey Date: October 7, 2013

Projection: NAD83, UTM zone 7N
Scale: 1 : 2,000
Inversion: M. Best
Plot: R. Daigle, I. Fage

GROUNDTRUTH EXPLORATION

CS-8 GOLDEN SADDLE

Final Inversions and Interpretation

Geological setting

The Golden Saddle deposit is located near the confluence of the White and Yukon rivers, 90 km south of Dawson City. The area is underlain by multiply-deformed Paleozoic metamorphic rocks of the Yukon-Tanana terrane, cut by a regional east-west sinistral transpressive fault system. The deposit was the focus of an MSc study by Bailey (2013) at the University of British Columbia; the description below is drawn primarily from his work.

Mineralization at Golden Saddle is hosted in a series of moderately northwest-dipping faults. Kinematic indicators link the faults and mineralization to the regional transpressive system. Gold occurs in quartz-carbonate veins and breccia infill, and is associated with galena, chalcopyrite, molybdenite, silver tellurides, bismuthinite, and barite. Although the mineralized faults cut all host rocks, the main part of the deposit occurs within a Late Permian feldspar augen orthogneiss that comprises part of the Sulphur Creek plutonic suite (Figure CS8-1).

Geophysical survey

Data were obtained for three pole-dipole configurations as well as dipole-dipole extended and inverse Schlumberger arrays for line L01 (location map and photo below).The length of the line was 415 m (single spread length). All 5 arrays were collected using the same 84 electrodes. However the location of the infinity current electrode is approximately 500 m from the north end, approximately 500 m from the south end, and approximately 500 m perpendicular to the line to the west. The average RMS error of fit for the five arrays is 5.27% with the highest being 7.53% indicating a good signal-to-noise level. The inverted resistivity and chargeability sections are provided as paired plots below after the map of the survey location map and surface geology.

Geophysical interpretation

The three pole-dipole arrays had a depth of exploration of approximately 150 m compared with the inverse Schlumberger and dipole-dipole extended arrays which had a depth of exploration of approximately 100 m. The deeper depth of exploration was able to outline the deeper mineralization on drillhole WD-043. The mineralization is associated with veins and alteration products with expected resistivity values in the low to moderate range. Generally the resistivity values of the mineralization is in the moderate range. The inverted resistivity features of all three pole-dipole arrays are similar. Similarly the dipole-dipole extended and inverse Schlumberger arrays have similar resistivity features; however they are different than the pole-dipole resistivity features. In particular the inverse Schlumberger and dipole-dipole extended array have lower resistivity values within the mineralized zones which provides better resolution of the mineralized zone.

The deeper mineralization is associated with higher values of chargeability as seen on the inverted IP pole-dipole arrays. The shallower mineralized zones have a mixture of low to moderated chargeability values. The disseminated sulphide and alteration products contribute to the observed chargeability on the inverted IP sections but their concentration and connectedness

determine their values. The deeper moderate to high chargeability values are only observed on the inverted pole-dipole arrays. Low to moderate values of chargeability are associated with all 5 inverted IP arrays for the shallower mineralization.

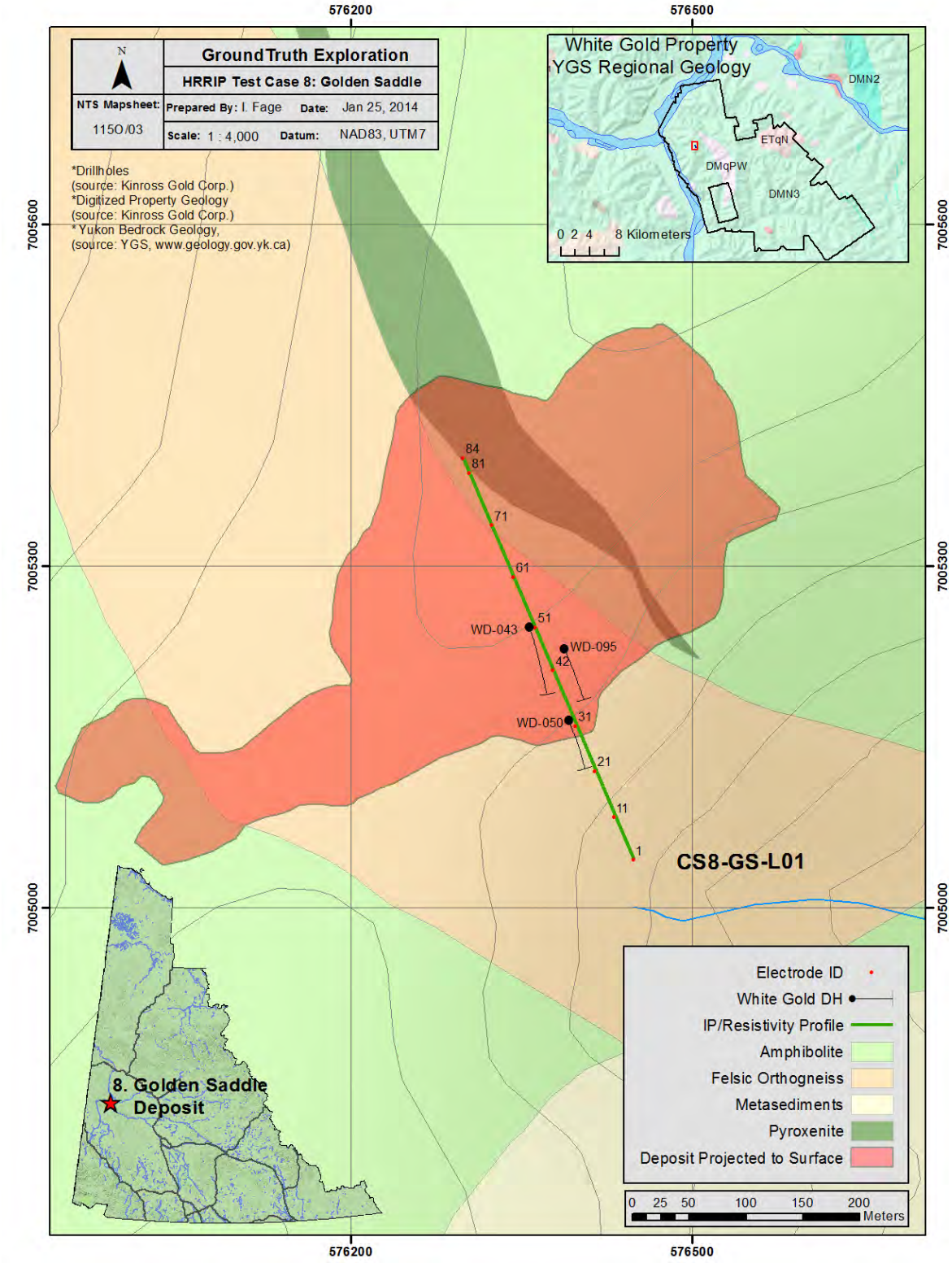

Figure CS8-1. *Location of the geophysical line and surface geology for CS-8, Golden Saddle.*

Figure CS8-2. *Survey line on CS-8, Golden Saddle.*

Figure CS8-3. *Shelter for Supersting at CS-8, Golden Saddle.*

PAIRED PLOTS

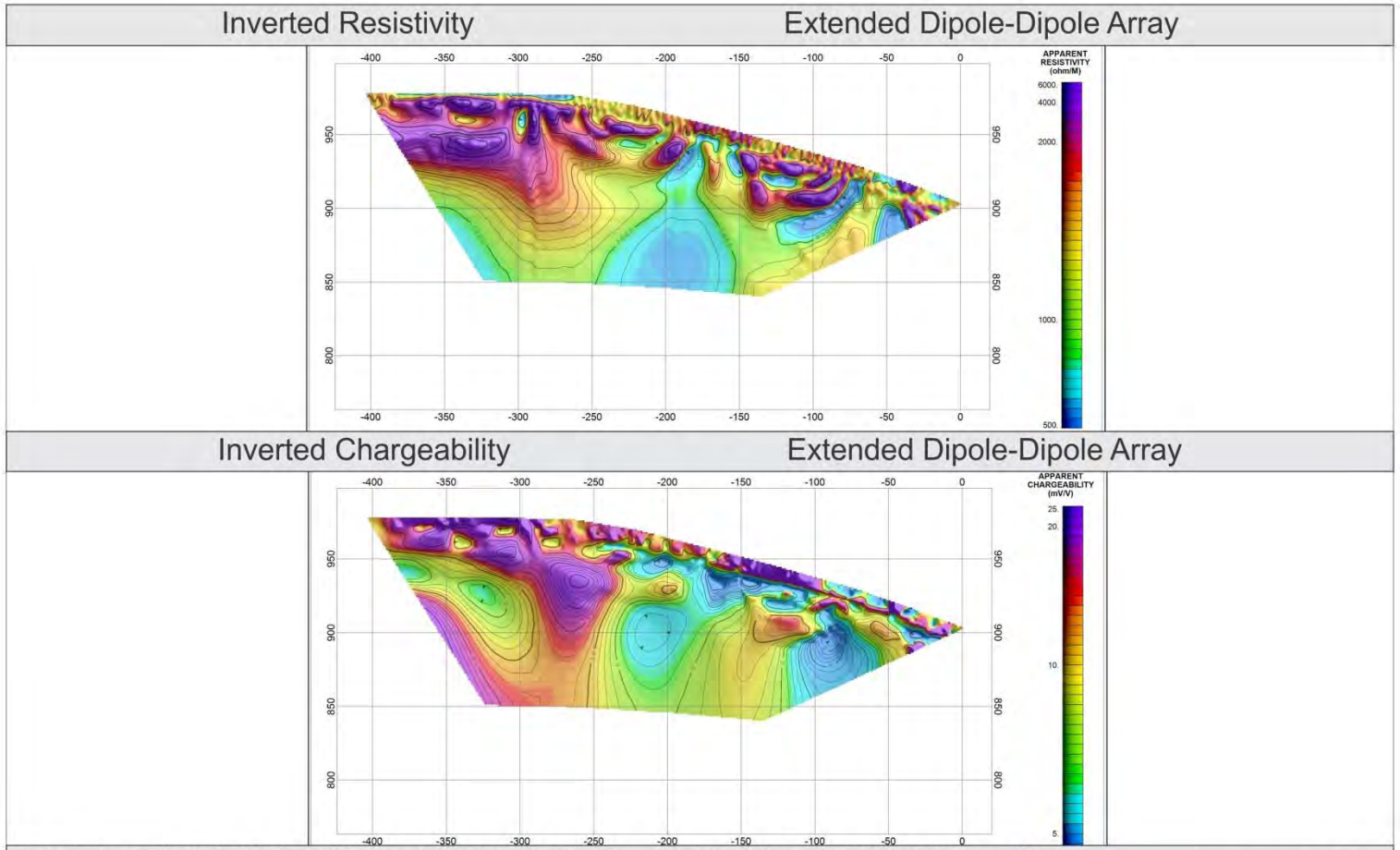

Inverted Resistivity — Inverse Schlumberger Array

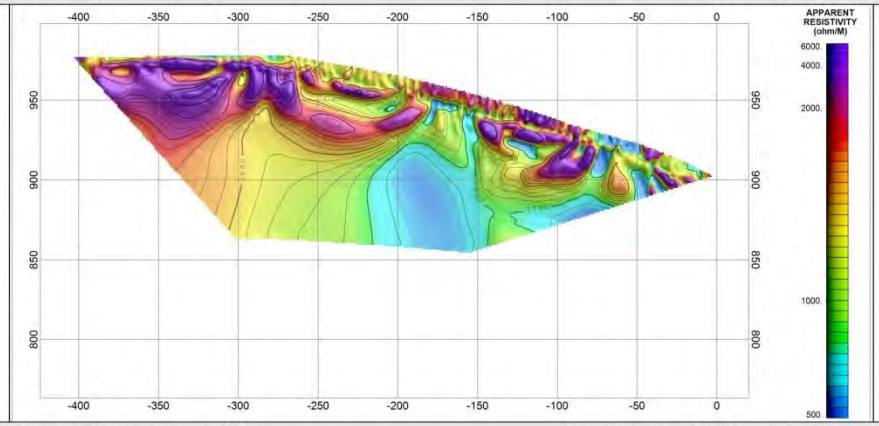

Inverted Chargeability — Inverse Schlumberger Array

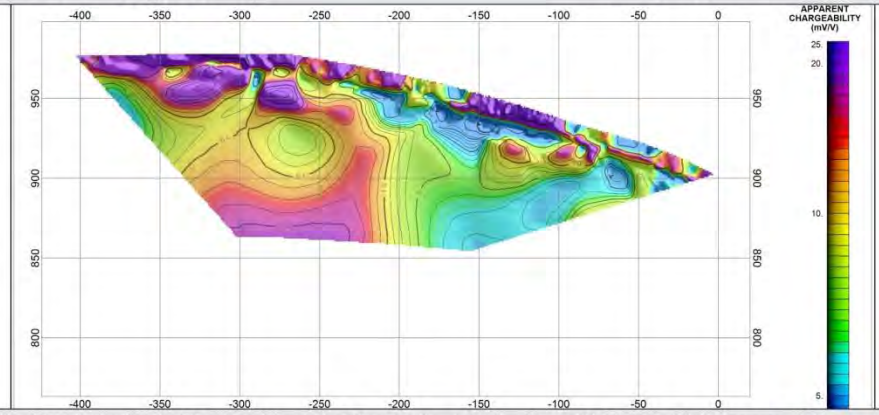

Project: Case Study 8, White Gold Project, Golden Saddle Deposit
Line: CS8-GS-L01
Look Direction: North East (66 deg)
Survey Date: October 8, 2013

Projection: NAD83, UTM zone 7N
Inversion: M. Best
Plot: R. Daigle, I. Fage

GROUNDTRUTH EXPLORATION

Inverted Resistivity — Pole-Dipole Array (N-Infinity)

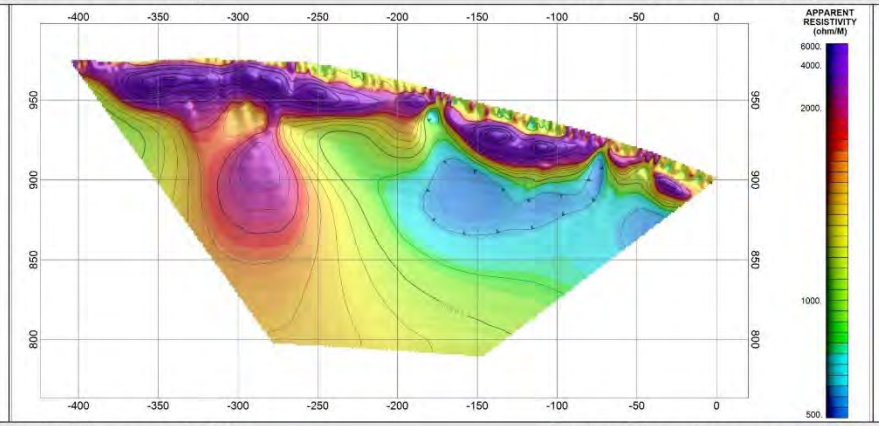

Inverted Chargeability — Pole-Dipole Array (N-Infinity)

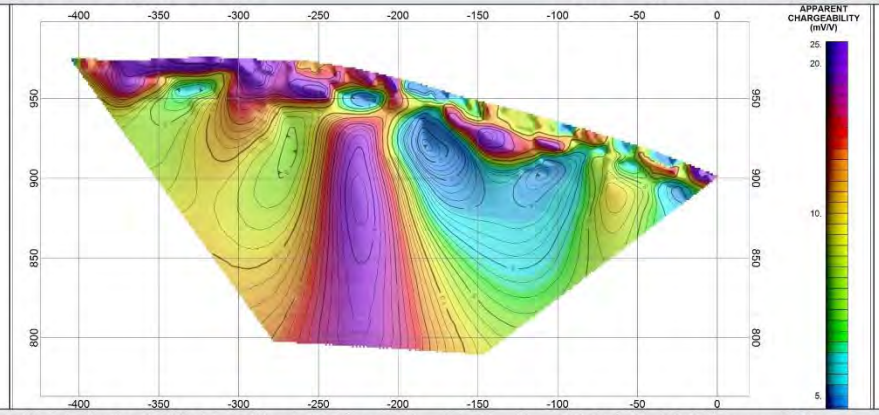

Project: Case Study 8, White Gold Project, Golden Saddle Deposit
Line: CS8-GS-L01
Look Direction: North East (66 deg)
Survey Date: October 8, 2013

Projection: NAD83, UTM zone 7N
Inversion: M. Best
Plot: R. Daigle, I. Fage

GROUNDTRUTH EXPLORATION

Inverted Resistivity — Pole-Dipole Array (S-Infinity)

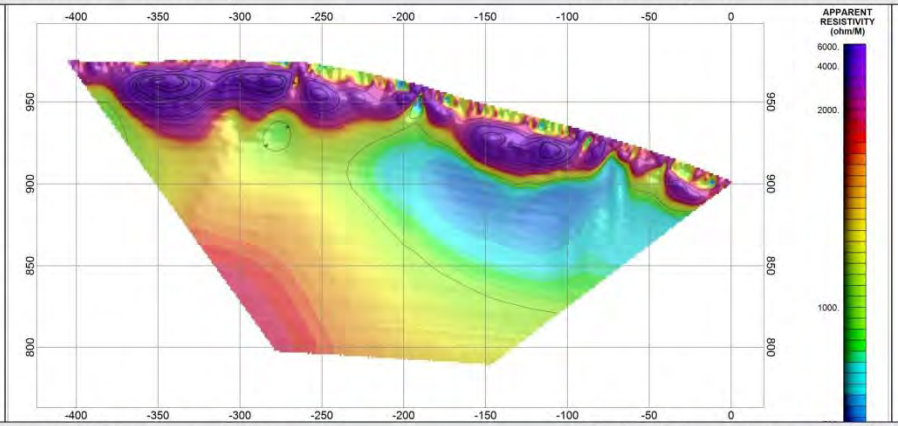

Inverted Chargeability — Pole-Dipole Array (S-Infinity)

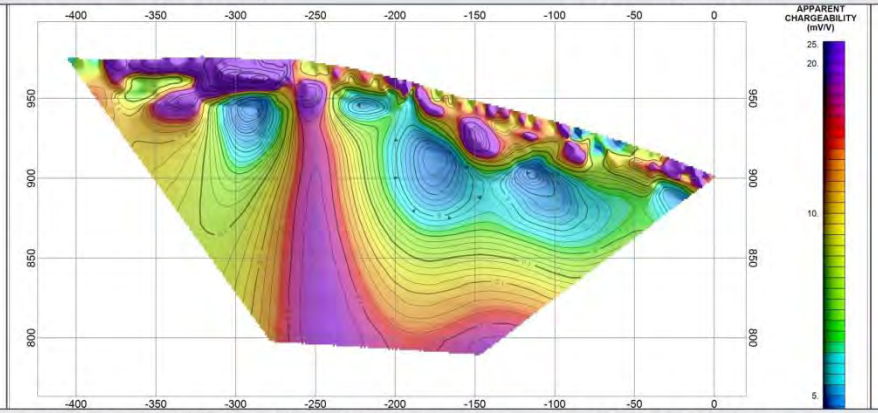

Project: Case Study 8, White Gold Project, Golden Saddle Deposit
Line: CS8-GS-L01
Look Direction: North East (66 deg)
Survey Date: October 8, 2013

Projection: NAD83, UTM zone 7N
Inversion: M. Best
Plot: R. Daigle, I. Fage

GROUNDTRUTH EXPLORATION

Inverted Resistivity — Pole-Dipole Array (W-Infinity)

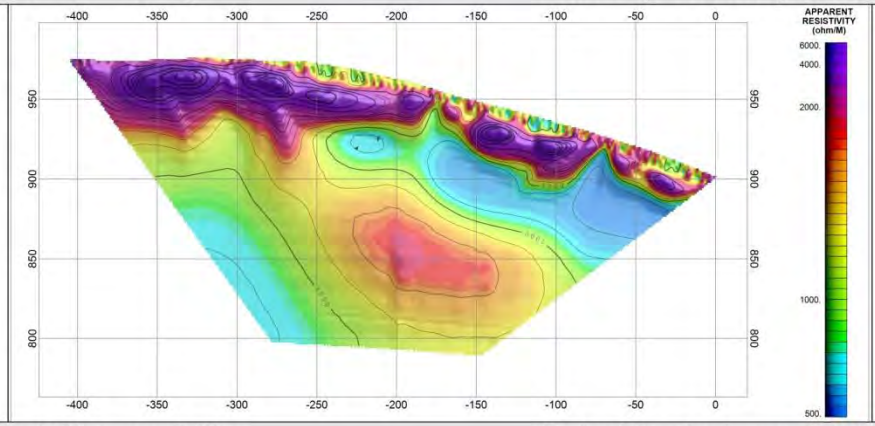

Inverted Chargeability — Pole-Dipole Array (W-Infinity)

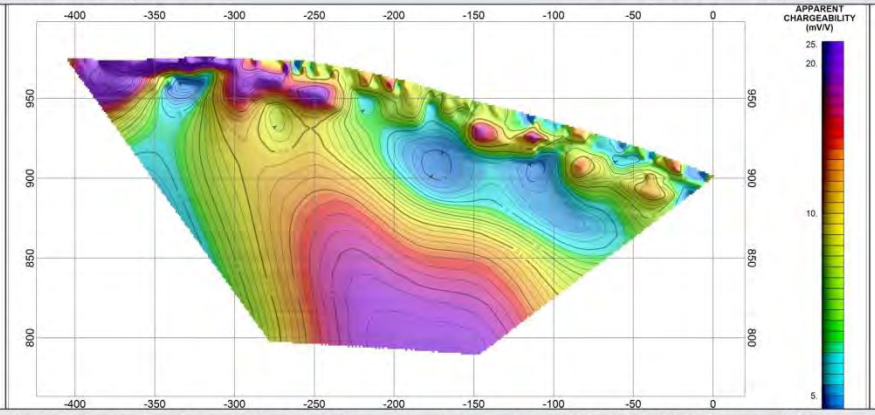

Project: Case Study 8, White Gold Project, Golden Saddle Deposit
Line: CS8-GS-L01
Look Direction: North East (66 deg)
Survey Date: October 8, 2013

Projection: NAD83, UTM zone 7N
Inversion: M. Best
Plot: R. Daigle, I. Fage

GROUNDTRUTH EXPLORATION

INTERPRETATION

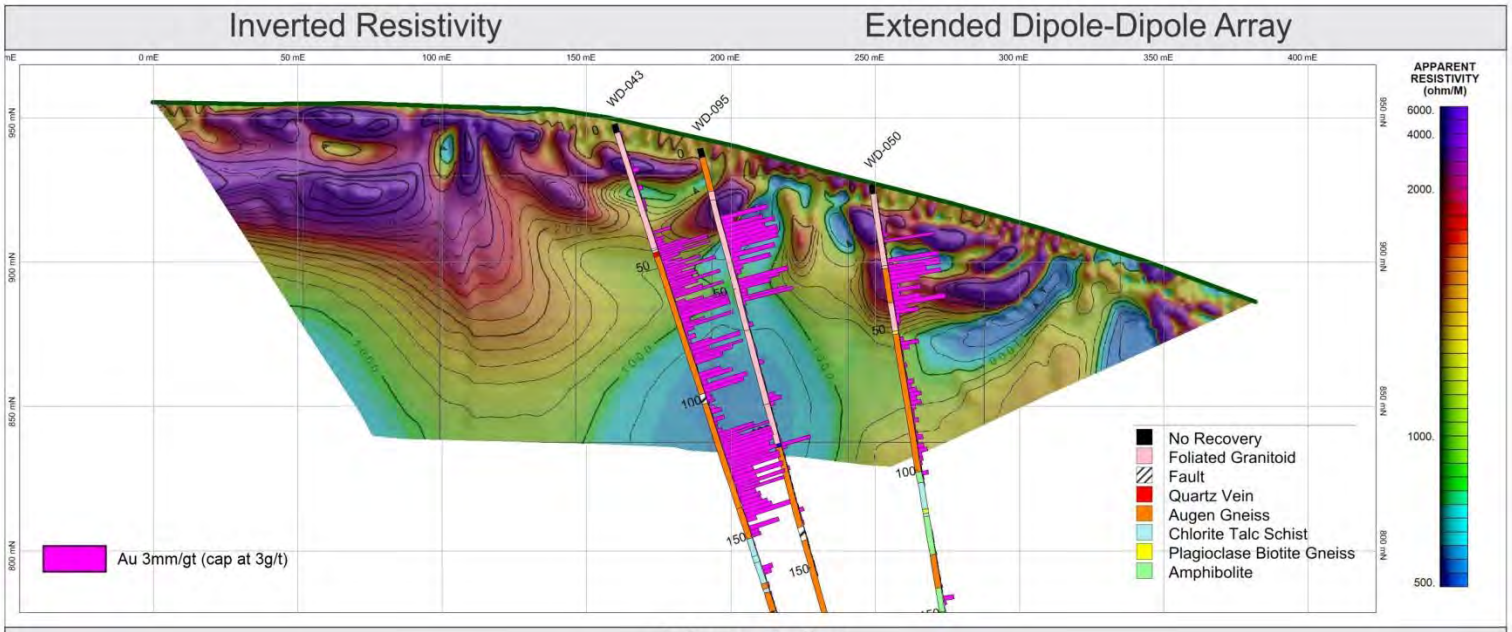

Interpretation

- mineralization associated with low resistivity zone
- dipole-dipole array maps low resistivity zone more effectively than pole-dipole arrays
- inverted inverse Schlumberger array has similar pattern to dipole-dipole array

Project: Case Study 8,White Gold Project, Golden Saddle Deposit	Projection: NAD83, UTM zone 7N
Line: CS8-GS-L01	Scale: 1 : 2,000
Look Direction: North East(66 deg)	Inversion: M. Best
Survey Date: October 8, 2013	Plot: R. Daigle, I. Fage

GROUNDTRUTH EXPLORATION

Inverted Resistivity — Pole-Dipole Array (S Infinity)

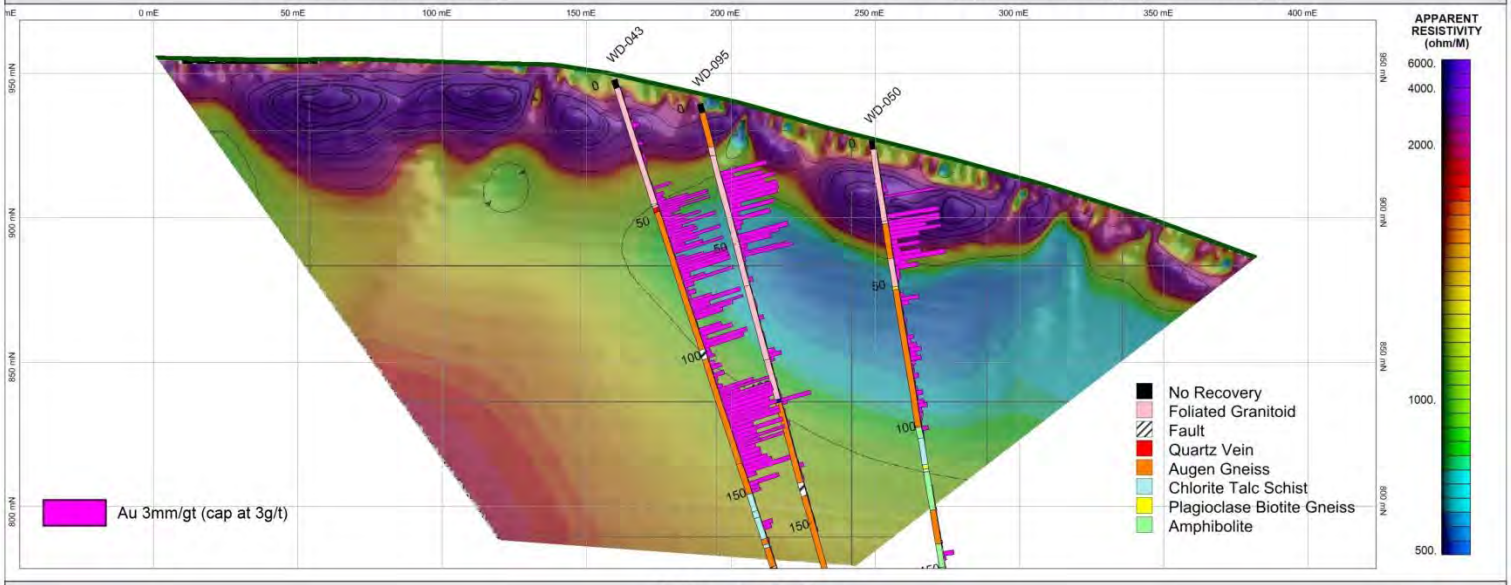

Interpretation

o all 3 pole-dipole arrays have depth of exploration approximately 150 m (over centre portion of array spread)
o dipole-dipole extended and inverse Schlumberger arrays have depth of exploration approximately 100 m
o mineralized zones associated with veins and alteration - consistent with low to moderate resistivity values although most mineralization is associated with moderate resistivity values
o inverted resistivity pattern of 3 pole-dipole arrays consistent; inverted resistivity pattern of inverted inverse Schlumberger and dipole-dipole extended arrays similar but different than pole-dipole arrays
o inverted dipole-dipole and inverse Schlumberger arrays have lower resistivity than corresponding pole-dipole arrays.

Project: Case Study 8,White Gold Project, Golden Saddle Deposit
Line: CS8-GS-L01
Look Direction: North East(66 deg)
Survey Date: October 8, 2013

Projection: NAD83, UTM zone 7N
Scale: 1 : 2,000
Inversion: M. Best
Plot: R. Daigle, I. Fage

GROUNDTRUTH EXPLORATION

Inverted Chargeability — Pole-Dipole Array (W Infinity)

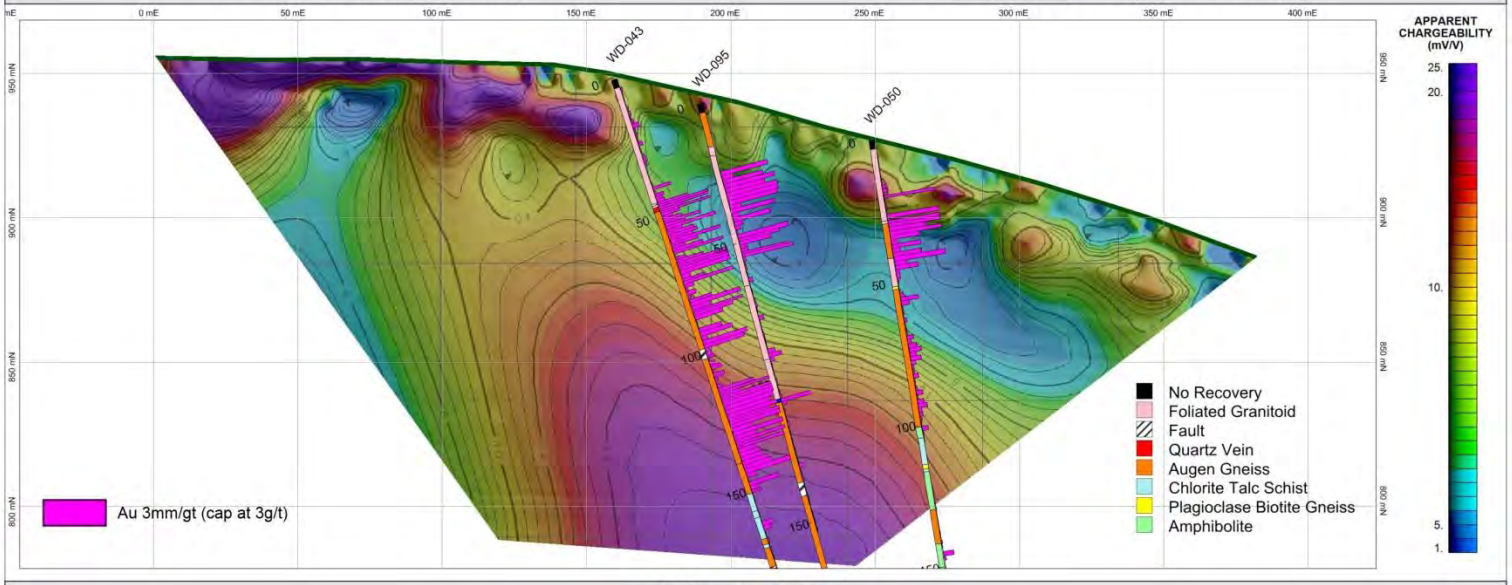

Interpretation

- o deeper mineralization generally associated with moderate to high chargeability
- o shallower mineralization mixed with zones of low to moderate chargeability
- o expect alteration and sulphides to contribute to chargeability but depends on their concentrations and connectedness
- o deeper mineralization not seen on inverted dipole-dipole extended and inverse Schlumberger sections
- o shallower low to moderate chargeability associated with mineralized zones consistent for all inverted IP arrays.

Project: Case Study 8,White Gold Project, Golden Saddle Deposit	Projection: NAD83, UTM zone 7N
Line: CS8-GS-L01	Scale: 1 : 2,000
Look Direction: North East(66 deg)	Inversion: M. Best
Survey Date: October 8, 2013	Plot: R. Daigle, I. Fage

GROUNDTRUTH EXPLORATION

CS-9 - WILLIAMS SOUTH

Final Inversions and Interpretation

Geological setting

The Williams Creek WS zone case study is located approximately 5 km south of the Carmacks (Copper North Mining Corp.) copper-gold deposits. This region is bounded by Stikinia terrane rocks to the east, Yukon Tanana terrane rocks to the north and the Coast Plutonic Complex rocks to the west. The WS property is hosted within foliated biotite rich granodiorite and granitic rocks of the Early Jurassic Aishihik Suite. On the WS property, the suite is represented by the Granite Mountain batholith (Dumas, 2014).

The WS zone (Figure CS9-1) is one of several copper porphyry targets located in the Minto-Carmacks region, where mineralization comprising bornite, chalcopyrite, and locally molybdenite is associated with foliated, heterogeneous biotite and amphibole-rich granodiorite to quartz-monzonite and granite pegmatite of Jurassic age. Tectonic fabrics and crosscutting relationships suggest porphyry emplacement and mineralization occurred during progressive ductile deformation.

Geophysical survey

Dipole-dipole, dipole-dipole extended, inverse Schlumberger and strong gradient array data were collected for the Williams Creek line L01 (see location map and photo). The length of the dipole-dipole and strong gradient array lines was 415 m (single spread length) but the dipole-dipole extended and inverse Schlumberger arrays had lengths of 55 m (2 additional roll-alongs). The RMS error of fits were around 6 % for the dipole-dipole arrays and was similar for the other two arrays; thus the data were of good quality. The paired plots for these 4 arrays and the location map are presented below.

Geophysical interpretation

Since there is only a single borehole on this line which does not have a geological description the interpretation is limited to a few qualitative comments. This is an excellent example though for comparing the dipole-dipole and dipole-dipole extended arrays along the same line. The inverted resistivity arrays for these two lines are presented below in the interpretation section. The overlapping portions of these two lines (the NE end of the line) have nearly identical resistivity values and features indicating that both arrays provide similar results. The advantage of the dipole-dipole extended array however is in the redundancy of data (large data volume) which is essential in areas with significant noise levels and/or high electrode contact resistance. The inverted chargeability sections for these two arrays also show excellent agreement in the overlap region.

The mineralization is contained within fractures and veins within intrusive rocks (granodiorite) and consists of disseminated sulphide. The resistivity values are therefore expected to have moderate to high values with chargeability values also moderate to high. The inverted chargeability values for all 4 arrays are consistent with these values, although the maximum chargeability is around 20 to 25 mV/V.

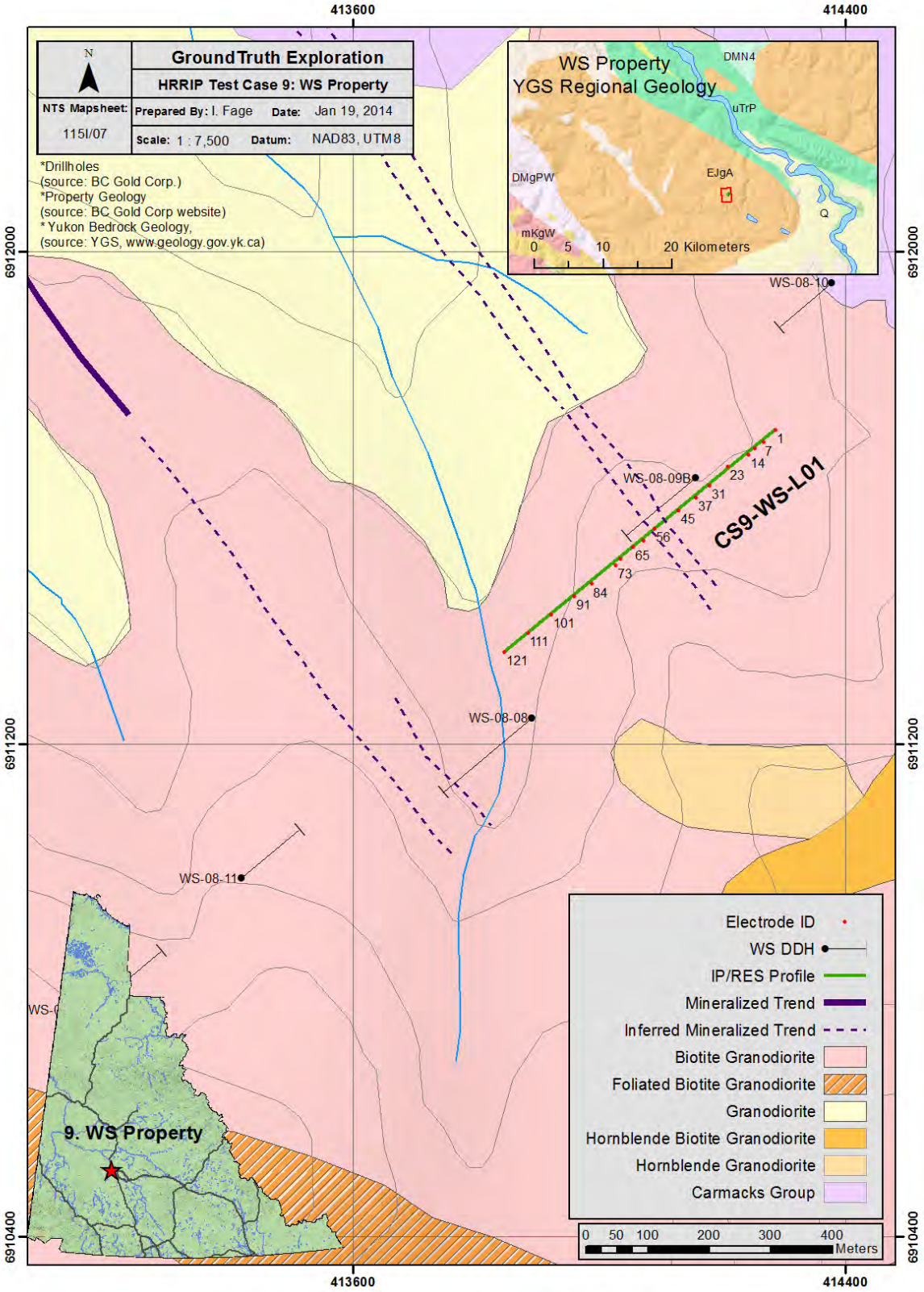

Figure CS9-1. *Location of geophysical line and surface geology for CS-9, Williams South project.*

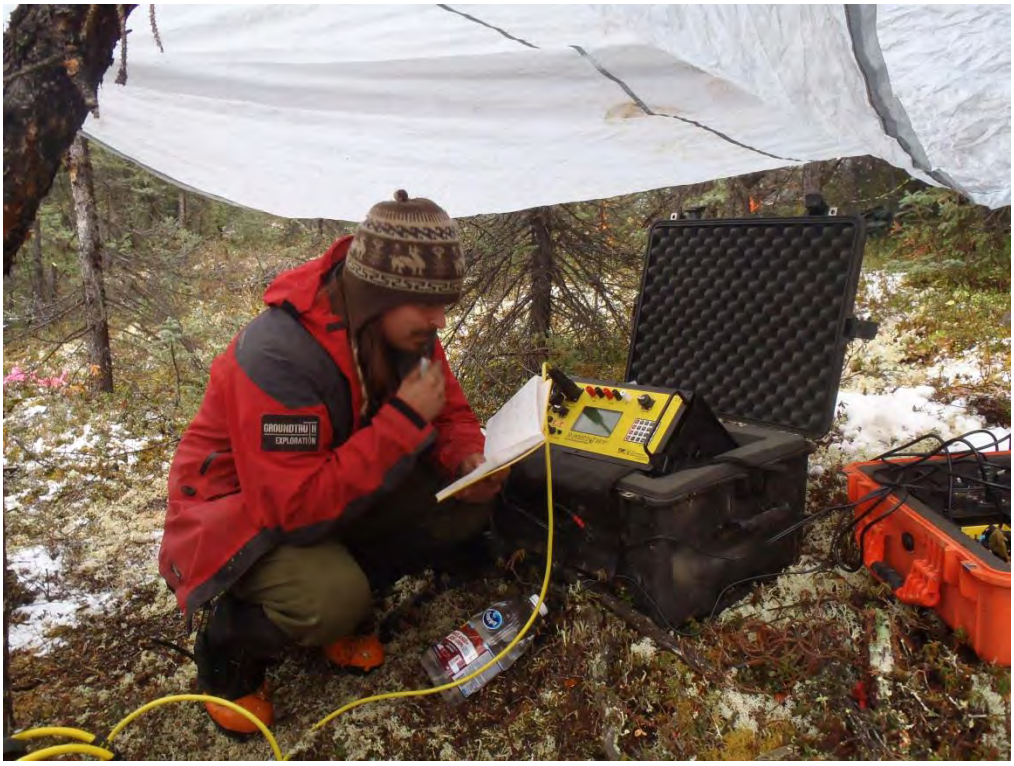

Figure CS9-2. *Chad Cote operating Supersting on CS-9, Williams South project.*

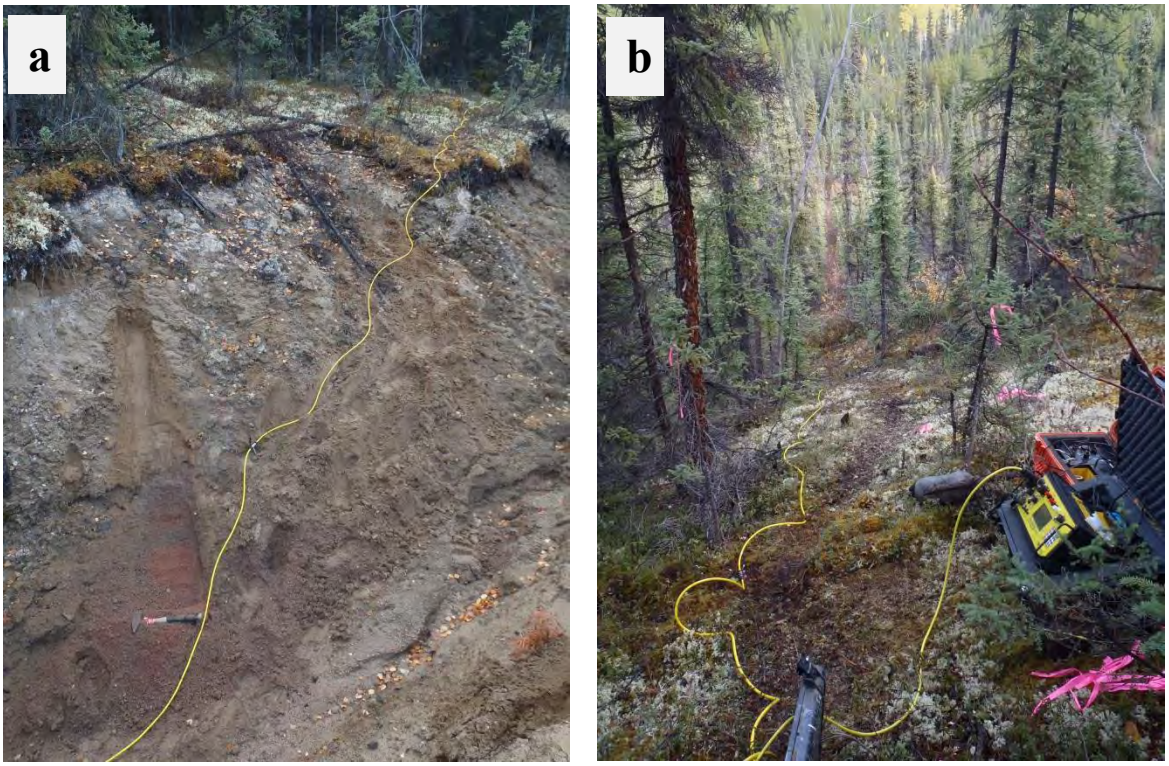

Figure CS9-3a,b. *Survey landscape & soil profile for CS-9, Williams South project.*

PAIRED PLOTS

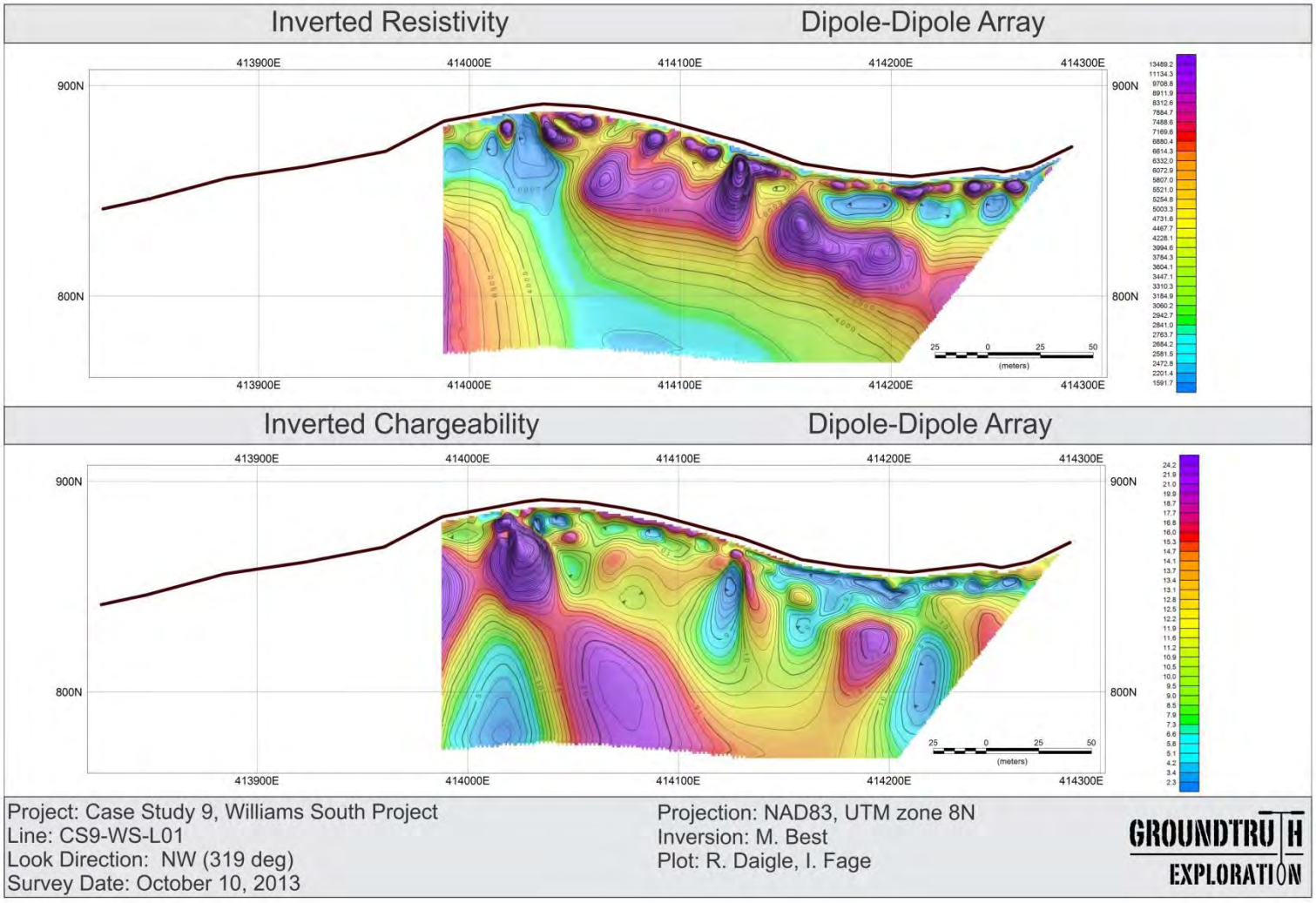

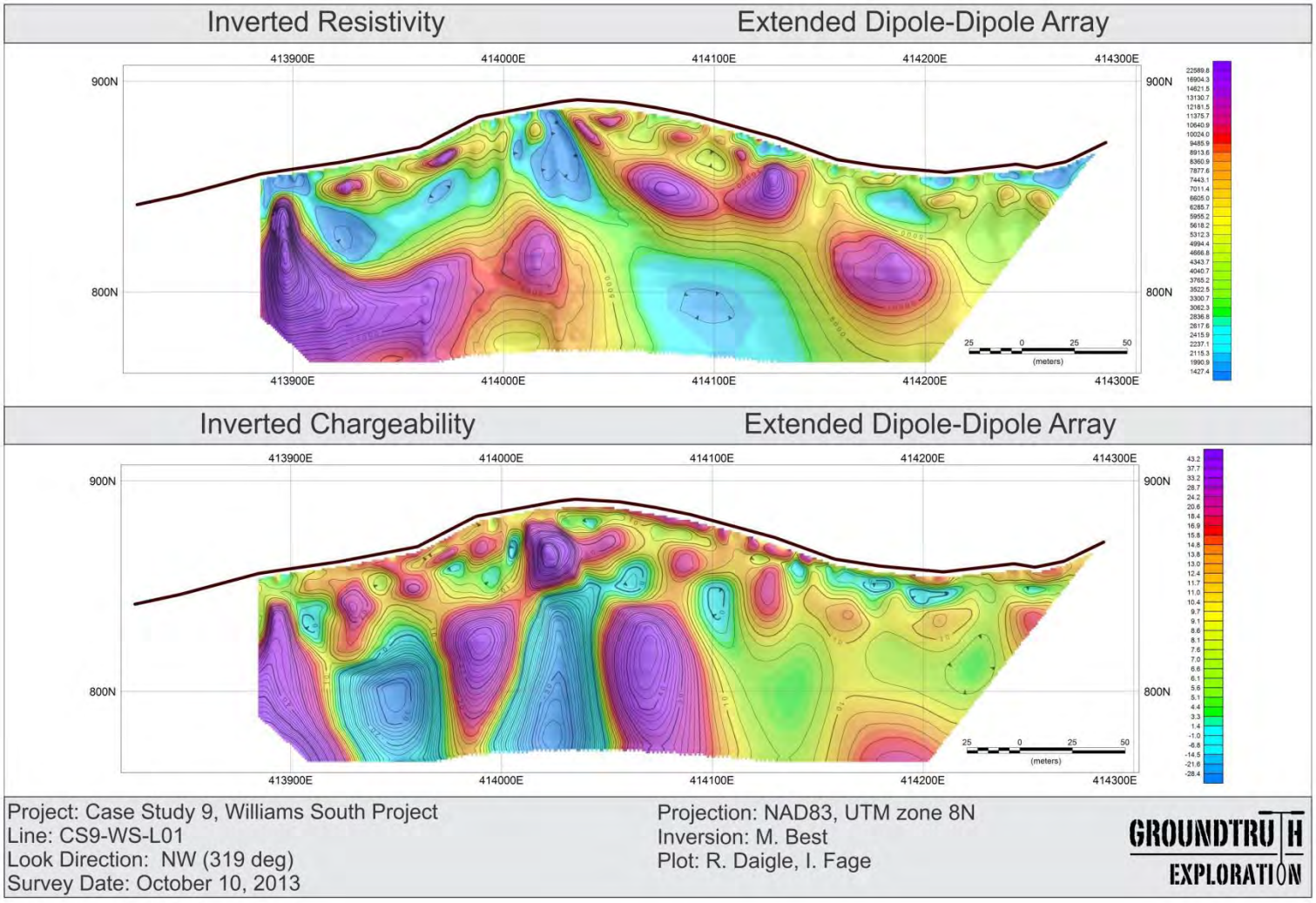
Inverted Resistivity
Extended Dipole-Dipole Array
413900E
414000E
414100E
414200E
414300E
900N
800N
25 0 25 50
(meters)
Inverted Chargeability
Extended Dipole-Dipole Array
Project: Case Study 9, Williams South Project
Line: CS9-WS-L01
Look Direction: NW (319 deg)
Survey Date: October 10, 2013
Projection: NAD83, UTM zone 8N
Inversion: M. Best
Plot: R. Daigle, I. Fage
GROUNDTRUTH
EXPLORATION

Inverted Resistivity — Inverse Schlumberger Array

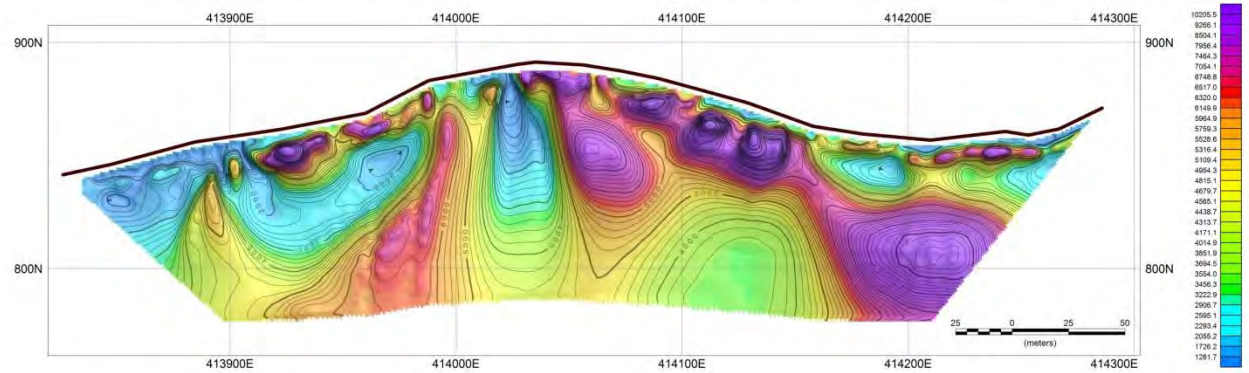

Inverted Chargeability — Inverse Schlumberger Array

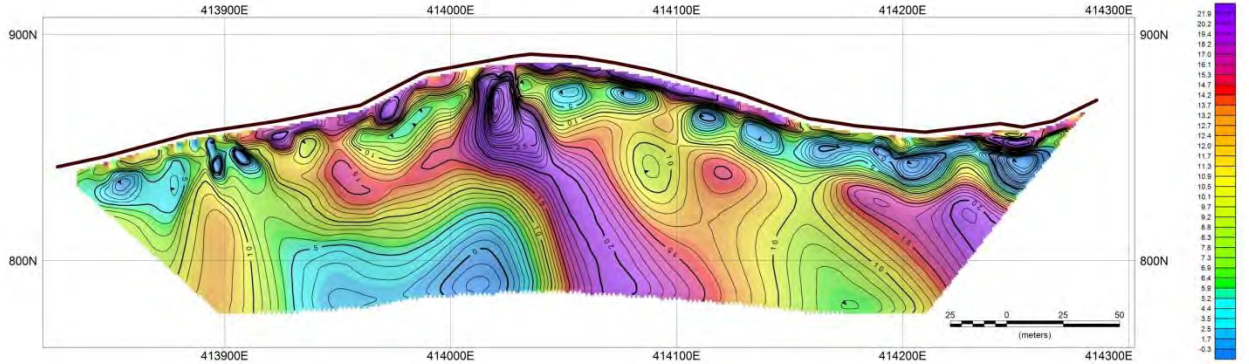

Project: Case Study 9, Williams South Project
Line: CS9-WS-L01
Look Direction: NW (319 deg)
Survey Date: October 10, 2013

Projection: NAD83, UTM zone 8N
Inversion: M. Best
Plot: R. Daigle, I. Fage

GROUNDTRUTH EXPLORATION

Inverted Resistivity — Strong Gradient Array

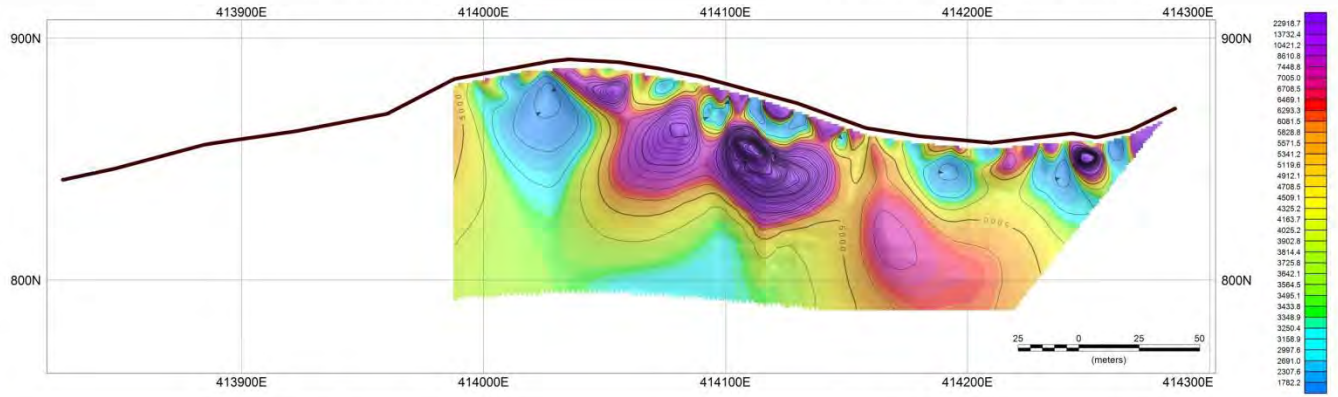

Inverted Chargeability — Strong Gradient Array

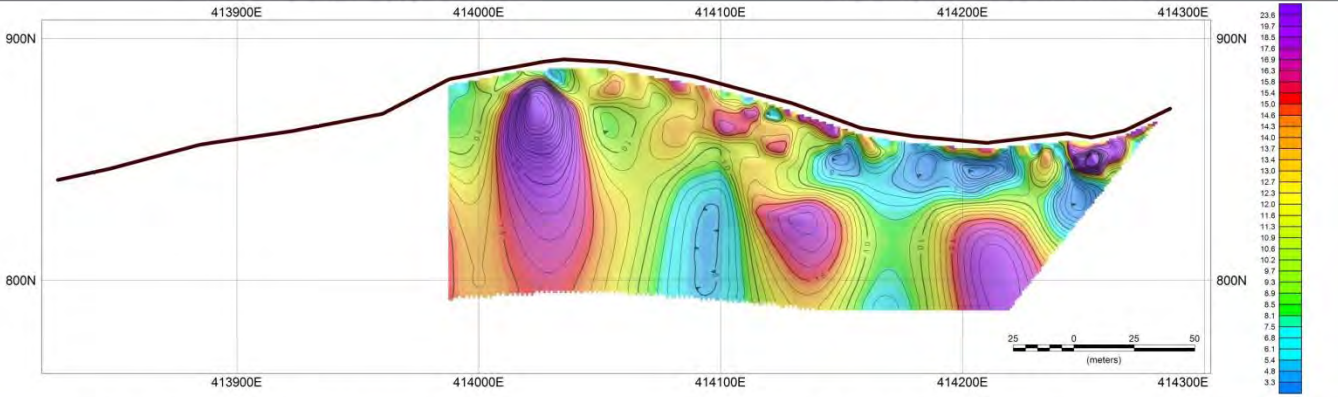

Project: Case Study 9, Williams South Project
Line: CS9-WS-L01
Look Direction: NW (319 deg)
Survey Date: October 10, 2013

Projection: NAD83, UTM zone 8N
Inversion: M. Best
Plot: R. Daigle, I. Fage

GROUNDTRUTH EXPLORATION

INTERPRETATION

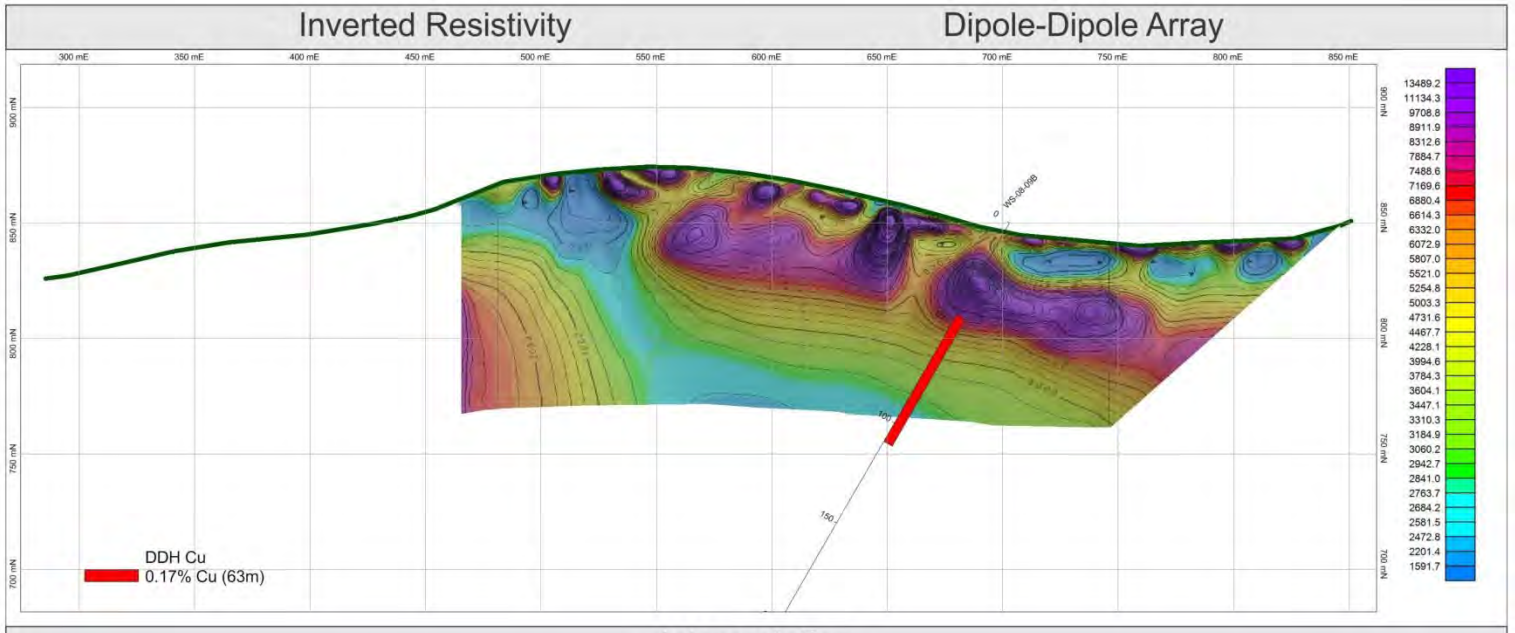

Interpretation

- o mineralization is in a moderate to high resistivity zone
- o all arrays have similar pattern of mineralization being in a moderate to high resistivity zone
- o expect resistivity values to be moderate to high for granodiorite rocks with disseminated sulphides.
- o opportunity to compare dipole-dipole with the extended version
- o only minor differences between the two arrays but generally they match well

Project: Case Study 9, Williams South Project	Projection: NAD83, UTM zone 8N
Line: CS9-WS-L01	Scale: 1 : 2,500
Look Direction: North West (319 deg)	Inversion: M. Best
Survey Date: October 10, 2013	Plot: R. Daigle, I. Fage

GROUNDTRUTH EXPLORATION

Inverted Resistivity — Extended Dipole-Dipole Array

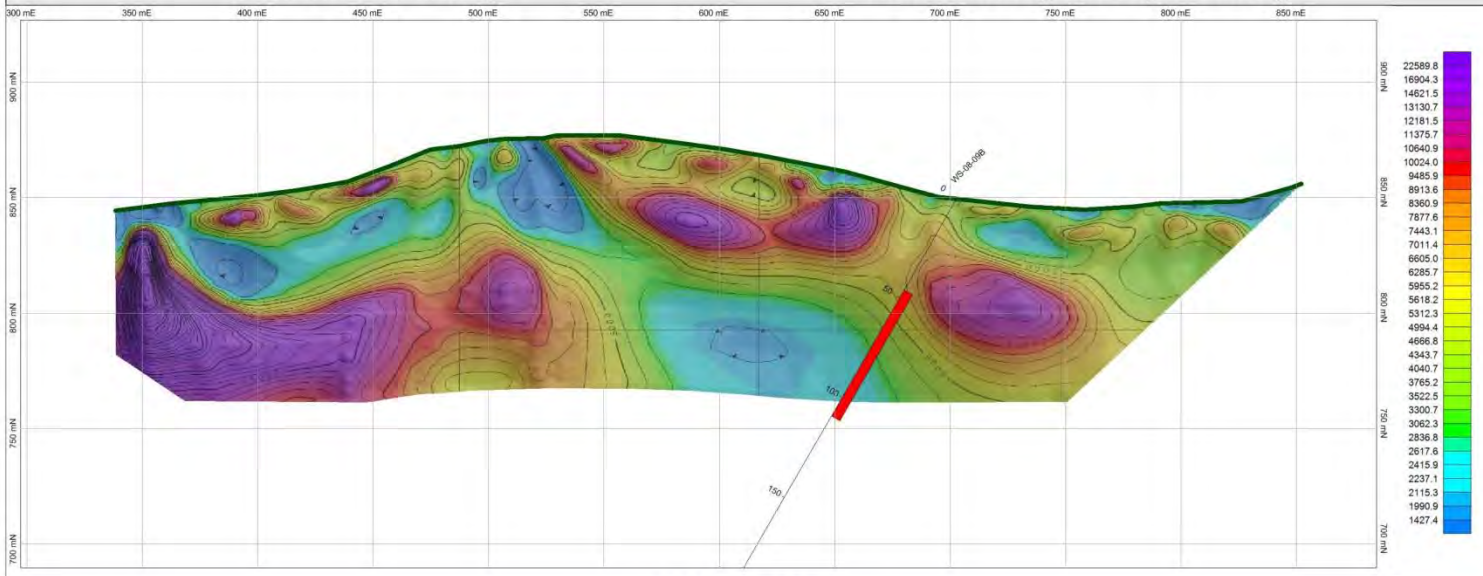

Interpretation

- dipole-dipole extended and dipole-dipole for inverse resistivity very similar
- dipole-dipole extended has several roll alongs to the SW so covers larger area but overlapping areas are nearly identical

Project: Case Study 9, Williams South Project	Projection: NAD83, UTM zone 8N
Line: CS9-WS-L01	Scale: 1 : 2,500
Look Direction: North West (319 deg)	Inversion: M. Best
Survey Date: October 10, 2013	Plot: R. Daigle, I. Fage

GROUNDTRUTH EXPLORATION

Inverted Chargeability — Inverse Schlumberger Array

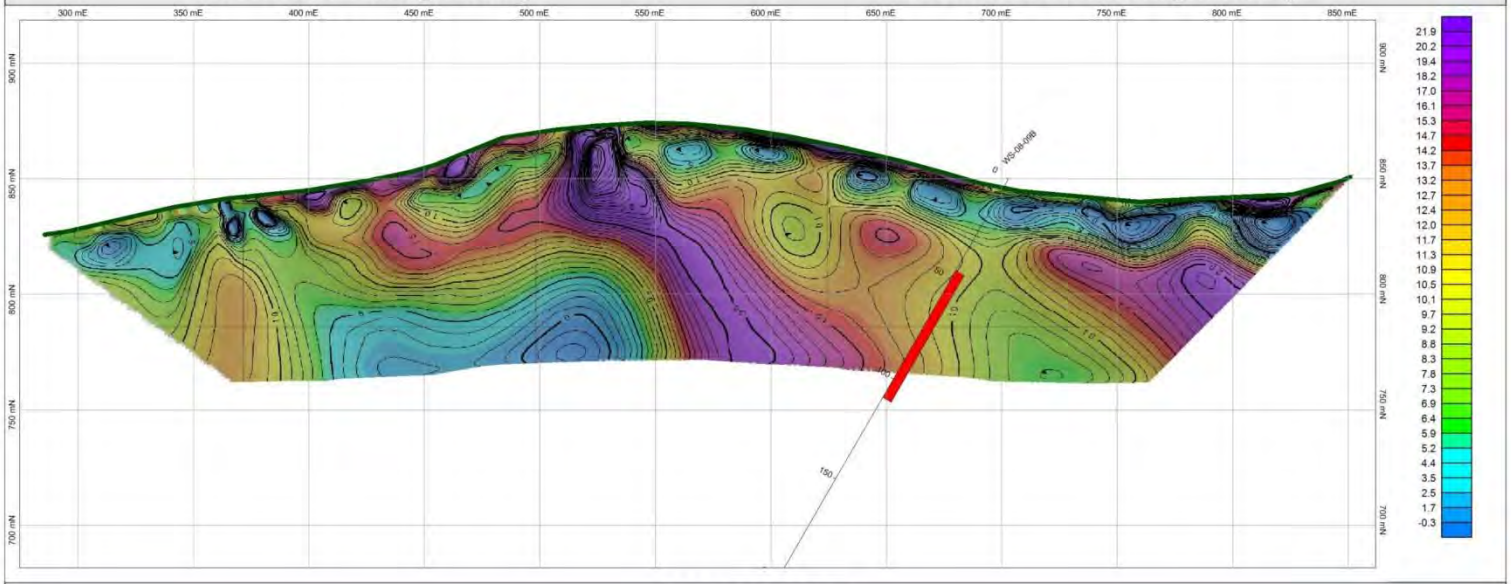

Interpretation

- moderate to high chargeability values associated with mineralization
- expect moderate to high chargeability values for disseminated sulphide systems for porphyry system
- all arrays exhibit similar moderate to high chargeability over mineralization

Project: Case Study 9, Williams South Project
Line: CS9-WS-L01
Look Direction: North West (319 deg)
Survey Date: October 10, 2013

Projection: NAD83, UTM zone 8N
Scale: 1 : 2,500
Inversion: M. Best
Plot: R. Daigle, I. Fage

GROUNDTRUTH EXPLORATION

ROCK PROPERTY MEASUREMENTS

Introduction

As a component of the HRRIP Test Case Project, representative drill core samples were obtained and resistivity/chargeability measurements were taken to assist in relating physical properties of representative rocks to the inverted survey data. Four test case projects had drill core samples loaned for rock property measurements: CS1- Brewery Creek, CS4- Klaza, CS6- Coffee, and CS7- QV project.

Rock properties were measured from drill core sampled at strategic intersections along resistivity/IP profiles. Samples were selected to represent mineralized and non-mineralized rock based on drill core logging, and to represent resistivity/IP highs and lows as indicated in the inversions. This gives ample opportunity to explore the relationships between the results presented in our resistivity/IP inversions and the geophysical characteristics of the various rock types and alterations present in assayed drill core.

Resistivity (ohm-m) and Induced Polarization (mV/V) were both measured using a GDD SCIP tester. Sample preparation and measurement protocol was followed from the Geological Survey of Canada Open File Report 7227: "Physical Property Measurements at the GSC Paleomagnetism and Petrophysical Laboratory including Electric Impedance Spectrum Methodology and Analysis" by R.J. Enkin, *et al.*, 2012.

Measurement Procedure Summary:

1. All samples were photographed and assigned a bar code ID for reference.
2. Samples were then cut to length of 10cm to provide consistent volumes for comparison and to flatten the ends for optimized contact while performing RES/IP measurements.
3. Physical dimensions and weight are measured
    a. Volumes of irregularly shaped samples were measured by displacement instead of being calculated using standard physical dimensions.
4. Samples were then rehydrated by:
    a. Immersing in distilled water
    b. Placing immersed samples in a 5 in/Hg vacuum chamber for 20 min.
    c. Letting sit for 30 days
5. Resistivity in Ohm-m and Chargeability in mV/V are then measured using:
    a. 2 second duty cycle
    b. 10 stacks
    c. 3 repeat measurements

Photos of Rock Property Testing

Photo 1:

Sample for physical property measurement. Half Core Cut to 10cm length.

Photo 2:

Samples in vacuum desiccator for rehydration prior to physical property measurement.

Photo 3:

Rehydrated core sample being tested for Chargeability and Resistivity using GDD, SCIP (Sample Core IP) Tester.

CASE STUDY 1: BREWERY CREEK, BOHEMIAN ZONE

The Brewery Creek drill core sample measurements show good agreement with inversion and drillhole overlay interpretation.

The majority of argillite core samples showed low resistivity values as expected. Two of the argillite samples showing high resistivity from drillhole BC12-417 (70 and 79 m) agree well with a resistivity high on the dipole-dipole inversion. Quartz monzonite shows variable resistivity even among strongly and weakly mineralized samples. Strongly mineralized QM sample measured from BC12-423, at 53 m showed a resistivity of 464 Ohm-m which completely agrees with dipole-dipole inversion overlay. Strongly mineralized QM samples from BC11-203 at 23 and 30 m depth had measured resistivity of 801 and 683 Ohm-m which also agrees very well with dipole-dipole resistivity inversion overlay.

The core samples logged as argillite all show very high chargeability measurements relative to the other rock types, except for sample at BC12-423, 72 m, which showed a moderate IP value. The one mineralized argillite sample registered the highest IP value of the population at 64.12 mV/V. Quartz monzonite core samples populated the lowest class of IP values while the SST sediments were of moderate chargeability. Agreement with chargeability measurements and inversion/ drillhole overlay is variable. The inverse Schlumberger inversion shows a trend of increasing chargeability at depth for holes BC12-423 and BC12-417 and correlating quartz monzonite near surface and argillite at depth. The inversion of dipole-dipole chargeability and BC11-203 overlay does not clearly demonstrate the measured low chargeability for strongly mineralized QM and moderate chargeability for weakly mineralized SST.

Overall, physical property measurements for this case are very useful for assisting to discriminate between argillite and quartz monzonite and aiding in interpretation of inverted data.

CS1-Brewery Creek			GDD Core	GDD Core		
HoleID	**from**	**to**	**IP (mV/V)**	**Res (Ohm-m)**	**Rock type**	**Au ppm**
BC12-423	53.20	53.34	4.60	464.19	LAQM	10.75
BC12-423	58.30	58.50	64.12	61.73	ARG	12.95
BC12-423	72.00	72.20	7.76	373.87	ARGG	0.07
BC12-423	74.50	74.68	21.76	228.34	ARGG	0.06
BC12-421	77.00	77.20	21.19	2206.25	ARGG	0
BC12-417	18.30	18.45	4.47	229.55	LAQM	1.26
BC12-417	20.50	20.70	5.55	475.22	LAQM	1.7
BC12-417	70.00	70.20	23.60	901.97	ARG	0
BC12-417	79.25	79.40	14.70	1801.63	ARG	0
BC11-203	23.00	23.30	9.21	801.43	LAQM	9.04
BC11-203	29.90	30.10	6.60	683.15	LAQM	8.89
BC11-203	47.30	47.40	13.16	662.49	SST	0.14
BC11-203	47.40	47.50	10.48	479.19	SST	0.14

CASE STUDY 4: KLAZA

The Klaza rock samples measured for resistivity and chargeability agree well with the geology of the deposit and inverted IP/res data. Representative rock samples for host rock (granodiorite), mineralization (sulphide veins/breccia) and associated porphyry dikes from survey area have been measured with results for chargeability and resistivity shown below. All inversions for Klaza, particularly on traverse CS4-KL-050E, show a distinct signature of resistivity low/chargeability high over the deposit area.

The sample of the porphyry dike (1340760) showed extremely low measured chargeability and low resistivity. The dikes follow adjacent to the mineralization, so low measured resistivity in the rock sample agrees with the inverted low resistivity from the field survey, but the low measured chargeability of the dikes is not reflected in the IP inversions showing a strong IP high.

Altered granodiorite samples showed different results based on alteration. The granodiorite sample with argillic/phyllic alteration (1340764) measured high IP response and a moderate resistivity value. High IP is expected with argillite, as was observed in the Brewery Creek sample IP measurements. The granodiorite with propylitic alteration showed high resistivity and is consistent with the interpretation of the host rock being higher resistivity than the mineralized zone. The mineralized zone had 4 samples measured with variable sulphide content. The samples containing massive sulphide (1340763, 1340758) both measured very high IP and very low resistivity. This is the deposit signature identified in the inversion. The 2 mineralized/brecciated samples (1340761, 1340762) also showed high IP values, consistent with IP inversion over mineralized zone, but also showed high resistivity.

Chargeability and resistivity measurements on Klaza drill core, are very useful for interpretation of inverted data, and discriminate rock units very well here. In the mineralized zone, chargeability highs in the inversions are resulting from chargeable sulphide in veins and breccia. Resistivity lows in the mineralized zone in inversions likely the result of conductive phyllic/argillic alteration and porphyry dikes associated with the mineralization.

CS4- KLAZA	GDD Core	GDD Core		
Sample Id	**IP (mV/V)**	**Res (Ohm-m)**	**Rock Type**	**Description**
1340760	1.88	136.78	Dike	Quartz-Feldspar-Porphyry
1340764	53.02	547.71	Granodiorite	Arg/phyllic Altered
1340759	6.80	5050.07	Granodiorite	Prop. Alteration
1340763	52.78	28.21	Mineralized Vein	py, semi massive
1340761	33.96	2922.53	Mineralized Vein	Brecciated Sulphide
1340762	16.22	415.80	Mineralized Vein	Brecciated Sulphide
1340758	314.41	2.54	Mineralized Vein	Gal-sphal-py, massive

CASE STUDY 6: COFFEE

The Coffee project had seven rock samples submitted for physical property measurements. Representative samples of mineralized silicified breccia, mineralized quartz mylonite, and felsic gneiss were measured for chargeability and resistivity.

The felsic gneiss samples, one altered (CFD0188, 127 m) and one fresh (CFD0258, 88 m) both had similar chargeability measurements in the range of 5 mV/V. The altered felsic gneiss had a higher resistivity of 2310 Ohm-m, where the fresh sample has moderate resistivity of 986 Ohm-m.

The three mineralized silicified-clast breccia samples have gold grades in the range of 1.07-1.77 grams per tonne. Two samples come from diamond drillhole CFD0188 which intersects the T3 structure on Kaminak section 4100 at a depth of 102 and 104 m. The 102 m depth silicified breccia sample has a low chargeability of 3.2 mV/V and low resistivity of 457 Ohm-m. The intensely clay altered sample from 104 m depth had a higher chargeability at 6.86 mV/V and a high resistivity of 3895 Ohm-m. The mineralized ribbon quartz mylonite had the highest chargeability of all samples at 12.2 mV/V and moderate resistivity of 1534 Ohm-m.

Inversion results from Latte and Supremo with drillhole overlays show the mineralized structures as resistivity lows and chargeability highs. Rock property testing suggests that the chargeability high signature in the mineralized zone can be attributed to clay alteration and ribbon quartz mylonite. Resistivity lows are interpreted to be caused by conductive iron oxides in the mineralized zone.

CS6-Coffee			GDD Core	GDD Core		
HoleID	**from**	**to**	**IP (mV/V)**	**Res (Ohm-m)**	**Rock units**	**Au ppm**
CFD0188	103.8	104.0	6.86	3895.446	Silicified-clast breccia/clay alt	1.07
CFD0188	127	127.2	5.583	2309.813	Felsic gneiss/altered	0
CFD0089	68.5	68.7	12.199	1534.104	Ribbon quartz mylonite	1.59
CFD0102	139.9	140.0	5.615	1458.393	Biotite-feldspar schist	0
CFD0258	88	88.35	5.133	985.569	Felsic gneiss/unaltered	0
CFD0102	55.5	55.7	4.102	809.165	Silicified-clast breccia	1.77
CFD0188	102	102.1	3.219	457.489	Silicified-clast breccia	1.26

CASE STUDY 7: QV

The QV project's VG zone had thirteen representative samples tested for chargeability and resistivity measurements. Samples were selected to test mineralized and non-mineralized specimens of the logged fault tectonic breccia (FTBX), biotite-quartz feldspar gneiss (BQFG) and quartz-eye schist (QES).

The FTBX unit had a total of 5 samples measured and is a significant contributor to the high grade intercepts in the deposit. We see that resistivity and chargeability values are variable within the unit and that significant mineralization can be hosted in both highly resistive and conductive environments.

The QES unit measurements showed similar chargeability measurements for both the strongly and weakly mineralized sample. The strongly mineralized QES sample measured with much lower resistivity, likely due to silicification or conductive sulphide.

The BQFG unit had 6 samples measured, 4 of which were non-mineralized and 2 mineralized. The non-mineralized samples had moderate resistivity values when compared to the extremely high resistivity values observed in the mineralized samples. The non-mineralized BQFG sample from hole QV12-007 had the highest chargeability value of all samples tested at 18.62 mV/V. All 4 BQFG samples from hole QV12-008 measured comparable chargeability values. Resistivity values increased at depth, as did the grade of the measured samples.

The samples measured from the VG zone showed mineralization to be associated with moderate to high resistivity values, which agrees with well with the pole-dipole inversions. Mineralization is associated with moderate chargeability values, also agreeing well with pole-dipole inversion.

CS7- VG Zone			GDD Core	GDD Core		
Hole_ID	**from**	**to**	**IP (mV/V)**	**Res (Ohm-m)**	**Rock type**	**Au ppm**
QV12-001	41.20	41.35	10.68	792.10	FTBX	3.41
QV12-001	70.00	70.15	7.48	5117.03	FTBX	2.94
QV12-001	101.60	101.75	12.27	1046.55	FTBX	0.73
QV12-002	51.00	51.15	8.45	1052.78	QES	0.77
QV12-004	50.85	51.00	6.57	326.50	QES	2.22
QV12-004	94.75	94.90	8.20	943.47	FTBX	1.41
QV12-006	91.80	91.95	6.07	7055.21	FTBX	3.89
QV12-007	111.20	111.35	18.62	2199.89	BQFG	0.05
QV12-008	50.35	50.50	9.97	1964.34	BQFG	0.11
QV12-008	51.35	51.50	8.57	1112.45	BQFG	0.05
QV12-008	80.70	80.85	11.63	10322.46	BQFG	0.11
QV12-008	100.95	101.10	6.72	11910.33	BQFG	2.07
QV12-008	104.90	105.05	9.91	13118.93	BQFG	2.37

RESULTS AND DISCUSSION

Approximately 50 2D resistivity/IP inversions using the Earthimager software program were carried out during the investigation (Table 2). Not all of these can be discussed at length in this report. However, all the inverted profiles are provided in the presentation of case study surveys section for readers interested in more detail. This section attempts to provide the reader with an overview of the main observations resulting from this investigation.

The HRRIP method produces the same results as any standard mineral exploration resistivity/IP system, except the HRRIP method is a faster, more environmentally sensitive, resistivity/IP technique that maps resistivity and chargeability variations within the upper 60 to 80 m of the subsurface. The method also has better lateral resolution in the upper 60 to 80 m since the electrode spacing is smaller than that used by conventional resistivity/IP systems employed in mineral exploration. Consequently the conclusions reached during this investigation are very similar to those from these conventional systems.

There is generally agreement between the known geology and mineralization of the case study examples and the inverted resistivity and IP results. The resistivity and chargeability sections reflect the geological structure and/or mineralization. In some cases chargeability is effective in locating areas of mineralization and in other cases the resistivity sections outline structure and geological formations. The present investigation helped us to understand the resistivity/IP responses mapped within the upper 60 to 80 m of the subsurface that were associated with the different types of deposits and mineralization styles investigated during the study. Below are a few general observations.

- gold mineralization associated with sulphide and/or clay alteration generally produced a chargeability response
- gold mineralization associated without sulphide and/or clay alteration did not produce a chargeability response
- a resistivity low is often related to metasedimentary rocks. Mineralization is often associated with the contact between metasediments and the surrounding resistive rocks (see CS-2 Eagle Deposit, inverse Schlumberger array on line CS2-S50NE for example)
- the inverted resistivity sections provided useful information about structure and geology which is useful for indirectly locating targets of potential mineralization
- most of the inverted resistivity profiles contain a near surface (approximately the upper 10 m) section containing numerous high resistivity features related to patches of permafrost

The case study survey section contains many more details on the relationship between the HRRIP inversions and the known mineralization and geological structure for the 9 deposits investigated.

The study however did identify inconsistencies between inversion results, both resistivity and IP, from different arrays along the same line. Generally these differences are slight and are related to the resolution of the different arrays. In a few cases however the differences were more pronounced. For example on line CS3-S102, case study CS-3 Flame and Moth, the inverted

resistivity section for the dipole-dipole array has low resistivity values near 250 m while the inverse Schlumberger array has high resistivity values near 250 m.

After inversion the data should, at least in principle, produce the same image for all arrays along the same line. However each array has a different current distributions within the earth. Although the different current distributions are taken into account in the mathematical treatment of the inversion codes the location of the current and voltage electrodes relative to the resistivity distribution within the ground can produce artifacts in the inversions. This is particularly true if the electrodes are planted in or near a strong conductive feature. Whether or not this is the reason for the difference noted for case study CS-3 is not clear.

There are examples where the same array, for example the inverse Schlumberger array along line CS2 Eagle Deposit, CS2-S35NE, has both chargeability lows and highs associated with mineralization. In this case the chargeability low at the south end of the line is associated with a zone of lower grade mineralization while the chargeability high around 300 m is associated with a zone of high grade mineralization. This points out the importance of using both chargeability and resistivity together to locate potential zones of mineralization.

The resolution of the resistivity and chargeability inverted sections depends, at least partially, on the array being used to collect the data. The dipole-dipole array and its extended version provided the best inverted resistivity lateral resolution. The inverse Schlumberger array and its extended version generally had slightly lower lateral resolution than the dipole-dipole arrays. However they often provided higher resolution chargeability inverted sections. The pole-dipole arrays provided information to depths of approximately 100 m but the lateral resolution is lower than the dipole-dipole and inverse Schlumberger arrays. The location of the "infinity" electrode can have a significant effect on the character of the inverted sections. The strong gradient array provided information similar to the dipole-dipole and inverse Schlumberger arrays.

The measurement of resistivity and chargeability of core samples provides additional information that can be used in conjunction with the inverted sections. Care must be exercised when interpreting the results though because of the different scales of measurement. The HRRIP method averages the measurements over volumes of at least 5 cubic metres while the core method averages the measurements over a few tens of cubic centimetres.

CONCLUSIONS

The investigation shows that different geological settings and/or type of mineralization influence the response of a given array type. The characteristics of one deposit type leads to low resistivity values, for example clay alteration and/or sulphide mineralization, whereas the characteristics of another deposit type leads to high resistivity values, for example quartz veins. Similar arguments hold for how deposit type affects chargeability. Dipole-dipole and extended dipole-dipole arrays have been shown to have excellent lateral resolution, particularly for inverted resistivity. On the other hand the inverse Schlumberger array, and its extended version are effective at locating chargeability features associated with mineralization. The strong gradient array is somewhere between these two with regard to resistivity resolution and imaging mineralized zones with the chargeability.

The location of the "infinity" current electrode influences the response of pole-dipole arrays and leads to asymmetry within the pseudosections and inverted resistivity and chargeability responses. The depth of exploration for a pole-dipole array is approximately 50% more than the other arrays for a given "a" spacing and a fixed number of electrodes. Near-surface resolution however is poorer for the pole-dipole array than for the other arrays.

Merging data from several arrays often improves the signal-to-noise. Subtle features observed on a single array however may be lost when inversion is carried out on the merged data set. Consequently care must be exercised when interpreting merged data sets; comparing the original inverted arrays with the merged inverted array provides insights into subtle features not seen on either of the original inverted data sets. Merging pole-dipole data with "infinity" electrodes placed at opposite ends of the spread eliminates any asymmetry associated with a single “infinity” location.

Measuring core sample resistivity and chargeability provides additional information to use when relating geology with the inverted resistivity/chargeability sections. Resistivity and chargeability measurements on cores from case studies 1, 4, 6 and 7 have provided useful information on expected resistivity and chargeability ranges of geological units and mineralized zones for a given case study as well as providing additional information for interpreting the inverted sections.

REFERENCES

Abbado, D., Slingerland, R.L., and Smith, N.D., 2005. The origin of anastomosis in the upper Columbia River, British Columbia, Canada. *In*: Fluvial Sedimentology VII, Blum, M.D., Marriott, S.B., and Leclair. S.F. (eds.), International Association of Sedimentologists, Special Publication 35, p. 3-15.

Bailey, L.A., 2013. Late Jurassic fault-hosted gold mineralization of the Golden Saddle deposit, White Gold district, Yukon Territory. Unpublished BSc thesis, University of British Columbia.

Berman, R.G., Ryan, J.J., Gordey, S.P., and Villeneuve, M., 2007. Permian to Cretaceous polymetamorphic evolution of the Stewart River region, Yukon-Tanana terrane, Yukon, Canada: P–T evolution linked with in situ SHRIMP monazite geochronology. Journal of Metamorphic Geology, vol. 25, no. 7, p. 803-827

Chartier, D., Couture, J.-F., Sim, R., and Starkey, J., 2013. Mineral Resource Evaluation, Coffee Gold Project, Yukon, Canada. Kaminak Gold Corporation, Vancouver, B.C., p 19.

Colpron, M., Nelson, J.L., and Murphy, D.C., 2006. A tectonostratigraphic framework for the pericratonic terranes of the northern Cordillera. *In*: Paleozoic evolution and metallogeny of pericratonic terranes at the ancient Pacific margin of North America, Canadian and Alaskan Cordillera, M. Colpron and J.L. Nelson (eds.), Geological Association of Canada, Special Paper 45, p. 1-23.

Constable, S.C., Parker, R.I., and Constable, C.G., 1987. Occam's inversion: A practical algorithm for generating smooth models from electromagnetic sounding data. Geophysics, vol. 52, p. 289-300.

Dey, A. and Morrison, H F., 1979. Resistivity modelling for arbitrarily shaped two-dimensional structures. Geophysical Prospecting, vol. 27, p. 106-136.

Enkin, R.J., Cowan, D., Tigner, J., Severide, A., Gilmour, D., Tkachyk, A., Kilduff, M., and Baker, J., 2012. Physical property measurements at the GSC paleomagnetism and petrophysics laboratory, including electric impedance spectrum methodology and analysis. Geological Survey of Canada, Open File 7227, p. 1-6.

Farrow, D. and McOnie, A., 2013. Updated technical report on the Flame & Moth deposit, Flame & Moth Property, Keno Hill District, Yukon. Flame and Moth NI 43-101 update final, March, 2013 Alexco Resource Corp., Vancouver, B.C., p. 32.

Gasperikova, E., Cuevas, N.H., and Morrison, H.F., 2005. Natural field induced polarization for mapping of deep mineral deposits: A field example from Arizona. Geophysics, vol. 70, p. B61–B66.

Gibson, J.L., 2013. Technical Report on the VG Zone - QV Property, Dawson Mining District, Yukon Territory, McLeod Williams Capital Corp., Vancouver, BC.

Gordey, S.P. and Makepeace, A.J., (compilers), 2003. Yukon Digital Geology, version 2.0. Geological Survey of Canada Open File 1749 and Yukon Geological Survey Open File 2003-9(D), 2 CD-ROMS.

Gustavson Associates, 2013. Technical report on resources, Brewery Creek project, Yukon, Canada. Report NI 43-101, Gustavson Associates, Lakewood, Colorado, p. 52.

Kearey, P. and Brooks, M., 1984. An introduction to geophysical exploration. Blackwell Scientific Publications, Oxford, 295 p.

Loke M.H. and Barker R.D., 1996a. Rapid least-squares inversion of apparent resistivity pseudosections using a quasi-Newton method. Geophysical Prospecting, vol. 44, p. 131-152.

Loke M.H. and Barker R.D., 1996b. Practical techniques for 3D resistivity surveys and data inversion. Geophysical Prospecting, vol. 44, p. 499-523.

Lowe, C., Thomas, M.D., and Morris, W. A., 1999. Geophysics in Mineral exploration: Fundamentals and case histories. Geological Association of Canada, Short course notes 14, 175 p.

Lewis, L.L. and Burke, M., 2011. Yukon hardrock mining, development and exploration overview 2010. *In:* Yukon Exploration and Geology Overview 2010, K.E. MacFarlane, L.H. Weston, and C. Relf (eds.), 2010. Yukon Geological Survey, p. 36.

MacKenzie, D., Craw, D., and Finnigan, C., 2014. Structural controls on alteration and mineralization at the Coffee gold deposits, Yukon. In: Yukon Exploration and Geology 2013, K.E. MacFarlane, M.G. Nordling, and P.J. Sack (eds.), Yukon Geological Survey, p. 119-131.

Maloof, T.L., Bakr, T., and Thompson, J.F.H., 2001. The Dublin Gulch intrusion- hosted deposit, Tombstone plutonic suite, Yukon Territory, Canada. Mineralium Deposita, vol. 36, p. 583-503.

Moran A., Marshall, B., Smith, C., Aurala, C., Kappes, D., Mosher, G., Newcomen, H.W., Ghaffari, H., Narciso, H., Myers, J., Collins, J., Mach, L., Guest, P., Powell, R., Billin, S., Meyer, T., and Hantelmann, T., 2012. Technical Report – Feasibility Study Eagle Gold Project, Yukon. Victoria Gold Corp., Vancouver B.C., p 7-3.

Mortensen, J.K., 1992. Pre-mid-Mesozoic tectonic evolution of the Yukon-Tanana Terrane, Yukon and Alaska. Tectonics, vol. 11, no. 4, p.836–853.

Nabighian, M.N. and Asten, M.W., 2002. Metalliferous mining geophysics—State of the art in the last decade of the 20th century and the beginning of the new millennium. Geophysics, vol. 67, p. 964–978.

Oldenberg, D. and Li, Y, 1994. Inversion of induced polarization data. Geophysics, vol. 59, p. 1327-1341.

Pare, P. and Legault, J.M., 2010. Ground IP-Resistivity, and airborne Spectrem and helicopter ZTEM survey results over Pebble copper-moly-gold porphyry deposit, Alaska. Society of Exploration Geophysicists Annual Meeting 2010, Denver, Colorado.

Rockhaven Resources Ltd., 2012. Rockhaven continues to step out. Company news release, November 14, 2012. <www.rockhavenresources.com/s/NewsReleases.asp?numCols=1&page=2>, accessed March 2014.

Stummer, J.S., Maurer, H. and Green, A G. 2004. Experimental design: Electrical resistivity data sets that provide optimum subsurface information. Geophysics, vol. 69, p. 120-139.

Sumner, J.S., 1976. Principles of induced polarization for geophysical exploration. Elsevier Scientific Publishing Company, Amsterdam 277 p.

Vallee, M.A., Smith R.S., and Keating, P., 2011. Metalliferous mining geophysics— State of the art after a decade in the new millennium. Geophysics, vol. 76, p. W31–W50.

Wainwright, A.J., Simmons, A.T., Finnigan, C.S., Smith, T.R., and Carpenter, R.L., 2011. Geology of new gold discoveries in the Coffee Creek area, White Gold District, west-central Yukon. In: Yukon Exploration and Geology 2010, K.E. MacFarlane, L.H. Weston and C. Relf (eds.), Yukon Geological Survey, p. 233-247.

Wannamaker, P.E., 1992. IP2d1-v1.00, Finite element program for dipole-dipole resistivity/IP forward modelling and parameterized inversion of two-dimensional earth resistivity structure. User documentation, University of Utah Research Institute, Earth Sciences Laboratory, Salt Lake City, Utah.

Ward, S.H (editor), 1990. Geotechnical and environmental geophysics, Volume 1, Review and tutorial, Investigations in Geophysics, No. 5, Society of Exploration Geophysicists.

Ward, S.H (editor), 1990. Geotechnical and environmental geophysics, Volume 2, Environmental and Groundwater, Investigations in Geophysics, No. 5, Society of Exploration Geophysicists.

Ward, S.H (editor), 1990. Geotechnical and environmental geophysics, Volume 3, Geotechnical, Investigations in Geophysics, No. 5, Society of Exploration Geophysicists.

APPENDIX A: AGI SUPERSTING SPECIFICATIONS

Key Benefits

- 8 channel simultaneous measure capability, cuts field time dramatically!
- High power transmitter. Can use both 12V and 24V batteries for added power.
- Field adapted rugged construction. Built to last in real conditions.
- Easy to use menu driven system.
- The best accuracy and noise performance in the industry!
- Large capacity internal memory for storage of measurement results.
- User programmed measure cycles can be loaded into memory from a PC and later executed in the field.
- Directly controls the Multi-Channel Swift Dual Mode Automatic Multi-electrode system (patent 6,404,203)!
- Induced Polarization mode records 6 individual IP chargeability windows.
- Manual measurements are available via four banana pole screws on the top of the instrument for connecting current and potential electrodes. Manual measurement array types include: Resistance, Schlumberger, Wenner, Dipole-dipole, Pole-dipole, and Pole-pole.

Technical Specifications

Measurement modes	Apparent resistivity, resistance, induced polarization (IP), battery voltage.
Measurement range	+/- 10V.
Measuring resolution	Max 30 nV, depends on voltage level.
Screen resolution	4 digits in engineering notation.
Output current intensity	1mA - 2000 mA continuous, measured to high accuracy.
Output voltage	800 Vp-p, actual electrode voltage depends on transmitted current and ground resistivity.
Output power	200W.
Input channels	Eight channels.
Input gain ranging	Automatic, always uses full dynamic range of receiver.
Input impedance	>150 MOhm.
Input voltage	Max 10 V.
SP compensation	Automatic cancellation of SP voltages during resistivity measurement. Constant and linearly varying SP cancels completely (V/I and IP measurements).
Type of IP measurement	Time domain chargeability (M), six time slots measured and stored in memory.

IP current transmission	ON+, OFF, ON-, OFF.
IP cycle times	0.5, 1, 2, 4 and 8 s.
Measure cycles	Running average of measurement displayed after each cycle. Automatic cycle stops when reading errors fall below user set limit or user set max cycles are done.
Resistivity cycle times	Basic measure time is 0.2, 0.4, 0.8, 1.2, 3.6, 7.2 or 14.4 s as selected by user via keyboard. Autoranging and commutation adds about 1.4 s.
Signal processing	Continuous averaging after each complete cycle. Noise errors calculated and displayed as percentage of reading. Reading displayed as resistance (dV/I) and apparent resistivity (ohmm or ohmft). Resistivity is calculated using user entered electrode distances.
Noise suppression	Better than 100 dB at f >20 Hz.
Powerline noise suppression	Better than 120 dB at power line frequencies (16 2/3, 20, 50 & 60 Hz) for measurement cycles of 1.2 s and above.
Total accuracy	Better than 1% of reading in most cases (lab measurements). Field measurement accuracy depends on ground noise and resistivity. Instrument will calculate and display running estimate of measuring accuracy.
System calibration	Calibration is done digitally by the microprocessor based on correction values stored in memory.
Supported configurations	Resistance, Schlumberger, Wenner, dipole-dipole, pole-dipole and pole-pole.
Operating system	Stored in re-programmable flash memory. Updated versions can be downloaded from our web site and stored in the flash memory.
Data storage	Full resolution reading average and error are stored along with user entered coordinates and time of day for each measurement. Storage is effected automatically in a job oriented file system.
Data display	Apparent resistivity (Ohmmeter), current intensity (mAmp) and measured voltage (mVolt) are displayed and stored in memory for each measurement.
Memory capacity	The memory can store more than 79,000 measurements (resistivity mode) and more than 26,000 measurements in combined resistivity/IP mode.
Data transmission	RS-232C channel available to dump data from instrument to a Windows type computer on user command.
Automatic multi-electrodes	The SuperSting is designed to run dipole-dipole, pole-dipole, pole-pole, Wenner and Schlumberger surveys including roll-along surveys completely automatic with the Swift Dual Mode Automatic Multi-electrode system (patent 6,404,203). The SuperSting can run any other array by using user programmed command files. These files are ASCII files and can be created using a regular text editor. The command files are downloaded to the SuperSting RAM memory and can at any time be recalled and run. Therefore there is no need for a fragile computer in the field.

Manual measurements	The instrument has four banana pole screws for connecting current and potential electrodes during manual resistivity measurements.
User controls	20 key tactile, weather proof keyboard with numeric entry keys and function keys. On/Off switch Measure button, integrated within main keyboard. LCD night light switch (push to illuminate).
Display	Graphics LCD display (16 lines x 30 characters) with night light.
Power supply, field	12V or 2x12V DC external power (one or two 12V batteries), connector on front panel. Maximum power output is increased when using 2x12V supply.
Power supply, office	Mains operated DC power supply.
Operating time	Depends on survey conditions and size of battery used. Internal circuitry in auto mode adjusts current to save energy.
Operating temperature	-5 to +50°C.
Weight	10.2 kg (22.5 lb), instrument only.
Dimensions	Width 184 mm (7.25"), length 406 mm (16") and height 273 mm (10.75").

(www.agiusa.com)

APPENDIX B: ARRAY THEORY

Survey Theory: Dipole-Dipole

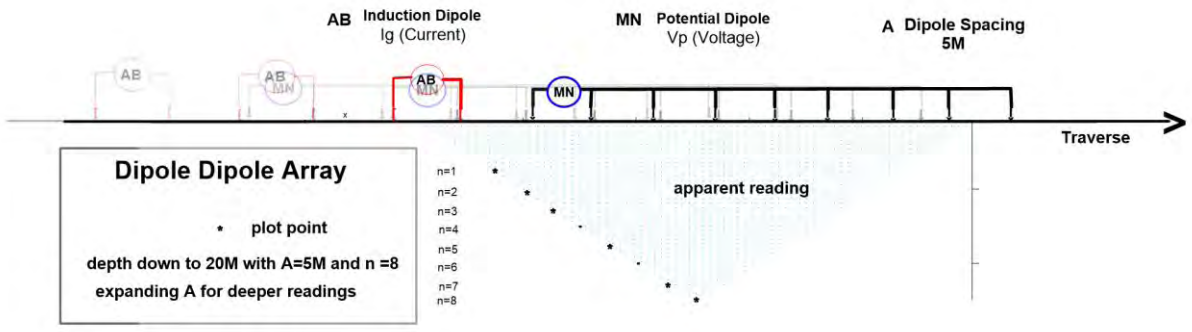

Geometry

Most common of arrays, directional current inductions mainly favored to delineate bodies having dip(s). Current electrodes always lag potential electrodes. Attention to direction of current inductions important when interpreting data. Known to produce typical pant-leg anomalies when both AB and MN electrodes cross a zone.

Set-up

Once a designated traverse is located, 84 electrodes are put into the ground pre extending 6 x cables of 14 connections amounting to a **415M Traverse.** The **Supersting** Transmitter/ Receiver (Tx/Rx) along with power-pack and switch-box are always centrally positioned.

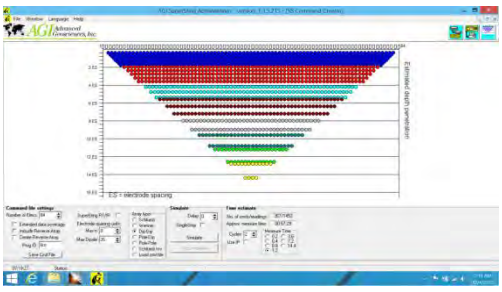

A designated Dipole Dipole Array command file was loaded in the Supersting performing:

1453 sample points, with an estimated 57.29min lapse-time, Maximum n (depth level) kept at 8 for best Signal/Noise, and Maximum dipoles of 26.

AB: 5, 10, 15, 20, 25, and 30M**, <u>5 x expansions</u>** reversed to traverse direction

MN: 5M till n=8, then 10M until n=8, then 20M until EOL

Extended Dipole Dipole

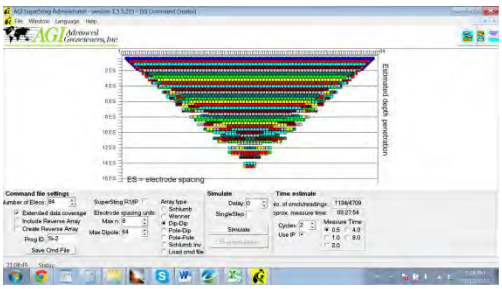

Extended Option:

4709 sample points, with an estimated 3hr:27Min lapse-time. Maximum n (depth level) kept at 8 for best Signal/Noise, and Maximum Dipoles of 26.

AB: 5, 10, 15… up to95M.

<u>19 expansions</u> reversed to traverse direction

MN: 5, 10, 15, 25, and 50M, 5 x expansions. Also reversed when best-fit.

Survey Theory: Pole Dipole

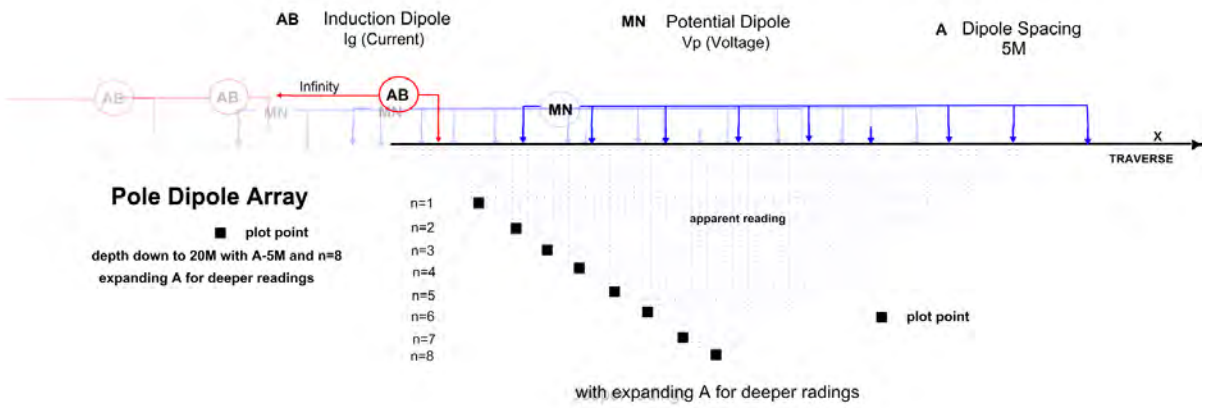

Geometry

Most common of arrays, directional current inductions mainly favored to delineate bodies having dip(s). Current electrodes always lag potential electrodes. Attention to direction of current inductions important when interpreting data. Known to produce typical pant-leg anomalies when both AB and MN electrodes cross a zone.

Set-up

Once a designated traverse is located, 84 electrodes are put into the ground pre extending 6 x cables of 14 connections amounting to a **415M Traverse.** The **Supersting** Transmitter/ Receiver (Tx/Rx) along with power-pack and switch-box are always centrally positioned.

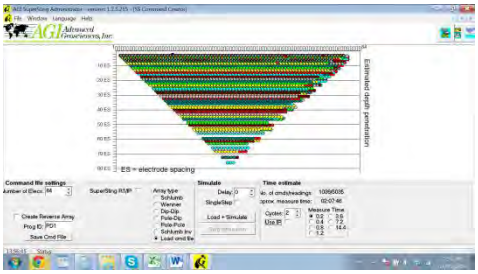

A designated Pole Dipole Array “PD1.CMD” command file was loaded in the Supersting performing:

5035 sample points, with an estimated 3:09:56 lapse-time, Maximum n (depth level) kept at 8 for best Signal/Noise, and Maximum dipoles of 26.

A electrode fixed: INFINITY
B electrode: 5M steps along traverse

MN: 14 x expansions (15M to 70M)

PD1.CMD; designed by R. Daigle at Groundtruth Exploration primarily for deeper investigations, eliminates early levels reducing technical <over-voltages> to speed up read time.

NOTE: Such high density requires additional time, thus choosing the proper array is crucial.

Survey Theory: Inverse Schlumberger

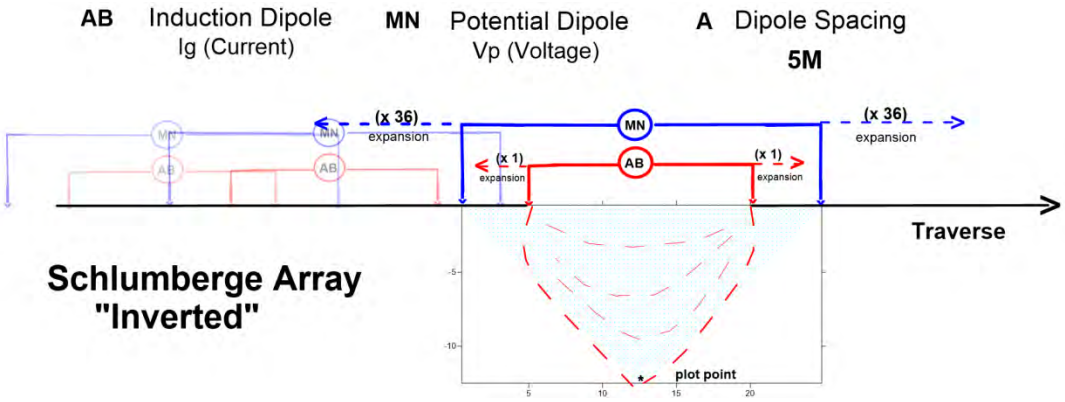

Geometry

Symmetric, vertical sounding technique is reliable delineating axis of zones. Termed inverse because the original design of the Schlumberger has inducing current electrodes outside potential electrodes. Also very useful isolating narrow, weak zones.

“Si-1” AB = 5M MN = 15M to 360M (36 expansions both directions). **For narrow nones**

“Si-2” AB = 5M and 15M MN = 15M to 65M first four levels. **For narrow & shallow.**

“Si-3” AB = 5M to 95M MN = 15M to 360M. **Best penetration of all three.**

Set-up

Once a designated traverse is located, 84 electrodes are put into the ground pre extending 6 x cables of 14 connections amounting to a **415M Traverse.** The **Supersting** Transmitter/ Receiver (Tx/Rx) along with power-pack and switch-box are always centrally positioned.

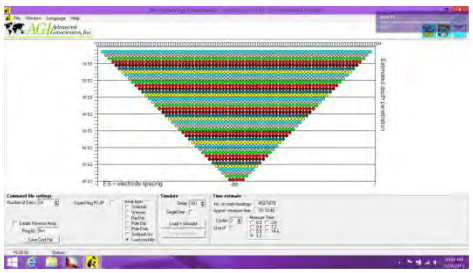

A designated Schlumberger Array command file was loaded in the Supersting performing:

1679 sample points, with an estimated 80:48min lapse-time, Maximum n kept at 8 (for best Signal/Noise), and Maximum dipoles of 26.

Si2.CMD: designed by R. Daigle at Groundtruth Exploration, for narrow/ shallow (limited depth extent) target.

Si3.CMD: primarily to improve S/N and target definitions. Early levels also kept for foot-print accuracy.